DOCTORAL THESIS

GEOGRAPHY, GENOMICS, AND EVOLUTIONARY SUCCESS IN AN INSULAR ENVIRONMENT

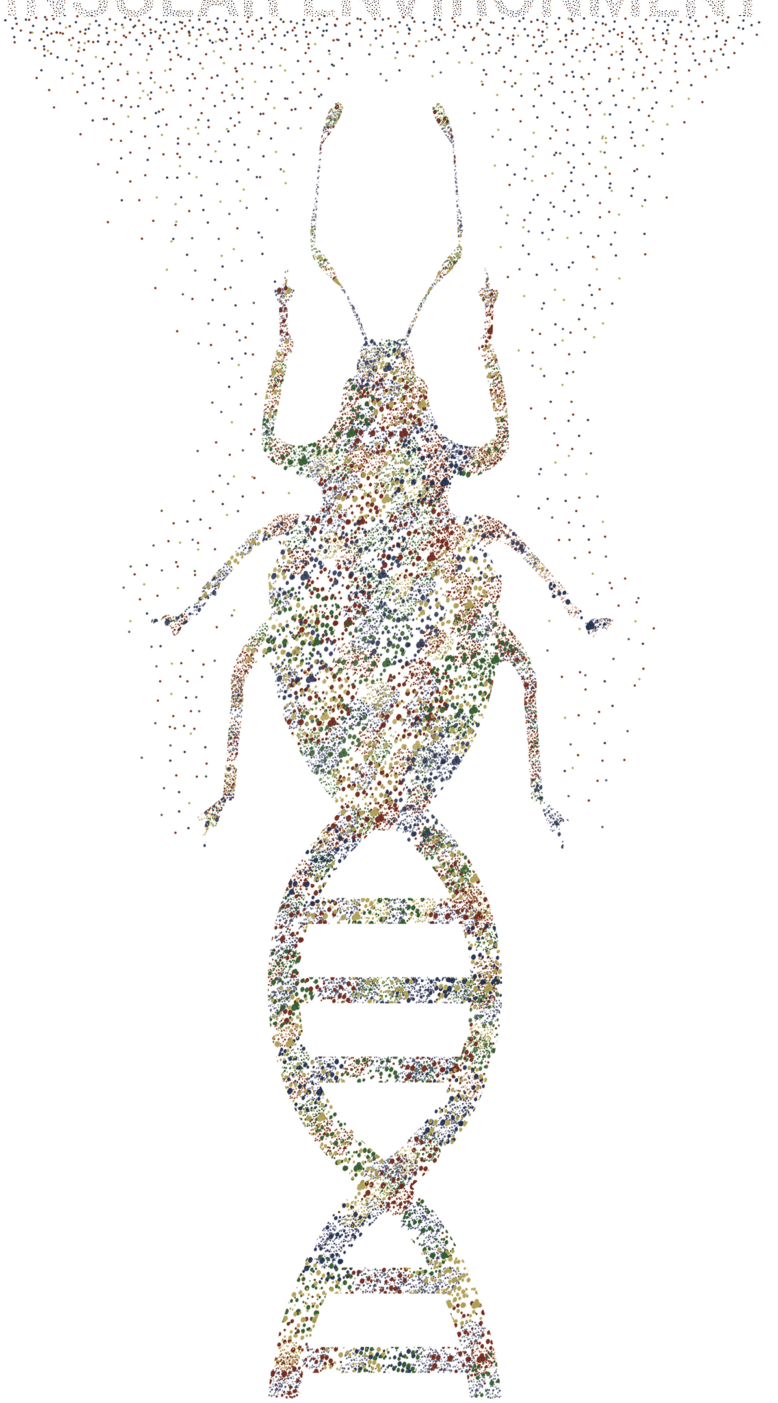

VÍCTOR M. GARCÍA OLIVARES

UNIVERSIDAD DE LA LAGUNA

SUPERVISORS

BRENT EMERSON | JAIRO PATIÑO

Geography, Genomics, and Evolutionary Success in an Insular Environment

2019

Autor : Víctor Manuel García Olivares

Director : Brent Charles Emerson

Co-Director : Jairo Patiño Llorente

Tutor : Mariano Nicolás Hernández Ferrer

Memoria presentada por el Licenciado Víctor Manuel García Olivares para optar al grado de Doctor con Mención Internacional por la Universidad de la Laguna (ULL)

Fdo : Brent Charles Emerson

Fdo : Jairo Patiño Llorente

Fdo : Mariano Hernández Ferrer

Geography, genomics, and evolutionary success in an insular environment

---

Víctor Manuel García Olivares

TESIS DOCTORAL - PH.D.
THESIS
SAN CRISTÓBAL DE LA LAGUNA, 2019

Instituto de Productos Naturales y Agrobiología
(IPNA-CSIC)

IPNA CSIC

CSIC
CONSEJO SUPERIOR DE INVESTIGACIONES CIENTÍFICAS

Esta Tesis Doctoral ha sido financiada por el Ministerio de Economía y Competitividad (proyecto de investigación: CGL2013-42589-P). Durante el desarrollo de mi Tesis Doctoral disfruté de una beca-contrato de Formación de Personal Investigador (FPI) (código de referencia: BES-2014-067868) y de diferentes ayudas para la realización de estancias breves en otros centros de investigación (códigos de referencia: EEBB-I-16-11213, EEBB-I-17-12649) concedidas por el Ministerio de Economía y Competitividad.

TABLE OF CONTENTS

THESIS ABSTRACT

Thesis abstract

Oceanic archipelagos are considered to serve as ideal natural laboratories for the study of ecology, evolution and conservation, providing a suitable framework to improve our understanding of the drivers of speciation. Evolutionary radiation is considered one of the more recognisable features of oceanic islands and represents a phenomenon that has long intrigued evolutionary biologists. Studies focusing on species radiations have provided a rich source of new insights into the evolutionary process and the mechanisms underlying diversification. Insular diversification is frequently associated with ecological drivers, however, non-ecological mechanisms may also drive diversification and speciation within insular settings by promoting geographic isolation. Applying phylogenetic and population genomic approaches, the present thesis investigates the dynamics of speciation within a super-radiation of weevils on the Canary Islands. The main objective is to understand the relative implications of geological events, climatic dynamics, geography and topography on the dynamics of diversification between and within islands. From the mitochondrial data analysed, strong evidence was found supporting a role for mega-landslides as drivers of island colonisation. The nuclear genome phylogeny revealed that, with some minor exceptions, species from each island are consistent with a single founding event for each island based on patterns of nuclear relatedness. In contrast, mitochondrial genetic variation shows more complex relationships among islands, reflecting multiple founding events for each island. The species complex from Gran Canaria, a geologically inactive island with high topographic complexity, points to the role for the interaction of topography and climate dynamics as a driver of diversification, revealing a complex speciation history involving repeated episodes of population isolation and admixture. Within the geologically more active island of Tenerife, the *L. tessellatus* species complex revealed a dynamic of more recent isolation and secondary contact, with the geography of individual relatedness implicating a role for gravitational flank collapses. These findings suggest that geologically active islands produce changes in the populations dynamic which may have a positive effect on regional genetic variation over the long term. Overall, the findings from this thesis

highlight the analytical power of next generation sequencing technologies to shed light into the fine-scale genomic understanding of evolutionary process.

GENERAL INTRODUCTION

General Introduction

Oceanic islands: Natural laboratories for evolutionary studies

Charles Darwin's five-year voyage around the world, studying and collecting animals, revolutionized evolutionary thinking, catalysed by an important stop in the Galapagos Islands and his study of the Galapagos finches (Darwin, 1859). Since Darwin's time, insular systems have been viewed as natural laboratories for the study of ecology and evolution (e.g. Roderick & Gillespie, 1998; Parent *et al.*, 2008). From a general point of view, islands can be classified into three categories: (i) those formed by volcanic activity in oceanic plates that have not been connected to continental landmasses (referred to as oceanic islands); (ii) those formed by relatively ancient fragmentation of larger landmasses of mainland that have been pushed away by tectonic activity (continental fragment islands); and (iii) those islands located within a continental shelf that have been commonly connected to mainland during Pleistocene glacial cycles (Whittaker & Fernandez-Palacios, 2007). Oceanic islands emerge from the ocean floor and their subaerial phase is initiated without life. Thus the initial assembly of oceanic biodiversity occurs through colonisation events that, together with the interaction of isolation and time, are the fundamental starting point for the generation of island biota (Gillespie & Roderick, 2002). By contrast, continental islands, due to their past connectivity with mainland, present a previous biological history such that elements of their contemporary biodiversity may predate the origin of the island. Of the different island types, oceanic islands are an attractive framework for evolutionary studies for a number of reasons: (i) they constitute discrete and isolated geographical entities with oceanic barriers limiting gene flow among them, (ii) their fauna and flora are often well understood, (iii) despite their reduced geographical size with respect continental systems, they often contain a considerable diversity of habitats, (iv) they are geologically dynamic (Emerson, 2002), and they present relative simplification in comparison with continental systems (Warren *et al.*, 2015).

Oceanic islands are geologically dynamic and typically follow a predictable geological trajectory throughout their life cycle comprised of several phases, which begins

with initial emergence from an underwater seamount, followed by a period of intense island-building, until reaching maximum area and elevation, followed by a latency stage, during which a slow erosional process leads to eventual island submergence (Price & Clague, 2002; Jackson, 2013). The dominant geological processes that characterize insular ontogeny are volcanic activity, flank collapses, tectonic subsidence and erosion, which are differentially associated with the different ontogenetic phases (Whittaker *et al.*, 2008). From an evolutionary perspective, the geological history of islands has frequently been inferred to have played a key role in generating within-island biogeographic boundaries, promoting the diversification of insular biotas (e.g. Carson, 1990; Pestano & Brown, 1999; Beheregaray *et al.*, 2003; Vandergast *et al.*, 2004; Bloor *et al.*, 2008; Macías-Hernández *et al.*, 2013). Given the evolutionary implications of geological dynamics for insular biodiversity, Whittaker *et al*., (2007; Whittaker *et al.*, 2008), in their General Dynamic Model (GDM), related the processes of immigration, speciation and extinction to the geological life cycle of an oceanic island. Otto *et al.* (2016), analyzing the distributions and richness of single island endemics (SIEs) with reference to GDM logic, revealed geological, geomorphological and evolutionary dynamics within islands as variables which best explain the distribution of SIEs at landscape scale. Together with geological processes, sea-level fluctuations provoked by Quaternary glacial cycles haven shaped island geography and archipelago configurations (Ali & Aitchison, 2014; Rijsdijk *et al.*, 2014; Fernández-Palacios *et al.*, 2016). Changes in island area, isolation and connectivity are promoted by sea-level fluctuations, the evolutionary impact of which has been implicated in the distribution patterns of island endemism across archipelagos (e.g. Papadopoulou & Knowles, 2015c; Papadopoulou & Knowles, 2015a; Weigelt *et al.*, 2016). Such a dynamic has been suggested to potentially promote a “species pump” through isolation and speciation during times of high sea-level stands, and range expansions and potential sympatry during periods of low sea-level stands (Gillespie & Roderick, 2014). Fernández-Palacios *et al.* (2016) have developed these processes into a conceptual model describing the role of Quaternary climatic dynamics over the variation of species distribution ranges in relationship with sea level changes. While the implications for speciation between islands is obvious, there has

been less focus on how Quaternary sea level changes and their environmental consequences might impact speciation within islands.

Canary Islands

The Canary Islands form part of the Macaronesian biogeographic region in the Atlantic Ocean, which is also comprised of the archipelagos of Azores, Madeira, Selvagens and Cape Verde. The archipelagos are of volcanic origin over the African plate, with the exception of Azores, the origin of which is associated with the oceanic mid-ocean ridge (Whittaker & Fernandez-Palacios, 2007). The Canary Islands stand out as one of the better-understood archipelagos from both a geological and biological point of view, helped in part due to a detailed investigation of the geological history of the islands (e.g. Ancochea *et al.*, 2006), and rich history of evolutionary and ecological investigation of the fauna and flora of the islands. Since Juan *et al.* (2000) first proposed expanding the scope of then available phylogenetic studies to develop existing understanding of community assembly on the archipelago, the archipelago has become a hot spot for evolutionary investigation (e.g. Emerson & Oromí, 2005; Jordal *et al.*, 2006; Sanmartín *et al.*, 2008; Kondraskov *et al.*, 2015; Patiño *et al.*, 2015). The origin of the Canary Island archipelago is controversial, diverses hypotheses have been proposed, which largely involve differing opinions over the hotspot concept of Wilson (1963), the mantle plume hypothesis of Morgan (1971), the propagating fracture hypothesis (Anguita & Hernan, 1975), the extensional ridges model (Fúster, 1975), and the uplifted tectonic blocks model (Araña, 1986). However, the current consensus seems to favour geological support for a hotspot origin (van den Bogaard, 2013). The archipelago is comprised of a chain of seven major islands and four islets which, at their closest point, are located 110 km from the northwestern coast of Africa, with their most distant point 494 km from Africa. The islands follow a sequential pattern of decreasing age from east to west (Fig. 1): Fuerteventura 22 Ma (Ancochea *et al.*, 1999; Carracedo & Day, 2002); Lanzarote 11.5 Ma (Coello *et al.*, 1992); Gran Canaria 14-15 Ma (Schimincke *et al.*, Sept. 1997); Tenerife 11.9 Ma (Guillou *et al.*, 2004); La Gomera 11-12 Ma (Cantagrel *et al.*, 1984; Ancochea *et al.*, 1990); La Palma 1.8 Ma (Carracedo *et al.*, 2001; Carracedo & Day,

2002), and; El Hierro 1.2 Ma (Guillou *et al.*, 1996; Carracedo *et al.*, 2001; Carracedo & Day, 2002). The broad age range of the islands, from 1.2 to 22 Ma, contrasts with many other oceanic archipelagos (e.g. the Hawaiian archipelago) due to their lack of older islands of substantial size. This represents a distinguishing feature of the Canary Islands, contributing to its uniqueness as an investigative model to understand the evolutionary effect of geological dynamics and their consequences across island biota.

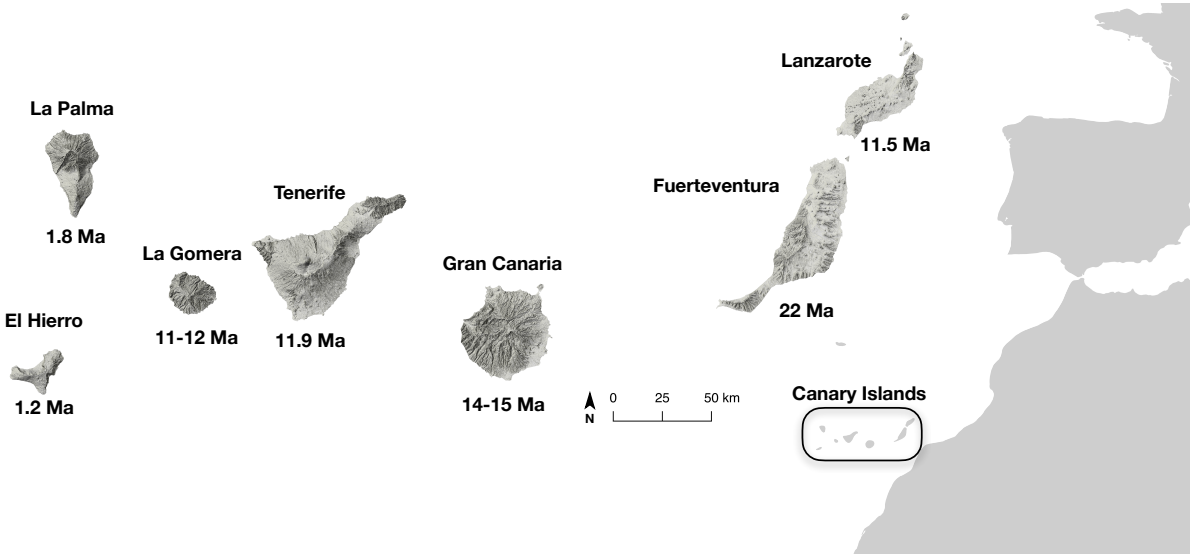

Figure 1. Canary Islands. Map showing the seven islands that compound the Archipelago indicating the name and age in Ma by each island.

The Canary Islands present a subtropical climate, with warm temperatures and limited seasonal variation. Higher altitude terrains act a barrier to low-level, moist trade winds, generating a toposequence of contrasting climatic conditions. This dynamic creates a marked zonation of vegetation, strongly differentiated between the windward and leeward sides of the islands (Fernández-Palacios & de Nicolás, 1995). Various ecological zones exist within the different islands, which vary depending of the height of an island. Different categorizations have been proposed (e.g. Oromí *et al.*, 2015), although from a general point of view one can describe, from the coast to the highest altitudes of the islands, the following: coastal desert, lowland vegetation which can be humid in the

northeast or arid in the southwest, laurel forest in the NE, pine forest mostly in the SW, and dry high mountain vegetation (Bramwell, 1972; Francisco-Ortega *et al.*, 1996; Juan *et al.*, 2000). The diversity of habitats present is considered to be one explanation for the high species diversity and endemicity across the archipelago, features which have led to the region being considered as a floral and faunal world hotspot for biodiversity (Sundseth, 2005). The Canary Islands are home to 14,254 known species of animal, plant and ground fungi, among which 27.3% are archipelago-level endemisms (Arechavaleta *et al.*, 2010). Approximately half of all species are arthropods (7,075 species), forming the most diverse assemblage within the archipelago. The native arthropod fauna is comprised of 3,301 endemic species and ninety-nine endemic genera, 49 of which belong to the order Coleoptera, within which the families Carabidae and Curculionidae stand out with 15 and 11 endemic genera, respectively. Among 12 non-endemic genera with more than 20 within Canary Islands species, 7 belong to the order Coleoptera (Oromí *et al.*, 2015).

Evolutionary radiations on oceanic islands

Evolutionary radiation, defined here as an extensive proliferation of a taxa within a clade, is one of the more recognisable features of oceanic islands (Losos & Ricklefs, 2009) and represents a phenomena that has intrigued evolutionary biologists for many decades. However, in many cases, the term adaptive radiation has been applied to describe radiation (e.g. Osborn, 1902; Simpson, 1953; Losos & Ricklefs, 2009; Givnish, 2015). Adaptive radiation is a specific definition of a radiation that is not reflective of the broader range of biotic and abiotic factors that can promote evolutionary radiation without adaptation, and as such usage of the term is now less universally applied (Harmon *et al.*, 2003; Olson & Arroyo-Santos, 2009; Lieberman, 2012; Moen & Morlon, 2014). Adaptive radiation is characterized by an increase of the rate of speciation within a clade driven primarily by biotic factors promoting adaptive change within lineages (Simoes *et al.*, 2016). Non-adaptive radiations are those that are unrelated to niche exploitation, and thus where reproductive isolation is not linked to the build-up of ecological niche diversification

(Gittenberger, 1991; Rundell & Price, 2009). Despite the fact that the term “non-adaptive radiation” was coined in the early part of the 20th century (Wright, 1931), this particular class of evolutionary radiation has remained largely unstudied, with the majority of radiations investigated having been adaptive. However, both concepts have been an object of discussion for some decades (e.g. Davis, 1993, 1994; Gittenberger, 2004).

Adaptive radiation describes an inherent link between ecology and evolution (Grant & Grant, 2008; Losos & Ricklefs, 2009; Mahler *et al.*, 2010; Moen & Morlon, 2014), and was defined by Givnish (1997) as ‘the rise of a diversity of ecological roles and attendant adaptations in different species within a lineage’. This process has been suggested to be a key evolutionary mechanism to explain the origin and maintenance of biodiversity in oceanic islands (Gillespie, 2002), including such iconic examples as Darwin’s finches in the Galapagos Islands, *Anolis* lizards in the Greater Antilles, and silverwords, honeycreepers and *Drosophila* in Hawaii (reviewed in Emerson, 2002; Gillespie, 2009).

From an evolutionary perspective, three general criteria describe non-adaptive radiation: (i) absence of clear niche differentiation; (ii) species typically present a low degree of phenotypical variation, and; (iii) species usually evolve in allopatry or peripatry (Brooks *et al.*, 1984; Gittenberger, 1991; Davis, 1993; Givnish, 1997; Gittenberger, 2004). In oceanic islands, the often complex landscapes formed by numerous volcanic events followed by erosional activity and flank collapses may generate landscapes of fragmented habitat, facilitating non-adaptive speciation, as has been suggested for terrestrial snails (Cameron *et al.*, 1996; Cook, 2008; Jordaens *et al.*, 2009). Thus, although insular diversification is frequently associated with ecological drivers, non-ecological mechanisms, such as the interaction of geology, topography and climate, are also expected to drive diversification and promote speciation within insular settings by promoting geographic isolation. Thus, oceanic islands may provide a suitable framework within which to understand the drivers of in situ insular speciation, and this has been recently highlighted and an important area of investigation (Patiño *et al.*, 2017).

Laparocerus a Macaronesian super-radiation

Within the Macaronesian region, the endemic weevil genus *Laparocerus* stands apart from all other invertebrate genera with its species richness of 237 species and subspecies. The majority of species are distributed in the Canary Islands, with a total of 196, follows by Madeira with 36, two in Selvagens, and three in Morocco. This vast species richness of the genus has been partitioned into higher-order taxonomic units and species complexes (e.g. Machado, 2006, 2008; Machado, 2011). Recently, a molecular phylogenetic approach has been used to assist with a taxonomical revision of the genus (Machado *et al.*, 2017). With only limited molecular sampling, using in the majority of the cases only one individual per species or subspecies, Machado *et al.* (2017) were able to resolve higher level relationships within the group. However, relationships among closely related species remain less clear. As a first approach to understand why *Laparocerus* has diversified so dramatically within Macaronesia, Faria *et al.* (2016), carried out a molecular study focused on the well-defined *Laparocerus tessellatus* species complex. From an evolutionary point of view, species complexes, in which closely related taxa present uncertain species boundaries, represent suitable models to study the speciation continuum (Coyne & Orr, 2004; Feder *et al.*, 2012), before evolutionary signal is eroded by demographic and selective processes. The *L. tessellatus* complex comprised of 10 taxonomically described species and an additional undescribed species distributed on four of the Canary Islands. All species are single endemic species, with four on Gran Canaria (*L. microphthalmus* Lindberg, 1950; *L. obsitus* Wollaston, 1864; *L. osorio* Machado, 2012; *L. tirajana* Machado, 2012) and one undescribed, four on Tenerife *(L. tessellatus* Brulle, 1839; *L. freyi* Uyttenboogaart, 1940; *L. punctiger* Machado, 2016; and *L. canescens* Machado, 2016), one on La Palma (*L. auarita* Machado, 2016) and one on El Hierro (*L. bimbache* Machado, 2011). Faria *et al.* (2016) analysed DNA sequence data from the mitochondrial COII gene and the nuclear ITS2 gene, sampled across the geographic range of each species, revealing inconsistencies between the two gene genealogies, with respect to their implications for species colonisation history. Nuclear DNA sequence variation was consistent with a simple colonization history, while mitochondrial

DNA sequence variation could only be explained by a more complex colonisation history. This incongruence was explained as a consequence of genetic admixture involving multiple founding species to the islands of La Palma and El Hierro, involving populations from more than one source island in each case. While able to broadly identify complex speciation histories involving genomic admixture, Faria *et al.* (2016) were unable to expand further on this dynamic. The results of Faria *et al.* (2016) highlight the need for more data rich approaches using new high throughput sequencing technologies for increased resolution for a fuller understanding of the recent diversification history within the *L. tessellatus* complex. Sub-genomic sequencing techniques provide a powerful molecular approach that has revolutionised evolutionary investigation in areas such as phylogeography, population genomics, and phylogenomics (Emerson, 2010; Keller *et al.*, 2013; Xu *et al.*, 2014).

New Generation Sequencing: A multilocus approach to unravelling recent species radiation

Since its development, the Sanger method for DNA sequencing (Sanger *et al.*, 1977) has been a key technology applied in a wide range of studies focussed on understanding biological diversity, and it remains the most commonly used sequencing method for routine molecular analyses (Escalante *et al.*, 2014). Sanger sequencing yields DNA sequence read lengths between 500-1000 bp (Shendure *et al.*, 2004) for a single fragment in a single reaction, approximately the length of an average gene (Escalante *et al.*, 2014). The method has been instrumental for obtaining comparable molecular markers within and across species, facilitating the development of the fields of phylogeography and phylogenetic analysis. In the early 1990s, Avise and Ball (1990), anticipated the use of larger multilocus data sets in order to distinguish between spurious phylogeographic breaks and true vicariant events, based on the assumption of the genealogical concordance across independent loci. Within the field of phylogenetics, it is recognized that the use of large datasets and thus more informative sites may increase nodal support (Brito & Edwards, 2008). Thus, using multiple loci to infer population-level and species-level histories has become the baseline in phylogeography and phylogenetics (McCormack *et al.*, 2013),

promoting further advances in the field of statistical phylogeography (Knowles & Maddison, 2002) while also fuelling the emerging species-tree paradigm of phylogenetics (Edwards, 2009). In spite of the increasing ability to generate multiple molecular markers for non-model organisms (Edwards, 2008; Thomson *et al.*, 2010), the generation of multilocus data requires a substantial laboratory effort (McCormack *et al.*, 2013). Logistical limitations for the acquisition of multilocus data have benefited from an important advance from Sanger to next-generation sequencing (NGS) technologies that utilise efficient and cost-effective nano sequencing developments (Lerner & Fleischer, 2010; Ekblom & Galindo, 2011).

Next-generation sequencing, also referred to as massive-parallel sequencing or high throughput sequencing, has become a key technology in biological sciences. This sequencing approach provides several important advantages in comparison with Sanger technology. First, the DNA amplification step is performed in cell-free systems, so it does not require a bacterial cloning process for the sequencing of single copy PCR product. Second, the detection of nucleotide base identity is performed in the absence of electrophoresis, with technologies such as sequencing-by-synthesis providing an alternative (Bentley *et al.*, 2008). Finally, thousands-to-many-millions of sequencing reactions can be performed in parallel. In addition, a wide spectrum of genomic polymorphisms can be characterised, from a point mutation within a single base pair (SNP), to insertions and deletions, genomic duplications (López de Heredia, 2016) or linked SNPs. The scale and idiosyncrasies of NGS data has resulted in significant computational challenges, leading to increased demands on bioinformatic tools for data analysis and management of big molecular data (van Dijk *et al.*, 2014). Due to the relatively short length and the high number of generated reads by NGS a large number of new algorithms have been developed to manage such data, as well as new algorithms for de novo assembly for non-model organisms (Hatem *et al.*, 2013), single nucleotide polymorphisms (SNP) detection (Zhang *et al.*, 2011), and to correct for biases introduced during library preparation (Hansen *et al.*, 2010). In addition, to overcome limitations in terms of computational time processing, High Performance Computing systems (HPC) are becoming

popular in bioinformatics by providing faster processing by utilizing high-throughput and parallel-processing techniques (Hager & Wellein, 2010; Zhang *et al.*, 2013).

The use of whole-genome sequencing to sample population diversity remains prohibitively expensive for population genetics laboratories due to the needed of a large number of individuals required for such studies (Gautier *et al.*, 2013), however the development of NGS approaches based on sequencing of reduced representation libraries (RRL), has facilitated the use of NGS technology for a wide range of organisms and research areas, including population genomics studies (e.g. Emerson, 2010; Hohenlohe *et al.*, 2010; Keller *et al.*, 2013). Restriction site associated DNA sequencing (RAD-seq) represents a low-cost and efficient technique for the analysis of potentially thousands of homologous DNA sequence regions sampled across multiple individuals from genomes of species with no prior information. The term of RAD-seq refers to a set of techniques base on a digestion step performed by restriction endonucleases which generate a range of loci to be sequenced. Within the range of RADseq methods, double-digested RAD-seq (ddRAD-seq) offers more potential to be applicable to a diversity of biological questions in a wide range of organisms (Peterson *et al.*, 2012). The main difference of ddRAD-seq with respect to the original technique (Baird *et al.*, 2008) is the use of two restriction endonucleases with different site specificities, generating fragments with known extremes, which are selected within a specific size range that will be a function of individual project requirements. This results in reduced genome sequencing with high repeatability and site-specific coverage (Peterson *et al.*, 2012). The unprecedented resolution provided by NGS technology and ddRAD-seq facilitates the analysis of species-level of genetic variation (Leache *et al.*, 2015; Potter *et al.*, 2016; Yoder *et al.*, 2016), and the evolutionary mechanisms involved in the early stages of speciation (Papadopoulou & Knowles, 2015b; Huang, 2016; Weir *et al.*, 2016).

1.6 Justification and aims

Given the above, this Doctoral Thesis is focused on investigating the dynamics of speciation within a super-radiation of weevils on the Canary Islands, using both phylogenetics and population genomics approaches. The general aim of this Doctoral Thesis is to understand the relative implications of geological events, climatic dynamics, geography and island topography on the dynamics of diversification between islands and within islands. The study model is the *Laparocerus tessellatus* complex, and the four specific aims developed through the four chapters can be summarised in the following points:

1. Explore the role of mega-landslides as a driver of colonization among islands for flightless invertebrates species (Chapter I).

2. Reconstruct the phylogenetic relationships of the *Laparocerus tessellatus* complex through mitochondrial and nuclear markers by using, respectively, Sanger and Next Generation Sequencing, in order to obtain a fuller understanding of the diversification history within complex (Chapter II).

3. Describe the patterns of individual genomic relatedness within and among species of the *Laparocerus tessellatus* complex on Gran Canaria to evaluate the potential role of the interaction of topography and climate on within-island diversification (Chapter III).

4. Evaluate the consequences of mega-landslides on within island population dynamics by quantifying individual genomic relatedness within and among areas of different geological stability through time within the island of Tenerife (Chapter IV).

References

Ali, J.R. & Aitchison, J.C. (2014) Exploring the combined role of eustasy and oceanic island thermal subsidence in shaping biodiversity on the Galápagos. *Journal of Biogeography*, **41**, 1227-1241.

Ancochea, E., Hernán, F., Huertas, M.J., Brändle, J.L. & Herrera, R. (2006) A new chronostratigraphical and evolutionary model for La Gomera: Implications for the overall evolution of the Canarian Archipelago. *Journal of Volcanology and Geothermal Research*, **157**, 271-293.

Ancochea, E., Huertas, M.J., Cantagrel, J.M., Coello, J., Fúster, J.M., Arnaud, N. & Ibarrola, E. (1999) Evolution of the Cañadas edifice and its implications for the origin of the Cañadas Caldera (Tenerife, Canary Islands). *Journal of Volcanology and Geothermal Research*, **88**, 177-179.

Ancochea, E., Fuster, J.M., Ibarrola, E., Cendrero, A., Coello, J., Hemán, F., Cantagrel, J.M. & Jamond, C. (1990) Volcanic evolution of the island of Tenerife (Canary Islands) in the light of new K-Ar data. *Journal of Volcanology and Geothermal Research* **44**, 231-249.

Anguita, F. & Hernan, F. (1975) A propagation fracture model versus a hot spot origin for the Canary Islands. *Earth and Planetary Science Letters*, **27**, 11-19.

Araña, V. (1986) Marco geodinamico del volcanismo canario. *An Fisica*, **82**, 202–231.

Arechavaleta, M., Rodríguez, S., Zurita, N. & García, A. (2010) *Lista de especies silvestres de Canarias. Hongos, plan- tas y animales terrestres*. Consejería de Medio Ambiente y Ordenación Territorial, Gobierno de Canarias.

Avise, J.C. & Ball, R.M.J. (1990) Principles of genealogical concordance in species concepts and biological taxonomy. *Oxford Surveys in Evolutionary Biology* (ed. by J.A. D. Futuyma), pp. 45-67. Oxford University Press, Oxford.

Baird, N.A., Etter, P.D., Atwood, T.S., Currey, M.C., Shiver, A.L., Lewis, Z.A., Selker, E.U., Cresko, W.A. & Johnson, E.A. (2008) Rapid SNP discovery and genetic mapping using sequenced RAD markers. *PLoS One*, **3**, e3376.

Beheregaray, L.B., Ciofi, C., Geist, D., Gibbs, J.P., Caccone, A. & Powell, J.R. (2003) Genes Record a Prehistoric Volcano Eruption in the Galápagos. *Science*, **302**, 75.

Bentley, D.R., Balasubramanian, S., Swerdlow, H.P., Smith, G.P., Milton, J., Brown, C.G., Hall, K.P., Evers, D.J., Barnes, C.L., Bignell, H.R., Boutell, J.M., Bryant, J., Carter, R.J., Keira Cheetham, R., Cox, A.J., Ellis, D.J., Flatbush, M.R., Gormley, N.A., Humphray, S.J., Irving, L.J., Karbelashvili, M.S., Kirk, S.M., Li, H., Liu, X., Maisinger, K.S., Murray, L.J., Obradovic, B., Ost, T., Parkinson, M.L., Pratt, M.R., Rasolonjatovo, I.M., Reed, M.T., Rigatti, R., Rodighiero, C., Ross, M.T., Sabot, A., Sankar, S.V., Scally, A., Schroth, G.P., Smith, M.E., Smith, V.P., Spiridou, A., Torrance, P.E., Tzonev, S.S., Vermaas, E.H., Walter, K., Wu, X., Zhang, L., Alam, M.D., Anastasi, C., Aniebo, I.C., Bailey, D.M., Bancarz, I.R., Banerjee, S., Barbour, S.G., Baybayan, P.A., Benoit, V.A., Benson, K.F., Bevis, C., Black, P.J., Boodhun, A., Brennan, J.S., Bridgham, J.A., Brown, R.C., Brown, A.A., Buermann, D.H., Bundu, A.A., Burrows, J.C., Carter, N.P., Castillo, N., Chiara, E.C.M., Chang, S., Neil Cooley, R., Crake, N.R., Dada, O.O., Diakoumakos, K.D., Dominguez-Fernandez, B., Earnshaw, D.J., Egbujor, U.C., Elmore, D.W., Etchin, S.S., Ewan, M.R., Fedurco, M., Fraser, L.J., Fuentes Fajardo, K.V., Scott Furey, W., George, D., Gietzen, K.J., Goddard, C.P., Golda, G.S., Granieri, P.A., Green, D.E., Gustafson, D.L., Hansen, N.F., Harnish, K., Haudenschild, C.D., Heyer, N.I., Hims, M.M., Ho, J.T.,

Horgan, A.M., Hoschler, K., Hurwitz, S., Ivanov, D.V., Johnson, M.Q., James, T., Huw Jones, T.A., Kang, G.D., Kerelska, T.H., Kersey, A.D., Khrebtukova, I., Kindwall, A.P., Kingsbury, Z., Kokko-Gonzales, P.I., Kumar, A., Laurent, M.A., Lawley, C.T., Lee, S.E., Lee, X., Liao, A.K., Loch, J.A., Lok, M., Luo, S., Mammen, R.M., Martin, J.W., McCauley, P.G., McNitt, P., Mehta, P., Moon, K.W., Mullens, J.W., Newington, T., Ning, Z., Ling Ng, B., Novo, S.M., O'Neill, M.J., Osborne, M.A., Osnowski, A., Ostadan, O., Paraschos, L.L., Pickering, L., Pike, A.C., Pike, A.C., Chris Pinkard, D., Pliskin, D.P., Podhasky, J., Quijano, V.J., Raczy, C., Rae, V.H., Rawlings, S.R., Chiva Rodriguez, A., Roe, P.M., Rogers, J., Rogert Bacigalupo, M.C., Romanov, N., Romieu, A., Roth, R.K., Rourke, N.J., Ruediger, S.T., Rusman, E., Sanches-Kuiper, R.M., Schenker, M.R., Seoane, J.M., Shaw, R.J., Shiver, M.K., Short, S.W., Sizto, N.L., Sluis, J.P., Smith, M.A., Ernest Sohna Sohna, J., Spence, E.J., Stevens, K., Sutton, N., Szajkowski, L., Tregidgo, C.L., Turcatti, G., Vandevondele, S., Verhovsky, Y., Virk, S.M., Wakelin, S., Walcott, G.C., Wang, J., Worsley, G.J., Yan, J., Yau, L., Zuerlein, M., Rogers, J., Mullikin, J.C., Hurles, M.E., McCooke, N.J., West, J.S., Oaks, F.L., Lundberg, P.L., Klenerman, D., Durbin, R. & Smith, A.J. (2008) Accurate whole human genome sequencing using reversible terminator chemistry. *Nature*, **456**, 53-9.

Bloor, P., Kemp, S.J. & Brown, R.P. (2008) Recent volcanism and mitochondrial DNA structuring in the lizard Gallotia atlantica from the island of Lanzarote. *Molecular Ecology*, **17**, 854-66.

Bramwell, D. (1972) *Endemism in the flora of the Canary Islands. Taxonomy, phytogeography, and evolution*. Academic Press, London.

Brito, P.H. & Edwards, S.V. (2008) Multilocus phylogeography and phylogenetics using sequence-based markers. *Genetica*, **135**, 439-455.

Brooks, D.R., O'Grady, R.T. & Glen, D.R. (1984) Phylogenetic analysis of the Digenea (Platyhelminthes: Cercomeria) with comments on their adaptive radiation. *Canadian Journal of Zoology*, **63**, 411-443.

Cameron, R.A.D., Cook, L.M. & Hallows, J.D. (1996) Land snails on Porto Santo: adaptive and non-adaptive radiation. *Philosophical Transactions of the Royal Society of London. Series B: Biological Sciences*, **351**, 309-327.

Cantagrel, J.M., Cendrero, A., Fuster, J.M., Ibarrola, E. & Jamond, C. (1984) K-Ar Chronology of the volcanic eruptions in the Canarian Archipelago: Island of La Gomera. *Bulletin of Volcanology*, **47**

Carracedo, J., Rodríguez-Badiola, E., Guillou, H., De La Nuez, J. & Pérez-Torrado, F.J. (2001) Geology and volcanology of La Palma and El Hierro, Western Canaries. *Estudios Geológicos*, **57**, 175-273.

Carracedo, J.C. & Day, S. (2002) *Canary Islands. Classic Geology in Europe Series Volume 4.* Terra Publishing, Harpenden.

Carson, H.L.L., J.P.; Craddock E.M. (1990) Extinction and recolonization of local populations on a growing shieldvolcano. *Proceedings of the National Academy of Sciences*, **87**, 7055-7057.

Coello, J., Cantagrel, J.M., Hernán, F., Fuster, J.M., Ibarrola, E., Ancochea, E., Casquet, C., Jamond, C., Díaz de Terán, J.R. & Cendrero, A. (1992) Evolution of the eastern volcanic ridge of the Canary Islands based on new K-Ar data. *Journal of Volcanology and Geothermal Research*, **53**, 251-274.

Cook, L.M. (2008) Species richness in Madeiran land snail and its causes. *Journal of Biogeography*, **35**, 647-653.

Coyne, J.A. & Orr, H.A. (2004) *Speciation*. Sinauer Associates, Inc., Sunderland, Massachusetts.

Darwin, C. (1859) *On the origin of species by means of natural selection, or preservation of favoured races in the struggle for life*. John Murray, 1859, London.

Davis, G.M. (1993) Evolution of Prosobranch Snails Transmitting Asian Schistosoma; Coevolution with Schistosoma: A Review. *Progress in Clinical Parasitology*. Sun T. (eds), New York, NY.

Davis, G.M. (1994) Molecular genetics and taxonomic discrimination. *The nautilus, Supplement*, **2**, 3-23.

Edwards, S.V. (2008) PERSPECTIVE: A smörgåsbord of markers for avian ecology and evolution. *Molecular Ecology*, **17**, 945-946.

Edwards, S.V. (2009) Is a new and general theory of molecular systematics emerging? *Evolution*, **63**, 1-19.

Ekblom, R. & Galindo, J. (2011) Applications of next generation sequencing in molecular ecology of non-model organisms. *Heredity (Edinb)*, **107**, 1-15.

Emerson, B. (2002) Evolution on oceanic islands: molecular phylogenetic approaches to understanding pattern and process. *Molecular Ecology*, **11**, 951–966.

Emerson, B.C. & Oromí, P. (2005) Diversification of the forest beetle genus Tarphius on the Canary Island, and the evolutionary origins of island endemics. *Evolution*, **59**, 586-598.

Emerson, K.J.M., Clayton R.; Catchen, Julian M.; Hohenlohe, Paul A.; Cresko, William A.; Bradshaw, William E.; Holzapfel, Christina M. (2010) Resolving postglacial phylogeography using high-throughput sequencing. *Proceedings of the National Academy of Sciences*, **107**, 16196-16200.

Escalante, A.E., Jardón Barbolla, L., Ramírez-Barahona, S. & Eguiarte, L.E. (2014) The study of biodiversity in the era of massive sequencing. *Revista Mexicana de Biodiversidad*, **85**, 1249-1264.

Faria, C.M.A., Machado, A., Amorim, I.R., Gage, M.J.G., Borges, P.A.V. & Emerson, B.C. (2016) Evidence for multiple founding lineages and genetic admixture in the evolution of species within an oceanic island weevil (Coleoptera, Curculionidae) super-radiation. *Journal of Biogeography*, **43**, 178-191.

Feder, J.L., Egan, S.P. & Nosil, P. (2012) The genomics of speciation-with-gene-flow. *Trends in Genetics*, **28**, 342-50.

Fernández-Palacios, J.M. & de Nicolás, J.P. (1995) Altitudinal pattern of vegetation variation on Tenerife. *Journal of Vegetation Science* **6**, 183-190.

Fernández-Palacios, J.M., Rijsdijk, K.F., Norder, S.J., Otto, R., de Nascimento, L., Fernández-Lugo, S., Tjørve, E. & Whittaker, R.J. (2016) Towards a glacial-sensitive model of island biogeography. *Global Ecology and Biogeography*, **25**, 817-830.

Francisco-Ortega, J., Jansen, R.K. & Santos-Guerra, A. (1996) Chloroplast DNA evidence of colonization, adaptive radiation, and hybridization in the evolution of the Macaronesian flora. *Proceedings of the Natural Academy of Sciences of Philadelphia*, **93**, 4085-4090.

Fúster, J.M. (1975) Las Islas Canarias: un ejemplo de evolución temporal y espacial del vulcanismo oceánico. *Estudios Geológicos*, **34**, 439-463.

Gautier, M., Foucaud, J., Gharbi, K., Cezard, T., Galan, M., Loiseau, A., Thomson, M., Pudlo, P., Kerdelhue, C. & Estoup, A. (2013) Estimation of population allele frequencies

from next-generation sequencing data: pool-versus individual-based genotyping. *Molecular Ecology*, **22**, 3766-79.

Gillespie, R.G. (2002) Biogeography of spiders on remote oceanic islands of the Pacific: archipelagoes as stepping stones? *Journal of Biogeography*, **29**, 655–662.

Gillespie, R.G. (2009) *Adaptive Radiation. Encyclopedia of Islands*. University of California Press, California, USA.

Gillespie, R.G. & Roderick, G.K. (2002) Arthropods on islands: colonization, speciation, and conservation. *Annual review of entomology*, **47**, 595-632.

Gillespie, R.G. & Roderick, G.K. (2014) Geology and climate drive diversification. *Nature*, **509**, 297 - 298.

Gittenberger, E. (1991) What about non-adaptive radiation? *Biological Journal of the Linnean Society*, **43**, 263-272.

Gittenberger, E. (2004) Radiation and adaptation, evolutionary biology and semantics. *Organisms Diversity & Evolution*, **4**, 135-136.

Givnish, T.J. (1997) Adaptive radiation and molecular systematics: Issues and approaches. *Evolution and Adaptive Radiation*, pp. 1-54. Cambridge University Press, Cambridge.

Givnish, T.J. (2015) Adaptive radiation versus 'radiation' and 'explosive diversification': why conceptual distinctions are fundamental to understanding evolution. *New Phytologist*, **207**, 297-303.

Grant, P.R. & Grant, B.R. (2008) *How and Why Species Multiply: The Radiation of Darwin's Finches*. Princeton University Press, New Jersey.

Guillou, H., Carracedo, J., Pérez-Torrado, F.J. & Rodríguez Badiola, E. (1996) K-Ar ages and magnetic stratigraphy of a hotspotinduced, fast grown oceanic island: El Hierro, Canary Islands. *Journal of Volcanology and Geothermal Research*, **73**, 141-155.

Guillou, H., Torrado, F.J.P., Hansen Machin, A.R., Carracedo, J.C. & Gimeno, D. (2004) The Plio–Quaternary volcanic evolution of Gran Canaria based on new K–Ar ages and magnetostratigraphy. *Journal of Volcanology and Geothermal Research*, **135**, 221-246.

Hager, G. & Wellein, G. (2010) *Introduction to High Performance Computing for Scientists and Engineers*. Chapman & Hall/CRC Press, Boca Raton, Florida.

Hansen, K.D., Brenner, S.E. & Dudoit, S. (2010) Biases in Illumina transcriptome sequencing caused by random hexamer priming. *Nucleic acids Research*, **38**, e131.

Harmon, L.J., Schulte, J.A., Larson, A. & Losos, J.B. (2003) Tempo and mode of evolutionary radiation in iguanian lizards. *Science*, **301**, 961-964.

Hatem, A., Bozda, D., Toland, A.E. & Çatalyüre, U.V. (2013) Benchmarking short sequence mapping tools. *BMC Bioinformatics*, **14**, 184.

Hohenlohe, P.A., Bassham, S., Etter, P.D., Stiffler, N., Johnson, E.A. & Cresko, W.A. (2010) Population genomics of parallel adaptation in threespine stickleback using sequenced RAD tags. *PLoS Genet*, **6**, e1000862.

Huang, J.P. (2016) Parapatric genetic introgression and phenotypic assimilation: testing conditions for introgression between Hercules beetles (Dynastes, Dynastinae). *Molecular Ecology*, **25**, 5513-5526.

Jackson, T.A. (2013) A review of volcanic island evolution and magma production rate: an example from a Cenozoic island arc in the Caribbean. *Journal of the Geological Society*, **170**, 547-556.

Jordaens, K., Van Riel, P., Frias Martins, A.M. & Backeljau, T. (2009) Speciation on the Azores islands: congruent patterns in shell morphology, genital anatomy, and molecular

markers in endemic land snails (Gastropoda, Leptaxinae). *Biological Journal of the Linnean Society*, **97**, 166-176.

Jordal, B.H., Emerson, B.C. & Hewitt, G.M. (2006) Apparent 'sympatric' speciation in ecologically similar herbivorous beetles facilitated by multiple colonizations of an island. *Molecular Ecology*, **15**, 2935-2947.

Juan, C., Emerson, B.C., Oromí, P. & Hewitt, G.M. (2000) Colonization and diversification: towards a phylogeographic synthesis for the Canary Islands. *Trends in Ecology & Evolution*, **15**, 104-109.

Keller, I., Wagner, C.E., Greuter, L., Mwaiko, S., Selz, O.M., Sivasundar, A., Wittwer, S. & Seehausen, O. (2013) Population genomic signatures of divergent adaptation, gene flow and hybrid speciation in the rapid radiation of Lake Victoria cichlid fishes. *Molecular Ecology*, **22**, 2848-63.

Knowles, L.L. & Maddison, W.P. (2002) Statistical phylogeography. *Molecular Ecology*, **11**, 2623-2635.

Kondraskov, P., Schutz, N., Schussler, C., de Sequeira, M.M., Guerra, A.S., Caujape-Castells, J., Jaen-Molina, R., Marrero-Rodriguez, A., Koch, M.A., Linder, P., Kovar-Eder, J. & Thiv, M. (2015) Biogeography of Mediterranean Hotspot Biodiversity: Re-Evaluating the 'Tertiary Relict' Hypothesis of Macaronesian Laurel Forests. *PLoS One*, **10**, e0132091.

Leache, A.D., Chavez, A.S., Jones, L.N., Grummer, J.A., Gottscho, A.D. & Linkem, C.W. (2015) Phylogenomics of phrynosomatid lizards: conflicting signals from sequence capture versus restriction site associated DNA sequencing. *Genome Biology Evolution*, **7**, 706-19.

Lerner, H. & Fleischer, R. (2010) Prospects for the Use of Next-Generation Sequencing Methods in Ornithology. *The Auk*, **127**, 4-15.

Lieberman, B.S. (2012) Adaptive Radiations in the Context of Macroevolutionary Theory: A Paleontological Perspective. *Evolutionary Biology*, **39**, 181-191.

López de Heredia, U. (2016) Las técnicas de secuenciación masiva en el estudio de la diversidad biológica. *Munibe Ciencias Naturales*, **64**, 7-31.

Losos, J.B. & Ricklefs, R.E. (2009) Adaptation and diversification on islands. *Nature*, **457**, 830-6.

Machado, A. (2006) The type material of the species of *Laparocerus* Schönherr, 1834 (Coleoptera, Curculionidae, Entiminae). *Journal of Natural History*, **40**, 2001-2055.

Machado, A. (2008) Three new endogean species of *Laparocerus* Schönherr, 1834 from the Canary Islands (Coleoptera, Curculionidae). *Journal of Natural History*, **42**, 1277-1288.

Machado, A. (2011) La morfología de *Laparocerus undatus* Wollaston, 1864 y consideraciones sobre la tribu Laparocerini Lacordaire, 1863 (Coleoptera, Curculionidae, Entiminae). *Graellsia*, **66**, 233-280.

Machado, A., Rodríguez-Expósito, E., López, M. & Hernandez, M. (2017) Phylogenetic analysis of the genus *Laparocerus*, with comments on colonisation and diversification in Macaronesia (Coleoptera, Curculionidae, Entiminae). *Zookeys*, **651**, 1-77.

Macías-Hernández, N., Bidegaray-Batista, L., Emerson, B.C., Oromí, P. & Arnedo, M. (2013) The imprint of geologic history on within-island diversification of woodlouse-hunter spiders (Araneae, Dysderidae) in the Canary Islands. *Journal of Heredity*, **104**, 341-56.

Mahler, D.L., Revell, L.J., Glor, R.E. & Losos, J.B. (2010) Ecological opportunity and the rate of morphological evolution in the diversification of Greater Antillean anoles. *Evolution*, **64**, 2731-45.

McCormack, J.E., Hird, S.M., Zellmer, A.J., Carstens, B.C. & Brumfield, R.T. (2013) Applications of next-generation sequencing to phylogeography and phylogenetics. *Molecular Phylogenetics and Evolution*, **66**, 526-38.

Moen, D. & Morlon, H. (2014) Why does diversification slow down? *Trends in Ecology and Evolution*, **29**, 190-197.

Morgan, W.J. (1971) Convection plumes in the lower mantle. *Nature*, **230**, 42-43.

Olson, M.E. & Arroyo-Santos, A. (2009) Thinking in continua: beyond the "adaptive radiation" metaphor. *Bioessays*, **31**, 1337-46.

Oromí, P., Zurita, N., Morales, H. & López, H. (2015) Diversidad de artrópodos terrestres en las Islas Canarias. *IDE@: Ibero Diversidad Entomológica @ccesible. Revista IDE@-SEA*, **4**, 1-14.

Osborn, H. (1902) The law of adaptive radiation. *American Naturalist*, **36**, 353-363.

Otto, R., Whittaker, R.J., von Gaisberg, M., Stierstorfer, C., Naranjo-Cigala, A., Steinbauer, M.J., Borregaard, M.K., Arévalo, J.R., Garzón-Machado, V., del Arco, M. & Fernández-Palacios, J.M. (2016) Transferring and implementing the general dynamic model of oceanic island biogeography at the scale of island fragments: the roles of geological age and topography in plant diversification in the Canaries. *Journal of Biogeography*, **43**, 911-922.

Papadopoulou, A. & Knowles, L.L. (2015a) Genomic tests of the species-pump hypothesis: Recent island connectivity cycles drive population divergence but not speciation in Caribbean crickets across the Virgin Islands. *Evolution*, **69**, 1501-1517.

Papadopoulou, A. & Knowles, L.L. (2015b) Species-specific responses to island connectivity cycles: refined models for testing phylogeographic concordance across a Mediterranean Pleistocene Aggregate Island Complex. *Molecular Ecology*, **24**, 4252-68.

Parent, C.E., Caccone, A. & Petren, K. (2008) Colonization and diversification of Galapagos terrestrial fauna: a phylogenetic and biogeographical synthesis. *Philosophical Transactions of the Royal Society B: Biological Sciences*, **363**, 3347-61.

Patiño, J., Carine, M., Mardulyn, P., Devos, N., Mateo, R.G., González-Mancebo, J.M., Shaw, A.J. & Vanderpoorten, A. (2015) Approximate Bayesian Computation Reveals the Crucial Role of Oceanic Islands for the Assembly of Continental Biodiversity. *Systematic Biologists*, **64**, 579-589.

Patiño, J., Whittaker, R.J., Borges, P.A.V., Fernández-Palacios, J.M., Ah-Peng, C., Araújo, M.B., Ávila, S.P., Cardoso, P., Cornuault, J., de Boer, E.J., de Nascimento, L., Gil, A., González-Castro, A., Gruner, D.S., Heleno, R., Hortal, J., Illera, J.C., Kaiser-Bunbury, C.N., Matthews, T.J., Papadopoulou, A., Pettorelli, N., Price, J.P., Santos, A.M.C., Steinbauer, M.J., Triantis, K.A., Valente, L., Vargas, P., Weigelt, P. & Emerson, B.C. (2017) A roadmap for island biology: 50 fundamental questions after 50 years of The Theory of Island Biogeography. *Journal of Biogeography*, **44**, 963-983.

Pestano, J. & Brown, R.P. (1999) Geographical structuring of mitochondrial DNA in Chalcides sexlineatus within the island of Gran Canaria. *Proceedings of the Royal Society of London*, **266**, 805-812.

Peterson, B.K., Weber, J.N., Kay, E.H., Fisher, H.S. & Hoekstra, H.E. (2012) Double digest RADseq: an inexpensive method for de novo SNP discovery and genotyping in model and non-model species. *PLoS One*, **7**, e37135.

Potter, S., Bragg, J.G., Peter, B.M., Bi, K. & Moritz, C. (2016) Phylogenomics at the tips: inferring lineages and their demographic history in a tropical lizard, Carlia amax. *Molecular Ecology*, **25**, 1367-80.

Price, J.P. & Clague, D.A. (2002) How old is the Hawaiian biota? Geology and phylogeny suggest recent divergence. *Proceedings of the Royal Society of London. Series B, Biological sciences*, **269**, 2429-35.

Rijsdijk, K.F., Hengl, T., Norder, S.J., Otto, R., Emerson, B.C., Ávila, S.P., López, H., van Loon, E.E., Tjørve, E., Fernández-Palacios, J.M. & Heaney, L. (2014) Quantifying surface-area changes of volcanic islands driven by Pleistocene sea-level cycles: biogeographical implications for the Macaronesian archipelagos. *Journal of Biogeography*, **41**, 1242-1254.

Roderick, G.K. & Gillespie, R.G. (1998) Speciation and phylogeography of Hawaiian terrestrial arthropods. *Molecular Ecology*, **7**, 519-531.

Rundell, R.J. & Price, T.D. (2009) Adaptive radiation, nonadaptive radiation, ecological speciation and nonecological speciation. *Trends in Ecology and Evolution*, **24**, 394-9.

Sanger, F., Nickelsen, C. & Coulson, R. (1977) DNA sequencingwithchain-terminatinginhibitors. *Proceedings of the National Academy of Sciences*, **74**, 5463-5467.

Sanmartín, I., van der Mark, P. & Ronquist, F. (2008) Inferring dispersal: a Bayesian approach to phylogeny-based island biogeography, with special reference to the Canary Islands. *Journal of Biogeography*, **35**, 428-449.

Schimincke, H.U., Sumita, M. & Funck, T. (Sept. 1997) Growth and destruction of Gran Canaria: evidence from land studies, bathymetry, offshore seismic studies and drilling during ODP Leg 157. *International workshop on Immature Oceanic Islands* (ed by, pp. 11-12. La Palma.

Shendure, J., Mitra, R.D., Varma, C. & Church, G.M. (2004) Advanced sequencing technologies: methods and goals. *Nature Reviews Genetics*, **5**, 335-44.

Simoes, M., Breitkreuz, L., Alvarado, M., Baca, S., Cooper, J.C., Heins, L., Herzog, K. & Lieberman, B.S. (2016) The Evolving Theory of Evolutionary Radiations. *Trends in Ecology & Evolution*, **31**, 27-34.

Simpson, G.G. (1953) *The major features of evolution*. Columbia University Press, Columbia.

Sundseth, K. (2005) *Natura 2000 in the Macaronesian region*. European Commision, Luxembourg.

Thomson, R.C., Wang, I.J. & Johnson, J.R. (2010) Genome-enabled development of DNA markers for ecology, evolution and conservation. *Molecular Ecology*, **19**, 2184-95.

van den Bogaard, P. (2013) The origin of the Canary Island Seamount Province - new ages of old seamounts. *Scientific Reports*, **3**, 2107.

van Dijk, E.L., Auger, H., Jaszczyszyn, Y. & Thermes, C. (2014) Ten years of next-generation sequencing technology. *Trends in Genetics*, **30**, 418-26.

Vandergast, A.G., Gillespie, R.G. & Roderick, G.K. (2004) Influence of volcanic activity on the population genetic structure of Hawaiian Tetragnatha spiders: fragmentation, rapid population growth and the potential for accelerated evolution. *Molecular Ecology*, **13**, 1729-43.

Warren, B.H., Simberloff, D., Ricklefs, R.E., Aguilee, R., Condamine, F.L., Gravel, D., Morlon, H., Mouquet, N., Rosindell, J., Casquet, J., Conti, E., Cornuault, J., Fernandez-Palacios, J.M., Hengl, T., Norder, S.J., Rijsdijk, K.F., Sanmartin, I., Strasberg, D., Triantis, K.A., Valente, L.M., Whittaker, R.J., Gillespie, R.G., Emerson, B.C. & Thebaud, C. (2015) Islands as model systems in ecology and evolution: prospects fifty years after MacArthur-Wilson. *Ecology Letters*, **18**, 200-17.

Weigelt, P., Steinbauer, M.J., Cabral, J.S. & Kreft, H. (2016) Late Quaternary climate change shapes island biodiversity. *Nature*, **532**, 99-102.

Weir, J.T., Haddrath, O., Robertson, H.A., Colbourne, R.M. & Baker, A.J. (2016) Explosive ice age diversification of kiwi. *Proceedings of the National Academy of Sciences*, **113**, E5580-E5587.

Whittaker, R.J. & Fernandez-Palacios, J.M. (2007) *Island Biogeography: Ecology, Evolution, and Conservation*. Oxford University Press, Oxford, UK.

Whittaker, R.J., Triantis, K.A. & Ladle, R.J. (2008) A general dynamic theory of oceanic island biogeography. *Journal of Biogeography*, **35**, 977-994.

Wilson, J.T. (1963) A possible origin of the Hawaiian islands. *Canadian Journal of Physics*, **41**, 863-870.

Wright, S. (1931) Evolution in Mendelian populations. *Genetics*, **16**, 97-159.

Xu, P., Xu, S., Wu, X., Tao, Y., Wang, B., Wang, S., Qin, D., Lu, Z. & Li, G. (2014) Population genomic analyses from low-coverage RAD-Seq data: a case study on the non-model cucurbit bottle gourd. *Plant Journal*, **77**, 430-42.

Yoder, A.D., Campbell, E.O., Blanco, M.B., dos Reis, M., Ganzhorn, J.U., Goodman, S.M., Hunnicutt, K.E., Larsen, P.A., Kappeler, P.M., Rasoloarison, R.M., Ralison, J.M., Swofford, D.L. & Weisrock, W. (2016) Geogenetic patterns in mouse lemurs (genus Microcebus) reveal the ghosts of Madagascar's forests past. *Proceedings of the National Academy of Sciences*, **113**, 8049-8056.

Zhang, J., Heshan, L., Balaji, P. & Feng, W. (2013) Optimizing Burrows-Wheeler Transform-Based Sequence Alignment on Multicore Architectures. In: *Cluster, Cloud and Grid Computing (CCGrid), 13th IEEE/ACM International Symposium*, pp. 377-384, IEEE.

Zhang, W., Chen, J., Yang, Y., Tang, Y., Shang, J. & Shen, B. (2011) A practical comparison of de novo genome assembly software tools for next-generation sequencing technologies. *PLoS One*, **6**, e17915.

CHAPTER I

Evidence for mega-landslides as drivers of island colonisation

Chapter published

García-Olivares, V., López, H., Patiño, J., Álvarez, N., Machado, A., Carracedo, J.C., Soler, V. & Emerson, B.C. (2017) Evidence for mega-landslides as drivers of island colonization. *Journal of Biogeography*, **44**, 1053-1064.

Evidence for mega-landslides as drivers of island colonisation

Abstract

Aim: How non-dispersive taxa colonise islands is generalised as being by wind, or rafting, with the implicit assumption that such events involve one (wind) or a few (rafting) individuals. However, because of the evolutionary timescale for colonisation events, the fit of individual species to a conceptual model of wind or rafting is difficult to assess. Here we describe an alternative testable geological model for inter-island colonisation that can result in larger effective founding population sizes than traditionally accepted colonisation mechanisms. We then test for the fit of genetic data to this model using weevils from the *Laparocerus tessellatus* species complex.

Location: Canary Islands.

Methods: Using a combination of geological data for the Canary Islands, and mtDNA data from a weevil radiation within the Canary Islands, we test three species-level predictions for mega-landslides as drivers of oceanic rafting between islands and subsequent speciation: (i) colonisation should involve multiple female lineages: (ii) founding lineages should have a common geographic origin, consistent with a mega-landslide event, and: (iii) colonisation direction should be consistent with ocean currents.

Results: Both individual-level and population-level analyses support a mega-landslide event as the driver of colonisation from the island of Tenerife to La Palma. At least four female lineages colonised La Palma from Tenerife, with the geographic range of ancestral sequences to these four lineages describing the limits of the La Orotava mega-landslide in Tenerife.

Main conclusions: In the context of island biogeographic theory, mega-landslides may be an important driver of colonisation, and subsequent lineage diversification. They provide a framework for hypothesis testing using genetic data from species, or closely related species, with ranges that encompass landslides and potential areas of colonisation.

Introduction

Our understanding of speciation within oceanic archipelagos has advanced considerably in recent decades (Warren *et al.*, 2015), in large part as a consequence of continued efforts to analyse phylogenetic data from a diversity of taxa with geographical, ecological and geological data. In contrast, there has been little investigation of the mechanisms promoting dispersal among islands within an archipelago, a process that underpins island biogeographic theory (MacArthur & Wilson, 1963, 1967). Dispersal from one island to another must be either airborne or waterborne. For invertebrate taxa, which typically comprise the dominant component of species richness on oceanic islands, airborne colonisation may involve secondary transport by birds, or wind. Secondary transport by birds is likely important for ectoparasitic invertebrate taxa, or non-ectoparasitic taxa transported through ingestion (e.g. Wada *et al.*, 2011). However, transport by ingestion is unlikely to account for more than a very small proportion of invertebrate species, and likely limited to those that feed within seeds (Gillespie *et al.*, 2012). Windborne colonisation should be important for flighted invertebrates, but less consequential for flightless invertebrates. Unless windborne colonisation involves a gravid female, a female with stored sperm, or a parthenogenetic individual, colonisation would not be followed by establishment, as it is unlikely that wind-transported individuals would arrive within the geographic proximity of each other required for subsequent mating. Even allowing for the colonisation of a multiply mated female, successful establishment of a windborne colonist could be challenging due to low genetic variation and inbreeding, although this is not always the case (e.g., see Edelaar *et al.*, 2015). In contrast to windborne dispersal, colonisation by oceanic rafting may result in multiple individuals arriving, but is expected to involve a limited number of individuals of coastal or riverine affinity (Gillespie *et al.*, 2012). Thus, the conceptual model of colonisation by wind or rafting is expected to result in extreme founder events, something seen as a potential driver of insular speciation (Carson & Kaneshiro, 1976; Templeton, 1980, 2008). It is also expected to be mostly relevant for flighted species, or flightless species with coastal distributions, or with freshwater connections to the coast. Colonisation by non-coastal flightless species is harder to explain.

In their consideration of long distance dispersal (i.e. from continents to archipelagos), Gillespie *et al.* (2012) point out that the ability of organisms to disperse by oceanic drift, or rafting on flotsam, is a function of the interaction of four variables: (i) ocean dynamics, (ii) survival *en route*, (iii) geomorphology and (iv) proximity to the ocean, given that rafts are initiated from areas proximate to oceans. With regard to ocean dynamics, although they may vary through geological time, they are idiosyncratic in nature and island or archipelago specific. However, the remaining three points suggest oceanic drift or rafting may be very consequential at the inter-island scale. Regarding point (ii), the comparatively short distances between islands must greatly increase survival probability, compared to the long distances that typically characterise continental source areas and isolated oceanic archipelagos. With regard to points (iii) and (iv), oceanic island geomorphology provides for periodic, expected and large-scale deposition of biota into the ocean, spanning large altitudinal ranges, through mega-landslide events. This has the potential to promote the synchronous rafting of individuals sampled across broad geographic areas, something that could result in much larger effective founding population sizes than traditionally accepted colonisation mechanisms.

Biotic consequences of volcanic flank collapse

When volcanic edifices reach high altitudes from the ocean floor they are prone to suffer flank collapses for several reasons, principally gravitational instability, volcanic or tectonic seismicity, and dyke injections (McGuire, 2003). Areas in excess of hundreds of km^2 can be affected, with flank collapse triggering substantial down slope movement of terrain, movements that can occur in only a few minutes at calculated velocities exceeding 100 km/h (Siebert, 1984). These mega-landslide events can generate ocean floor deposits of hundreds of km^2, measuring hundreds of km in length, involving volumes in the order of thousands of km^3 (Canals *et al.*, 2000). Such mega-landslides are not infrequent events, as revealed by terrestrial geological studies, sonar, three-dimensional bathymetry, offshore seismic analysis, and even historical records (e.g. Ward & Day, 2003). There is both inland and sea floor evidence for numerous mega-landslides in the Hawaiian Islands (e.g. Moore *et al.*, 1994), Canary Islands (e.g. Carracedo *et al.*, 2009), Réunion (e.g. Oehler *et al.*, 2004), French Polynesian Islands (e.g. Clément *et al.*, 2002), Tristan da Cunha Island (e.g.

Holcomb & Searle, 1991), Cape Verde Islands (e.g. Masson *et al.*, 2008) and the Lesser Antilles Islands (e.g. Samper *et al.*, 2008), among others. The most detailed long-term data on flank collapses within an archipelago comes from a 17 Ma (million years) record for the Canary Islands. Hunt et al. (2014) reveal that the mean recurrence of landslides across the Canary Islands over the last 17 Ma is 135 ka (thousand years), with the last 7 Ma characterised by a similar mean recurrence of 135 ka.

Within the Canary Islands the biggest recorded mega-landslides occurred on the island of Tenerife, with 11 documented events that affected vast areas of the island, in some cases from more than 2000 macsl (metres above current sea level) to the coast, resulting in the transfer of enormous debris deposits to the seafloor (Fig. 1, Table S1.1 in Appendix S1 in Supporting Information). While many landslides have been overwritten by subsequent lava deposits, the Orotava and Güímar valleys present clear evidence, with flat floors flanked by steep scarps defining most of their perimeter (Masson *et al.*, 2002). The within island evolutionary significance of such landslides is well understood, as they have produced important habitat discontinuities implicated in divergent evolution between populations on opposing flanks (e.g. Brown *et al.*, 2006; Macías-Hernández *et al.*, 2013; Mairal *et al.*, 2015), the biogeographic relevance of which has also been recognised (Whittaker *et al.*, 2008). What is less understood is the fate of the vast biomass that was deposited into the ocean.

The landslide of La Orotava was initiated at sea level, followed by the rapid downslope movement of higher altitude terrains up to several hundred meters deep. During the subaerial phase of this process, maximum terrain destruction occurs at depth, with limited transformation of the surface, meaning that surface organic material likely remains relatively intact prior to entering the ocean. An obvious consequence of this dynamic would be the flotation of organic matter, derived from more than 100 km^2 of diverse habitat, from the coastline to altitudes exceeding 2000 macsl (Fig. 2). Oceanic rafting on this scale, with favourable ocean currents, could potentially favour the synchronous transport of many individuals to neighbouring islands, providing a suitable scenario for testable predictions.

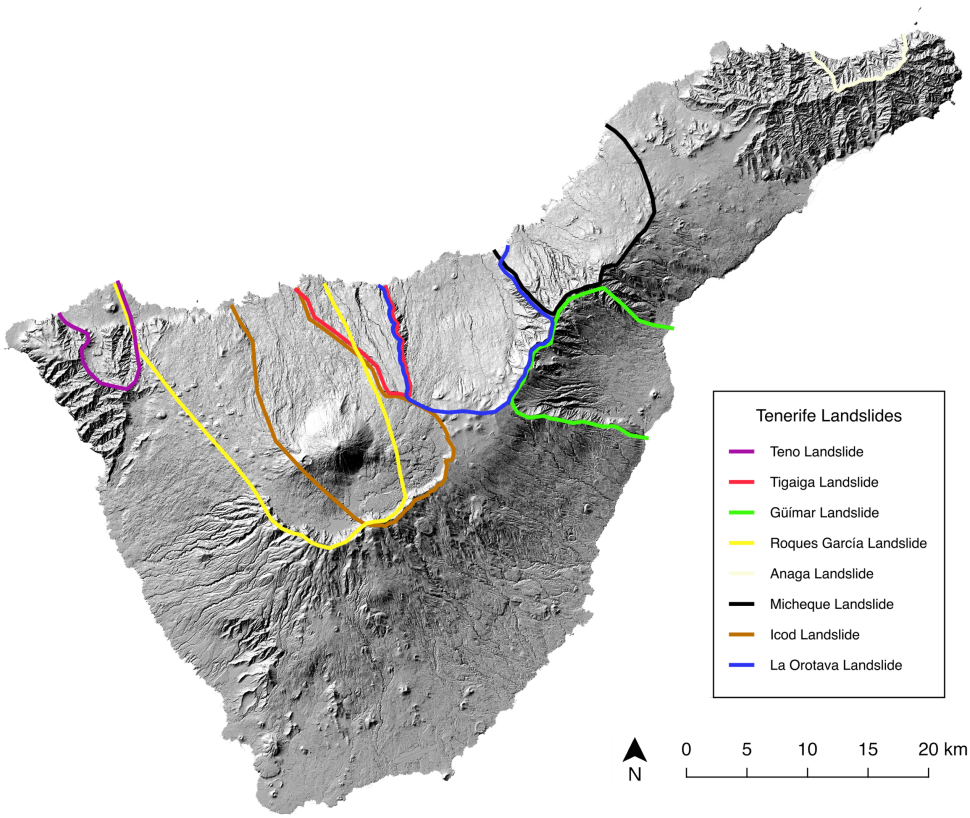

Figure 1. Mega-landslides on the island of Tenerife. Seven of the 11 documented landslides are sufficiently unaffected by subsequent volcanic activity to be able to identify their geographic limits. Landslides are colour-coded according to the inset that provides approximate ages for each mega-landslide. See Table S1.1 in Appendix S1 for more details.

Predictions for colonisation from a mega-landslide

Three testable predictions can be made for the colonisation of an invertebrate species originating from a mega-landslide. The first is that colonisation should have involved multiple female lineages. The second is that founding lineages should share a common geographic origin that is spatially consistent with a mega-landslide event. The third is that colonisation direction should be consistent with ocean currents. Here we evaluate evidence for these predictions using mtDNA sequence data for a complex of flightless beetle species on the Canary Islands. Among the more than 128 species within the weevil genus *Laparocerus* in the Canary Islands, the *L. tessellatus* complex comprises 11 taxonomically described species, each being a single island endemic. A recent molecular genetic analysis of the complex (Faria *et al.*, 2016) sampled nine species (two new species were subsequently described by Machado, 2016) revealed complex relationships among

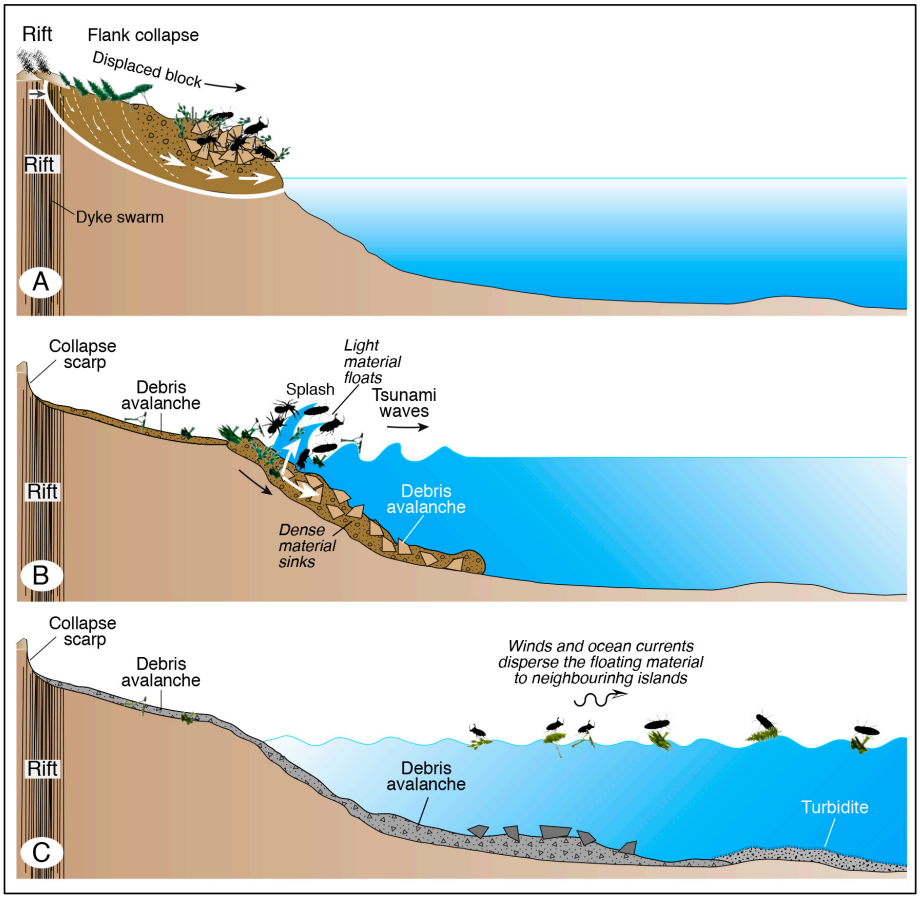

Figure 2. Biotic consequences of a volcanic flank collapse. (A) Flank collapse is initiated near sea-level, causing the downslope movement of a block of terrain. The surface of the affected terrain suffers limited transformation, with maximum transformation occurring along the sliding plane. (B) A consequence of the dynamic described in A is that much of the organic surface layer may enter in the ocean practically intact, with a high proportion remaining on the surface due to its high floatability. (C) The ocean surface will contain a vast amount of organic debris derived from the surface of the landslide, including living animals and plant material. This flotsam, together with favourable winds and marine currents, would favour the dispersal of animals and plant species between islands.

individual-level patterns of nuclear and mtDNA sequence relatedness, and taxonomy (see Faria *et al.*, 2016 for details). Of relevance to the above-mentioned predictions, it was revealed that the single species from the island of La Palma was founded by individuals of related species from the islands of Tenerife and Gran Canaria (Faria *et al.*, 2016). In the case of Tenerife, two founding mtDNA haplotypes to La Palma were inferred from sequences sampled from several localities above the steep scarps defining the perimeter of the Orotava valley. This provides a minimum estimate of two colonising female lineages, and is suggestive of a possible role for the La Orotava mega-landslide. We evaluate this hypothesis by sampling the *L. tessellatus* complex to specifically test the prediction of multiple founding female lineages to La Palma from the region of the

Orotava valley. We use DNA sequence data from the mitochondrial genome, as its characteristic female inheritance and absence of recombination allows for robust inferences of the minimum number of founding female lineages through the reconstruction of coalescent ancestry.

Materials and Methods

Sampling and laboratory procedures

We increased previous geographic sampling for the *L. tessellatus* complex (Faria *et al.*, 2016) by visiting collecting localities for species of the *L. tessellatus* complex within the collection of AM, and several other new localities. From two to five individuals were sequenced from each locality on the island of Gran Canaria. As our focus is on the mtDNA relatedness between La Palma and Tenerife, we took an iterative approach to sequencing. Two individuals from each sampling locality were sequenced in the first instance for the mtDNA COII gene region for joint analysis with published data (Faria *et al.*, 2016). Localities in Tenerife yielding mtDNA sequences closely related to La Palma were then sequenced for a further three individuals (unless limited by sample numbers). Similarly, all localities in La Palma with mtDNA sequences closely related to sequences from Tenerife were sequenced for a further three individuals. Total genomic DNA was extracted from the two hind legs using a Chelex extraction protocol (Casquet *et al.*, 2012). The mitochondrial COII gene was amplified using previously described conditions (Faria *et al.*, 2016) and sequenced using the Sanger DNA sequencing service of Macrogen (www.macrogen.com). Sequences were edited with Geneious R8 8.0.3 (http://geneious.com, Kearse *et al.*, 2012), aligned using MEGA 6.06 (Tamura *et al.*, 2013), and unique haplotypes were collapsed Fabox 1.41 (Villesen, 2007).

Haplotype network and Bayesian phylogenetic tree construction

Statistical parsimony was used to infer a haplotype network using PopART (Leigh & Bryant, 2015). Predictions from coalescent theory, related to the frequency and geographical

distribution of haplotypes, are often applied to resolve reticulations within haplotype networks (Posada & Crandall, 2001). However, the strong geographic structuring of mtDNA variation within the *L. tessellatus* complex (Faria *et al.*, 2016) precludes the use of probability-based predictions derived from coalescent theory to solve reticulations (Posada & Crandall, 2001). We therefore used an alternative probability-based approach where, for each reticulation, we evaluated alternative solutions under an appropriate model of DNA sequence evolution. This was achieved by constructing a Bayesian tree from the sequence data with MrBayes v3.2.5 (Ronquist, 2012) under a general time reversible model of sequence evolution with a gamma correction (GTR+G) without modelling invariant sites (I), as in Faria *et al.* (2016). Four analyses were each run for 100 million generations using 4 MCMC (Markov chain Monte Carlo) chains, starting from a random tree, and sampling trees every 1000 generations. For both the network and Bayesian analyses a sequence from the closely related species *L. vicinus* was used as an outgroup. Stationarity and convergence of the chains were determined by graphical inspection of the values of the log-likelihoods of the four MCMC analyses; confirmation that the average standard deviation of split frequencies was below 0.01 at the completion of the analysis; and verification that effective sample size (ESS) values were above 200 using the log files in Tracer 1.6 (Rambaut, 2016). A burn-in of 25% was removed from each run, and the remaining trees were used to construct a majority-rule consensus tree.

Minimum estimation of founding female lineages

We used a rooted haplotype network of geographically referenced mtDNA sequences, to infer the dispersal history of maternal lineages (e.g. Emerson *et al.*, 2006). The rooted mtDNA haplotype network was used to estimate the minimum number of mtDNA haplotypes that are, or have been, shared between islands, with the direction of dispersal inferred from the order of geographic state change from the root of the network (Fig. 3). This provides a minimum estimate of the number of female lineages that have dispersed between islands. One or more geographic states (islands) can be assigned to each sampled haplotype, and on the basis of these known states, one can infer the geographic states of missing (extinct or unsampled) haplotypes within the network. We inferred

haplotype sharing (female dispersal) either (i) directly, when a sampled haplotype had two geographic states (Fig. 3A), or (ii) indirectly, when the geographic state changed between an ancestral and descendent haplotype (Fig. 3B-F).

Analyses of population structure

We defined three geographic regions based upon the relatedness of mtDNA haplotypes between La Palma and Tenerife. The first region consists of all sites on La Palma sampled for mtDNA lineages derived from Tenerife. The second region is a polygon describing the minimum geographic range of mtDNA haplotypes and their descendants from Tenerife that are ancestral to La Palma haplotypes. To construct the polygon we applied an iterative approach, using the minimum convex polygon method (Mohr, 1947). In a first iteration, a polygon describing the geographic range of this group of haplotypes was constructed. Subsequent iterations removed haplotypes from populations at the periphery of the polygon if they were also present within interior population, until no more haplotypes could be removed. The third region comprises the remaining sampling sites on Tenerife that fall outside the polygon.

To test whether the distribution of mtDNA genetic diversity reveals a phylogeographic pattern within the *L. tessellatus* complex distributed across the three regions, genetic differentiation among populations was estimated using both F_{ST} (genetic distance among haplotypes is unweighted) and N_{ST} (genetic distance among haplotypes is weighted). When mutation rate exceeds dispersal rate, haplotypes within regions will be more closely related than haplotypes compared among regions (Pons & Petit, 1996). Under these conditions N_{ST} will exceed F_{ST}, indicating a greater role of mutation and the phylogeographic structuring of genetic variation over evolutionary time scales, compared to the structuring of genetic variation by gene flow and genetic drift over ecological time scales. To test whether N_{ST} was significantly higher than F_{ST}, a randomization procedure permuting haplotype assignation in the matrix of genetic distances among haplotypes was performed and repeated 10,000 times in SPaGeDi 1.4b (Hardy & Vekemans, 2002).

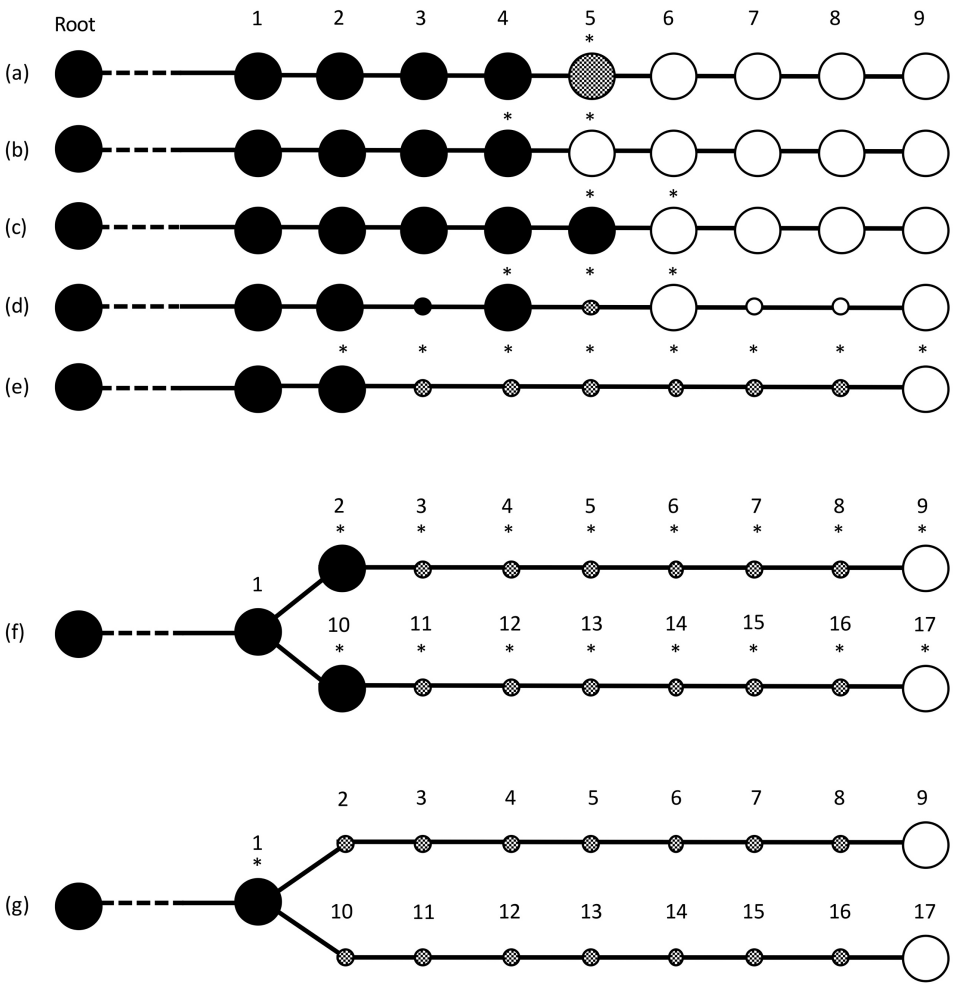

Figure 3. Inferring sets of potential colonist (geographically shared) haplotypes, and the minimum number of colonising haplotypes. Haplotypes from an ancestral island (X) are represented as black filled circles. Haplotypes from a colonised island (Y) are represented as white filled circles. Haplotypes found on both X and Y are shown in hatching. Large circles represent sampled haplotypes. Small circles represent missing (extinct or unsampled) haplotypes, whose *potential* geographic states are inferred based on the known geographic states of immediately ancestral and descendent sampled haplotypes. For each of the scenarios A-G, asterisks indicate the set of haplotypes from which a minimum of one haplotype is inferred to have colonised from X to Y. (A) represents no haplotype extinction and sampling of all haplotypes, while C-E represent the same scenario but with some extinct or unsampled haplotypes, while F-G represent alternative scenarios with coalescence. (A) 5 is identified as the colonising haplotype as it is shared across both islands. (B) Either 4 or 5 is the colonising haplotype: 4 colonised Y and is unsampled or extinct on Y, or 5 colonised Y and is unsampled or extinct on X. (C) Either 5 or 6 is the colonising haplotype: 5 colonised Y and is unsampled or extinct on Y, or 6 colonised Y and is unsampled or extinct on X. (D) Either 4, 5 or 6 is the colonising haplotype: 4 colonised Y and is unsampled or extinct on Y, or 5 colonised Y and is unsampled or extinct on both islands, or 6 colonised Y and is unsampled or extinct on X. (E) Any of haplotypes 2-9 may have colonised from X to Y: 2 colonised Y and is unsampled or extinct on B, or one of haplotypes 3-8 colonised Y and is unsampled or extinct on both islands, or 9 colonised Y and is unsampled or extinct on X. (F) At least two colonising haplotypes are inferred, due to the sampling of haplotypes 2 and 10 on X, with a minimum of one shared haplotype between haplotypes 2-9, and the other between 10-17. (G) Similar to F, but unsampled or extinct haplotypes 2 and 10 result in a minimum inference of 1 colonising haplotype.

Results

Haplotype network and Bayesian phylogenetic tree

Forty-seven sites were sampled in Tenerife, 32 in La Palma, and 21 in Gran Canaria (Fig. 4, Table S2.2 in Appendix S2). A total of 255 new individuals were sequenced, yielding 394 DNA sequences together with previously published sequences (Faria *et al.*, 2016). DNA sequences were collapsed to 195 unique haplotypes, characterised by 164 polymorphic sites across 633 bp, 127 of which were parsimony informative. A single haplotype network was obtained from the statistical parsimony analysis, with a total of 44 reticulations, of which all but two were solved with the Bayesian phylogenetic reconstruction (Fig. S2.1 in Appendix S2). The resolved network (Fig. 5) thus presents comparable geographic clusters of sequences, branching relationships among them, and root location, as those obtained in the Bayesian phylogenetic analysis (Fig. S2.1 in Appendix S2).

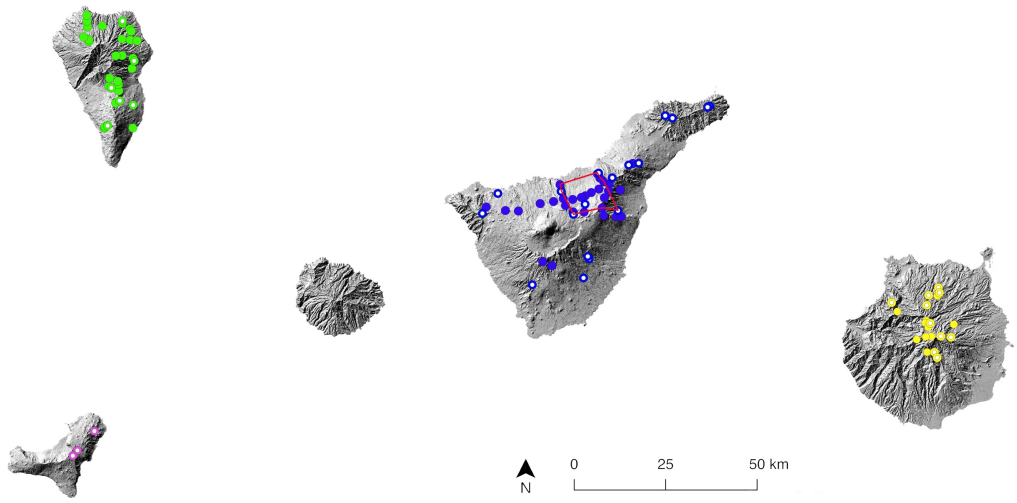

Figure 4. Map of sampling sites for the *Laparocerus tessellatus* complex. The eleven taxonomically defined species within the complex are all single island endemics. Gran Canaria (5 species): *L. microphthalmus* Lindberg, 1950, *L. obsitus* Wollaston, 1864, *L. osorio* Machado, 2012, *L. tirajana* Machado, 2012, and *L.* sp. aff. *tirajana*. Tenerife (4 species) *L. tessellatus* (Brulle, 1839), *L. freyi* Uyttenboogaart, 1940, *L. punctiger* Machado, 2016, and *L. canescens* Machado, 2016. La Palma (1 species): *L. auarita* Machado, 2016. El Hierro (1 species): *L. bimbache* Machado, 2011. Sampling sites are colour coded to be consistent with island colour coding in Figure 5 and Figure S1. Geographic coordinates of sampling sites, and the taxonomic species assignment of samples from each location are provided in Table S2.2 in Appendix 2. Also shown is a polygon describing the minimum geographic range of mtDNA haplotypes and their descendants from Tenerife that are ancestral to La Palma haplotypes (see text). Sampling sites from Faria *et al.* (2016) are indicated with a white dot inside the coloured circle.

Number and origin of founding female lineages from Tenerife to La Palma

The rooted haplotype network reveals that the mtDNA variation of the *L. tessellatus* complex across the four islands has involved the establishment of at least 11 female lineages by inter-island colonisation (Fig. 5). Our sampling reveals a total of six colonising haplotypes to the island of La Palma, doubling a previous estimate (Faria *et al.*, 2016), of which two are derived from Gran Canaria, with the remaining four derived from Tenerife. Twenty mtDNA haplotypes from Tenerife were identified either as ancestral to La Palma (2), or derived from ancestral haplotypes (18) by no more than 4 mutations (Fig. 5) and were sampled from 18 of the 47 sampling sites. For ease of understanding we refer to these as TF-LP haplotypes. The mean divergence between the 18 derived TF-LP haplotypes and the most closely related sampled or unsampled ancestral haplotype was 1 mutation. A polygon describing the minimum geographic range of the 20 TF-LP haplotypes was arrived at after 4 iterations, and included a total of 18 sampling sites, 14 of which contain TF-LP haplotypes, which broadly describes the Orotava valley (Fig. 4). All but two of the 18 sites are above the steep escarpments or within the Orotava valley, with the remaining two sites on the geographically proximate southern slope of the Güímar valley. The 18 sampling sites within the polygon were sampled for a total of 80 individuals, of which 49 presented a TF-LP haplotype, with the remaining 31 presenting one of the 18 other haplotypes sampled within this region. The remaining 29 Tenerife sampling sites outside the polygon were sampled for a total of 89 individuals and 39 haplotypes.

The global N_{ST} of 0.34 is significantly higher ($P<0.001$) than the global F_{ST} of 0.03 ($P<0.001$), indicating the dominant role of geographic isolation and mutation over gene flow and genetic drift for the structuring of genetic variation across the three regions. All pairwise F_{ST} and N_{ST} comparisons are significantly different from zero and N_{ST} were consistently significantly higher than F_{ST} ($P<0.001$; Table 1). The two regions of Tenerife are the least differentiated from each other. La Palma is similarly differentiated from the Orotava valley and all other Tenerife sampling sites for F_{ST} (0.04 for both), but less differentiated from the polygon representing the Orotava valley for N_{ST} (0.38 from the Orotava valley and 0.45 from the rest of Tenerife). Thus, mtDNA variation in La Palma is less differentiated from mtDNA variation in the Orotava valley than it is from the rest of

Tenerife, supporting the hypothesis that the Orotava valley is the source area for individuals that colonised La Palma.

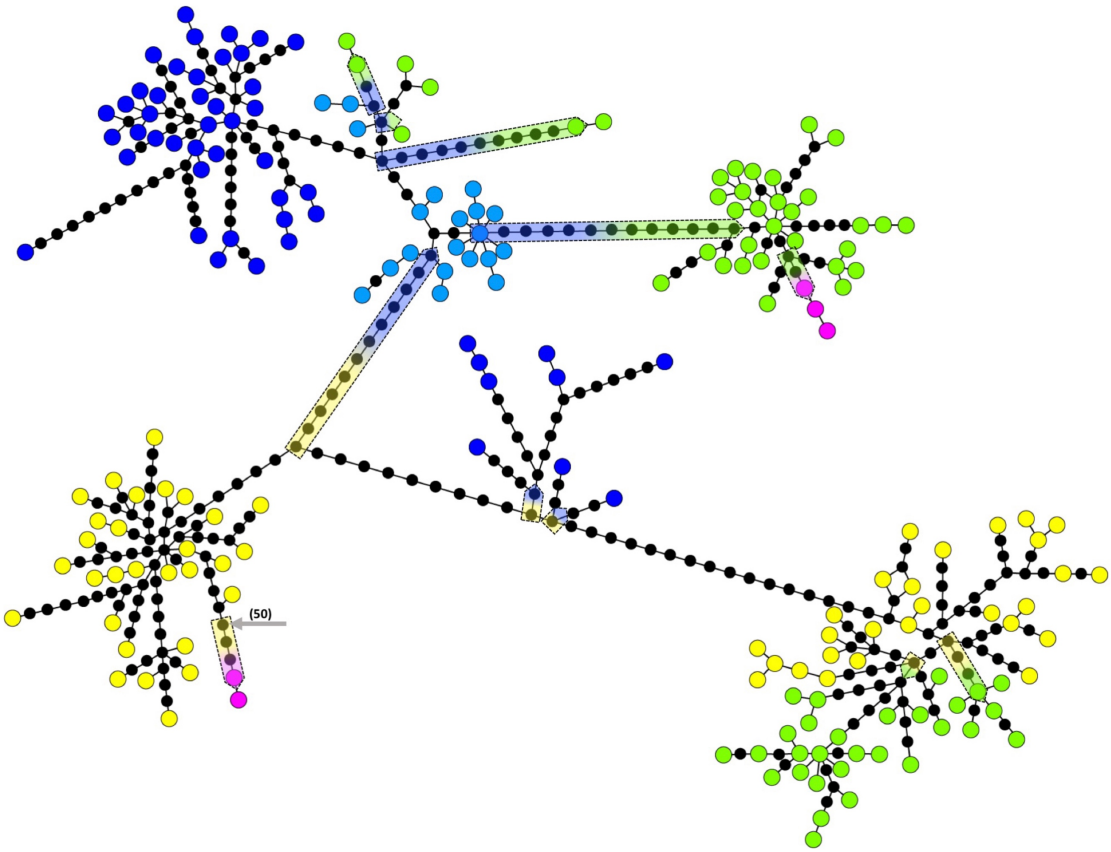

Figure 5. Haplotype network. A resolved haplotype network representing the relationships among 195 mtDNA haplotypes obtained from 633 bp of mtDNA sequence data for the COII gene for 396 individuals of the *Laparocerus tessellatus* complex. Haplotypes are colour coded with respect to island: yellow - Gran Canaria, blue - Tenerife, green - La Palma, pink - El Hierro. Haplotypes from Tenerife that are ancestral to La Palma, or closely related to haplotypes that are ancestral to La Palma (referred to as TF-LP haplotypes in the text), are shown in light blue. Extinct or unsampled haplotypes are shown as small black filled circles. The grey arrow indicates the most recent common ancestral haplotype of the complex, determined by rooting with the closely related species *L. vicinus* Lindberg, 1953. Coloured pointed rectangles represent sets of potential ancestral haplotypes, from which at least one haplotype colonised a new island, with colonisation direction indicated by a colour gradient and pointed end to the rectangle (see Figure 3)

Discussion

In support of predictions one and two, we find that multiple founding individuals to La Palma share a common geographic origin consistent with the mega-landslide event of the Orotava valley. Marine currents between Tenerife and La Palma provide support for

prediction three. The Canary Current is estimated to have been relatively unchanged over the past 22 Ma, passing southward along the northwest African coast, until reaching the Canary Islands, the geomorphology of which forces it to pass among the islands. Of particular relevance is the trade wind season which results in currents that flow to the south between islands, but also an offshore current that swings around the archipelago (Mittelstaedt, 1991), providing a connection between Tenerife and La Palma. The Canary Current has an estimated flow speed of 10-30 $cm \cdot s^{-1}$ (Wooster *et al.*, 1976), suggesting that the offshore current would carry floating organic material deposited from the Orotava valley over the minimum distance of 120 km between the coast of La Orotava and the coast of La Palma in a period between 4 and 13 days.

Table 1. Pairwise F_{ST} (below) and N_{ST} (above) values calculated using mtDNA COII sequence data for the *Laparocerus tessellatus* complex sampled from the Orotava Valley, Tenerife (excluding the Orotava valley) and La Palma. P-values indicate the probability that F_{ST} is significantly different from zero after 10.000 permutations of specimens among the three regions. P-values for N_{ST} indicate the probability that N_{ST} is significantly different from F_{ST} after 10.000 permutations of the matrix of genetic distances among haplotypes.

	Orotava Valley	Tenerife	La Palma
Orotava Valley	-	0.130***	0.377***
Tenerife	0.022***	-	0.452***
La Palma	0.042***	0.041***	-

***P < 0.001.

Mega-landslide, or small raft?

Rafts of vegetation are recognised as an important mechanism for the arrival of species to oceanic islands from more distant continental source areas, and rafts of a similar nature are also likely to play a role in inter-island colonisation. However, as highlighted by Gillespie et al. (2012), such rafts will be initiated from areas proximate to oceans (e.g. coastal areas, or upriver), and are thus more relevant for flora and fauna of coastal or riverine affinity. The *L. tessellatus* complex in Tenerife is typical of altitudes between 764 macsl and 1424 macsl (first and third quartiles of species distribution records), and is rarely observed below an altitude of 300 macsl (see Appendix S3), meaning that transportation by rafts, in the classical sense of coastal or freshwater origin, is

improbable. In contrast, a landslide event on the scale of that forming the Orotava Valley would yield rafting organic matter from higher altitudes (Fig. 2). There is little direct data on what would happen to this organic matter once it enters the sea, but an important insight comes from the eruption of Mount St. Helens in May 1980. The eruption itself was preceded, and probably in part promoted, by a mega-landslide that carried tens of thousands of trees into Spirit Lake, where a giant log raft formed and persisted for years (Coffin, 1983; see Appendix S3). The behaviour of the Mount St. Helens landslide highlights the potential for large scale oceanic rafting of organic material derived from a mega-landslide. For the Orotava landslide, the estimated surface area 136 km^2 (Table S1.1 in Appendix S1), would have contributed many millions of individual plants and invertebrates to floating organic matter.

Mega-landslides, tsunamis, and their consequences for island biogeography

Mega-landslides from volcanic island flank collapses are expected to directly deposit a large amount of organic material into the ocean (Fig. 2). An additional consequence of such landslide events is that they also trigger tsunamis when entering energetically into the sea (McGuire, 1996), and there are records of tsunamis from landslides in recent times (Evans *et al.*, 2006; Furukawa *et al.*, 2008 and references therein), as well as coastal deposits for more historical events (e.g. McMurtry *et al.*, 1999; McMurtry *et al.*, 2004b; Pérez-Torrado *et al.*, 2006; Coello *et al.*, 2014; Ramalho *et al.*, 2015). The resulting tsunami waves are propagated both offshore and onshore (Didenkulova *et al.*, 2010; Sue *et al.*, 2011), and can reach heights of hundreds of metres, as recorded by coastal deposits (e.g. McMurtry *et al.*, 2004b: 240-356 m; McMurtry *et al.*, 2004a: 400 m; Pérez-Torrado *et al.*, 2006: 188 m; Ramalho *et al.*, 2015: 270 m). Thus, tsunamis not only wash up the coasts of islands and mainland areas in their trajectory, but also the coast of the island suffering the landslide.

Given that there are both offshore and onshore tsunami waves propagating from a mega-landslide (Didenkulova *et al.*, 2010; Sue *et al.*, 2011), deposition of organic material into the ocean is also expected from (i) areas of the source island affected by the onshore tsunami, and (ii) islands impacted by the offshore tsunami. Thus, mega-landslides are expected to promote the ocean deposition and rafting of significantly more organic

material than that associated with the landslide itself, although the altitude of secondary deposition will be a function of the tsunami height. In the context of island biogeographic theory, for which colonisation is a fundamental component (MacArthur & Wilson, 1963, 1967), mega-landslides may be an important driver of colonisation, mediated by ocean currents and archipelago geomorphology.

Limitations and further considerations

A general limitation that applies to the present study is a lack of power to estimate the timing of colonisation of mtDNA lineages, which are expected to be synchronous when driven by a mega-landslide event, and consistent with the timing of the mega-landslide event. This is because the estimation of colonisation times of mtDNA lineages that are derived from coalescent mtDNA variation within a source population is subject to multiple sources of error, including unsampled or extinct haplotypes (see Fig. 5, and Fig. 2 for a conceptual explanation), mean substitution rate uncertainty and high rate variance over a coalescent time-scale. We suggest that some of these challenges may be alleviated in future studies with reduced representation genome sequencing approaches, such as restriction site-associated DNA sequencing (RADseq). With access to geographically referenced patterns of relatedness across potentially thousands of nuclear loci, it may be possible to estimate demographic parameters such as the number of founding events, their timing, and their founding population size(s).

For a given mega-landslide event, ocean currents and archipelago geomorphology will influence the dispersal of organic material deposited into the ocean, potentially providing for model-based hypothesis testing. However, obtaining supporting evidence is expected to be challenging for older mega-landslide events. This is because lineage sorting will erode patterns of shared genetic variation across islands with time, until all individuals coalesce back to a single source lineage. Thus, the older a landslide event is, the less likely it will be to find signatures of colonisation involving multiple individuals. We therefore suggest that it will be advantageous to investigate mega-landslides of recent geological origin. Given the potential for mega-landslides to result in the synchronous colonisation of a large number species to a neighbouring island, we also suggest sampling multiple species with distributions that could be explained by a mega-landslide. Taking a

multi-species, multi-locus approach, with a focus on geologically recent mega-landslides should shed light on their general importance in oceanic island biogeography.

References

Brown, R.P., Hoskisson, P.A., Welton, J.H. & Báez, M. (2006) Geological history and within-island diversity: a debris avalanche and the Tenerife lizard *Gallotia galloti*. *Molecular Ecology*, **15**, 3631-3640.

Brullé, G.A. (1839) Insectes. *Histoire naturelle des îles Canaries* (ed. by P.B. Webb and S. Berthelot), pp. 54-95. Bethune, Paris.

Canals, M., Urgeles, R., Masson, D. & Casamor, J.L. (2000) Los deslizamientos submarinos de las Islas Canarias. *Makaronesia: Boletín de la Asociación de Amigos del Museo de Ciencias Naturales de Tenerife*, **2**, 57-69.

Carracedo, J.C., Pérez-Torrado, F.J., Paris, R. & Rodríguez, E. (2009) Megadeslizamientos en las Islas Canarias. *Enseñanza de las Ciencias de la Tierra*, **17**, 44-56.

Carson, H.L. & Kaneshiro, K.Y. (1976) Drosophila of Hawaii: systematics and ecological genetics. *Annual Review of Ecology and Systematics*, **7**, 311-345.

Casquet, J., Thebaud, C. & Gillespie, R.G. (2012) Chelex without boiling, a rapid and easy technique to obtain stable amplifiable DNA from small amounts of ethanol-stored spiders. *Molecular Ecology Resources*, **12**, 136-141.

Clément, J.-P., Legendre, C., Caroff, M., Guillou, H., Cotten, J., Bollinger, C. & Guille, G. (2002) Epiclastic deposits and 'horseshoe-shaped' calderas in Tahiti (Society Islands) and Ua Huka (Marquesas Archipelago), French Polynesia. *Journal of Volcanology and Geothermal Research*, **120**, 87-101.

Coello, J.J., Martín, E. & Hernández Gutiérrez, L. (2014) Depósitos de tsunami originados por un deslizamiento gravitacional masivo en Tenerife (Islas Canarias). *Vieraea*, **42**, 79-102.

Coffin, H.G. (1983) Erect floating stumps in Spirit Lake, Washington. *Geology*, **11**, 298-299.

Didenkulova, I., Nikolkina, I., Pelinovsky, E. & Zahibo, N. (2010) Tsunami waves generated by submarine landslides of variable volume: analytical solutions for a basin of variable depth. *Natural Hazards and Earth System Science*, **10**, 2407-2419.

Edelaar, P., Roques, S., Hobson, E.A., Gonçalves da Silva, A., Avery, M.L., Russello, M.A., Senar, J.C., Wright, T.F., Carrete, M. & Tella, J.L. (2015) Shared genetic diversity across the global invasive range of the monk parakeet suggests a common restricted geographic origin and the possibility of convergent selection. *Molecular Ecology*, **24**, 2164-2176.

Emerson, B.C., Forgie, S., Goodacre, S.L. & Oromi, P. (2006) Testing phylogeographic predictions on an active volcanic island: *Brachyderes rugatus* (Coleoptera: Curculionidae) on La Palma (Canary Islands). *Molecular Ecology*, **15**, 449-458.

Evans, S.G., Scarascia Mugnozza, G., Strom, A.L., Hermanns, R.L., Ischuk, A. & Vinnichenko, S. (2006) Landslides from massive rock slope failure and associated phenomena. *Landslides from Massive Rock Slope Failure* (ed. by S.G. Evans, G. Scarascia Mugnozza, A.L. Strom and R.L. Hermanns), pp. 3-52. Springer, Netherlands.

Faria, C.M.A., Machado, A., Amorim, I.R., Gage, M.J.G., Borges, P.A.V. & Emerson, B.C. (2016) Evidence for multiple founding lineages and genetic admixture in the evolution of species within an oceanic island weevil (Coleoptera, Curculionidae) super-radiation. *Journal of Biogeography*, **43**, 178-191.

Furukawa, R., Nanayama, F. & Yoshimoto, M. (2008) Volcanic Debris-Avalanche as a Cause of a Historic Tsunami: The AD 1640 Eruption of the Hokkaido-Komagatake

Volcano, Northern Japan. *Solutions to Coastal Disasters 2008* (ed by L. Wallendorf, L. Ewing, C. Jones and B. Jaffe), pp. 235-247. Turtle Bay, Oahu, Hawaii.

Gillespie, R.G., Baldwin, B.G., Waters, J.M., Fraser, C., Nikula, R. & Roderick, G.K. (2012) Long-distance dispersal – a framework for hypothesis testing. *Trends in Ecology & Evolution*, **27**, 47-56.

Hardy, O.J. & Vekemans, X. (2002) SPAGeDi: a versatile computer program to analyse spatial genetic structure at the individual or population levels. *Molecular Ecology Notes*, **2**, 618-620.

Holcomb, R.T. & Searle, R.C. (1991) Large landslides from oceanic volcanoes. *Marine Georesources & Geotechnology*, **10**, 19-32.

Hunt, J.E., Talling, P.J., Clare, M.A., Jarvis, I. & Wynn, R.B. (2014) Long-term (17Ma) turbidite record of the timing and frequency of large flank collapses of the Canary Islands. *Geochemistey, Geophysics, Geosystems*, **15**, 3322-3345.

Kearse, M., Moir, R., Wilson, A., Stones-Havas, S., Cheung, M., Sturrock, S., Buxton, S., Cooper, A., Markowitz, S., Duran, C., Thierer, T., Ashton, B., Mentjies, P. & Drummond, A.J. (2012) Geneious Basic: an integrated and extendable desktop software platform for the organization and analysis of sequence data. *Bioinformatics*, **28**, 1647-1649.

Leigh, J.W. & Bryant, D. (2015) Popart: Full-Feature Software for Haplotype Network Construction. *Methods in Ecology and Evolution*, **6**, 1110-1116.

Lindberg, H. (1953) Zweiter Beitrag zur Kenntnis der Käferfauna der Kanarischen Inseln. *Commentationes Biologicae*, **13**, 1-8.

MacArthur, R.H. & Wilson, E.O. (1963) An equlilbrium theory of insular zoogeography. *Evolution*, **17**, 373-387.

MacArthur, R.H. & Wilson, E.O. (1967) *The theory of island biogeography*. Princeton University Press, Princeton.

Machado, A. (2011) Nuevos taxones de *Laparocerus* Schoenherr, 1834 de El Hierro y La Gomera, Islas Canarias (Coleoptera, Curculionidae, Entiminae). *Graellsia*, **67**, 57-90.

Machado, A. (2012) Nuevos taxones de *Laparocerus* Schoenherr, 1834 de la isla de Gran Canaria (Coleoptera, Curculionidae, Entiminae). *Boletín de la Sociedad Entomológica Aragonesa*, **51**, 5-46.

Machado, A. (2016) *Laparocerus* Schoenherr, 1834 nuevos de Canarias y claves de las especies de la isla de Tenerife (Coleoptera, Curculionidae, Entiminae). *Graellsia*, **72**, e049.

Macías-Hernández, N., Bidegaray-Batista, L., Emerson, B.C., Oromí, P. & Arnedo, M.A. (2013) The imprint of geologic history on within-island diversification of woodlouse-hunter spiders (Araneae, Dysderidae) in the Canary Islands. *Journal of Heredity*, **104**, 341-356.

Mairal, M., Sanmartín, I., Aldasoro, J., Culshaw, V., Manopoulou, I. & Alarcón, M. (2015) Palaeo-islands as refugia and sources of genetic diversity within volcanic archipelagos: the case of the widespread endemic *Canarina canariensis* (Campanulaceae). *Molecular Ecology*, **24**, 3944-3963.

Masson, D., Le Bas, T., Grevemeyer, I. & Weinrebe, W. (2008) Flank collapse and large-scale landsliding in the Cape Verde Islands, off West Africa. *Geochemistry, Geophysics, Geosystems*, **9**, Q07015.

Masson, D., Watts, A., Gee, M., Urgeles, R., Mitchell, N., La Bas, T. & Canals, M. (2002) Slope failures on the flanks of the western Canary Islands. *Earth-Science Reviews*, **57**, 33-45.

McGuire, W.J. (2003) Volcano instability and lateral collapse. *Revista*, **1**, 33-45.

McGuire, W.J. (1996) Volcano instability: a review of contemporary themes. *Geological Society London Special Publications*, **110**, 1-23.

McMurtry, G., Watts, P., Fryer, G., Smith, J. & Imamura, F. (2004a) Giant landslides, mega-tsunamis, and paleo-sea level in the Hawaiian Islands. *Marine Geology*, **203**, 219-233.

McMurtry, G., Fryer, G., Tappin, D.R., Wilkinson, I.P., Williams, M., Fietzke, J., Garbe-Schoenberg, D. & Watts, P. (2004b) Megatsunami deposits on Kohala volcano, Hawaii, from flank collapse of Mauna Loa. *Geology*, **32**, 741-744.

McMurtry, G.M., Herro-Bervera, E., Cremer, M.D., Smith, J.R., Resig, J., Sherman, C. & Torresan, M.E. (1999) Stratigraphic constraints on the timing and emplacement of the Alika 2 giant Hawaiian submarine landslide. *Journal of Volcanology and Geothermal Research*, **94**, 35-58.

Mittelstaedt, E. (1991) The ocean boundary along the northwest African coast: Circulation and oceanographic properties at the sea surface. *Progress in Oceanography*, **26**, 307-355.

Mohr, C.O. (1947) Table of equivalent populations of North American small mammals. *American Midland Naturalist*, **37**, 223-249.

Moore, J.G., Normark, W.R. & Holcomb, R.T. (1994) Giant hawaiian landslides. *Annual Review of Earth and Planetary Sciences*, **22**, 119-144.

Oehler, J.-F., Labazuy, P. & Lénat, J.-F. (2004) Recurrence of major flank landslides during the last 2-Ma-history of Reunion Island. *Bulletin of Volcanology*, **66**, 585-598.

Pérez-Torrado, F.J., Paris, R., Cabrera, M.C., Schneider, J.-L., Wassmer, P., Carracedo, J.C., Rodríguez-Santana, Á. & Santana, F. (2006) Tsunami deposits related to flank collapse in oceanic volcanoes: the Agaete Valley evidence, Gran Canaria, Canary Islands. *Marine Geology*, **227**, 135-149.

Pons, O. & Petit, R.J. (1996) Measuring and testing genetic differentiation with ordered versus unordered alleles. *Genetics*, **144**, 1237-1245.

Posada, D. & Crandall, K.A. (2001) Intraspecific gene genealogies: trees grafting into networks. *Trends in Ecology and Evolution*, **16**, 37-45.

Ramalho, R.S., Winckler, G., Madeira, J., Helffrich, G.R., Hipólito, A., Quartau, R., Adena, K. & Schaefer, J.M. (2015) Hazard potential of volcanic flank collapses raised by new megatsunami evidence. *Scientific Advances*, **1**, e1500456.

Rambaut, A. (2016) *FigTree v1.4.3, Available from* http://tree.bio.ed.ac.uk/software/figtree/.

Ronquist, F., M. Teslenko, P. van der Mark, D. L. Ayres, A. Darling, S. Hohna, B. Larget, L. Liu, M. A. Suchard, J. P. Huelsenbeck (2012) MrBayes 3.2: Efficient bayesian phylogenetic inference and model choice across a large model space. *Systematic Biology*, **61**, 539-542.

Samper, A., Quidelleur, X., Boudon, G., Le Friant, A. & Komorowski, J. (2008) Radiometric dating of three large volume flank collapses in the Lesser Antilles Arc. *Journal of Volcanology and Geothermal Research*, **176**, 485-492.

Siebert, L. (1984) Large volcanic debris avalanches: characteristics of source areas, deposits, and associated eruptions. *Journal of Volcanology and Geothermal Research*, **22**, 163-197.

Sue, L., Nokes, R. & Davidson, M. (2011) Tsunami generation by submarine landslides: comparison of physical and numerical models. *Environmental fluid mechanics*, **11**, 133-165.

Tamura, K., Stecher, G., Peterson, D., Filipski, A. & Kumar, S. (2013) MEGA6: Molecular Evolutionary Genetics Analysis Version 6.0. *Molecular Biology and Evolution* **30**, 2725-2729.

Templeton, A.R. (1980) The theory of speciation via the founder principle. *Genetics*, **94**, 1011-1038.

Templeton, A.R. (2008) The reality and importance of founder speciation in evolution. *Bioessays*, **30**, 470-479.

Uyttenboogaart, D.L. (1940) Voyages de M. Ch. Alluaud aux Iles Canaries (1889–90) et à l'archipel de Madère (1938). Coléoptères Curculionides. *Revue Française d'Entomologie, Paris*, **7**, 49-69.

Villesen, P. (2007) Fabox: An online fasta sequence toolbox. *Molecular Ecology Notes*, **7**, 965-968.

Wada, S., Kawakami, K. & Chiba, S. (2011) Snails can survive passage through a bird's digestive system. *Journal of Biogeography*, **39**, 69-73.

Ward, S.N. & Day, S. (2003) Ritter Island Volcano—lateral collapse and the tsunami of 1888. *Geophysical Journal International*, **154**, 891-902.

Warren, B.H., Simberloff, D., Ricklefs, R.E., Aguilée, R., Condamine, F.L., Gravel, D., Morlon, H., Mouquet, N., Rosindell, J., Casquet, J., Conti, E., Cornualt, J., Fernández-Palacios, J.M., Hengl, T., Norder, S.J., Rijsdijk, K.F., Sanmartín, I., Strasberg, D., Triantis, K.A., Valente, L.M., Whattaker, R.J., Gillespie, R.G., Emerson, B.C. & Thébaud, C. (2015) Islands as medel systems in ecology and evolution: fifty years after MacArthur-Wilson. *Ecology Letters*, **18**, 200-217.

Whittaker, R.J., Triantis, K.A. & Ladle, R.J. (2008) A general dynamic theory of oceanic island biogeography. *Journal of Biogeography*, **35**, 977-994.

Wollaston, T.V. (1864) *Catalogue of the coleopterous insects of the Canaries in the collection of the British Museum*. Taylor & Francis, London.

Wooster, W.S., Bakum, A. & McLain, D.R. (1976) The seasonal upwelling cycle along the eastern boundary of the North Atlantic. *Journal of Marine Research*, **34**, 131-140.

Supporting information

Appendix S1. Details of documented landslides on the island of Tenerife

Table S1.1 Summary of documented landslides on the island of Tenerife, with marine deposit data when known. The area of each major plant community affected was calculated for those landslides where the limits of the surface area affected are clearly described by geomorphological evidence, such as landslide scars on island flanks. GIS shapes for the limits of the affected landslide areas were created based on previous published approximations, and on scars visualized on maps within the Canary Island cartography website (http://visor.grafcan.es/visorweb/). GIS shapes were then imported into maps of potential vegetation, and areas of each plant community were estimated using proprietary tools within the grafcan website.

		Marine deposits			*Area of the landslide in inland (km^2)*						
Landslide	Age (Ma)	Length (km)	Area (km^2)	Volume (km^3)	High mountain scrub	Pine forest	Laurel forest	Thermophilous woodland	Xeric shrub	Other	Total
Masca	5.89-6.65[a,b]	-	-	-	-	-	-	-	-	-	-
Carrizales	5.89-6.27[a,b]	-	-	-	-	-	-	-	-	-	-
Teno	6[c,d,e]	35[e]	400[e]	-	-	-	-	-	-	-	-
Anaga	4.1-4.7[f]	33[e]	>400[d]; 500[e,g]	36[g]	0	0	5.6	6.26	3.53	0	15.39
Tigaiga	2.3-2.6[c,e]	30[e]	200[e]	-	1.38	14.34	18.8	7.12	0.31	0	41.95
Bandas del Sur	<2[h]	30[h]	500[h]	25[h]	-	-	-	-	-	-	-
Roques de García	0.6-1.3[c,i]	95[e]; 130[d]	2200-4500[e,d]	500[c,d]	-	-	-	-	-	-	-
Micheque	0.83[j]	25[k]	400[k]	100[k]	-	-	-	-	-	-	-
Güímar	0.83-0.85[l,m]; 0.78-0.84[d]	85[e]; >50[d]	1600[d, h]; 2600[e]	120[d, h]	5.14	38.68	5.01	15.07	37.71	28.39	130
La Orotava	0.54-0.69[e]; 0.5-0.8[h]	75[e]; 90[d]	2100[d]; 2200[e]	500[d]	23.64	23.71	65.43	14.92	8.35	0	136.05
Icod	0.15-0.17[d]; 0.165[n]	105[d]	1700[d,i]	320[n]	-	-	-	-	-	-	-

a: Longpré et al. (2009); b: Walter and Schmincke (2002); c: Cantagrel et al. (1999); d: Masson et al. (2002); e: Acosta et al. (2003); f: Walter et al. (2005); g: Llanes et al. (2003); h: Krastel et al. (2001); i: Watts and Masson (1998); j: Carracedo et al (2011); k: Ablay and Hürlimann (2000); l: Hunt et al. (2013); m: Giachetti et al. (2011); n: Wynn et al. (2002).

Ablay, G., and M. Hürlimann. (2000). Evolution of the north flank of Tenerife by recurrent giant landslides. *Journal of Volcanology and Geothermal Research*, **103**, 135– 159.

Acosta, J., E. Uchupi, A. Muñoz, P. Herranz, C. Palomo, M. Ballesteros, and ZEE Working Group. (2003). Geologic evolution of the Canary Islands of Lanzarote, Fuerteventura, Gran Canaria and La Gomera and comparison of the landslides at these islands with those at Tenerife, La Palma and El Hierro. *Mar. Geophys. Res*., **24**, 1–40.

Cantagrel, J. M., N. O. Arnaud, E. Ancochea, J. M. Fuster, and M. J. Huertas. (1999). Repeated debris avalanches on Tenerife and genesis of Las Cañadas caldera wall (Canary Islands). *Geology*, **27**, 739–742.

Carracedo, J. C. H. Guillou, S. Nomade, E. Rodríguez-Badiola, F. J. Pérez-Torrado, A. Rodríguez-González, R. Paris, V. R. Troll, S. Wiesmaier, A. Delcamp and J. L. Fernández-Turiel. (2011). Evolution of ocean-island rifts: The northeast rift zone of Tenerife, Canary Islands. *Geological Society of America Bulletin*. **123**, 562–584.

Giachetti, T., R. Paris, K. Kelfoun, and F. J. Perez-Torrado. (2011). Numerical modelling of the tsunami triggered by the Güímar debris avalanche, Tenerife (Canary Islands): Comparison with field-based data. *Mar. Geol*., **284**, 189–202.

Hunt, J. E., R. B. Wynn, P. J. Talling, and D. G. Masson. (2013). Turbidite record of frequency and source of large volume (>100 km3) Canary Island landslides in the last 1.5 Ma: Implications for landslide triggers and geohazards. *Geochem. Geophys. Geosyst*., **14**, 2100–2123.

Krastel, S., H.-U. Schmincke, C. L. Jacobs, R. Rihm, T. P. Le Bas, and B. Alibes. (2001). Submarine landslides around the Canary Islands, *J. Geophys*. Res., **106**, 3977–3997.

Llanes, P., A. Muñoz, A. Muñoz-Martın, J. Acosta, P. Herranz, A. Carbo, and C. Palom. (2003). Morphological and structural analysis in the Anaga offshore massif, Canary Islands: fractures and debris avalanches relationships. *Mar. Geophys*. Res., **24**, 91–112

Longpré, M.-A., V. R. Troll, T. R. Walter, and T. H. Hansteen. (2009). Volcanic and geochemical evolution of the Teno massif, Tenerife, Canary Islands: Some repercussions of giant landslides on ocean island magmatism, Geochem. *Geophys. Geosyst*., **10**, Q1201.

Masson, D. G., A. B. Watts, M. R. J. Gee, R. Urgeles, N. C. Mitchell, T. Le Bas, and M. Canals. (2002). Slope failures on the flanks of the Western Canary Islands. Earth *Science Reviews* **57**, 1–35.

Walter, T., and H.-U. Schmincke. (2002). Rifting, recurrent landsliding and Miocene structural reorganisation of NW-Tenerife (Canary Islands), *Int. J. Earth Sci*., **91**, 615– 628.

Walter, T. R., V. R. Troll, B. Cailleau, A. Belousov, H.-U. Schmincke, F. Amelung, and P. v.d. Bogaard. (2005). Rift zone reorganization through flank instability in ocean island volcanoes: an example from Tenerife, Canary Islands. *Bull. Volcanol*., **67**, 281–291.

Watts, A. B., and D. G. Masson. (1998). Reply to comment on: A giant land-slide on the northern flank of Tenerife, Canary Islands, by A. B. Watts and D. G. Masson. J. *Geophys. Res*., **103**, 9948–9951.

Wynn, R. B., P. P. E. Weaver, D. A. V. Stow, and D. G. Masson. (2002). Turbidite depositional architecture across three interconnected deepwater basins on the northwest African margin. *Sedimentology*, **49**, 1441–1462.

Appendix S2: Details of sampling locations and the taxonomic assignment of samples, and the Bayesian phylogenetic tree constructed from 194 unique mtDNA haplotypes.

Figure S2.1. Bayesian phylogenetic tree constructed from 195 haplotypes for the mtDNA COII gene sampled from the *Laparocerus tessellatus* complex. Haplotype colour represents island of origin (see Fig. 4).

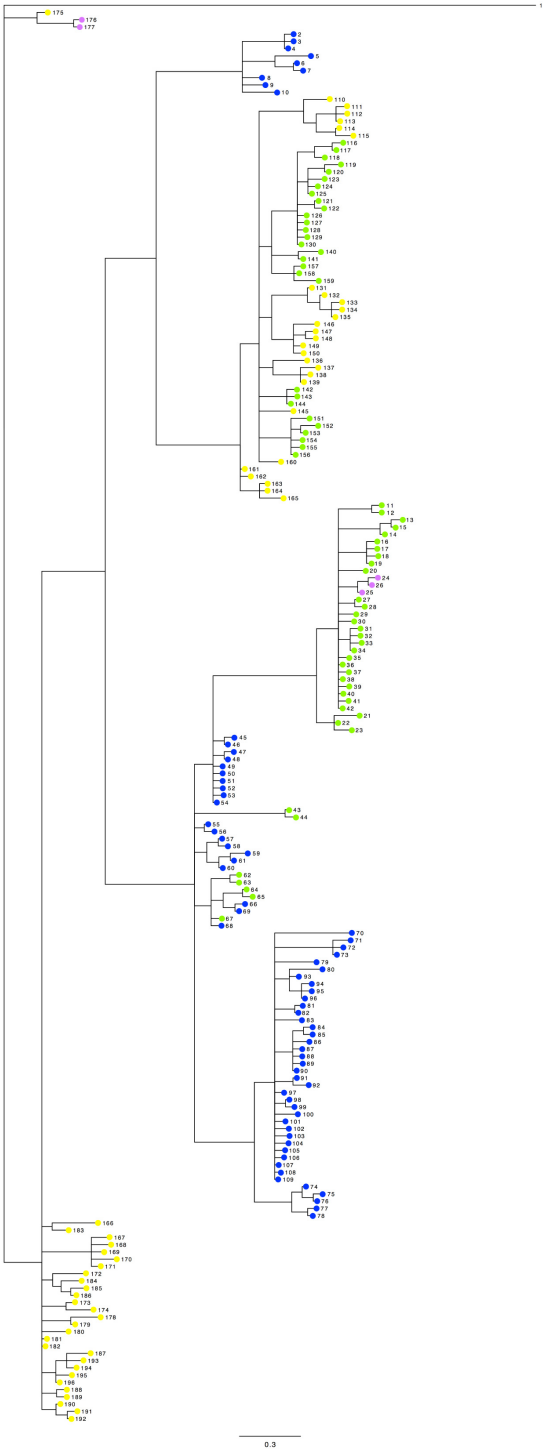

Table S2.2. Details of sampling locations, the number of individuals sampled at each location, and their taxonomic assignment.

Island	Locality	Locality Code	Lat.	Long.	Taxonomic assignment	No. Individuals	Source
Gran Canaria	Las Huertecillas	C01	28.08554312	-15.55989249	*L. obsitus*	2	This study
Gran Canaria	Las Huertecillas	C01	28.08554312	-15.55989249	*L. osorio*	1	Faria et al. 2015
Gran Canaria	Degollada de Osorio	C02	28.07254322	-15.55794230	*L. sp. aff. tirajana*	5	Faria et al. 2015
Gran Canaria	Laguna de Valleseco	C03	28.06506291	-15.56382636	*L. obsitus*	2	This study
Gran Canaria	Barranco Oscuro	C04	28.06775026	-15.58813215	*L. obsitus*	4	Faria et al. 2015; this study
Gran Canaria	Barranco Oscuro	C04	28.06775026	-15.58813215	*L. osorio*	6	Faria et al. 2015; this study
Gran Canaria	Barranco los Cazadores	C05	28.04327617	-15.59488702	*L. obsitus*	2	This study
Gran Canaria	Barranco los Cazadores	C05	28.04327617	-15.59488702	*L. osorio*	3	Faria et al. 2015
Gran Canaria	Casa Forestal de Tamadaba	C06	28.05323863	-15.69192219	*L. microphthalmus*	9	Faria et al. 2015; this study
Gran Canaria	Pico del Majadal	C07	28.03067996	-15.67753554	*L. microphthalmus*	2	This study
Gran Canaria	Cruz de Tejeda	C08	28.00513303	-15.59791167	*L. obsitus*	3	This study
Gran Canaria	Infra Cruz de Tejeda	C09	27.99958826	-15.60048465	*L. tirajana*	2	This study
Gran Canaria	Barranco de la Mina	C10	27.99852595	-15.58727789	*L. obsitus*	2	Faria et al. 2015
Gran Canaria	Barranco de la Mina	C10	27.99852595	-15.58727789	*L. osorio*	3	This study
Gran Canaria	Las Casillas	C11	27.99277738	-15.52195750	*L. obsitus*	2	This study
Gran Canaria	Degollada de Becerra	C12	27.98854334	-15.59328465	*L. tirajana*	2	This study
Gran Canaria	Barranco de los Cernícalos	C13	27.96126336	-15.53148454	*L. sp. aff. tirajana*	5	Faria et al. 2015; this study
Gran Canaria	Cumbre. Pico Redondo	C14	27.96466481	-15.55926738	*L. sp. aff. tirajana*	5	Faria et al. 2015; this study
Gran Canaria	Llanos de la Pez	C15	27.96539529	-15.58548187	*L. tirajana*	2	This study
Gran Canaria	Supra Ayacata	C16	27.96511834	-15.60155445	*L. tirajana*	2	This study
Gran Canaria	Lomo Aserrador	C17	27.95949872	-15.62689883	*L. tirajana*	4	This study
Gran Canaria	Casa forestal Pilancones	C18	27.92719590	-15.59940314	*L. tirajana*	1	This study
Gran Canaria	Barranco Tirajana	C19	27.92605460	-15.57921238	*L. tirajana*	3	Faria et al. 2015; this study
Gran Canaria	San Bartolome de Tirajana	C20	27.91562810	-15.57493941	*L. tirajana*	2	This study
Gran Canaria	San Bartolomé, Km 1	C21	27.91213562	-15.57252269	*L. tirajana*	12	Faria et al. 2015
El Hierro	Monte Ajares, 600 m	H02	27.80306251	-17.91735339	*L. bimbache*	2	Faria et al. 2015
El Hierro	Piedras Blancas, San Andrés	H06	27.75615779	-17.96588963	*L. bimbache*	2	Faria et al. 2015
El Hierro	Infra Montaña Masilva	H08	27.74329951	-17.97906625	*L. bimbache*	2	Faria et al. 2015
La Palma	Ermita Santa Cecilia	P01	28.55312588	-17.86759048	*L. auarita*	2	This study
La Palma	Don Mendo Inferior	P02	28.55635515	-17.86673813	*L. auarita*	1	This study

La Palma	Don Mendo Superior	P03	28.55918404	-17.85878435	*L. auarita*	5	Faria et al. 2015; this study
La Palma	Caldereta de Mazo	P04	28.55171613	-17.78852885	*L. auarita*	4	This study
La Palma	Montaña de Venijobre	P05	28.60832065	-17.78591420	*L. auarita*	12	Faria et al. 2015; this study
La Palma	Refugio del Pilar	P06	28.61465974	-17.83430130	*L. auarita*	2	This study
La Palma	Pared Vieja	P07	28.61991369	-17.82330969	*L. auarita*	5	Faria et al. 2015; this study
La Palma	Fuente Guairín 1400 m	P08	28.64466749	-17.82496467	*L. auarita*	5	This study
La Palma	Supra El Paso, 870 m.	P09	28.65230896	-17.84558086	*L. auarita*	7	Faria et al. 2015
La Palma	Supra El Paso, 837 m	P10	28.65633803	-17.85215283	*L. auarita*	2	This study
La Palma	Cumbre Nueva, 1400 m	P11	28.66020837	-17.82546337	*L. auarita*	5	This study
La Palma	Pista de la Cumbre Nueva km 6	P12	28.66844581	-17.82710614	*L. auarita*	5	This study
La Palma	Pista de Ferrer Inferior	P13	28.67692853	-17.84972415	*L. auarita*	2	This study
La Palma	Barranco de la Madera	P14	28.69902060	-17.78647300	*L. auarita*	2	This study
La Palma	Montaña Tagoja B	P15	28.71770148	-17.77949856	*L. auarita*	3	Faria et al. 2015
La Palma	Montaña Tagoja A	P16	28.72455336	-17.78274993	*L. auarita*	5	This study
La Palma	Fuente de Olén	P17	28.73150875	-17.81321665	*L. auarita*	5	This study
La Palma	Picos de las Nieves	P18	28.73144181	-17.83024401	*L. auarita*	2	This study
La Palma	Las Moradas 2000	P19	28.76854840	-17.90470811	*L. auarita*	3	This study
La Palma	Pinar de la Garafía 1900 m	P20	28.77295172	-17.90463565	*L. auarita*	2	This study
La Palma	Pinar de la Garafía 1450 m	P21	28.78029274	-17.91932624	*L. auarita*	2	This study
La Palma	Cueva de la Zarza	P22	28.80500749	-17.90804415	*L. auarita*	6	This study
La Palma	Montaña de las Varas	P23	28.81950108	-17.90894892	*L. auarita*	5	This study
La Palma	Juan Adalid, 600 m	P24	28.83406532	-17.90866785	*L. auarita*	1	This study
La Palma	Barranco de las Traviesas, 924 m	P25	28.80646150	-17.86624023	*L. auarita*	5	This study
La Palma	Llanada de Barlovento	P26	28.81725810	-17.80925143	*L. auarita*	5	Faria et al. 2015
La Palma	Laguna de Barlovento	P27	28.81173517	-17.80936941	*L. auarita*	5	This study
La Palma	Los Tilos	P28	28.79697693	-17.78941412	*L. auarita*	5	This study
La Palma	Las Lomadas	P29	28.79118302	-17.78605468	*L. auarita*	5	This study
La Palma	Marcos y Cordero	P30	28.77274777	-17.81202970	*L. auarita*	5	This study
La Palma	Infra Marcos y Cordero	P31	28.76956776	-17.78921668	*L. auarita*	5	This study
La Palma	Cubo de la Galga	P32	28.76701695	-17.76984079	*L. auarita*	5	This study
Tenerife	Chinobre A	T04	28.55855948	-16.17519235	*L. tessellatus*	1	Faria et al. 2015
Tenerife	El Pijaral A	T05	28.55558324	-16.18118025	*L. tessellatus*	12	Faria et al. 2015

Tenerife	Cruz del Carmen	T08	28.53192475	-16.28007026	*L. tessellatus*	2	Faria et al. 2015
Tenerife	Pista Las Yedras	T10	28.53869269	-16.30013310	*L. tessellatus*	1	Faria et al. 2015
Tenerife	Los Morros (Altos Vilaflor)	T100	28.17835785	-16.63134339	*L. canescens*	1	This study
Tenerife	Granadilla (Las Vegas)	T105	28.14503420	-16.54520667	*L. canescens*	6	Faria et al. 2015
Tenerife	El Contador	T112	28.19143403	-16.52742558	*L. canescens*	2	Faria et al. 2015
Tenerife	Cumbres de Arico	T113	28.19770104	-16.53115154	*L. canescens*	3	Faria et al. 2015
Tenerife	Lomo del Retamar	T122	28.29691862	-16.48256482	*L. canescens*	4	This study
Tenerife	Montaña Las Raíces	T123	28.29323746	-16.44797825	*L. punctiger*	2	This study
Tenerife	Montaña de Anocheza A	T124	28.29324808	-16.43328514	*L. punctiger*	5	This study
Tenerife	Las Raíces	T20	28.42382434	-16.37923736	*L. punctiger*	11	Faria et al. 2015
Tenerife	Montaña Pico las Flores	T21	28.42380586	-16.39610270	*L. punctiger*	1	This study
Tenerife	Fuente Fría. Tacoronte	T22	28.42011452	-16.40749833	*L. tessellatus*	1	Faria et al. 2015
Tenerife	Barranco de Bensa	T41	28.39007943	-16.45466060	*L. tessellatus*	3	Faria et al. 2015
Tenerife	Gorgo	T43	28.35900553	-16.43337186	*L. tessellatus*	1	This study
Tenerife	Mirador de Chipeque	T46	28.37382697	-16.46375524	*L. tessellatus*	5	This study
Tenerife	Choza Almadi	T50	28.38142911	-16.47936090	*L. tessellatus*	4	This study
Tenerife	Las Lajitas	T51	28.39031952	-16.48924102	*L. tessellatus*	7	This study
Tenerife	Supra La Corujera	T53	28.40303863	-16.49228702	*L. tessellatus*	5	Faria et al. 2015; this study
Tenerife	El Nogalito	T54	28.40120553	-16.49567039	*L. tessellatus*	5	This study
Tenerife	Montaña de Ayosa	T55	28.35769475	-16.46666606	*L. tessellatus*	5	This study
Tenerife	Peña Rajada	T56	28.36350078	-16.49300887	*L. tessellatus*	5	This study
Tenerife	Corral de los Lucas	T57	28.34126307	-16.47890596	*L. punctiger*	5	This study
Tenerife	Barranco del Agua. Güimar	T59	28.30806238	-16.44235595	*L. punctiger*	9	Faria et al. 2015
Tenerife	Lomo los Pajales	T60	28.31639226	-16.48613925	*L. punctiger*	5	This study
Tenerife	Lomo Chillero	T61	28.35539266	-16.51460597	*L. tessellatus*	5	This study
Tenerife	Morro Quemado	T62	28.34795435	-16.53172067	*L. tessellatus*	5	This study
Tenerife	Las Jaritas	T63	28.34422815	-16.54282729	*L. tessellatus*	2	This study
Tenerife	Montaña Bermeja	T64	28.32716206	-16.53319714	*L. freyi*	2	Faria et al. 2015
Tenerife	Roque Caramujo	T65	28.30758082	-16.53692392	*L. freyi*	5	This study
Tenerife	Los Amontaderos	T66	28.34006167	-16.56709584	*cf. L. freyi*	5	This study
Tenerife	El Portillo	T67	28.30291210	-16.56654085	*L. freyi*	3	Faria et al. 2015
Tenerife	Infra El Portillo	T68	28.30911349	-16.56722319	*L. freyi*	2	This study
Tenerife	Vista la Chapa	T69	28.32568840	-16.58786491	*L. freyi*	3	This study
Tenerife	Cruz de Joaquín	T70	28.34281845	-16.59322010	*L. freyi*	5	This study
Tenerife	Icod el Alto	T71	28.36095843	-16.59862289	*L. freyi*	4	Faria et al. 2015
Tenerife	La Corona	T72	28.37783472	-16.60094739	*cf L. tessellatus*	2	This study
Tenerife	Lomo Blanco	T73	28.33658388	-16.62065758	*L. freyi*	2	This study
Tenerife	Hoya Benjaminas	T74	28.33271255	-16.65817491	*L. tessellatus*	2	This study

Tenerife	Llano de los Cuervos	T75	28.31620449	-16.71956612	*L. tessellatus*	2	This study
Tenerife	Tanque Bajo	T76	28.36146458	-16.77505070	*L. tessellatus*	1	Faria et al. 2015
Tenerife	Arenas Negras	T77	28.31853497	-16.75554195	*L. tessellatus*	1	This study
Tenerife	El Lomito	T79	28.32895645	-16.80887055	*L. tessellatus*	2	This study
Tenerife	Cumbre de Bolico	T80	28.31338338	-16.82018098	*L. tessellatus*	2	Faria et al. 2015
Tenerife	Ifonche	T94	28.13267228	-16.68803953	*L. punctiger*	2	Faria et al. 2015
Tenerife	Fuente Fría Altos Vilaflor	T96	28.18892538	-16.65694869	*L. canescens*	1	This study

Appendix S3: Altitudinal sampling data for the *L. tessellatus* complex in Tenerife, and photographic evidence of floating vegetation resulting from the 1980 eruption of Mount St. Helens.

Table S3.1. Summary of the number of localities known in Tenerife for the *tessellatus* complex and the other species of *Laparocerus*, in altitudinal intervals of 100 macsl. Locality data from a collection of *Laparocerus* maintained by one of us (AMC) was used to estimate the altitudinal range of the *Laparocerus tessellatus* complex in Tenerife. Six hundred and forty-two sampling localities, encompassing all ecosystems in an altitudinal gradient from sea level to the highest altitudes of the island, were sampled for *Laparocerus*. Data are summarised within altitudinal intervals of 100 macsl in Table S3.1. Two hundred and forty-four localities included samples from the *L. tessellatus* complex, while the remaining 398 were sampled only for other species from the genus. Of the 83 localities sampled for *Laparocerus* at altitudes ≤ 300 macsl, the *L. tessellatus* complex was sampled at only 4, meaning that more than 98% of occurrence records for *L. tessellatus* are > 300 macsl. The *L. tessellatus* complex is typical of altitudes above 764 macsl and below 1424 macsl (first and third quartiles of species distribution records), with a median and mean altitude of 1102 m and 1000 m respectively.

Latitudinal intervals	*Frequency L.tessellatus*	*Frequency other species*	*Total*
0--99	0	35	35
100--199	3	21	24
200--299	1	23	24
300--399	3	21	24
400--499	5	18	23
500--599	10	26	36
600--699	18	30	48
700--799	27	37	64
800--899	30	47	77
900--999	22	20	42
1000--1099	22	30	52
1100--1199	15	10	25
1200--1299	18	11	29
1300--1399	5	4	9
1400--1499	11	8	19
1500--1599	4	5	9
1600--1699	16	12	28
1700--1799	9	4	13
1800--1899	3	3	6
1900--1999	7	1	8
2000--2099	8	8	16
2100--2199	2	9	11
2200--2299	4	7	11
2300--2399	1	2	3
2400--2499	0	0	0
2500--2599	0	2	2
2600--2699	0	2	2
2700--2799	0	0	0
2800--2899	0	0	0
2900--2999	0	0	0
3000--3099	0	2	2
> 3100	0	0	0
Total	244	398	642

During the eruption of Mt. St. Helens in 1980, a mega-landslide resulted in the deposition of tens of thousands of trees into Spirit Lake, producing a giant log raft that persisted for many years. The following photos, taken between two and three decades after the eruption, demonstrate the high floatability and temporal persistence of plant material deposited into a water body from a mega-landslide.

Photo 1. Agglomeration of logs on Spirit Lake, 22 years after the eruption and landslide (Author: Xpda). Logs are indicated with a black arrow added by the authors.

Photo 2. Trees drifting on Spirit Lake, with the open crater of Mount St. Helens open in the background, 32 years after the landslide and eruption (Author: Stephan Schulz).

Photo 3. Hikers gazing at the logs covering Spirit Lake, near Mount St. Helens, 29 years after the eruption and landslide (Author: Etliebe).

▶CHAPTER II

Phylogenomic reconstruction of the *Laparocerus tessellatus* species complex

Phylogenomic analysis of the *Laparocerus tessellatus* species complex

Abstract

Evolutionary radiation is one of the more recognisable features of oceanic islands. They have long intrigued evolutionary biologists and are considered fertile ground to investigate the mechanisms underlying diversification. Within the Macaronesian region, the endemic weevil genus *Laparocerus* stands apart from all other invertebrate genera with its species richness of 237 species and subspecies. The majority of these taxa, 196 species and subspecies, are endemic to the Canary Islands, where they represent more than one-third of all native weevil species within the archipelago, being the most species-rich of any animal or plant genus. A species complex within the genus has been the focus of recent investigation to understand the factors that explain the evolutionary success of the genus. Molecular data from the complex has revealed significant inconsistencies between nuclear and mitochondrial markers, leading to speculation of species formation on younger islands by genetic admixture among founding species from different islands. Here we applied a multi-locus approach to investigate the evolutionary history of the complex using double-digest restriction site associated DNA sequencing to obtain a fuller understanding of the diversification history within complex. Our nuclear genome phylogeny inferred for the *Laparocerus tessellatus* species complex provide strong support for a Gran Canaria origin for the complex, and is consistent with the origin of each island from a single founding event, although with some minor exceptions.

Introduction

Charles Darwin's five-year voyage around the world, studying and collecting animals, revolutionized evolutionary thinking, catalysed by an important stop in the Galapagos Islands and his study of the Galapagos finches (Economo *et al.*, 2015). Since then, insular systems have been viewed as natural laboratories for the study of ecology and evolution (e.g. Roderick & Gillespie, 1998; Parent *et al.*, 2008). Evolutionary radiation is one of the more recognisable features of oceanic islands (Losos & Ricklefs, 2009) and represents a phenomena that has long intrigued evolutionary biologists. Studies focused on species radiation have provided a rich source of new insights into the evolutionary processes underlying diversification (Schluter, 2001; Gavrilets & Vose, 2005).

During the last two decades, the Macaronesian archipelagos have increasingly become the focus of research to further understand the processes of diversification and radiation (Whittaker & Fernandez-Palacios, 2007). Within this region, the endemic weevil genus *Laparocerus* stands apart from all other invertebrate genera, with 237 species and subspecies, distributed almost exclusively in the Canary and Madeira archipelagos, and the Selvagens Islands, with several species found in West Morocco (Machado *et al.*, 2017). The vast majority of these taxa, 196 species and subspecies, are endemic to the Canary Islands, where they represent more than one third of all native weevil species within the archipelago, being the most species-rich of any animal or plant genus (Arechavaleta *et al.*, 2010). Within the superfamily Curculionoidea, *Laparocerus* shows twelve times higher species richness than the second most species-rich genus, *Acalles*, comprised of 16 species (Oromí *et al.*, 2010). This unbalanced species diversity raises an important question, why are some lineages more diverse than others? This disparity among lineages with regard to diversification is a recurrent pattern across biodiversity, particularly within island environments, being recognized as a fundamental question in evolutionary biology (Hutchinson, 1959; Warren *et al.*, 2015; Patiño *et al.*, 2017). From an ecological perspective, species of *Laparocerus* can be found across much of the habitat diversity of the islands: dune ecosystems, semi-arid succulent shrub land, sclerophyllous forest, azonal cliff

vegetation, humid cloud forest, pine forest, high mountain shrublands and grassland, and the subterranean environment (Machado *et al.*, 2017). The extensive radiation within the genus *Laparocerus*, together with its apparent adaptation to diverse habitats, makes the genus something of an enigma for evolutionary biologists.

A recent molecular phylogenetic analysis of the genus *Laparocerus* has described relationships among morphologically described species (Machado *et al.*, 2017). Within the genus, a complex of species falling within the 'Pecoudius' subclade (Fig. 1), has been the subject of more fine-scale molecular analysis to address the evolutionary success of the genus from an intraspecific perspective. Faria *et al.* (2016) investigated inter-island colonization within the *Laparocerus tessellatus* complex, revealing significant inconsistencies among nuclear (ITS2) and mitochondrial DNA (COII) pattern of relatedness, both of which were also inconsistent with taxonomy. Faria *et al.* (2016) suggest that such incongruencies are compatible with a history of potential genetic admixture among multiple colonizing lineages arriving to the same island. García-Olivares *et al.* (2017, Chapter I) increased the number of localities and samples of Faria *et al.* (2016) to describe dispersal between islands by mega-landslides involving the establishment of multiple individuals from the same source. While both studies offer some insight to dispersal history between islands, and its evolutionary consequences, mechanisms explaining within-island diversification and speciation are limited, although Faria *et al.* (2016) were able to speculate that environmental barriers may promote isolation and secondary contact within Tenerife.

The use of one or a few molecular markers for phylogenetic and phylogeographic analysis can constrain the power and resolution of inferences, something that is well documented (Edwards & Beerli, 2000; Edwards, 2009; Andrews *et al.*, 2014). In the case of Faria *et al.* (2016), only two markers were used, the mitochondrial COII gene region and the nuclear ITS2 gene region. While both were consistent with the progression rule hypothesis (Funk & Wagner), each implied a very different colonisation history. A simple colonization history from eastern to western islands was inferred by the nuclear topology. However, the colonisation history reflected by the mitochondrial marker is more complex. Species from the younger islands of La Palma and El Hierro are derived from multiple

mitochondrial lineages from more than one island. *Laparocerus auarita* from La Palma shares mitochondrial DNA (mtDNA) variation with taxa from both the island of Tenerife and Gran Canaria. In the case of *L. bimbache* from El Hierro, divergent mtDNA lineages within

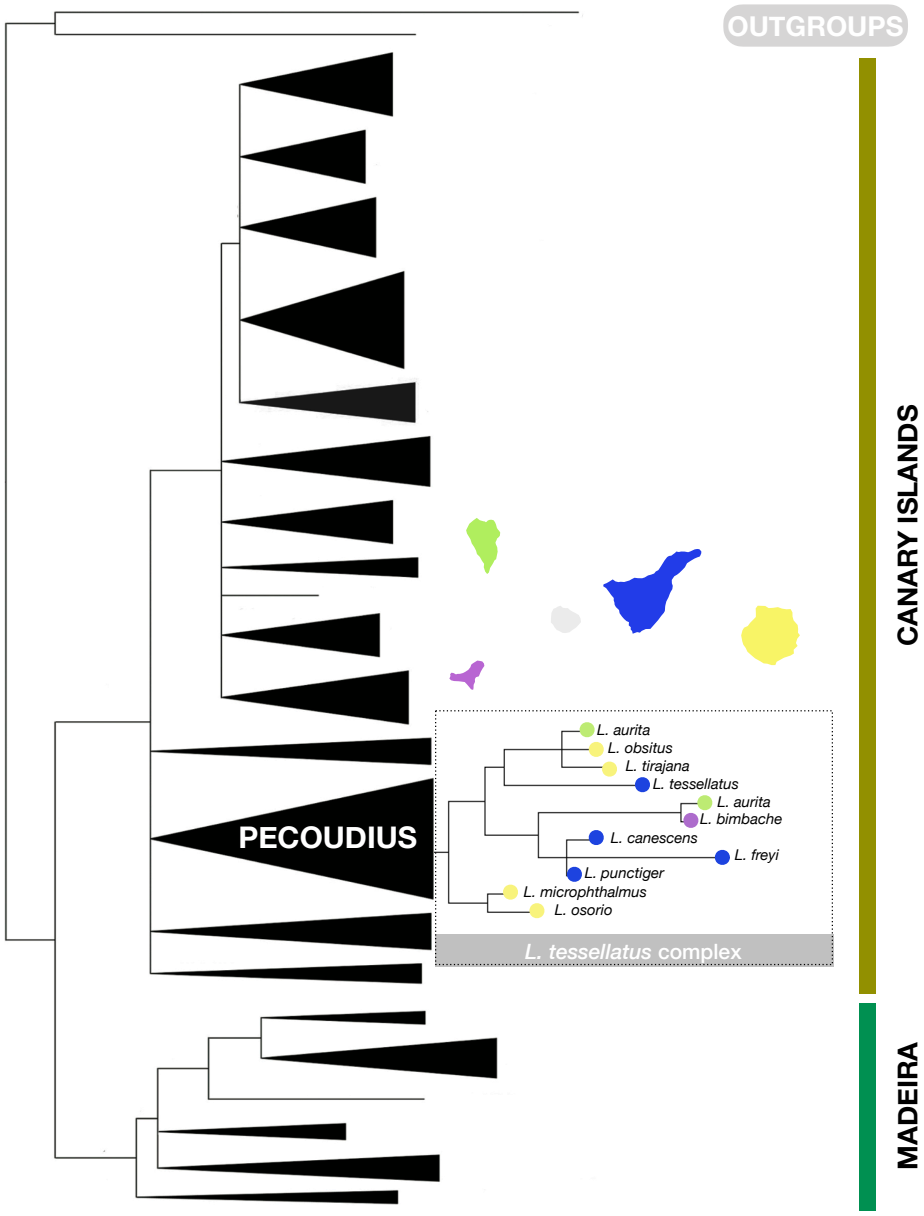

Figure 1. Bayesian phylogenetic tree of the genus *Laparocerus* Schönherr, 1834, from Machado *et al.* (2017), representing the different subclades which comprise the genus. Of particular note is the Pecoudius subclade, and the phylogenetic relationships and geographic origins among species related to the *L. tessellatus* complex. The species complex is compound by 11 taxonomically defined species which them are all single-island endemics. Gran Canaria (5 species): *L. microphthalmus* Lindberg, 1950, *L. obsitus* Wollaston, 1864; *L. osorio* Machado, 2012; *L. tirajana* Machado, 2012; and *L. sp. aff. tirajana* Tenerife (4 species) *L. tessellatus* Brulle, 1839; *L. freyi* Uyttenboogaart, 1940; *L. punctiger* Machado, 2016; and *L. canescens* Machado, 2016; La Palma (1 species): *L. auarita* Machado, 2016; El Hierro (1 species): *L. bimbache* Machado, 2011.

this species share independent common ancestry with different taxa from La Palma and Gran Canaria. Thus, the topologies recovered by both markers show strong conflicting signatures of colonisation history. Recently diverged taxa may present conflicting topologies for different loci due to interspecific gene flow or incomplete lineage sorting (Maddison, 1997; Wendel & Doyle, 1998; Degnan & Rosenberg, 2009). However, Faria *et al.* (2016) were able to discard an explanation of incomplete lineage sorting, concluding instead that topological inconsistencies between both markers were the result of genetic admixture involving multiple founding species.

Increasing the number of loci in an analysis of population history increases the power to take into account the stochasticity of the coalescent process, allowing for improved inference resolution (Knowles & Maddison, 2002; Knowles, 2009; Carstens *et al.*, 2013). In this context the advent of next generation sequencing (NGS) technology has notably improved our ability to sample hundreds to thousands of loci from non-model organisms (Emerson, 2010). Restriction site associated DNA sequencing (RAD-seq) is an application of NGS technology that allows parallel sequencing of millions of DNA fragments sampled from the genomes of potentially hundreds of individuals at the same time within a cost-effective experiment. The unprecedented resolution provided by NGS technology and RAD-seq facilitates the analysis of species-level genetic variation (Leache *et al.*, 2015; Potter *et al.*, 2016; Yoder *et al.*, 2016), and is thus a promising tool for the inference of phylogenetic relationships among recently diversified taxa using multi-locus data (McCormack *et al.*, 2013). Such an approach has already proven useful for species delimitation and phylogenetic resolution in recently diversified taxa (e.g. swordtails in Jones *et al.*, 2013; Heliconius butterflies in Nadeau *et al.*, 2013; cichlids in Wagner *et al.*, 2013; geckos in Leache *et al.*, 2014).

In order to further understand dispersal and speciation history within the *Laparocerus tessellatus* complex, we have improved both geographical and molecular sampling performed by Faria *et al.* (2016) and García-Olivares *et al.* (2017, Chapter I). We use double-digest restriction site associated DNA sequencing (ddRAD-seq; Peterson *et al.*, 2012), a method considered suitable to infer recent evolutionary histories (<3 Ma) in other

taxa (e.g. Jones *et al.*, 2013; Nadeau *et al.*, 2013), consistent with the estimated age of onset of diversification of the *L tessellatus* species complex (2.7 Ma, Faria *et al.*, 2016; 1.24 Ma, Machado *et al.*, 2017).

Methods

Sampling

The *Laparocerus tessellatus* complex is comprised of 10 taxonomically described species and an additional undescribed species, which form a monophyletic group based on a Bayesian phylogenetic analysis using both nuclear and mitochondrial markers (Fig. 1; Machado *et al.*, 2017). All species are single island endemics, distributed across four islands: five on Gran Canaria (*L. microphthalmus* Lindberg, 1950, *L. obsitus* Wollaston, 1864, *L. osorio* Machado, 2012, *L. tirajana* Machado, 2012, and *L.sp. aff. tirajana*), four on Tenerife (*L. tessellatus* Brullé, 1839; *L. freyi*, Uyttenboogaart, 1940; *L. canescens*, Machado, 2016; *L. punctiger*, Machado 2016) and one on each of La Palma (*L. auarita*, Machado, 2016) and El Hierro (*L. bimbache,* Machado, 2011). Here we increase the previous sampling performed for the species complex (Faria *et al.*, 2016; García-Olivares *et al.*, 2017), Chapter I) with 77 new localities, by adding 14 localities in El Hierro and 63 in Tenerife (Fig. 2).

MtDNA sequencing

From each locality, a minimum of 3 individuals per taxon were sequenced (unless limited by sample number). DNA extraction was performed using the two hind legs and a Chelex extraction protocol (Casquet et al., 2012). The mitochondrial COII marker was amplified using previously described conditions (Faria *et al.*, 2016) and sequenced using the Sanger DNA sequencing service of Macrogen (www.macrogen.com). Sequence editing was performed using GENEIOUS R10.2.2 (http://geneious.com, Kearse *et al.*, 2012) and aligned

with sequences from Faria *et al.* (2016) and García-Olivares *et al.* (2017, Chapter I) using MAFFT 6.814 (Katoh *et al.*, 2002).

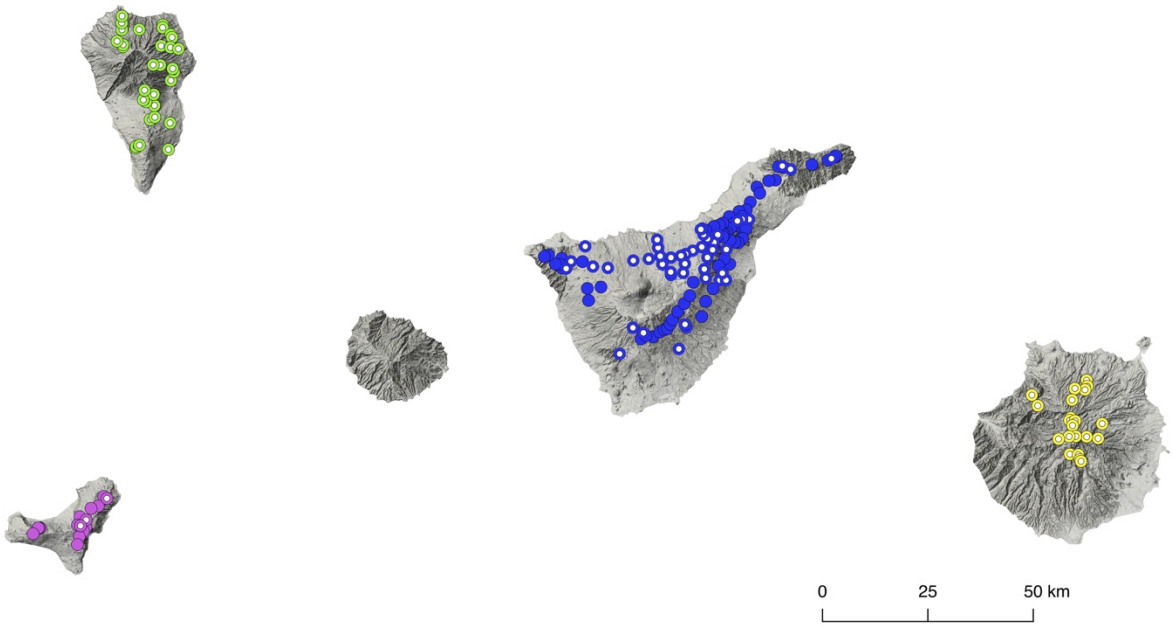

Figure 2. Map of sampling sites for the *Laparocerus tessellatus* complex across the Canarian Archipelago. Sampling sites are colour coded with respect to island: yellow – Gran Canaria, blue – Tenerife, green – La Palma, pink – El Hierro. Sampling sites from Faria et al. (Faria *et al.*, 2016) and García-Olivares et al. (2017) are indicated with a white dot inside the coloured circle.

ddRAD-seq library preparation

For the preparation of genomic libraries, at least one individual per taxon and sampling site was selected, increasing that number of individuals in localities with divergent mtDNA lineages in sympatry, by adding one individual per each divergent lineage shown. Individuals selected for ddRAD-seq analysis were subject to DNA extraction using the Qiagen DNeasy Blood & Tissue kit following the manufacturer's instructions. A total of 275 individuals of the *L. tessellatus* complex from 174 different localities, plus an individual of *L. vicinus* (Lindberg, 1953), used as an outgroup, were chosen for a ddRAD-seq analysis following modifications to the protocol of Mastretta-Yanes *et al.* (2015, full details of the protocol are included in Appendix S1). Individuals were sequenced across two experiments, the first included 48 samples (including four replicates and two negative controls)

performed using two sequencing indexes (ddRAD-seq libraries hereafter). Both ddRAD-seq libraries from the first experiment were sequenced across a single lane of an Illumina HiSeq2500 (Lausanne Genomic Technologies Facility, University of Lausanne, Switzerland). The mean depth estimates from this experiment (see results) was used to optimise the maximum number of samples per Illumina lane with sufficient depth, determined to be 80 individuals per lane. The remaining 234 individuals were thus sequenced across three different lanes, in which each lane was comprised of 80 samples (78 individuals, plus 1 replicate and 1 negative control) distributed across four ddRAD-seq libraries. Within each lane, samples were randomly assigned to one of four libraries for each (3 libraries with 24 samples, 1 library with 8 samples).

Bioinformatic steps

The bioinformatic processing of the ddRAD-seq raw data provided by Illumina was performed with IPYRAD 0.7.19 (Eaton & Overcast, 2016). For the demultiplexing step, a strict filter was applied for which only reads with unambiguous barcodes and with fewer than 5 low quality bases (Phred quality score < 20) were retained. To identify optimal parameter values a sensitivity analysis was performed using a reduced dataset. Individuals from Gran Canaria species were selected as a representative dataset, due to the higher genetic distances among individuals within the nuclear phylogeny (Faria *et al.*, 2016). A range of parameter values were explored for clust_threshold (0.85, 0.87, 0.90 and 0.93), max_SNPs_locus (5, 10, 15, 20, 40) and min_samples_locus (40%, 60%, 80% and 90%), with all remaining parameter values set to their default values, yielding a total of 80 different combinations. Outputs from each analysis were processed using VCFTOOLS (Danecek *et al.*, 2011) to calculate: (i) total number of loci, (ii) the distribution of SNPs across loci, (iii) mean depth, and (iv) missing data. Results from the 80 parameter combinations were used to evaluate the effect of each parameter on the number of loci recovered as (i) the parameter value varies in a background of fixed values for other parameters and (ii) as other parameter values are varied while the parameter of interest remains constant. These

observations were then used to (i) identify and exclude parameter values that indicate assembly problems, and then (ii) identify parameter combinations that yield a high number of loci.

MtDNA analysis

A Bayesian tree was constructed applying the same parameters described in Faria *et al.* (2016) using MRBAYES 3.2.6 (Ronquist *et al.*, 2012). Four independent analyses were run, each for 25 million generations using 4 Markov chain Monte Carlo (MCMC) chains, and sampling trees every 10000 generations discarding 25% of samples as burn-in. Stationarity and convergence of chains were visualized in TRACER 1.7 (Rambaut *et al.*, 2018) with only estimated sample size above 200 for all parameters being accepted. The final tree was visualized in FIGTREE 1.4.2 (Rambaut & Drummond, 2014).

Phylogenomic analysis

In order to investigate phylogenomic relationships among individuals within the complex, we adopted a supermatrix approach (de Queiroz & Gatesy, 2007), generating a single alignment by concatenating all SNPs. Maximum-likelihood analysis was then conducted with RAxML v.8.2.9 (Stamatakis, 2014) using a GTR+G+I model (inferred using a Smart Model and Bayesian Information Criterion in PhyML; Lefort *et al.*, 2017) of sequence evolution and 1,000 rapid bootstrap replicates. The resulting tree was visualized and edited in FIGTREE 1.4.2 (Rambaut & Drummond, 2014) and rooted with *L. vicinus* (Lindberg, 1953). Furthermore, in order to evaluate the consistency of the topology recovered by maximum-likelihood approach and to compare the nuclear data with the mitochondrial Bayesian tree, we carried out a Bayesian inference phylogenetic analysis using the same supermatrix. In order to optimize the computation time in MRBAYES, we reduced the number of generations for each of the four independent analyses from 25 to 1 million employing 4 MCMC chains, sampling trees every 1000 generations and discarding 25% of samples as burn-in. For the

rest of parameters, we used the same scheme described by Faria *et al.* (2016). Pairwise genetic distances between individuals across the archipelago were estimated using an uncorrected p-distance with SplitsTree v4 (Huson & Bryant, 2006). Differences among islands, with respect to within island genetic divergences, were tested using a non-parametric Kruskal-Wallis test followed by a Games-Howell Test's nonparametric all-pairs comparison test performed in the R package PMCMRplus (Pohlert, 2018) in R v. 3.4.2 (R Core Team 2013).

Mitochondrial DNA and nuclear DNA topology comparison

In order to compare the same individuals across both data sets, the mitochondrial matrix was reduced to include only individuals for which ddRAD-seq data was obtained, yielding a total of 257 individuals. To evaluate dissimilarity between mitochondrial and nuclear topologies, a Robinson-Foulds (RF) distance was calculated (Robinson & Foulds, 1981) using the ETE Toolkit (Huerta-Cepas *et al.*, 2016), exploring a range of parameter values for branch support limit (0.7, 0.9 and 1). Furthermore, trees were visually compared using the 'cophyloplot' function from the R package ape (Paradis & Schliep, 2019) and plotted as ultrametric phylogenetic trees. Interaction lines connecting branch to branch were drawn in order to show unshared branching events and evaluate inconsistencies between topologies.

Results

Mitochondrial COII marker

From the 72 sampling sites, a total of 442 individuals were sequenced for the mtDNA COII marker, that together with the 394 individuals from 103 localities analysed in García-Olivares *et al.* (2017, Chapter I) generated a dataset comprised of 836 individuals

representing 182 localities across the geographic range of the *L. tessellatus* complex (Table S1). The aligned sequence data matrix comprised 630 nucleotides, characterized by 213 polymorphic sites, of which 166 were parsimony informative.

Phylogenetic analysis of mtDNA

The four independent MCMC Bayesian runs showed suitable mixing with large effective sample sizes (ESS > 200), and converged successfully to a stationary phase, with an average standard deviation of split frequencies of 0.027 and an average potential scale reduction factor for parameter values of 1. The general patterns inferred by our phylogeny were consistent with those of Faria *et al.* (2016), indicating that mtDNA lineage variation within the complex is currently well characterised, and it is unlikely there are unsampled lineages. Early branching events are poorly supported, with higher support at more derived nodes (Fig. 3). Two independent well-supported clades revealed a polyphyletic origin for the single endemic species *L. auarita* from La Palma. One clade comprised individuals from La Palma together with individuals from Gran Canaria, with high support (PP = 1), while the other clade includes individuals from Tenerife, with moderate support (PP = 0.93). Within this last clade, individuals from La Palma are distributed among several subclades, and are clearly not monophyletic. The single endemic species from El Hierro, *L. bimbache*, reveals two monophyletic lineages of independent origin, albeit one with limited support. A highly supported clade of *L. bimbache* was nested within a clade of individuals from La Palma. The remaining individuals from El Hierro were most closely related to individuals from Gran Canaria, although with limited support.

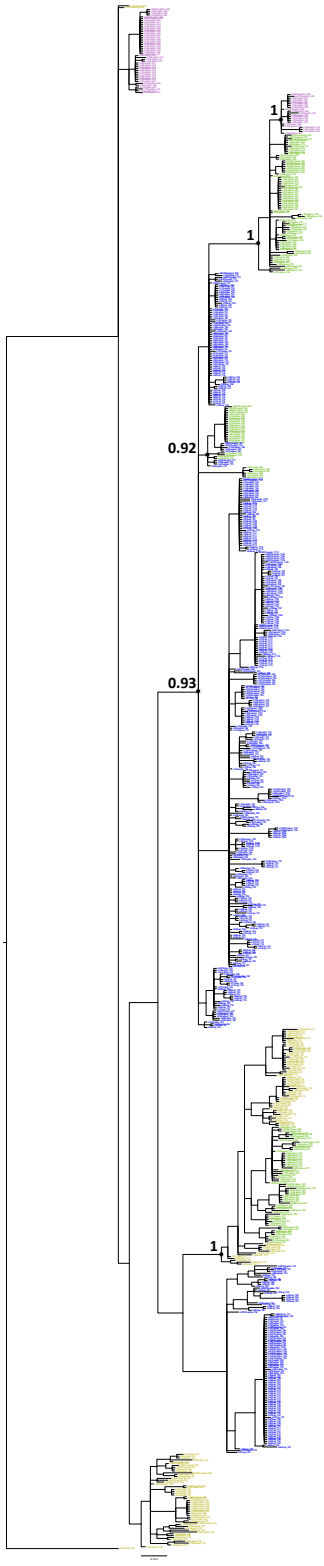

Figure 3. Bayesian tree. Bayesian phylogenetic tree constructed from 836 individuals for the mtDNA COII gene sampled from the *Laparocerus tessellatus* complex. Individuals are colour coded to represent their island of origin (see Fig. 2). Gran Canaria: *L. microphthalmus* = Lapmic, *L. obsitus* = Lapobs, *L. osorio* = Laposo, *L. tirajana* = Laptir, and *L. sp. aff. tirajana* = Lapaft. Tenerife: *L. tessellatus* = Laptes, *L. freyi* = Lapfre, *L. punctiger* = Lappun, and *L. canescens* = Lapcan; La Palma: *L. auarita* = Lapaua. El Hierro: *L. bimbache* = Lapbim. A full version of the tree with all sampled individuals is provided in Fig. S3.1 (in Appendix S3).

Sensitivity analysis of ddRAD-seq data

A total of 178.37 million reads were sequenced for the dataset from Gran Canaria, of which 169.85 million reads passed the quality filtering steps of IPYRAD pipeline. Per sample an average of 3.46 (± 1.58 SD) million reads were recovered. Results from the optimization step are summarised in Figure S2 (Supporting Information). Lower values for min_samples_locus resulted in the recovery of more loci across the 80 parameter combinations explored within IPYRAD for genotype assembly. However, a trend toward a decreasing number of recovered loci was observed at values of 40% and 60% as the value of clust_threshold was reduced, at a given value for max_SNPs_locus, being more pronounced for lower values of min_samples_locus. This counterintuitive trend suggests that at lower values for min_samples_locus, divergent alleles may be excluded during clustering, allowing for the partial assembly of loci across a subset of individuals presenting a subset of less divergent alleles. Thus, while lower values of min_samples_locus may be appealing for the larger number of loci they can potentially retrieve, we chose to avoid such parameter combinations (i.e. those with min_samples_locus of 40% and 60%) due to concerns that they may increase genotyping error. In contrast, the number of recovered loci increased as clust_threshold was reduced for values of 80% and 90% for min_samples_locus, consistent with the expectation that, for a given value of max_SNPs_locus, as clust_threshold is decreased, loci with more divergent alleles are assembled.

From the remainder of the sensitivity analyses including min_samples_locus = 80% or 90%, the parameter combination yielding the highest number of loci was as follows: clust_threshold = 0.85, max_SNPs_locus = 40, min_samples_locus = 80%, yielding a total of 4576 (± 228.14 SD) loci per sample, with 11.12% of missing data. In contrast to this relaxed parameter combination, the most conservative parameter combination (clust_threshold = 0.93, max_SNPs_locus = 5, min_sample_locus = 90%) yielded an average of 512 (± 19.98 SD) loci per sample with 4.84% of missing data. The relaxed approach was selected as the optimal parameter combination to apply for the complete dataset, in order to recover a

suitable number of locus through the species forming the complex, given divergence among taxa. Locus and allele error rates were calculated using the sample replicate approach of Mastretta-Yanes *et al.* (2015) for this parameter combination revealing error rates of 0.029 and 0.002 respectively.

Bioinformatic processing of full ddRADseq dataset

The combination of relaxed parameters was applied to the full dataset of all individuals. From this dataset, 11 individuals were discarded, due to a low number of reads or a high level of missing data (more than 40%), reducing the final dataset from 276 to 265 individuals, from 172 different localities (Table S1). A total of 913.18 million reads were recovered, of which 895.71 million reads passed the quality filtering steps of the pipeline, and an average of 3.38 (± 1.79 SD) millions reads were recovered per sample. A total of 46,801 linked SNPs distributed across 1814 loci were recovered, with 11.51% (± 10.20 SD) of missing data. The average pairwise p-distance between individuals across the archipelago was 1.89%, with a maximum genetic distance of 5.27%. Gran Canaria presented the highest average p-distance within an island, with 2.72%, followed by Tenerife with an average of 0.09%. Both younger islands, La Palma and El Hierro, presented lower average p-distance with 0.05% and 0.03% respectively (Fig. 4). For all possible pair of islands combinations, we found highly significant differences (Games-Howell Test, $p < 0.05$).

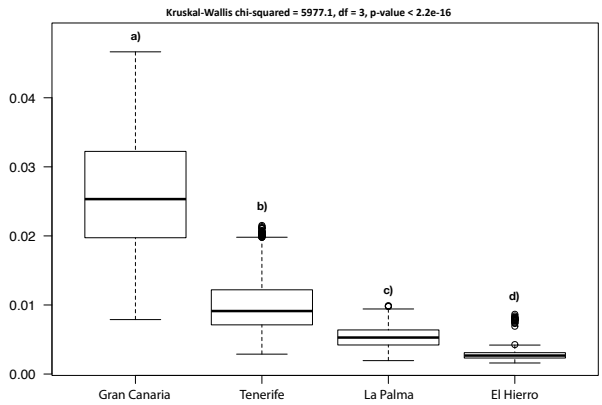

Figure 4. Box-plot diagram. Box-plot showing pairwise genetic distance among individuals per island. Significant differences ($p<0.05$) were found between all pairs of islands (a, b, c, d).

Phylogenomic reconstruction

A concatenation of ddRADseq data, comprising 46,801 SNPs, was used to obtain a maximum likelihood (ML) phylogeny (Fig. 5). The nuclear genome data reveals a clear pattern of structuring within the *L. tessellatus* species complex by island, in the majority of the cases highly supported by bootstrap (100), with the exception of the La Palma clade which was less supported (85). The earliest branching events comprise three well-supported clades from Gran Canaria, each supported with a bootstrap value of 100. A single individual belonging to the Gran Canaria species *L. osorio* is closely related to a clade comprising all individuals from Tenerife, La Palma and El Hierro, with high support (100), and placed as a sister lineage, but with only moderate support (75). Two lineages, each belonging to the respective single endemic species from La Palma and El Hierro, are highly supported as sister lineages (100), and nested within a bigger clade that includes all individuals from Tenerife. One individual from El Hierro was found nested within the clade of individuals from La Palma.

Phylogeny comparison

Bayesian phylogenetic trees derived from mtDNA and nuclear DNA (nDNA) analyses of the same set of individuals are presented in Figure 6. The average RF distance between both trees across the three different thresholds was 0.93. With minor exceptions, the nuclear topology recovered a pattern of structuring of individuals by island contrasting strongly with the mitochondrial topology, which presents a more complex pattern of relatedness among islands. Both trees recovered individuals from Gran Canaria within the earliest branching events, highly supported by the nuclear data (PP = 1.0). Relationships among individuals within the species from the younger islands of La Palma and El Hierro present clear phylogenetic conflict between mtDNA and nDNA. The mitochondrial topology infers a polyphyletic origin for each island. In contrast, the nuclear data strongly supports a single origin for each island. *Laparocerus auarita* and *L. bimbache* are each recovered as

monophyletic, with the exception of one individual of *L. bimbache* falling within the *L. auarita* clade.

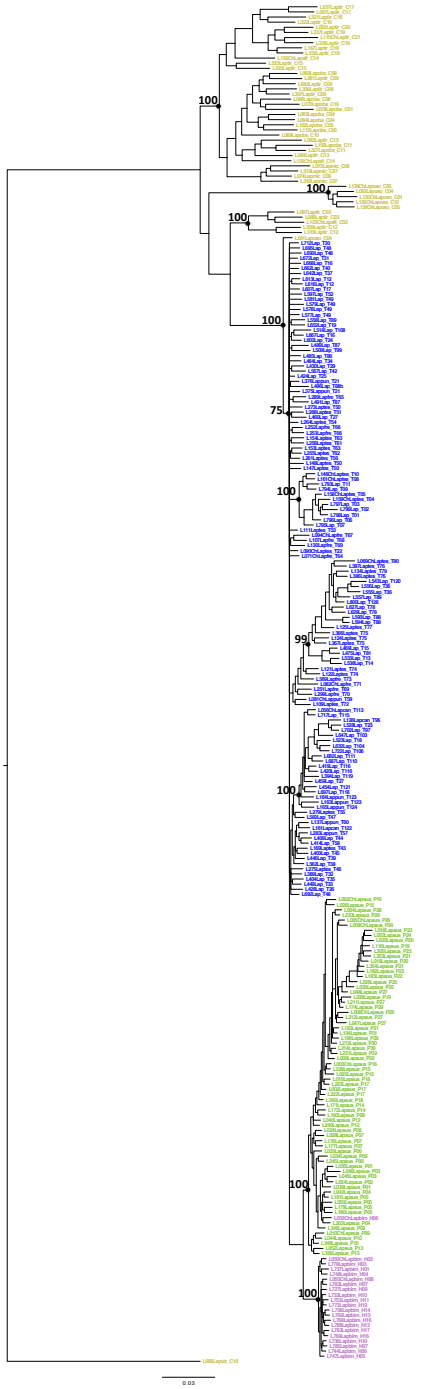

Figure 5. Maximum-likelihood tree. Maximum-likelihood phylogenetic tree constructed using a nuclear sub-genomic alignment of concatenated SNPs, sampled from 265 individuals of the *Laparocerus tessellatus* complex. Individuals are colour coded to represent their island of origin (see Fig. 2). Gran Canaria: *L. microphthalmus* = Lapmic, *L. obsitus* = Lapobs, *L. osorio* = Laposo, *L. tirajana* = Laptir, and *L. sp. aff. tirajana* = Lapaft. Tenerife: *L. tessellatus* = Laptes, *L. freyi* = Lapfre, *L. punctiger* = Lappun, and *L. canescens* = Lapcan; La Palma: *L. auarita* = Lapaua. El Hierro: *L. bimbache* = Lapbim. A full version of the tree with all sampled individuals is provided in Fig. S3.2 (in Appendix S3).

Discussion

The nuclear genomic (ddRAD-seq) data provide strong evidence for a Gran Canaria origin for the species complex, due to the earliest branching events involving lineages that are solely comprised of individuals from Gran Canaria. Faria *et al.* (2016) pointed out that the almost exclusively Gran Canarian origin of all lineages within the higher level *Pecoudius* taxonomic group that the complex belongs to Machado *et al.* (2017) argues for a Gran Canarian origin of the *L. tessellatus* complex, and provided suggestive population-level genetic data to support this. The data presented here reinforces this suggestion, providing a compelling argument for a Gran Canarian origin.

Within the nuclear genomic phylogeny, strong phylogeographic signal was found, with relationships among individuals consistent with a single founding event for each island, with only two minor exceptions involving single individuals on Gran Canaria and El Hierro. An individual sampled on El Hierro and assigned to *L. bimbache*, clustered within a clade exclusively formed by individuals sampled from La Palma identified as *L. auarita*. In the other case, an individual which is unequivocally assigned to *L. osorio* from Gran Canaria, the largest sized and therefore the most clearly differentiated species within the complex, was inferred by nuclear genomic data to be more related to individuals from Tenerife, but with contrasting positions under both phylogenetic approaches. Under the maximum-likelihood approach, this individual was found as a sister lineage to Tenerife, while within the Bayesian tree it was recovered to be nested within the Tenerife clade. One potential explanation for the phylogenetic position of this individual is a back colonisation event, whereby Tenerife was first colonised from Gran Canaria, followed by a latter colonisation event from Tenerife to Gran Canaria. Back colonisation among islands has been demonstrated in other taxa (Juan *et al.*, 2000; Arnedo *et al.*, 2008; González-Pérez *et al.*, 2009), particularly within the Canarian archipelago. A study of the spider species *Titanidiops canariensis* revealed a potential back colonisation between the south of Lanzarote and Fuerteventura islands, using both nuclear and mitochondrial markers within a phylogeographic approach (Opatova & Arnedo, 2014). However, such an explanation

would imply the independent and convergent evolution of the distinct *L. osorio* morphology twice from a Tenerife ancestor. It would seem that the history of this lineage is more complex than simple back colonisation, and the contrasting phylogenetic positions inferred by Bayesian and maximum likelihood analyses are suggestive of a history including both back colonisation and introgression.

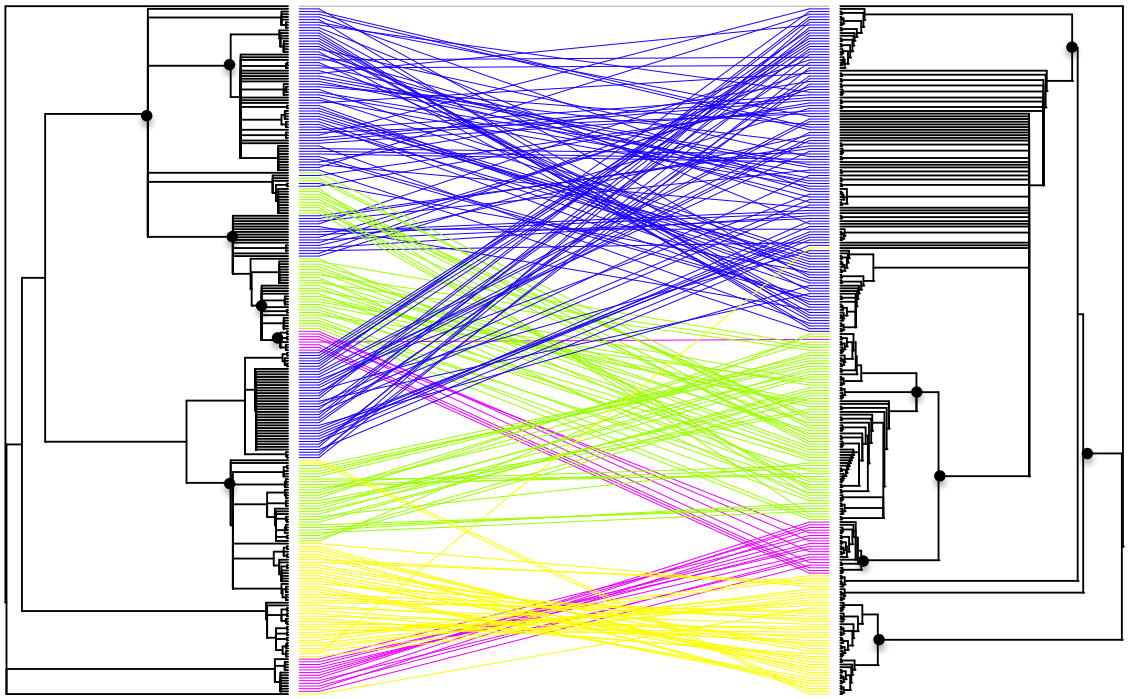

Figure 6. Phylogeny comparison. Comparison between mitochondrial DNA (left), and nuclear DNA (right) phylogenetic trees. Interaction lines connecting branch to branch with each colour representing island of origin (see Fig. 2). The interaction line between the outgroup *L. vicinus* is representing by grey colour. Black dots indicate a posterior probability more than 0.99.

The strong structuring by island of the nuclear genomic data contrasts with the mitochondrial topology that infers more complex relationships among islands. The clear structuring by island with nuclear genomic data, with no clear signatures of introgression among species from different islands, also argues against the hypothesis of admixture among multiple colonizing lineages, proposed by Faria *et al.* (2016) for the islands of La Palma and El Hierro. Mitochondrial introgression seems a simpler explanation for the patterns observed by Faria *et al.* (2016). The two older islands of Gran Canaria and Tenerife

revealed contrasting nuclear genomic patterns. In Gran Canaria, the presence of highly divergent and well-supported clades contrasts with the shallower divergences within Tenerife, which were also observed in the lineages occurring on El Hierro and La Palma.

Extensive divergence and lineage formation within Gran Canaria

Individuals sampled from Gran Canaria are clearly structured into several well-supported and highly divergent clades at the nuclear genome level. Two of the clades are exclusively comprised of all sampled individuals from the single taxonomic species, *L. microphthalmus* and *L. osorio*. These results clearly indicate that the evolution of divergent lineages is associated more with the island of Gran Canaria than the other islands, possibly due to one of two explanations, or a combination of both. Gran Canaria is the origin of the species complex, and has thus had more time for diversification in comparison with the remaining more recently colonised islands. A second potential explanation is related to geological activity and the topography of Gran Canaria. Gran Canaria has a complex topography. This, together with the relatively geological quiescence of Gran Canaria over the last 3 million years, which predates estimates for the initiation of diversification within the *L. tessellatus* species complex (2.7 Ma, Faria *et al.*, 2016; 1.24 Ma, Machado *et al.*, 2017), may explain the high levels of divergence through greater opportunity for population isolation, divergence and persistence. In order to understand the drivers of structure within Gran Canaria, a more detailed process-oriented analyses of the data are required.

Limited divergence within Tenerife

The nuclear genomic tree reveals three well-supported lineages within the island of Tenerife, each with a discrete geographic distribution, representing with minor exceptions three regions within Tenerife, the northern and southern flanks of the island, and the north-east of the island (Fig. 7). The remaining individuals within the tree presented unresolved relationships. Two potential explanations can be put forward for this pattern: (1) a history

involving longer-term persistence and stability of populations in some regions, with admixture among these populations in intermediate geographic areas, or (2) incomplete lineage sorting (Funk & Omland, 2003; Toews & Brelsford, 2012). Both explanations, or a combination of both, are plausible. Although geological elements of Tenerife date back more than 10 million years, much of the island is geologically young, and gravitational flank collapses have featured substantially over a large area of the island over then last 2 million years García-Olivares *et al.* (2017, Chapter I). Thus, compared to Gran Canaria, much of the surface area of Tenerife is the product of recent eruptive volcanic activity and catastrophic flank collapses. The island-wide signature of high relatedness among individuals derived from a relatively young common ancestor is thus suggestive of a causal relationship between geological process and population-level process. But similar to the case for Gran Canaria, a more detailed process-based investigation of the data is required to test this explicitly.

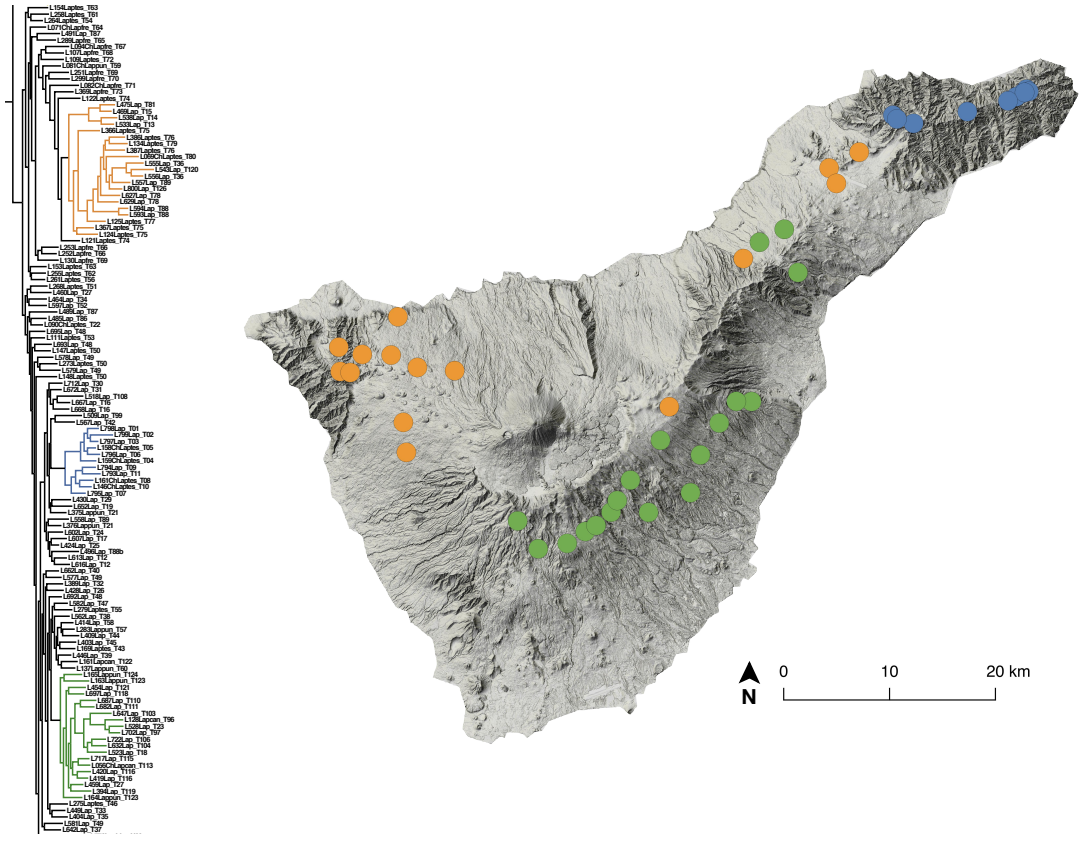

Figure 7. Geographic distribution of the three well-supported lineages inferred within the maximum-likelihood phylogenetic tree using the nuclear genome data. Individuals within the topology and their respective sampling points within the geographic map are colour coded representing each one lineage. *L. tessellatus* = Laptes, *L. freyi* = Lapfre, *L. punctiger* = Lappun, and *L. canescens* = Lapcan.

References

Andrews, K.R., Hohenlohe, P.A., Miller, M.R., Hand, B.K., Seeb, J.E. & Luikart, G. (2014) Trade-offs and utility of alternative RADseq methods: reply to Puritz et al. *Molecular Ecology*, **23**, 5943-6.

Arechavaleta, M., Rodríguez, S., Zurita, N. & García, A. (2010) *Lista de especies silvestres de Canarias. Hongos, plan- tas y animales terrestres*. Consejería de Medio Ambiente y Ordenación Territorial, Gobierno de Canarias.

Arnedo, M.A., Oromí, P., MartÍN De Abreu, S. & Ribera, C. (2008) Biogeographical and evolutionary patterns in the Macaronesian shield-backed katydid genusCalliphonaKrauss, 1892 (Orthoptera: Tettigoniidae) and allies as inferred from phylogenetic analyses of multiple mitochondrial genes. *Systematic Entomology*, **33**, 145-158.

Carstens, B.C., Pelletier, T.A., Reid, N.M. & Satler, J.D. (2013) How to fail at species delimitation. *Molecular Ecology*, **22**, 4369-83.

Danecek, P., Auton, A., Abecasis, G., Albers, C.A., Banks, E., DePristo, M.A., Handsaker, R.E., Lunter, G., Marth, G.T., Sherry, S.T., McVean, G. & Durbin, R. (2011) The variant call format and VCFtools. *Bioinformatics*, **27**, 2156-2158.

de Queiroz, A. & Gatesy, J. (2007) The supermatrix approach to systematics. *Trends in Ecology & Evolution*, **22**, 34-41.

Degnan, J.H. & Rosenberg, N.A. (2009) Gene tree discordance, phylogenetic inference and the multispecies coalescent. *Trends in Ecology & Evolution*, **24**, 332-40.

Eaton, D.A. & Overcast, I. (2016) ipyrad: interactive assembly and analysis of RADseq data sets. *Available from:* http://ipyrad.readthedocs.io/.

Economo, E.P., Sarnat, E.M., Janda, M., Clouse, R., Klimov, P.B., Fischer, G., Blanchard, B.D., Ramirez, L.N., Andersen, A.N., Berman, M., Guenard, B., Lucky, A., Rabeling, C., Wilson, E.O. & Knowles, L.L. (2015) Breaking out of biogeographical modules: range expansion and taxon cycles in the hyperdiverse ant genus Pheidole. *Journal of Biogeography*, **42**, 2289-2301.

Edwards, S.V. (2009) Is a new and general theory of molecular systematics emerging? *Evolution*, **63**, 1-19.

Edwards, S.V. & Beerli, P. (2000) Perspective: gene divergence, population divergence, and the variance in coalescence time in phylogeographic studies. . *Evolution*, **54**, 1839-1854.

Emerson, K.J.M., Clayton R.; Catchen, Julian M.; Hohenlohe, Paul A.; Cresko, William A.; Bradshaw, William E.; Holzapfel, Christina M. (2010) Resolving postglacial phylogeography using high-throughput sequencing. *Proceedings of the National Academy of Sciences*, **107**, 16196-16200.

Faria, C.M.A., Machado, A., Amorim, I.R., Gage, M.J.G., Borges, P.A.V. & Emerson, B.C. (2016) Evidence for multiple founding lineages and genetic admixture in the evolution of species within an oceanic island weevil (Coleoptera, Curculionidae) super-radiation. *Journal of Biogeography*, **43**, 178-191.

Funk, D.J. & Omland, K.E. (2003) Species-Level Paraphyly and Polyphyly: Frequency, Causes, and Consequences, with Insights from Animal Mitochondrial DNA. *Annual Review of Ecology, Evolution, and Systematics*, **34**, 397-423.

Funk, V.A. & Wagner, W.L. *Biogeographic patterns in the Hawaiian islands. Hawaiian biogeography: evolution on a hot spot archipelago*. Smithsonian Inst Press, Washington DC.

García-Olivares, V., López, H., Patiño, J., Alvarez, N., Machado, A., Carracedo, J.C., Soler, V. & Emerson, B.C. (2017) Evidence for mega-landslides as drivers of island colonization. *Journal of Biogeography*, **44**, 1053-1064.

Gavrilets, S. & Vose, A. (2005) Dynamic patterns of adaptive radiation. *Proceedings of the National Academy of Sciences*, **102**, 18040-18045.

González-Pérez, M.A., Sosa, P.A. & Batista, F.J. (2009) Genetic variation and conservation of the endangered endemic Anagyris latifolia Brouss. ex Willd. (Leguminosae) from the Canary Islands. *Plant Systematics and Evolution*, **279**, 59-68.

Huerta-Cepas, J., Serra, F. & Bork, P. (2016) ETE 3: Reconstruction, Analysis, and Visualization of Phylogenomic Data. *Molecular Biology and Evolution*, **33**, 1635-8.

Huson, D.H. & Bryant, D. (2006) Application of phylogenetic networks in evolutionary studies. *Molecular Biology and Evolution*, **23**, 254-67.

Hutchinson, G.E. (1959) Homage to Santa Rosalia or why are these so many kinds of animals? *American Naturalist*, **93**, 145-159.

Jones, J.C., Fan, S., Franchini, P., Schartl, M. & Meyer, A. (2013) The evolutionary history of Xiphophorus fish and their sexually selected sword: a genome-wide approach using restriction site-associated DNA sequencing. *Molecular Ecology*, **22**, 2986-3001.

Juan, C., Emerson, B.C., Oromí, P. & Hewitt, G.M. (2000) Colonization and diversification: towards a phylogeographic synthesis for the Canary Islands. *Trends in Ecology & Evolution*, **15**, 104-109.

Katoh, K., Misawa, K., Kuma, K.I. & Miyata, T. (2002) MAFFT: a novel method for rapid multiple sequence alignment based on fast Fourier transform. *Nucleic acids research*, **30**, 3059-3066.

Kearse, M., Moir, R., Wilson, A., Stones-Havas, S., Cheung, M., Sturrock, S., Buxton, S., Cooper, A., Markowitz, S., Duran, C., Thierer, T., Ashton, B., Meintjes, P. & Drummond, A. (2012) Geneious Basic: An integrated and extendable desktop software platform for the organization and analysis of sequence data. *Bioinformatics*, **28**, 1647-1649.

Knowles, L.L. (2009) Statistical Phylogeography. *Annual Review of Ecology, Evolution, and Systematics*, **40**, 593-612.

Knowles, L.L. & Maddison, W.P. (2002) Statistical phylogeography. *Molecular Ecology*, **11**, 2623-2635.

Leache, A.D., Fujita, M.K., Minin, V.N. & Bouckaert, R.R. (2014) Species delimitation using genome-wide SNP data. *Systematic Biology*, **63**, 534-42.

Leache, A.D., Chavez, A.S., Jones, L.N., Grummer, J.A., Gottscho, A.D. & Linkem, C.W. (2015) Phylogenomics of phrynosomatid lizards: conflicting signals from sequence capture versus restriction site associated DNA sequencing. *Genome Biology Evolution*, **7**, 706-19.

Lefort, V., Longueville, J.E. & Gascuel, O. (2017) SMS: Smart Model Selection in PhyML. *Molecular Biology and Evolution*, **34**, 2422-2424.

Losos, J.B. & Ricklefs, R.E. (2009) Adaptation and diversification on islands. *Nature*, **457**, 830-6.

Machado, A., Rodríguez-Expósito, E., López, M. & Hernandez, M. (2017) Phylogenetic analysis of the genus *Laparocerus*, with comments on colonisation and

diversification in Macaronesia (Coleoptera, Curculionidae, Entiminae). *Zookeys*, **651**, 1-77.

Maddison, W.P. (1997) Gene Trees in Species Trees. *Systematic Biologists*, **46**, 523-536.

Mastretta-Yanes, A., Arrigo, N., Álvarez, N., Jorgensen, T.H., Pinero, D. & Emerson, B.C. (2015) Restriction site-associated DNA sequencing, genotyping error estimation and de novo assembly optimization for population genetic inference. *Molecular Ecology Resources*, **15**, 28-41.

McCormack, J.E., Hird, S.M., Zellmer, A.J., Carstens, B.C. & Brumfield, R.T. (2013) Applications of next-generation sequencing to phylogeography and phylogenetics. *Molecular Phylogenetics and Evolution*, **66**, 526-38.

Nadeau, N.J., Martin, S.H., Kozak, K.M., Salazar, C., Dasmahapatra, K.K., Davey, J.W., Baxter, S.W., Blaxter, M.L., Mallet, J. & Jiggins, C.D. (2013) Genome-wide patterns of divergence and gene flow across a butterfly radiation. *Molecular Ecology*, **22**, 814-26.

Opatova, V. & Arnedo, M.A. (2014) Spiders on a Hot Volcanic Roof: Colonisation Pathways and Phylogeography of the Canary Islands Endemic Trap-Door Spider Titanidiops canariensis (Araneae, Idiopidae). *PLoS One*, **9**, e115078.

Oromí, P., Cruz, S. & Báez, M. (2010) *Psocoptera, Mallophaga, Anoplura, Hemiptera, Thysanoptera, Coleoptera, Strepsiptera, Siphonaptera.* ed. by M. Arechavaleta, S. Rodrígues, N. Zurita and A. García, Gobierno de Canarias, Santa Cruz de Tenerife.

Paradis, E. & Schliep, K. (2019) ape 5.0: an environment for modern phylogenetics and evolutionary analyses in R. *Bioinformatics*, **35**, 526-528.

Parent, C.E., Caccone, A. & Petren, K. (2008) Colonization and diversification of Galapagos terrestrial fauna: a phylogenetic and biogeographical synthesis. *Philosophical Transactions of the Royal Society B: Biological Sciences*, **363**, 3347-61.

Patiño, J., Whittaker, R.J., Borges, P.A.V., Fernández-Palacios, J.M., Ah-Peng, C., Araújo, M.B., Ávila, S.P., Cardoso, P., Cornuault, J., de Boer, E.J., de Nascimento, L., Gil, A., González-Castro, A., Gruner, D.S., Heleno, R., Hortal, J., Illera, J.C., Kaiser-Bunbury, C.N., Matthews, T.J., Papadopoulou, A., Pettorelli, N., Price, J.P., Santos, A.M.C., Steinbauer, M.J., Triantis, K.A., Valente, L., Vargas, P., Weigelt, P. & Emerson, B.C. (2017) A roadmap for island biology: 50 fundamental questions after 50 years of The Theory of Island Biogeography. *Journal of Biogeography*, **44**, 963-983.

Peterson, B.K., Weber, J.N., Kay, E.H., Fisher, H.S. & Hoekstra, H.E. (2012) Double digest RADseq: an inexpensive method for de novo SNP discovery and genotyping in model and non-model species. *PLoS One*, **7**, e37135.

Pohlert, T. (2018) Calculate Pairwise Multiple Comparisons of Mean Rank Sums Extended. *Available from :* https://cran.r-project.org/package=PMCMRplus,

Potter, S., Bragg, J.G., Peter, B.M., Bi, K. & Moritz, C. (2016) Phylogenomics at the tips: inferring lineages and their demographic history in a tropical lizard, Carlia amax. *Molecular Ecology*, **25**, 1367-80.

Rambaut, A. & Drummond, A. (2014) FigTree v.1.4.2: Tree Figure Drawing Tool. *Available from :* http://tree.bio.ed.ac.uk/software/figtree,

Rambaut, A., Drummond, A.J., Xie, D., Baele & G., S., M. A (2018) Posterior summarisation in Bayesian phylogenetics using Tracer 1.7. *Systematic Biology*, **10**, 1-3.

Robinson, D.F. & Foulds, L.R. (1981) Comparison of Phylogenetic Trees. *Mathematical Biosciences*, **53**, 131-147.

Roderick, G.K. & Gillespie, R.G. (1998) Speciation and phylogeography of Hawaiian terrestrial arthropods. *Molecular Ecology*, **7**, 519-531.

Ronquist, F., Teslenko, M., van der Mark, P., Ayres, D.L., Darling, A., Hohna, S., Larget, B., Liu, L., Suchard, M.A. & Huelsenbeck, J.P. (2012) MrBayes 3.2: efficient Bayesian phylogenetic inference and model choice across a large model space. *Systematic Biology*, **61**, 539-42.

Schluter, D. (2001) *A synthesis of adaptive radiation*. Oxford University, New York.

Stamatakis, A. (2014) RAxML Version 8: A tool for Phylogenetic Analysis and Post-Analysis of Large Phylogenies. *Bioinformatics*, **30**, 1312-1313.

Toews, D.P. & Brelsford, A. (2012) The biogeography of mitochondrial and nuclear discordance in animals. *Molecular Ecology*, **21**, 3907-30.

Wagner, C.E., Keller, I., Wittwer, S., Selz, O.M., Mwaiko, S., Greuter, L., Sivasundar, A. & Seehausen, O. (2013) Genome-wide RAD sequence data provide unprecedented resolution of species boundaries and relationships in the Lake Victoria cichlid adaptive radiation. *Molecular Ecology*, **22**, 787-98.

Warren, B.H., Simberloff, D., Ricklefs, R.E., Aguilee, R., Condamine, F.L., Gravel, D., Morlon, H., Mouquet, N., Rosindell, J., Casquet, J., Conti, E., Cornuault, J., Fernandez-Palacios, J.M., Hengl, T., Norder, S.J., Rijsdijk, K.F., Sanmartin, I., Strasberg, D., Triantis, K.A., Valente, L.M., Whittaker, R.J., Gillespie, R.G., Emerson, B.C. & Thebaud, C. (2015) Islands as model systems in ecology and evolution: prospects fifty years after MacArthur-Wilson. *Ecology Letters*, **18**, 200-17.

Wendel, J.F. & Doyle, J.J. (1998) *Phylogenetic incongruence: window into genome history and molecular evolution.* Kluwer Academic Publishers, Boston.

Whittaker, R.J. & Fernandez-Palacios, J.M. (2007) *Island Biogeography: Ecology, Evolution, and Conservation*. Oxford University Press, Oxford, UK.

Yoder, A.D., Campbell, E.O., Blanco, M.B., dos Reis, M., Ganzhorn, J.U., Goodman, S.M., Hunnicutt, K.E., Larsen, P.A., Kappeler, P.M., Rasoloarison, R.M., Ralison, J.M., Swofford, D.L. & Weisrock, W. (2016) Geogenetic patterns in mouse lemurs (genus Microcebus) reveal the ghosts of Madagascar's forests past. *Proceedings of the National Academy of Sciences*, **113**, 8049-8056.

Supporting information

Appendix S1. Double digest RAD (ddRAD) sequencing protocol

GEEI lab double digest RAD (ddRAD) sequencing protocol

Sept 2018

This protocol is a modification of that presented in Mastretta-Yanes et al. (2015, doi: 10.1111/1755-0998.12291). It has been prepared for the analysis of beetles, which have a typical genome size of around 0.6 Gb (there seems to be very little variation around this value based on published genome size estimates). We've applied it to species from 14 different genera sampled from across the beetle tree of life, with fairly consistent results, in terms of fragment analysis profiles and final data yield.

The protocol applies barcoding with indexing which allows one to pool 288 samples per library for the price of 61 oligos (24x2 for P1 adapters + 2 for P2 adapter + 1 PCR1 primer + 12 ILLPCR2 primers). It can be easily adapted to a pool of 1,152 samples if using 96 P1 barcoded adapters instead of 24.

Although we have yet to explore it, we think this protocol should be easily adapted to larger genomes. For any clarifications, you can contact:
Brent Emerson: bemerson@ipna.csic.es
Jairo Patiño: jpatino.llorente@gmail.com
Víctor García Olivares: victor.garcia.olivares@gmail.com

Glossary

Adapter: fully or partially double-stranded product of annealing two oligos. Adapters are ligated to genomic DNA at restriction enzyme cut sites in order to add barcodes and common PCR priming sequences.

Barcode: short DNA sequence downstream of the sequencing primer annealing region of an adapter. Used to resolve products of different ligation reactions (usually separate individuals) after sequencing pooled libraries.

Fragment: section of genomic DNA resulting from restriction enzyme cleavage.

Index: short DNA sequence introduced during PCR amplification of the final library that uniquely identifies products of that PCR reaction. Used combinatorially with Adapter P1 barcodes to resolve multiplexed sample pools.

Index Pool: the pool of all individuals with a particular index. Useful for grouping individuals from the same species for fragment analysis (step) and the subsequent size selection procedure.

Library: a collection of sequencing-competent fragments. Comprised of one or more index pools.

Notice that the dual indexing involves a barcode and an index, while other protocols use a single sequence-tag.

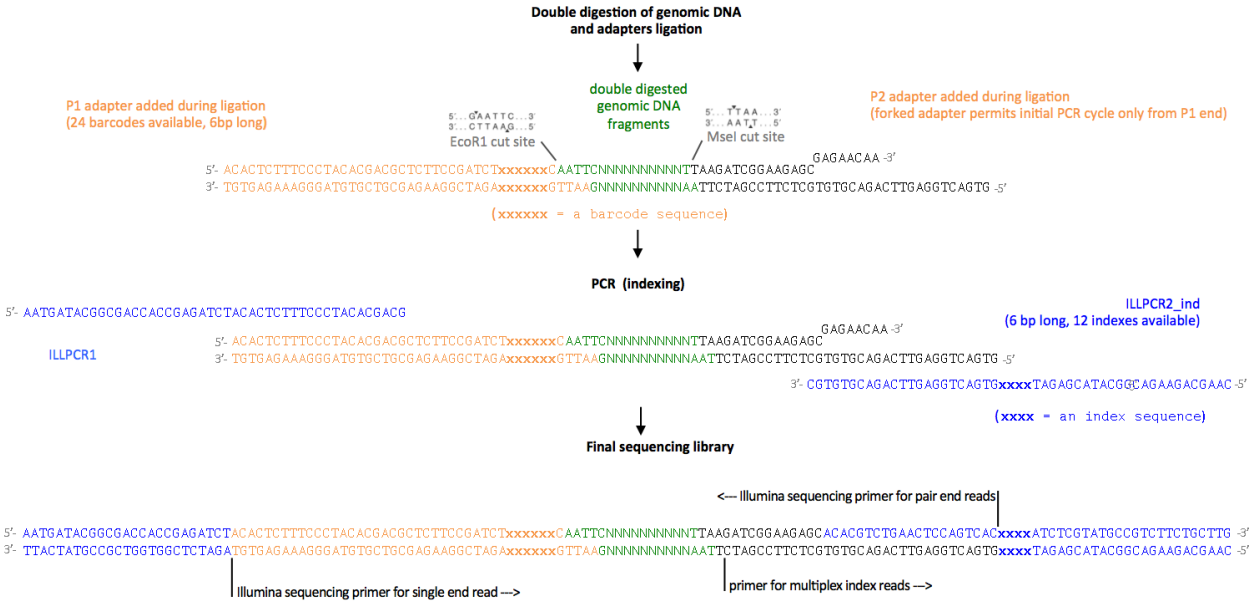

Figure 1. Diagram of library preparation and the final structure of the sequencing library.

Note on experimental design

Include replicates of some of the samples and a negative control. Randomize the position of the samples in the plate. The negative control should be treated as a normal sample though the whole protocol. If you are going to include species from different genera in the final library, then it will be wise to use a different index for each species. This means that species are treated individually until index pools are combined in the final step of library preparation, and will facilitate decisions about size selection for each index pool. I.e. index pools for different species, due to their different genomes, are likely to present different fragment distributions in Step VI, which helps decision making about the size selection for the library. If individuals from species were randomised across different indices, then any unusual spikes in the fragment distribution of a given species (which we want to avoid selecting) could have their signal diluted.

Note on starting DNA material

DNA should ideally be at a minimum concentration of 20 ng/µL and a maximum concentration of 150 ng/µL, but lower concentrations (down to ~ 2 ng/µl) may still work. It is advisable to homogenize sample's concentration before digestion if the variation is orders of magnitude larger.

DNA is extracted using a Qiagen extraction kit, and the tissue used will depend on the size of the species. E.g. for a beetle with a body length of 2-3cm, a pair of legs should be appropriate. For smaller body sizes one can (i) increase the number of legs extracted, (ii) include the head and pronotum, (iii) use the whole individual. The important point is to standardise within species. We elute DNA in a final volume of 100ul of elution buffer.

Enzymes

We used New England Biolabs enzymes: EcoRI-HF (R3101S), MseI (R0525S), T4 DNA Ligase (M0202S), Q5 polymerase (M0493), and their corresponding buffers.

0. Preparation of adaptors and primer working solutions

P1 adapters:

The P1 adapters consist of 24 barcodes of 6bp long (Table 1) at the end of core sequence ACACTCTTTCCCTACACGACGCTCTTCCGATCT, and an overhang (AATT) at the 5' end of the P1_n.2 oligo that matches the cut site of the EcoR1 restriction enzyme (change this overhang to adapt to other enzymes). The barcodes were designed using the Python script at https://bioinf.eva.mpg.de/multiplex/. In this set of 24, all of the barcodes are separated from each other by at least 3 substitutions.

To prepare the adapter mix for P1 add 98 µl of water to as many PCR wells as P1 barcoded adapters are desired (24 in this case). Then add primer pairs (P1_n.1 with P1_n.2) by mixing 1 µL of each oligo in a pair (100 µM stock). If organized as in Figure 2, from the oligos 100 µM stock plate mix column 1 with column 4, column 2 with column 5, column 3 with column 6 f to generate the plate of annealed 1 µM P1 adapters. Heat to 95ºC for 5 minutes and bring to 20ºC with a ramp of 0.1 ºC/s to slowly cool down. Once they are ready it is possible to freeze it for later use. Keep the set of adaptors organized in plate format that is convenient for later use in setting up reactions. Notice that the barcodes of these adapters are "base balanced", thus if using less than the full complement provided here you must subset them according with the suggest_subset.py script from https://bioinf.eva.mpg.de/multiplex/.

Plate oligos P1 100µM stock

	1	2	3	4	5	6
A	P1_01.1	P1_09.1	P1_17.1	P1_01.2	P1_09.2	P1_17.2
B	P1_02.1	P1_10.1	P1_18.1	P1_02.2	P1_10.2	P1_18.2
C	P1_03.1	P1_11.1	P1_19.1	P1_03.2	P1_11.2	P1_19.2
D	P1_04.1	P1_12.1	P1_20.1	P1_04.2	P1_12.2	P1_20.2
E	P1_05.1	P1_13.1	P1_21.1	P1_05.2	P1_13.2	P1_21.2
F	P1_06.1	P1_14.1	P1_22.1	P1_06.2	P1_14.2	P1_22.2
G	P1_07.1	P1_15.1	P1_23.1	P1_07.2	P1_15.2	P1_23.2
H	P1_08.1	P1_16.1	P1_24.1	P1_08.2	P1_16.2	P1_24.2

Plate 1µM annealed P1 adapters

	1	2	3
A	P1_01	P1_9	P1_17
B	P1_02	P1_10	P1_18
C	P1_03	P1_11	P1_19
D	P1_04	P1_12	P1_20
E	P1_05	P1_13	P1_21
F	P1_06	P1_14	P1_22
G	P1_07	P1_15	P1_23
H	P1_08	P1_16	P1_24

Figure 2. Oligos and annealed P1 adapters

P2 adapter

The P2 adapters presented here (Table 2) are compatible with MseI. To prepare the working solution mix 100 µL of the P2.1_MseI and P2.2_MseI oligos (100 µM stock) with 800 µL of water to make 1000 µL of 10 pmole/µL (10 µM) stock. Heat to 95ºC for 5 minutes and bring to 20ºC with a ramp of 0.1 ºC/s to slowly cool down. Freeze for later use.

PCR primers

Mix 50 µL of the ILLPCR1 and ILLPCR2_ind oligos (Table 2) with 900 µL of water to make a working solution (5 µM of each oligo). The dual-indexing barcode is incorporated in the ILLPCR2_ind oligo, so **this step must be repeated for each dual-indexing barcode** (mixing each uniquely barcoded version of ILLPCR2 with ILLPCR1, which will be the same oligo in all working solutions).

Note: If using only 2 indexed primers (i.e. to pool 24x2=48 samples) Illumina recommends to use the ILLPCR2_ind06 and ILLPCR2_ind12. If three primers, use 4, 6, 12. If six primers: 2,4,5,6,7,12.

I. Double restriction digest

1. Prepare master mix I (see below, 3 µL prepared per sample), mix and centrifuge. We have found that making 1.2x per sample is sufficient to avoid running out due to high viscosity and/or pipetting error. Work on ice all times.

MASTER MIX I: DIGESTION	
EcoR1-MseI	**Vol (µl) 1x**
10X T4 Buffer	0.9
1 M NaCl	0.45
1 mg/mL BSA	0.45
H2O	0.85
MseI (10,000 U/ml)	0.1
EcoR1 (HF) (20,000 U/ml)	0.25
Total mix volume per sample	3

2. Place 6 µL of sample DNA in each well of a plate.
3. Add 3 µL of the combined master mix I to each well. The total reaction volume should be 9 µL.
4. Cover and seal the plate, centrifuge and incubate at 37°C for 10 hours* on a thermal cycler with a heated lid. Heat kill the enzyme with 20 mins at 65ºC. Keep at 4ºC afterwards.

Total volume of each sample available for the next step is 9µl

* The digestion time can be reduced to 3 hrs, but if the genome size is large it is advisable to perform the reaction during a long time to ensure complete digestion.

II. Adaptor Ligation

1. Thaw P1 and P2 adaptors. These adaptors should already be annealed (step 0).

2. Prepare master mix II (see below, 1.6 µL prepared per sample), mix well. As above, it is best to prepare an extra 20% (1.2x/sample).

MASTER MIX II: LIGATION	
EcoRI-MseI	**Vol (µl) 1x**
10x T4 Buffer	0.16
1M NaCl	0.13
1 mg/mL BSA	0.13
Water	0.0125
P2 (MseI) adapter 10 uM	1
T4 DNA Ligase (400,000 U/ml)	0.1675
Total mix volume per sample	1.6

3. Add 1.6 µL to each well of the restriction digested DNA.

4. Add 1 µL of the P1 (EcoR1) adaptor to each well (a unique barcoded adaptor for each DNA sample).

5. The total reaction volume should now be 11.6 µL. Cover and seal the plate, vortex softly, centrifuge and incubate at 16° C for 6 hours on a thermocycler.

6. Dilute the Restriction-Ligation reaction with 100 µL of 10 mM Tris-HCl pH 8.5 (or 0.1x TE for long-term storage). Store at 4° C for a month, or -20° C for longer.

Total volume of each sample available for the next step is 111.6 µl (11.6 + 100)

III. Purification

Clean the ligation product with XP beads following the protocol below, using a magnetic plate or a magnetic tube rack to separate beads from the solution. The AMPure XP original protocol recommends using a volume of beads equal to 1.8X the volume of the solution being cleaned, however ratios of 1X or 1.5X are successful.

This step reduces the presence of adapter dimers and increases the success of the PCR in samples that otherwise may fail. The AMPure reagent contains polyethylene glycol (PEG), and lower molecular mass DNA (i.e. primer dimers etc) precipitates at higher PEG concentrations. To perform the purification with the diluted ligation product from the previous step follow the protocol below. The original Agencourt AMPure XP protocol recommends a starting sample volume of 40 µl, but it can be done with 20 µl if pipetting with special care. We work with a sample volume of 20 µl.

On lab bench:

1. Take Agencourt AMPure XP bottle out from the fridge 30 minutes before starting.

2. Shake and vortex the Agencourt AMPure XP bottle (several times) to fully resuspend magnetic particles.
3. Samples to purify should be ready in a PCR plate (if using magnetic bead) or 1.5ml eppendorf tubes (if using tube rack).
4. To a sample volume of 20µl add 30ul of Agencourt AMPure XP to obtain the desired ratio of 1.5X). Pipette mix 10 times.
5. Incubate at room temperature for 5 minutes.
6. Place the reaction plate/tubes onto the magnetic plate/rack.

On magnetic plate/rack

7. Let it stand for 5 minutes to separate beads from solution.
8. Aspirate the supernatant from the reaction plate and discard (do not disturb the beads)
9. Dispense 200 µl of 70% ethanol (use a fresh preparation) and incubate at room temperature for 1 minute. Aspirate out the ethanol and discard. Repeat once for a total of two washes.
10. Wait until the ethanol gets completely dry (5-10 minutes, or maybe more depending on lab conditions - check for small ethanol drops until they totally disappear) after the 2nd wash and remove from the magnet.

On lab bench

11. Add a volume of elution buffer (10 mM Tris-HCl pH 8.5) equal (or smaller, to concentrate) to the starting sample volume (20 µl), pipette mix 10 times or until the magnetic particles are fully resuspended (brown color).
12. Incubate at room temperature for 5 minutes.
13. Place the reaction plate/tubes onto the magnetic plate/rack.

On magnetic plate/rack

14. Let it stand for 5 minutes to separate beads from solution.
15. Transfer the solution to a new plate and label it. This is the purified product. Be careful do not carry over the magnetic particles when aspirating (it is advisable to aspirate 2 µl less than the elution volume).

Total volume of each sample available for the next step should be approximately 18 µl (20 – 2µl)

IV. PCR Amplification

This PCR step uses the Illumina PCR primers to amplify fragments that have our adapters + barcodes ligated onto the ends. To ameliorate stochastic differences in PCR production of fragments in reactions, we run two separate 10 µL reactions per restriction-ligation product (i.e. perform next two steps twice with the same samples), and later combine them. If your sequencing batch includes fewer than 32 individuals, run each PCR at double volume (20 µl) to produce sufficient library quantity.

1. Prepare master mix III (see below, 8 µl l per sample, but remember to prepare 2 PCR reactions per sample), vortex and centrifuge. **If you are running the dual-indexing protocol, be sure to prepare separate master mixes for samples to be indexed with different Illumina barcodes- these will each require a different primer mix (see step 0).** Remember, if only 2 index primers will be used use the ILLPCR2_ind06 and ILLPCR2_ind12, if three primers, use 4, 6, 12. If six primers use 2,4,5,6,7,12.

MASTER MIX III: PCR

	Vol (µl) 1x
Water	3.150
Q5 Buffer	2
GC enhancer	2
dNTP (25mM)	0.08
PCR Primer Mix	0.67
Q5 polymerase	0.1
Total mix volume per sample	8

2. Add 8 µl of the combined master mix III to each well of a plate.
3. Add 2 µl of the diluted ligation product from step II or of the purification product if step III was done.
4. Thermal cycler profile for this PCR: 98ºC for 30s; 20 cycles of: 98 ºC for 20s, 60 ºC for 30s, 72 ºC for 40s; final extension at 72 ºC for 10 min.
5. Prepare master mix IV (see below, 1 µl per sample), **remember to account for dual-indexing primers; they need to be prepared in separate mixes.** It is not necessary to add more polymerase or $MgCl_2$ as there is still enough from the previous PCR. This step reduces production of single-stranded or heteroduplex PCR products.

MASTER MIX IV: PCR final cycle

	Vol (µl) 1x
Water	0.385
Buffer (Q polymerase)	0.2
PCR primer mix	0.335
dNTP (25 mM)	0.08
Total mix volume per sample	1

6. Add 1 µl to each PCR product (keep cold), run thermocycler profile as follows: 98 ºC for 3 min, 60 ºC for 2 min, 72 ºC for 12 min.

Note: it is advisable to run all the reactions in the same thermocycler and block.

Total volume of each sample available for the next step should be 22 µl (2 x [10+1])

V. Confirm reaction success of each sample and estimate relative concentration of each library to normalize concentrations for pooling

Ensuring each sample contributes approximately the same concentration of sample library to the pooled library within an index

Pool equal samples of the two PCR reactions into the same plate ("stack" the plates) and run 3-5 µl of each PCR product on a 1.5% agarose gel for 20-30 minutes with an appropriately sized ladder that will let you estimate the relative concentration of each RAD-library (i.e. use a ladder that has bands of different concentrations). You should see a smear of PCR product from 150-300 bp to between 500 and 1000 bp, often with a bright band of primer dimer at 130 bp. Samples that failed to amplify, or amplified only the adapter dimer, can be excluded from the pool (except negative controls, those must be pooled).

Samples will probably vary in terms of the intensity of both the RAD-library and primer dimer. If there is an evident difference in the yield of some samples compare to others, it is probable that the samples with the much brighter smears will take over the sequencing reaction if equal volumes of each sample are combined into a pool (especially if sequencing a low number of samples). One way to deal with this is to perform a AMPure purification as in step III, then measure the concentrations (Qubit), and then pool the samples in equimolar ratios.

An alternative, and perhaps less precise option is to categorise samples into three or four classes of intensity when run on the gel by using the ladder concentrations to estimate the relative concentration of each category. Then, use these estimations to dilute samples such that they have equimolar concentrations.

Once concentrations have been normalized, samples can then be pooled (**important – pool by index. For example, 48 samples with 2 indexes will produce 2 pools of 24).**

VI. Size selection

Size selection of the index pools (i.e. samples pooled by index) should be done with a BluePippin (Sage Science, product code BDF2010), or an analogous instrument. First run samples pooled by index on the fragment analyser, to identify the best size interval. We have found that selecting between 200-250 or 225-275 (i.e. there is flexibility to avoid any odd looking spikes in the fragment distribution of a given species) provides a rich return for species of beetle when sequencing between 62 and 80 individuals in a single Illumina run (single end sequencing on a 2500). Quite probably the number of individuals could be increased before low coverage becomes an issue.

After BluePippin size selection, re-run the index pools on a fragment analyser to be sure that only the desired fragment range has been selected, (i.e. that primers, primer dimers, and other ligated fragments outside the desired size range have been removed). Then measure the concentration of each index pool with a Qubit and perform equimolar pooling of indexes in the final library.

VII. Preparing final library template for Illumina sequencing

1. Measure concentration on a Qubit. A total concentration of >25 ng/µL is ideal for Illumina sequencing, but it has been suggested that one can go as low as 2 ng/µL.
2. Make an aliquot of the library and submit it to Fragment Analyzer or Bioanalyzer. You should expect to see a curve with a peak in the middle of the range of the size selection. A peak around 130 bp indicates that there was primer dimer carry over. It is possible to perform a 0.9X or 1X ampure purification to discard the primer dimers, but if the peak is small relatively to the library, it is possible to sequence the as it is, as they will represent a small percentage of the total reads.
3. If the Fragment Analyzer profile and concentration are as desired, the library is now ready for sequencing. The library can be submitted for sequencing on an Illumina HiSeq2500 (or similar) system in a single or pair-end run. But bear in mind that if you size selected fragments from 200-250 then the genomic inserts will be from 70-120 (approximately), so to do paired end sequencing would perhaps be throwing money away. The index sequencing is done separately from the insert sequencing, and the index sequence is not affected by the insert length, so it is not necessary to run the pair end to get the indexes sequence. If you used this protocol with more than one index, then you will be asked by the sequencing facility to provide their ID and sequence (Table 2) so that they can demultiplex the reads by index. Then your pipeline will have to include a second demultiplexing step to separate the reads by individual. Happy sequencing.

Table 1. Oligos sequence for P1 adapters.

barcode #	barcode sequence	reverse complement	ID	P1_EcoR1_n.1 sequence (5'-3')		ID	P1_EcoRI_n.2 sequence
1	GGTCTT	AAGACC	P1_EcoR1_01.1	ACACTCTTTCCCTACACGACGCTCTTC CGATCTGGTCTTC		P1_EcoR1_01.2	AATTGAAGACCAGATCGGAAGAGCGT CGTGTAGGGAAAGAGTGT
2	CTGGTT	AACCAG	P1_EcoR1_02.1	ACACTCTTTCCCTACACGACGCTCTTC CGATCTCTGGTTC		P1_EcoR1_02.2	AATTGAACCAGAGATCGGAAGAGCGT CGTGTAGGGAAAGAGTGT
3	AAGATA	TATCTT	P1_EcoR1_03.1	ACACTCTTTCCCTACACGACGCTCTTC CGATCTAAGATAC		P1_EcoR1_03.2	AATTGTATCTTAGATCGGAAGAGCGT CGTGTAGGGAAAGAGTGT
4	ACTTCC	GGAAGT	P1_EcoR1_04.1	ACACTCTTTCCCTACACGACGCTCTTC CGATCTACTTCCC		P1_EcoR1_04.2	AATTGGGAAGTAGATCGGAAGAGCG TCGTGTAGGGAAAGAGTGT
5	TTACGG	CCGTAA	P1_EcoR1_05.1	ACACTCTTTCCCTACACGACGCTCTTC CGATCTTTACGGC		P1_EcoR1_05.2	AATTGCCGTAAAGATCGGAAGAGCGT CGTGTAGGGAAAGAGTGT
6	AACGAA	TTCGTT	P1_EcoR1_06.1	ACACTCTTTCCCTACACGACGCTCTTC CGATCTAACGAAC		P1_EcoR1_06.2	AATTGTTCGTTAGATCGGAAGAGCGT CGTGTAGGGAAAGAGTGT
7	ATTCAT	ATGAAT	P1_EcoR1_07.1	ACACTCTTTCCCTACACGACGCTCTTC CGATCTATTCATC		P1_EcoR1_07.2	AATTGATGAATAGATCGGAAGAGCGT CGTGTAGGGAAAGAGTGT
8	CCGACC	GGTCGG	P1_EcoR1_08.1	ACACTCTTTCCCTACACGACGCTCTTC CGATCTCCGACCC		P1_EcoR1_08.2	AATTGGGTCGGAGATCGGAAGAGCG TCGTGTAGGGAAAGAGTGT
9	ATCGTC	GACGAT	P1_EcoR1_09.1	ACACTCTTTCCCTACACGACGCTCTTC CGATCTATCGTCC		P1_EcoR1_09.2	AATTGGACGATAGATCGGAAGAGCGT CGTGTAGGGAAAGAGTGT
10	CATCAA	TTGATG	P1_EcoR1_10.1	ACACTCTTTCCCTACACGACGCTCTTC CGATCTCATCAAC		P1_EcoR1_10.2	AATTGTTGATGAGATCGGAAGAGCGT CGTGTAGGGAAAGAGTGT
11	GCCTGG	CCAGGC	P1_EcoR1_11.1	ACACTCTTTCCCTACACGACGCTCTTC CGATCTGCCTGGC		P1_EcoR1_11.2	AATTGCCAGGCAGATCGGAAGAGCGT CGTGTAGGGAAAGAGTGT
12	TGCTTG	CAAGCA	P1_EcoR1_12.1	ACACTCTTTCCCTACACGACGCTCTTC CGATCTTGCTTGC		P1_EcoR1_12.2	AATTGCAAGCAAGATCGGAAGAGCGT CGTGTAGGGAAAGAGTGT
13	TCGCAT	ATGCGA	P1_EcoR1_13.1	ACACTCTTTCCCTACACGACGCTCTTC CGATCTTCGCATC		P1_EcoR1_13.2	AATTGATGCGAAGATCGGAAGAGCGT CGTGTAGGGAAAGAGTGT
14	GGTAGA	TCTACC	P1_EcoR1_14.1	ACACTCTTTCCCTACACGACGCTCTTC CGATCTGGTAGAC		P1_EcoR1_14.2	AATTGTCTACCAGATCGGAAGAGCGT CGTGTAGGGAAAGAGTGT
15	GGAGCG	CGCTCC	P1_EcoR1_15.1	ACACTCTTTCCCTACACGACGCTCTTC CGATCTGGAGCGC		P1_EcoR1_15.2	AATTGCGCTCCAGATCGGAAGAGCGT CGTGTAGGGAAAGAGTGT
16	TTGAAC	GTTCAA	P1_EcoR1_16.1	ACACTCTTTCCCTACACGACGCTCTTC CGATCTTTGAACC		P1_EcoR1_16.2	AATTGGTTCAAAGATCGGAAGAGCGT CGTGTAGGGAAAGAGTGT
17	GATTAC	GTAATC	P1_EcoR1_17.1	ACACTCTTTCCCTACACGACGCTCTTC CGATCTGATTACC		P1_EcoR1_17.2	AATTGGTAATCAGATCGGAAGAGCGT CGTGTAGGGAAAGAGTGT
18	CGAGGC	GCCTCG	P1_EcoR1_18.1	ACACTCTTTCCCTACACGACGCTCTTC CGATCTCGAGGCC		P1_EcoR1_18.2	AATTGGCCTCGAGATCGGAAGAGCGT CGTGTAGGGAAAGAGTGT
19	CAACCG	CGGTTG	P1_EcoR1_19.1	ACACTCTTTCCCTACACGACGCTCTTC CGATCTCAACCGC		P1_EcoR1_19.2	AATTGCGGTTGAGATCGGAAGAGCGT CGTGTAGGGAAAGAGTGT
20	GTATGA	TCATAC	P1_EcoR1_20.1	ACACTCTTTCCCTACACGACGCTCTTC CGATCTGTATGAC		P1_EcoR1_20.2	AATTGTCATACAGATCGGAAGAGCGT CGTGTAGGGAAAGAGTGT

21	TGGATT	AATCCA	P1_EcoR1_21.1	ACACTCTTTCCCTACACGACGCTCTTC CGATCTTGGATTC		P1_EcoR1_21.2	AATTGAATCCAAGATCGGAAGAGCGT CGTGTAGGGAAAGAGTGT
22	CCAGCT	AGCTGG	P1_EcoR1_22.1	ACACTCTTTCCCTACACGACGCTCTTC CGATCTCCAGCTC		P1_EcoR1_22.2	AATTGAGCTGGAGATCGGAAGAGCGT CGTGTAGGGAAAGAGTGT
23	AACTCG	CGAGTT	P1_EcoR1_23.1	ACACTCTTTCCCTACACGACGCTCTTC CGATCTAACTCGC		P1_EcoR1_23.2	AATTGCGAGTTAGATCGGAAGAGCGT CGTGTAGGGAAAGAGTGT
24	ACCAGA	TCTGGT	P1_EcoR1_24.1	ACACTCTTTCCCTACACGACGCTCTTC CGATCTACCAGAC		P1_EcoR1_24.2	AATTGTCTGGTAGATCGGAAGAGCGT CGTGTAGGGAAAGAGTGT

These oligos include a protective base - a C added immediately after the barcode, thus before the restriction enzyme overhang. Order sequences as unmodified oligos with HPSF purification.

Table 2. Oligos sequence (5'-3') for P2 adapter and PCR primers.

P2.1_MseI	GTGACTGGAGTTCAGACGTGTGCTCTTCCGATCT	
p2.2_MseI	/5Phos/TAAGATCGGAAGAGCGAGAACAA	
ILLPCR1	AATGATACGGCGACCACCGAGATCTACACTCTTTCCCTACACGACG	**Index sequence ****
ILLPCR2_ind01	CAAGCAGAAGACGGCATACGAGATCGTGATGTGACTGGAGTTCAGACGTGTGC	ATCACG
ILLPCR2_ind02	CAAGCAGAAGACGGCATACGAGATACATCGGTGACTGGAGTTCAGACGTGTGC	CGATGT
ILLPCR2_ind03	CAAGCAGAAGACGGCATACGAGATGCCTAAGTGACTGGAGTTCAGACGTGTGC	TTAGGC
ILLPCR2_ind04	CAAGCAGAAGACGGCATACGAGATTGGTCAGTGACTGGAGTTCAGACGTGTGC	TGACCA
ILLPCR2_ind05	CAAGCAGAAGACGGCATACGAGATCACTGTGTGACTGGAGTTCAGACGTGTGC	ACAGTG
ILLPCR2_ind06	CAAGCAGAAGACGGCATACGAGATATTGGCGTGACTGGAGTTCAGACGTGTGC	GCCAAT
ILLPCR2_ind07	CAAGCAGAAGACGGCATACGAGATGATCTGGTGACTGGAGTTCAGACGTGTGC	CAGATC
ILLPCR2_ind08	CAAGCAGAAGACGGCATACGAGATTCAAGTGTGACTGGAGTTCAGACGTGTGC	ACTTGA
ILLPCR2_ind09	CAAGCAGAAGACGGCATACGAGATCTGATCGTGACTGGAGTTCAGACGTGTGC	GATCAG
ILLPCR2_ind10	CAAGCAGAAGACGGCATACGAGATAAGCTAGTGACTGGAGTTCAGACGTGTGC	TAGCTT
ILLPCR2_ind11	CAAGCAGAAGACGGCATACGAGATGTAGCCGTGACTGGAGTTCAGACGTGTGC	GGCTAC
ILLPCR2_ind12	CAAGCAGAAGACGGCATACGAGATTACAAGGTGACTGGAGTTCAGACGTGTGC	CTTGTA

Modifications key: /5Phos/ = 5' phosphate. Note: it is optional to add phosphorothioate bonds (*) to the first two bases of the PCR2 primers to add resistance to degradation by exonucleases. Order HPSF purification for the unmodified oligos and HPLC for the modified. ** As needed for demultiplexing, the reverse complement of each sequence is inside the ILLPCR2 primer.

Table S1. Details of sampling locations and the number of individuals sequenced at each location for the *Laparocerus tessellatus* complex.

Island	Locality Code	Latitude	Longitude	Source	No. total of individuals COII	No. total of individuals ddRADseq
Gran Canaria	C01	28.08554	-15.55989	Faria et al. 2016 / García-Olivares et al. 2017	5	3
Gran Canaria	C02	28.07254	-15.55794	Faria et al. 2016 / García-Olivares et al. 2017	5	2
Gran Canaria	C03	28.06506	-15.56383	Faria et al. 2016 / García-Olivares et al. 2017	2	2
Gran Canaria	C04	28.06775	-15.58813	Faria et al. 2016 / García-Olivares et al. 2017	13	4
Gran Canaria	C05	28.04328	-15.59489	Faria et al. 2016 / García-Olivares et al. 2017	5	4
Gran Canaria	C06	28.05324	-15.69192	Faria et al. 2016 / García-Olivares et al. 2017	10	2
Gran Canaria	C07	28.03068	-15.67754	Faria et al. 2016 / García-Olivares et al. 2017	5	2
Gran Canaria	C08	28.00513	-15.59791	Faria et al. 2016 / García-Olivares et al. 2017	4	2
Gran Canaria	C09	27.99959	-15.60049	Faria et al. 2016 / García-Olivares et al. 2017	4	4
Gran Canaria	C10	27.99853	-15.58728	Faria et al. 2016 / García-Olivares et al. 2017	5	4
Gran Canaria	C11	27.99278	-15.52196	Faria et al. 2016 / García-Olivares et al. 2017	5	2
Gran Canaria	C12	27.98854	-15.59329	Faria et al. 2016 / García-Olivares et al. 2017	5	2
Gran Canaria	C13	27.96126	-15.53149	Faria et al. 2016 / García-Olivares et al. 2017	6	2
Gran Canaria	C14	27.96466	-15.55927	Faria et al. 2016 / García-Olivares et al. 2017	7	2
Gran Canaria	C15	27.96540	-15.58548	Faria et al. 2016 / García-Olivares et al. 2017	4	2
Gran Canaria	C16	27.96512	-15.60155	Faria et al. 2016 / García-Olivares et al. 2017	5	2
Gran Canaria	C17	27.95950	-15.62690	Faria et al. 2016 / García-Olivares et al. 2017	5	2
Gran Canaria	C18	27.92720	-15.59940	Faria et al. 2016 / García-Olivares et al. 2017	4	3
Gran Canaria	C19	27.92605	-15.57921	Faria et al. 2016 / García-Olivares et al. 2017	5	2
Gran Canaria	C20	27.91563	-15.57494	Faria et al. 2016 / García-Olivares et al. 2017	3	2
Gran Canaria	C21	27.91214	-15.57252	Faria et al. 2016 / García-Olivares et al. 2017	12	2
El Hierro	H01	27.80727	-17.92477	This study	4	1
El Hierro	H02	27.80306	-17.91735	Faria et al. 2016 / García-Olivares et al. 2017	2	1
El Hierro	H03	27.78638	-17.93754	This study	5	1
El Hierro	H04	27.78091	-17.95486	This study	5	1
El Hierro	H05	27.76258	-17.98112	This study	1	1
El Hierro	H06	27.75616	-17.96589	Faria et al. 2016 / García-Olivares et al. 2017	7	2
El Hierro	H07	27.74480	-17.98625	This study	5	2
El Hierro	H08	27.74330	-17.97907	Faria et al. 2016 / García-Olivares et al. 2017	2	2

El Hierro	H09	27.74066	-17.96595	This study	5	1
El Hierro	H10	27.73189	-17.97164	This study	5	2
El Hierro	H11	27.71986	-17.98152	This study	4	1
El Hierro	H12	27.70303	-17.98551	This study	5	1
El Hierro	H13	27.73662	-18.07559	This study	5	2
El Hierro	H14	27.73638	-18.07862	This study	4	1
El Hierro	H16	27.73641	-18.08063	This study	5	2
El Hierro	H17	27.72378	-18.09258	This study	4	1
La Palma	P01	28.55313	-17.86759	Faria et al. 2016 / García-Olivares et al. 2017	5	2
La Palma	P02	28.55636	-17.86674	Faria et al. 2016 / García-Olivares et al. 2017	1	1
La Palma	P03	28.55918	-17.85878	Faria et al. 2016 / García-Olivares et al. 2017	5	2
La Palma	P04	28.55172	-17.78853	Faria et al. 2016 / García-Olivares et al. 2017	4	2
La Palma	P05	28.60832	-17.78591	Faria et al. 2016 / García-Olivares et al. 2017	12	4
La Palma	P06	28.61466	-17.83430	Faria et al. 2016 / García-Olivares et al. 2017	5	4
La Palma	P07	28.61991	-17.82331	Faria et al. 2016 / García-Olivares et al. 2017	6	3
La Palma	P08	28.64467	-17.82497	Faria et al. 2016 / García-Olivares et al. 2017	4	2
La Palma	P09	28.65231	-17.84558	Faria et al. 2016 / García-Olivares et al. 2017	7	1
La Palma	P10	28.65634	-17.85215	Faria et al. 2016 / García-Olivares et al. 2017	5	2
La Palma	P11	28.66845	-17.82711	Faria et al. 2016 / García-Olivares et al. 2017	6	0
La Palma	P12	28.66845	-17.82711	Faria et al. 2016 / García-Olivares et al. 2017	5	2
La Palma	P13	28.67693	-17.84972	Faria et al. 2016 / García-Olivares et al. 2017	3	2
La Palma	P14	28.69902	-17.78647	Faria et al. 2016 / García-Olivares et al. 2017	4	2
La Palma	P15	28.71770	-17.77950	Faria et al. 2016 / García-Olivares et al. 2017	7	3
La Palma	P16	28.72455	-17.78275	Faria et al. 2016 / García-Olivares et al. 2017	3	2
La Palma	P17	28.73151	-17.81322	Faria et al. 2016 / García-Olivares et al. 2017	7	3
La Palma	P18	28.73144	-17.83024	Faria et al. 2016 / García-Olivares et al. 2017	5	2
La Palma	P19	28.76855	-17.90471	Faria et al. 2016 / García-Olivares et al. 2017	3	2
La Palma	P20	28.77295	-17.90464	Faria et al. 2016 / García-Olivares et al. 2017	5	2
La Palma	P21	28.78029	-17.91933	Faria et al. 2016 / García-Olivares et al. 2017	5	2
La Palma	P22	28.80501	-17.90804	Faria et al. 2016 / García-Olivares et al. 2017	6	2
La Palma	P23	28.81950	-17.90895	Faria et al. 2016 / García-Olivares et al. 2017	5	2
La Palma	P24	28.83407	-17.90867	Faria et al. 2016 / García-Olivares et al. 2017	1	1
La Palma	P25	28.80646	-17.86624	Faria et al. 2016 / García-Olivares et al. 2017	6	2

La Palma	P26	28.81726	-17.80925	Faria et al. 2016 / García-Olivares et al. 2017	5	3
La Palma	P27	28.81174	-17.80937	Faria et al. 2016 / García-Olivares et al. 2017	6	4
La Palma	P28	28.79698	-17.78941	Faria et al. 2016 / García-Olivares et al. 2017	6	2
La Palma	P29	28.79118	-17.78606	Faria et al. 2016 / García-Olivares et al. 2017	7	2
La Palma	P30	28.77275	-17.81203	Faria et al. 2016 / García-Olivares et al. 2017	6	2
La Palma	P31	28.76957	-17.78922	Faria et al. 2016 / García-Olivares et al. 2017	6	2
La Palma	P32	28.76702	-17.76984	Faria et al. 2016 / García-Olivares et al. 2017	7	2
Tenerife	T01	28.56202	-16.17140	Faria et al. 2016 / García-Olivares et al. 2017	0	1
Tenerife	T02	28.56020	-16.16920	This study	0	1
Tenerife	T03	28.55930	-16.17323	This study	0	1
Tenerife	T04	28.55856	-16.17519	Faria et al. 2016 / García-Olivares et al. 2017	1	1
Tenerife	T05	28.55558	-16.18118	Faria et al. 2016 / García-Olivares et al. 2017	12	1
Tenerife	T06	28.55196	-16.18923	This study	0	1
Tenerife	T07	28.54243	-16.22830	This study	0	1
Tenerife	T08	28.53192	-16.28007	Faria et al. 2016 / García-Olivares et al. 2017	2	1
Tenerife	T09	28.53550	-16.29620	This study	0	1
Tenerife	T10	28.53869	-16.30013	Faria et al. 2016 / García-Olivares et al. 2017	1	1
Tenerife	T11	28.53731	-16.30938	This study	0	1
Tenerife	T12	28.50834	-16.31650	This study	5	2
Tenerife	T13	28.50689	-16.33227	This study	5	1
Tenerife	T14	28.49309	-16.36113	This study	5	1
Tenerife	T15	28.48003	-16.35396	This study	5	1
Tenerife	T16	28.46071	-16.37668	This study	5	2
Tenerife	T17	28.44379	-16.38644	This study	5	1
Tenerife	T18	28.44044	-16.40373	This study	5	1
Tenerife	T19	28.42999	-16.39546	This study	5	1
Tenerife	T20	28.42382	-16.37924	Faria et al. 2016 / García-Olivares et al. 2017	11	0
Tenerife	T21	28.42381	-16.39610	Faria et al. 2016 / García-Olivares et al. 2017	5	2
Tenerife	T22	28.42011	-16.40750	Faria et al. 2016 / García-Olivares et al. 2017	1	1
Tenerife	T23	28.42914	-16.42744	This study	5	1
Tenerife	T24	28.41455	-16.41713	This study	5	1
Tenerife	T25	28.40815	-16.40306	This study	4	1
Tenerife	T26	28.40458	-16.39634	This study	5	1
Tenerife	T27	28.40373	-16.39002	This study	4	2
Tenerife	T28	28.40426	-16.38607	This study	2	1
Tenerife	T29	28.38285	-16.39437	This study	1	1
Tenerife	T30	28.40399	-16.42423	This study	5	1

Tenerife	T31	28.39480	-16.43165	This study	5	1
Tenerife	T32	28.37345	-16.40509	This study	5	1
Tenerife	T33	28.37479	-16.41268	This study	5	1
Tenerife	T34	28.37879	-16.42473	This study	5	1
Tenerife	T35	28.39203	-16.43736	This study	4	1
Tenerife	T36	28.41501	-16.44293	This study	5	2
Tenerife	T37	28.39117	-16.44142	This study	5	1
Tenerife	T38	28.41115	-16.45066	This study	5	1
Tenerife	T39	28.38607	-16.44199	This study	2	1
Tenerife	T40	28.38550	-16.45585	This study	5	1
Tenerife	T41	28.39008	-16.45466	Faria et al. 2016 / García-Olivares et al. 2017	3	0
Tenerife	T42	28.40752	-16.46434	This study	5	1
Tenerife	T43	28.35901	-16.43337	Faria et al. 2016 / García-Olivares et al. 2017	6	1
Tenerife	T44	28.32805	-16.42484	This study	4	1
Tenerife	T45	28.33887	-16.43794	This study	4	1
Tenerife	T46	28.37383	-16.46376	Faria et al. 2016 / García-Olivares et al. 2017	5	1
Tenerife	T47	28.36885	-16.46501	This study	4	1
Tenerife	T48	28.37258	-16.46783	This study	5	3
Tenerife	T49	28.37591	-16.47281	This study	5	4
Tenerife	T50	28.38143	-16.47936	Faria et al. 2016 / García-Olivares et al. 2017	4	4
Tenerife	T51	28.39032	-16.48924	Faria et al. 2016 / García-Olivares et al. 2017	7	1
Tenerife	T52	28.39917	-16.48384	This study	5	1
Tenerife	T53	28.40304	-16.49229	Faria et al. 2016 / García-Olivares et al. 2017	5	1
Tenerife	T54	28.40121	-16.49567	Faria et al. 2016 / García-Olivares et al. 2017	6	1
Tenerife	T55	28.35769	-16.46667	Faria et al. 2016 / García-Olivares et al. 2017	6	1
Tenerife	T56	28.36350	-16.49301	Faria et al. 2016 / García-Olivares et al. 2017	5	1
Tenerife	T57	28.34126	-16.47891	Faria et al. 2016 / García-Olivares et al. 2017	6	1
Tenerife	T58	28.32366	-16.45176	This study	4	1
Tenerife	T59	28.30806	-16.44236	Faria et al. 2016 / García-Olivares et al. 2017	8	1
Tenerife	T60	28.31639	-16.48614	Faria et al. 2016 / García-Olivares et al. 2017	7	1
Tenerife	T61	28.35539	-16.51461	Faria et al. 2016 / García-Olivares et al. 2017	5	1
Tenerife	T62	28.34795	-16.53172	Faria et al. 2016 / García-Olivares et al. 2017	5	1
Tenerife	T63	28.34423	-16.54283	Faria et al. 2016 / García-Olivares et al. 2017	4	2
Tenerife	T64	28.32716	-16.53320	Faria et al. 2016 / García-Olivares et al. 2017	3	1
Tenerife	T65	28.30758	-16.53692	Faria et al. 2016 / García-Olivares et al. 2017	5	1
Tenerife	T66	28.34006	-16.56710	Faria et al. 2016 / García-Olivares et al. 2017	5	2

Tenerife	T67	28.30291	-16.56654	Faria et al. 2016 / García-Olivares et al. 2017	3	1
Tenerife	T68	28.30911	-16.56722	Faria et al. 2016 / García-Olivares et al. 2017	5	1
Tenerife	T69	28.32569	-16.58787	Faria et al. 2016 / García-Olivares et al. 2017	3	2
Tenerife	T70	28.34282	-16.59322	Faria et al. 2016 / García-Olivares et al. 2017	7	1
Tenerife	T71	28.36096	-16.59862	Faria et al. 2016 / García-Olivares et al. 2017	4	1
Tenerife	T72	28.37783	-16.60095	Faria et al. 2016 / García-Olivares et al. 2017	5	1
Tenerife	T73	28.33658	-16.62066	Faria et al. 2016 / García-Olivares et al. 2017	5	1
Tenerife	T74	28.33271	-16.65818	Faria et al. 2016 / García-Olivares et al. 2017	5	2
Tenerife	T75	28.31620	-16.71957	Faria et al. 2016 / García-Olivares et al. 2017	5	3
Tenerife	T76	28.36146	-16.77505	Faria et al. 2016 / García-Olivares et al. 2017	4	2
Tenerife	T77	28.31853	-16.75554	Faria et al. 2016 / García-Olivares et al. 2017	1	1
Tenerife	T78	28.32877	-16.78105	This study	4	2
Tenerife	T79	28.32896	-16.80887	Faria et al. 2016 / García-Olivares et al. 2017	2	1
Tenerife	T80	28.31338	-16.82018	Faria et al. 2016 / García-Olivares et al. 2017	2	1
Tenerife	T81	28.31413	-16.82984	This study	5	1
Tenerife	T82	28.32199	-16.83505	This study	1	0
Tenerife	T83	28.32282	-16.84648	This study	5	0
Tenerife	T86	28.34167	-16.86331	This study	3	1
Tenerife	T87	28.33848	-16.87357	This study	5	2
Tenerife	T88	28.27160	-16.76831	This study	6	2
Tenerife	T88b	28.27495	-16.73553	This study	4	2
Tenerife	T89	28.24605	-16.76495	This study	4	2
Tenerife	T94	28.13267	-16.68804	Faria et al. 2016 / García-Olivares et al. 2017	2	0
Tenerife	T96	28.18893	-16.65695	Faria et al. 2016 / García-Olivares et al. 2017	6	1
Tenerife	T97	28.16540	-16.63680	This study	5	1
Tenerife	T99	28.17253	-16.62525	This study	5	1
Tenerife	T100	28.17836	-16.63134	Faria et al. 2016 / García-Olivares et al. 2017	5	1
Tenerife	T103	28.17035	-16.60902	This study	5	1
Tenerife	T104	28.18068	-16.59173	This study	5	1
Tenerife	T105	28.14503	-16.54521	Faria et al. 2016 / García-Olivares et al. 2017	6	0
Tenerife	T106	28.18591	-16.58145	This study	5	1
Tenerife	T108	28.18815	-16.57393	This study	5	1
Tenerife	T110	28.19746	-16.56724	This study	5	1
Tenerife	T111	28.20746	-16.56141	This study	5	1
Tenerife	T112	28.19143	-16.52743	Faria et al. 2016 / García-Olivares et al. 2017	2	0
Tenerife	T113	28.19770	-16.53115	Faria et al. 2016 / García-Olivares et al. 2017	3	1

Tenerife	T115	28.22499	-16.54904	This study	5	1
Tenerife	T116	28.21490	-16.49102	This study	5	2
Tenerife	T117	28.24211	-16.53368	This study	5	1
Tenerife	T118	28.25931	-16.52052	This study	4	1
Tenerife	T119	28.24721	-16.48191	This study	4	1
Tenerife	T120	28.28796	-16.51247	This study	5	1
Tenerife	T121	28.27462	-16.46414	This study	3	1
Tenerife	T122	28.29692	-16.48257	Faria et al. 2016 / García-Olivares et al. 2017	6	1
Tenerife	T123	28.29324	-16.44798	Faria et al. 2016 / García-Olivares et al. 2017	2	2
Tenerife	T124	28.29325	-16.43329	Faria et al. 2016 / García-Olivares et al. 2017	6	1
Tenerife	T126	28.33486	-16.83157	This study	3	1

Appendix S2. Sensitivity analysis results.

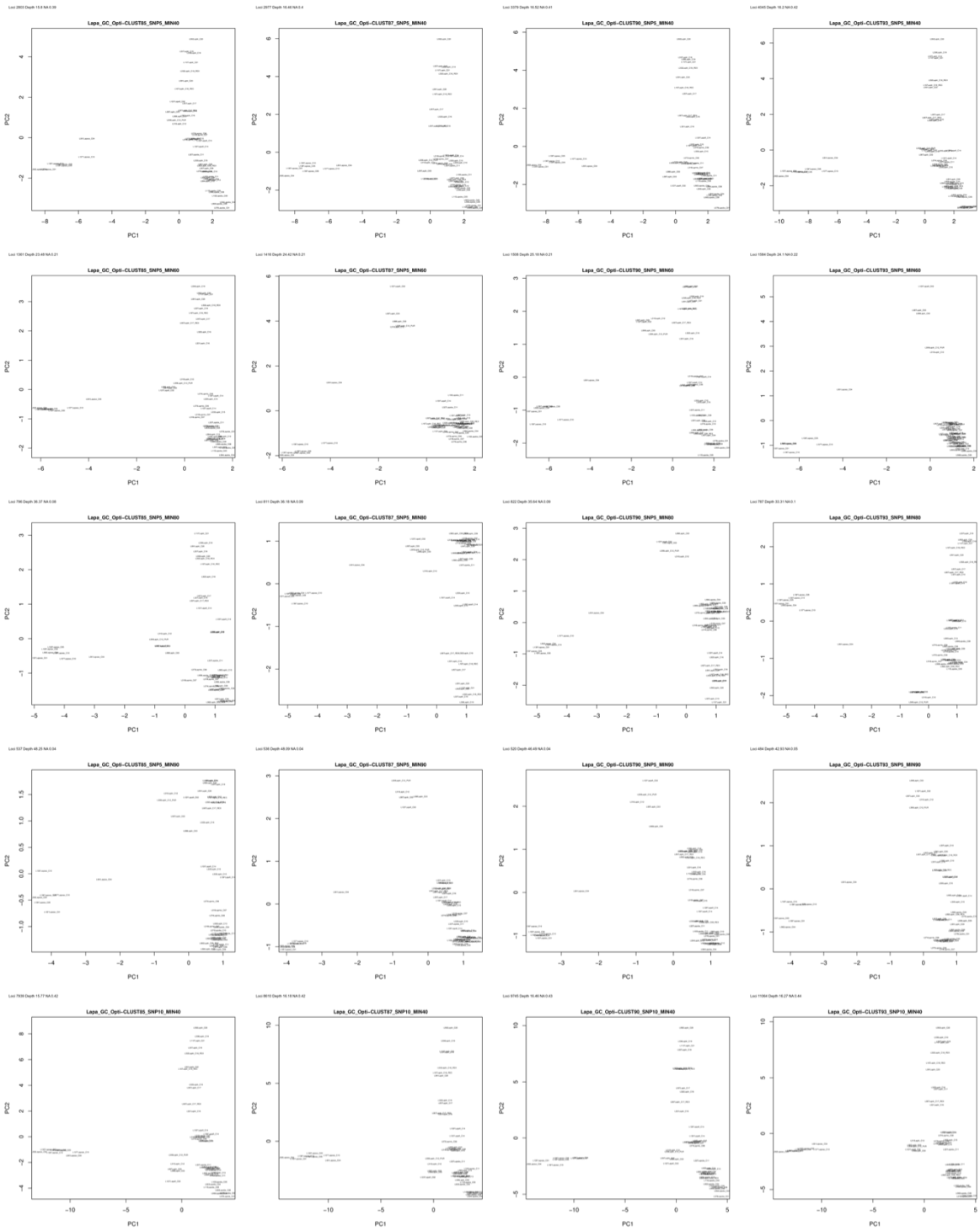

Figure S2.1. Principal component analyses (PCA) from the optimization step. Each plot represents a specific parameter combination from the 80 different combinations explored. Details of each parameter combination is presented at the top of each plot. Each row represents a fixed combination of parameters for max_SNPs_locus and min_samples_locus, with each column represented a different value for clust_threshold.

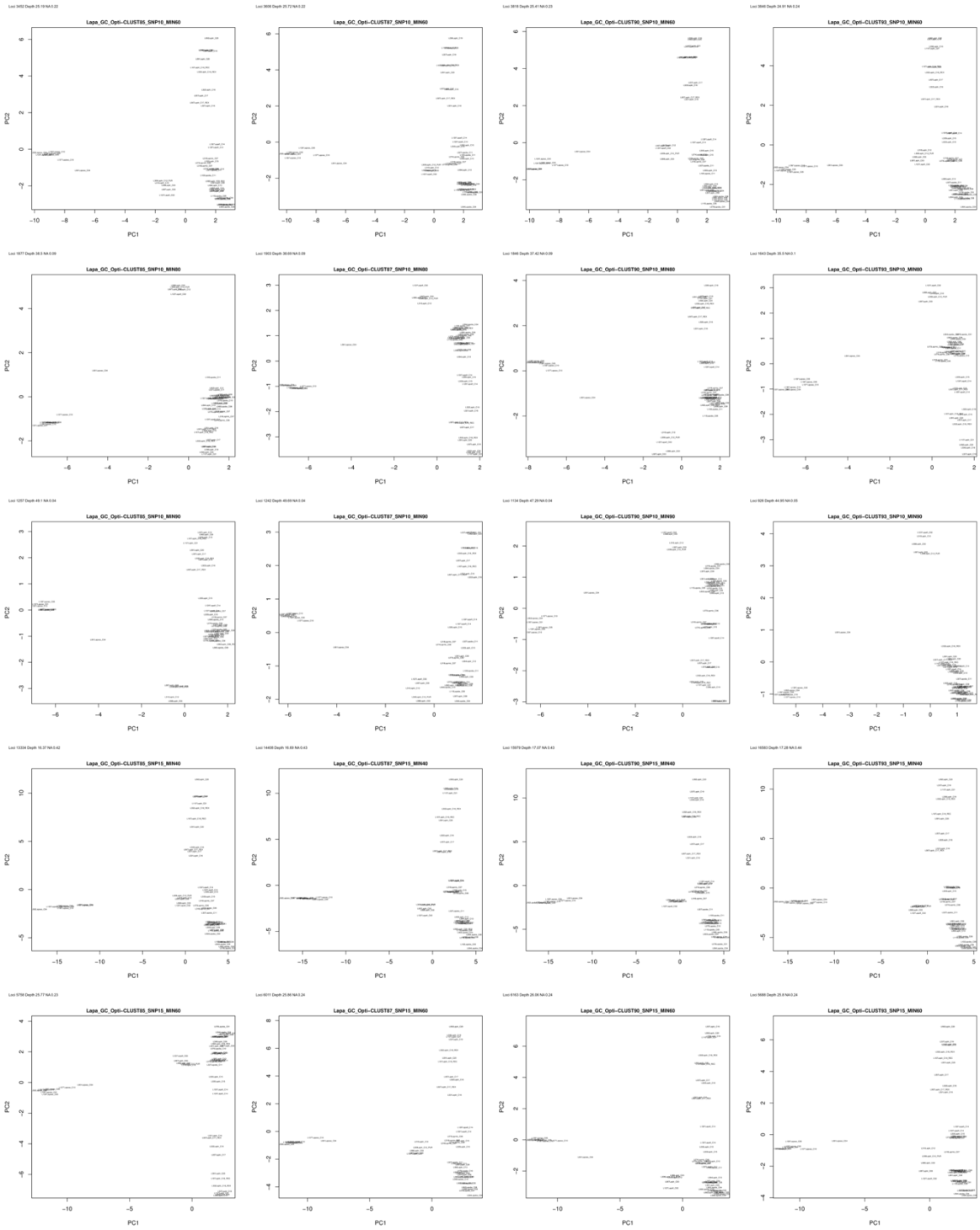

Figure S2.1., continued

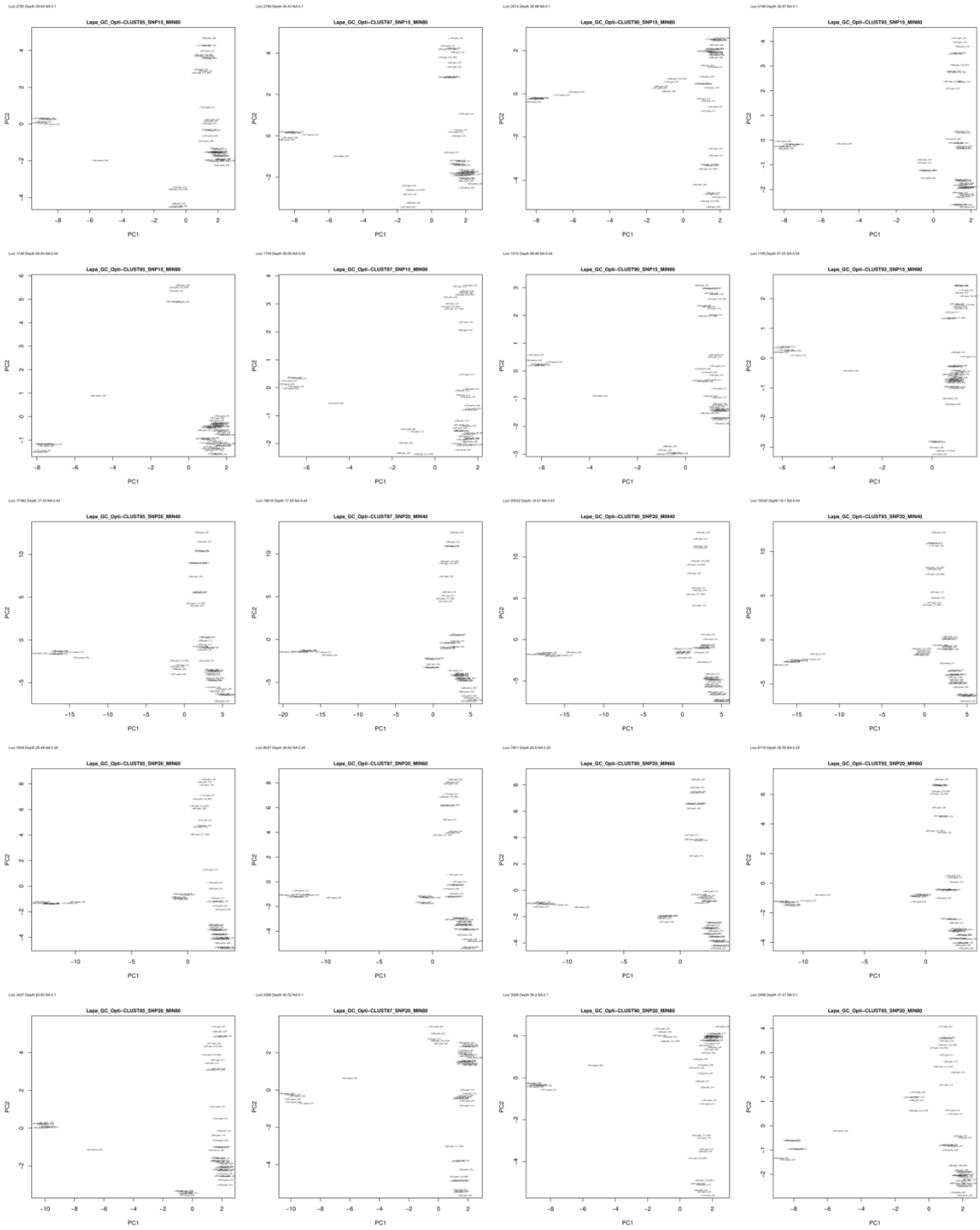

Figure S2.1., continued

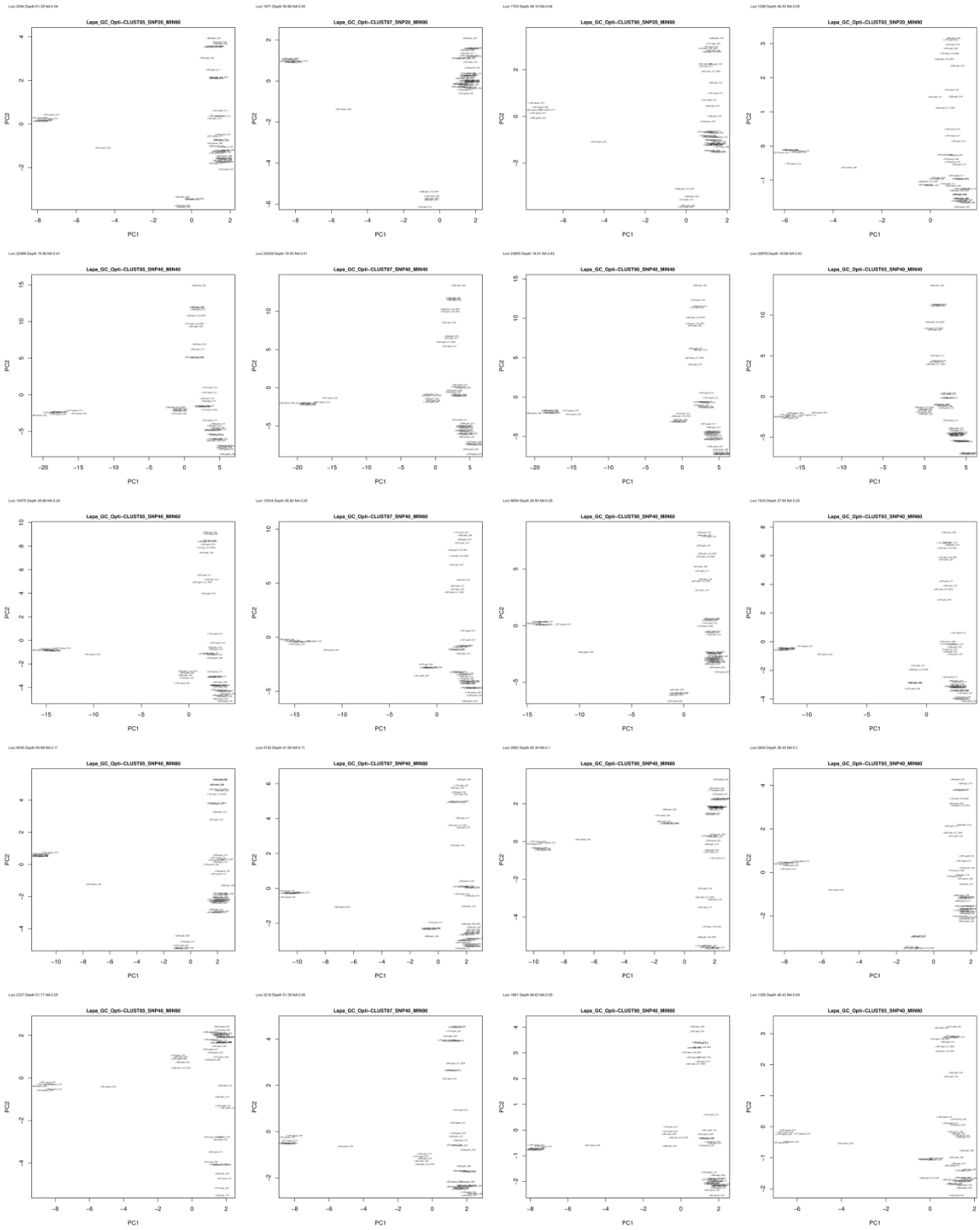

Figure S2.1., continued

Appendix S3. Bayesian phylogenetic tree of the complete mtDNA COII data set and Maximum-likelihood phylogenetic tree of the nuclear sub-genomic data.

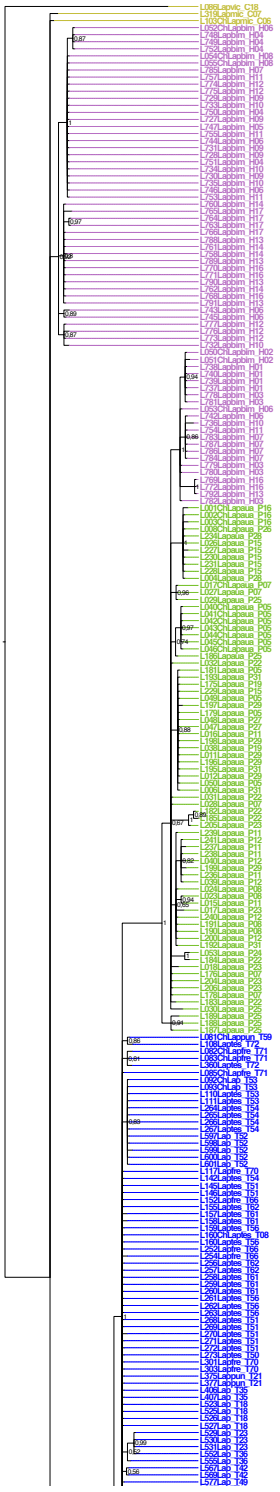

Figure S3.1. Bayesian phylogenetic tree constructed from 836 individuals for the mtDNA COII gene sampled from the *Laparocerus tessellatus* complex. Individuals are colour coded to represent their island of origin (see Fig. 2). Gran Canaria: *L. microphthalmus* = Lapmic, *L. obsitus* = Lapobs, *L. osorio* = Laposo, *L. tirajana* = Laptir, and *L. sp. aff. tirajana* = Lapaft. Tenerife: *L. tessellatus* = Laptes, *L. freyi* = Lapfre, *L. punctiger* = Lappun, and *L. canescens* = Lapcan; La Palma: *L. auarita* = Lapaua. El Hierro: *L. bimbache* = Lapbim.

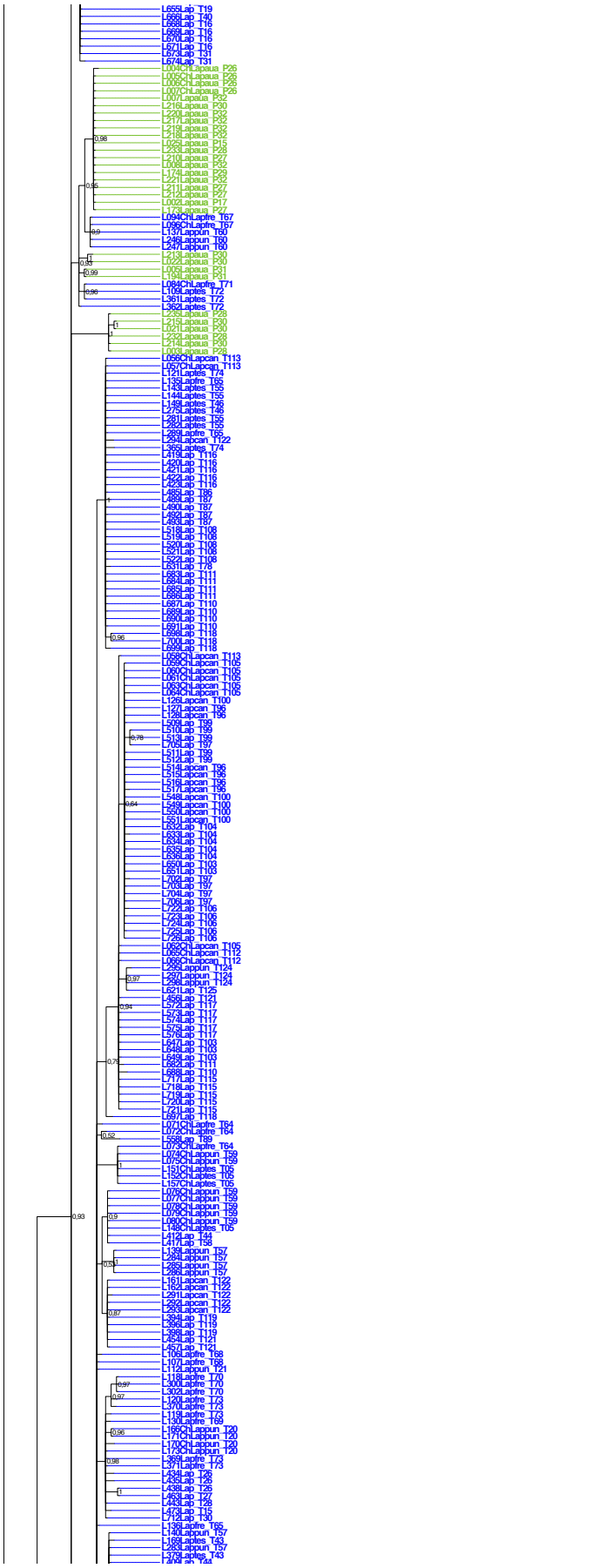

Figure S3.1., continued

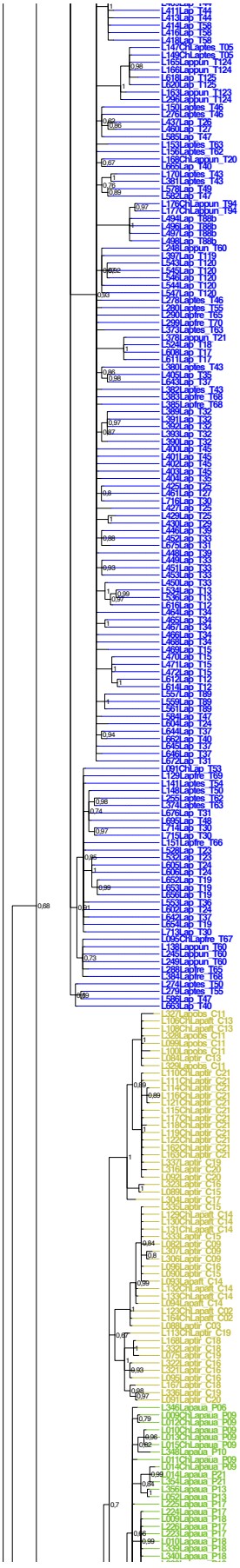

Figure S3.1., continued

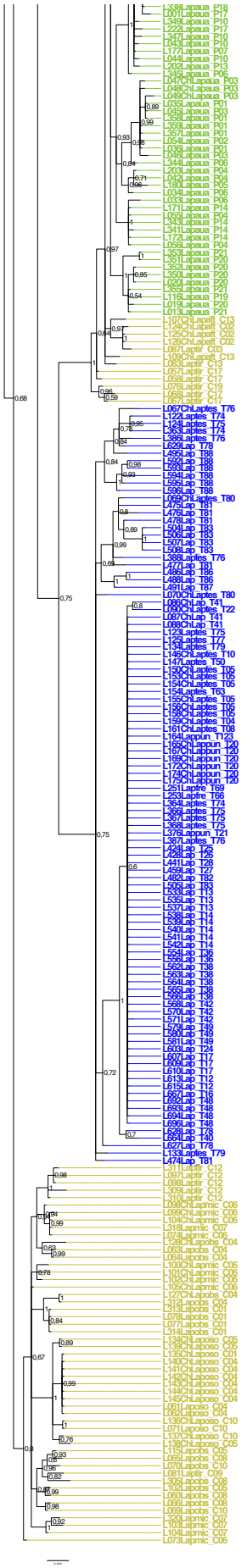

Figure S3.1., continued

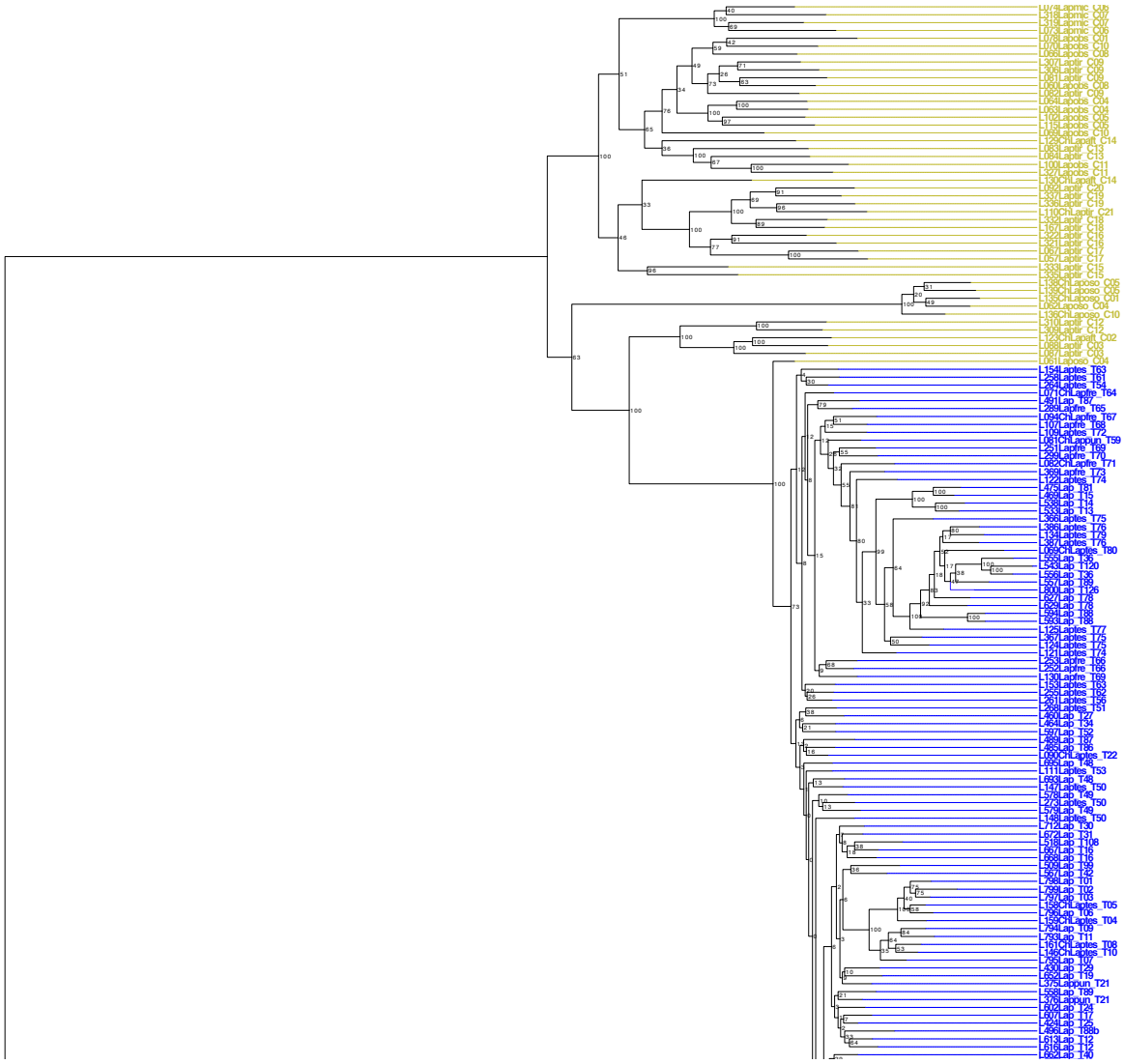

Figure S3.2. Maximum-likelihood phylogenetic tree constructed using a nuclear sub-genomic alignment of concatenated SNPs, sampled from 265 individuals of the *Laparocerus tessellatus* complex. Individuals are colour coded to represent their island of origin (see Fig. 2). Gran Canaria: *L. microphthalmus* = Lapmic, *L. obsitus* = Lapobs, *L. osorio* = Laposo, *L. tirajana* = Laptir, and *L. sp. aff. tirajana* = Lapaft. Tenerife: *L. tessellatus* = Laptes, *L. freyi* = Lapfre, *L. punctiger* = Lappun, and *L. canescens* = Lapcan; La Palma: *L. auarita* = Lapaua. El Hierro: *L. bimbache* = Lapbim.

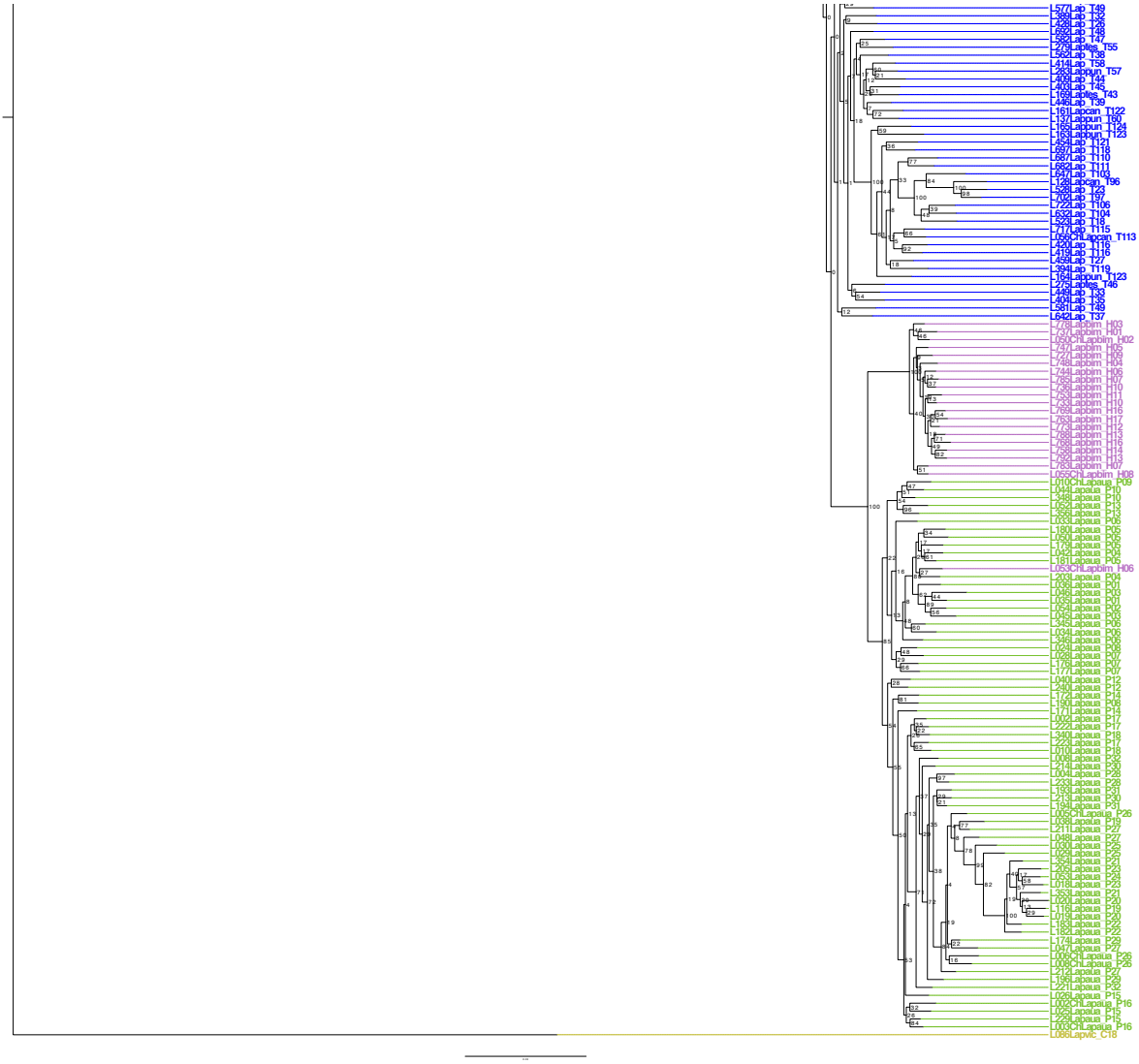

Figure S3.2., continued

▶CHAPTER III

A topoclimate model for Quaternary insular speciation

Chapter accepted

García-Olivares, V., Patiño, J., Overcast, I., Salces-Castellano, A., López de Heredia, U., Mora-Márquez, F., Machado A., Hickerson, M., & Emerson, B.C. (2019) A topoclimate model for Quaternary insular speciation. *Journal of Biogeography*

A topoclimate model for Quaternary insular speciation

Abstract

Aim. Understanding speciation as a process on islands, particularly speciation within individual islands, is key to explain the high levels of invertebrate speciation that characterise many oceanic islands and archipelagos. Here we propose an insular topoclimate model for Quaternary diversification (ITQD), and test the general prediction that glacial climate conditions facilitate the divergence of populations within species across valleys.

Location. Gran Canaria, Canary Islands.

Taxon. The *Laparocerus tesselatus* species complex (Curculionidae).

Methods. We characterise individual-level genomic relationships using single nucleotide polymorphisms produced by double-digest restriction site associated DNA sequencing (ddRAD-seq). A range of parameter values were explored in order to filter our data. We assess individual relatedness, species boundaries, demographic history and spatial patterns of connectivity.

Results. The total number of ddRAD-seq loci per sample ranges from 4576 to 512, with 11.12% and 4.84% of missing data respectively, depending on the filtering parameter combination. We consistently infer four genetically distinct ancestral populations and two presumed cases of admixture, one of which is largely restricted to high altitudes. Bayes factor delimitation support the hypothesis of four species, which is consistent with the four inferred ancestral gene pools. Landscape resistance analyses identified genomic relatedness among individuals in two out of the four inferred species to be best explained by annual precipitation during the last glacial maximum rather than geographic distance.

Main conclusions. Our data reveal a complex speciation history involving population isolation and admixture, with broad support for the ITQD model here proposed. We suggest that further studies are needed to test the generality of our model, and enrich our understanding of the evolutionary process in island invertebrates. Our results demonstrate the power of ddRAD-seq data to provide a detailed understanding of the temporal and spatial dynamics of insular biodiversity.

Introduction

The study of invertebrate speciation on oceanic archipelagos has been the focus of much attention due to the well-defined geographic boundaries of individual islands, the typical historical geographic isolation of islands from each other (but see Rijsdijk *et al.*, 2014), their dynamic and complex history of volcanism, and an often-strong endemic species component of their biodiversity. Molecular phylogenetic approaches have been an important source of information to understand both the tempo and geography of species origins in oceanic island settings (e.g. Shapiro *et al.*, 2006; Contreras-Diaz *et al.*, 2007; Dimitrov *et al.*, 2008; Sequeira *et al.*, 2008; Shaw & Gillespie, 2016), contributing to our understanding of patterns of community assembly and turnover (e.g. Emerson, 2003; Emerson & Oromi, 2005; Emerson & Gillespie, 2008). Population-level approaches have revealed the importance of colonisation dynamics among islands in the speciation process, highlighting how repeated colonisations of an island and gene exchange among different populations and species among islands can play an important role in speciation (Jordal *et al.*, 2006; Hendrickx *et al.*, 2015). Population-level studies are informative about divergence, gene flow, establishment of reproductive isolation and speciation, and the factors that promote it. However, compared to phylogenetic analyses of speciation history, studies that specifically address the speciation process in invertebrates within oceanic islands are few. Thus, understanding the drivers of invertebrate speciation within islands, in particular the potential for interactions among geology, topography and climate to promote speciation by local geographic isolation, is a key challenge (Patiño *et al.*, 2017).

It is increasingly recognised that Quaternary glacial cycles have impacted oceanic islands due to coincident sea-level and climate changes (e.g. Ali *et al.*, 2014; Rijsdijk *et al.*, 2014). Sea-level changes can cause substantial changes in island area, isolation and connectivity, now seen as consequential for patterns of island endemism across oceanic archipelagos and their underlying evolutionary dynamics (e.g. Papadopoulou & Knowles, 2015a, b; Weigelt *et al.*, 2016). At the archipelago scale, Gillespie and Roderick (2014) point out that such a dynamic can act as a “species pump”, potentially facilitating isolation and speciation, with subsequent range expansions leading to sympatry in periods of higher connectivity. Fernández-Palacios *et al.* (2016) present a model describing how variation in Quaternary climatic factors must have enforced species elevational changes, further

exaggerating isolation distances between islands caused by sea level changes alone during glacial conditions. While the implications for speciation between islands is obvious, there has been less focus on how Quaternary sea level changes and their environmental consequences might impact speciation within islands.

The dynamic highlighted by Fernández-Palacios *et al.* (2016) raises interesting potential outcomes when considering topographically more complex islands. Using a conically shaped island as an example, Fernández-Palacios *et al.* (2016) illustrate how rising sea levels and upward-shifted climatic zones would simultaneously shift species distributions upslope and reduce their overall range size (Fig. 1). The uniform topography considered by Fernández-Palacios *et al.* (2016) models expectations for a geologically young island, where erosional and catastrophic flank loss events are of minor consequence. In such a uniform landscape, climate is expected to change predictably with distance from the coast to the centre of the island. However, in older more eroded islands, spatial variation in local climate will be less uniform, and less predictable based on radial distance. The topographically complex island of Gran Canaria in the Canary Islands provides a useful example of this. Local climate station data has been used to demonstrate that pluviseasonal bioclimatic conditions are structured by variation in elevation and exposition (Fig. 2), resulting in a complex matrix of climate discontinuity across the island (del-Arco *et al.*, 2002).

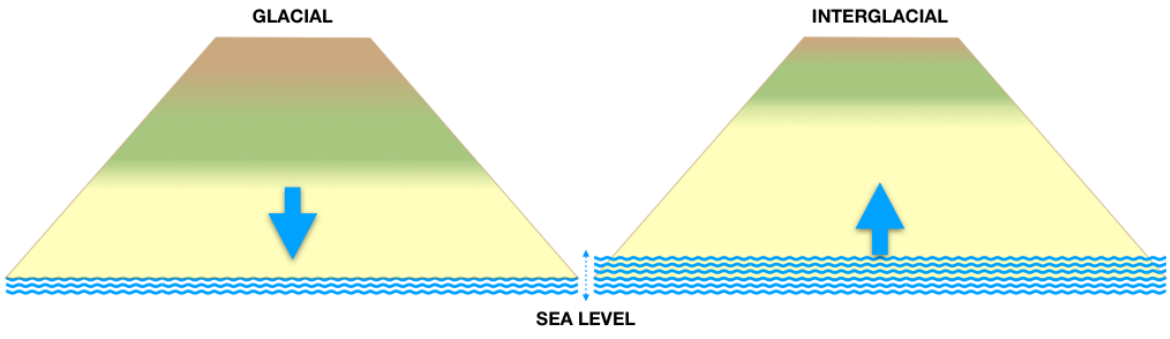

Figure 1. Quaternary climate change and oceanic island species distributions. Rising sea levels and upward-shifted climate zones during interglacial conditions are expected to impact upon the glacial distributions of individual species and habitats within oceanic islands. As climate transitions from glacial to interglacial conditions, a general tendency for upslope shifts is expected (modified from Fernández-Palacios *et al.*, 2015).

Variation in climate across topographically complex islands, together with (i) climatically sensitive species with limited dispersal ability, and (ii) cyclical alternation between glacial and interglacial conditions, could promote a dynamic of population divergence and coalescence, with potentially profound population genetic and evolutionary consequences. Dispersal limitation is a frequent feature of insular arthropods, and it has been recognised that together with landscape variation, such dispersal limitation can promote isolation and initiate speciation (Roesch *et al.*, 2012), even at a relatively small geographic scales (Vandergast *et al.*, 2004). In this respect, a mounting number of studies addressing the hypothesized "species pump" action of rising and falling sea levels under the "Pleistocene Aggregate Island Complex" (PAIC) (Heaney, 1985; Brown & Diesmos, 2002; Brown *et al.*, 2009; Esselstyn & Brown, 2009) have provided evidence for maximum levels of isolation in insular arthropods during present day interglacial conditions (e.g. Jordan *et al.*, 2005; Papadopoulou & Knowles, 2015a, b), potentially driving diversification.

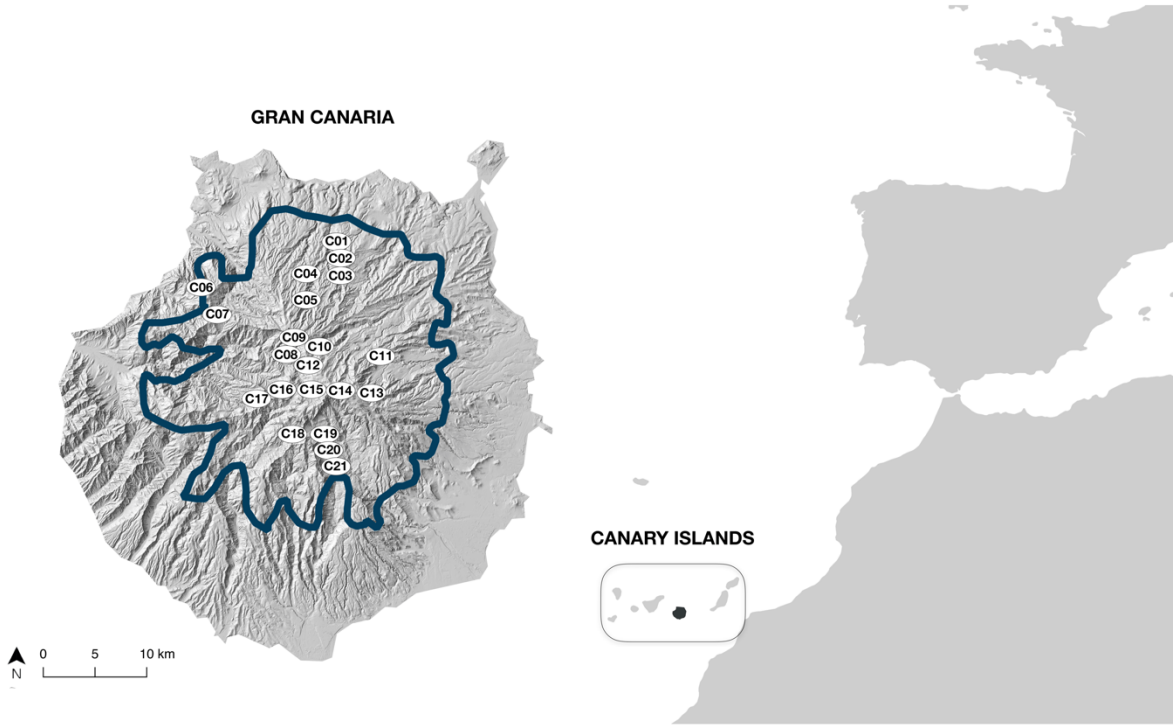

Figure 2. Sampling of the *Laparocerus tessellatus* complex in Gran Canaria. Map showing the location of the Canary Islands relative to Northwest Africa, and the geography of the archipelago with Gran Canaria highlighted in black. Sampling sites are shown within the island of Gran Canaria, together with the estimated distribution limits of the pluviseasonal bioclimate.

Here we used genomic data from beetles to develop and test predictions for a new model, which we refer to as an insular topoclimate model for Quaternary diversification (hereafter termed as ITQD). Within this model we propose that, during temporally more persistent glacial conditions, species ranges would have been at their lowest elevations, reaching their broadest potential range sizes, but also the greatest potential for spatial isolation by climate within islands (Fig. 3). As conditions transitioned from glacial to interglacial, distributions would have shifted to higher elevations and a simpler geographic climate matrix, something that should facilitate secondary contact (Fig. 3). We evaluate predictions from the ITQD model using a candidate system of dispersal limited beetles from the weevil genus *Laparocerus* on Gran Canaria. This is an ideal model system for a number of reasons related to both the biology of the focal group, the *Laparocerus tessellatus* species complex, and the geology of the island of Gran Canaria.

The *L. tessellatus* complex comprises 10 taxonomically described species and an additional undescribed species distributed across four islands, with each species being a single island endemic. Species are dispersal limited and patchily distributed, with a clear association to local humidity (Machado & Aguiar, 2005). The five taxonomically recognised species within the topographically and climatically complex island of Gran Canaria, have ranges that fall within the pluviseasonal bioclimate of the island (Fig. 2). A recent phylogenetic analysis for the genus *Laparocerus* revealed speciation within islands to be an important driver for the diversification of the 196 taxonomically described species and subspecies in the Canary Islands (Machado *et al.*, 2017). Recent population level analyses of closely related species within the *L. tessellatus* complex have further revealed less than simple patterns of individual relatedness among islands (Faria *et al.*, 2016), subsequently explained by mega-landslides facilitating movement between islands involving multiple individuals (García-Olivares *et al.*, 2017). However, there is less understanding about what factors have promoted divergence and speciation within islands, although Faria *et al.* (2016) present suggestive evidence for environmental barriers promoting both isolation and secondary contact.

Several recent DNA sequence-based analyses provide consistent evidence that Gran Canaria is the origin of the *L. tessellatus* complex. A Bayesian phylogenetic analysis concluded that the *L. tessellatus* complex belongs to a monophyletic group of potential subgenus status (Machado *et al.*, 2017) that includes a further 21 species. All but three of

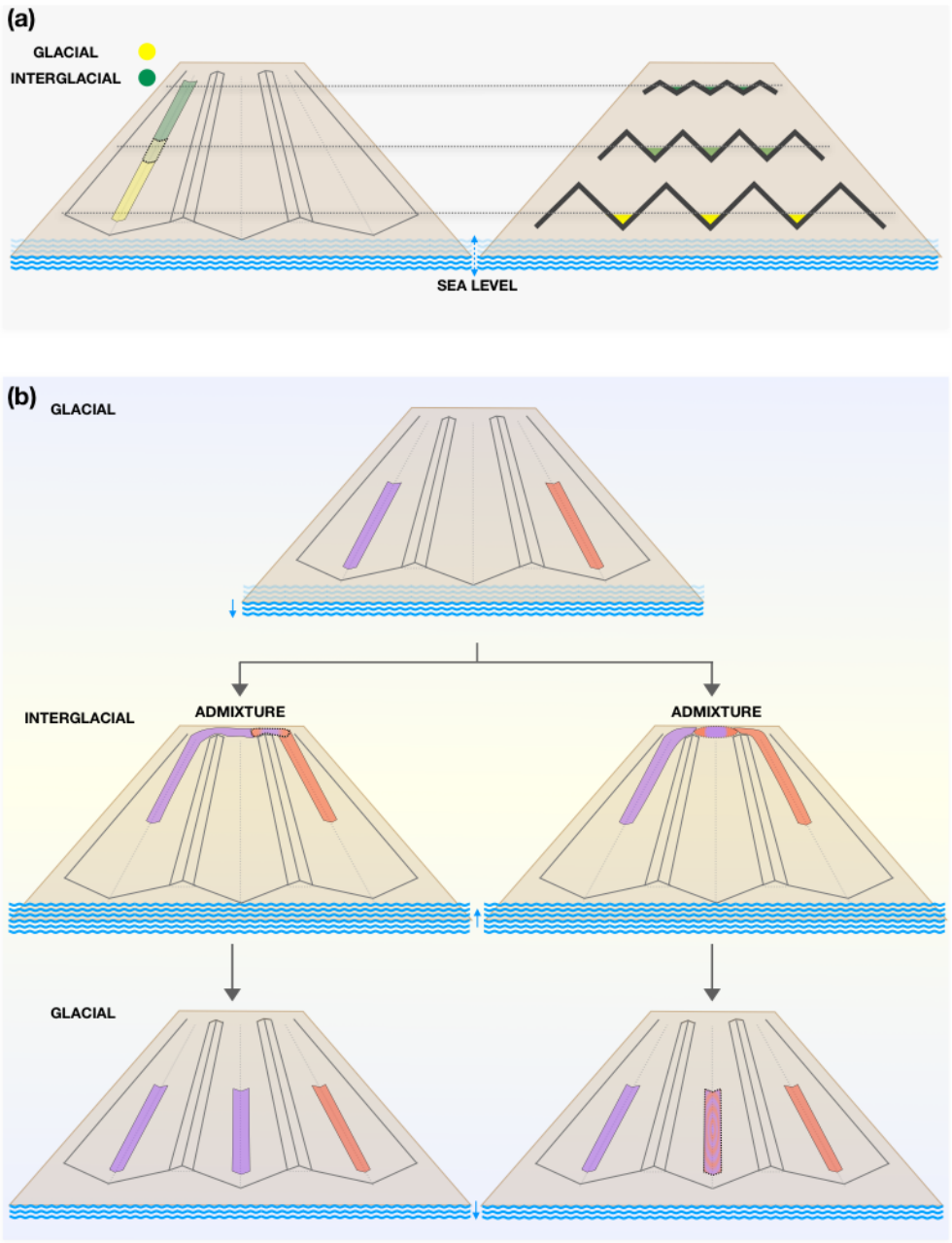

Figure 3. An insular topoclimate model for Quaternary diversification (ITQD). (a) A simplified island model is shown in the left panel, where topography is marked by erosional activity and the formation of valleys. Hypothetical species distributions are depicted as polygons representing range limits during glacial and interglacial climate conditions. Yellow represents interglacial conditions, when sea levels are at their lowest and global climate conditions at their coolest. Green represents range limits during warmer interglacial conditions, with overlap between glacial and interglacial ranges denote with an intermediate colour. The right panel represents isolation by bioclimate across valleys at different altitudes. In this example, a species with favourable climate associated with valley floors experiences reduced isolation by environment at higher elevations where the amplitude of topographic separation among valleys is reduced. (b) Two potential outcomes of glacial-scale climate change for two species (purple and red) distributed in different valleys during glacial climate conditions (top panel). During the transition from glacial to interglacial climate conditions, rising sea-level and upward-shifted climate zones result in upslope shifts in the distribution limits of both species, with contact and admixture in high elevation areas of low topographic complexity (middle panel). As climate transitions back to glacial conditions, species range limits shift downslope, potentially facilitating the colonisation of new valley by parental species (bottom panel, left), or even by new admixed populations (bottom panel, right).

the additional 21 species are endemic to Gran Canaria, consistent with a Gran Canarian origin for the complex. Faria *et al.* (2016) arrived to the same conclusion based on the geographic distribution of *ITS*2 variation across the four islands of the complex, although mtDNA variation was less informative. However, increased mtDNA sampling and network analyses in García-Olivares *et al.* (2017) confirmed the inferred ancestral mtDNA haplotype for the complex to have a Gran Canarian origin. Gran Canaria is represented by four taxonomically described species from the *L. tessellatus* complex: *L. microphthalmus* Lindberg, 1950; *L. obsitus* Wollaston, 1864; *L. osorio* Machado, 2012; and *L. tirajana* Machado, 2012. However, there are inconsistencies between these taxonomic entities and relationships inferred from both mtDNA and nuclear sequence data (see Faria *et al.*, 2016 for details), highlighting the need for different sequencing technologies that can increase resolution in order to infer the recent diversification history of the *L. tessellatus* complex. Due to their potential to yield data from thousands of loci, reduced representation genome sequencing approaches offer the opportunity to quantify individual relatedness and population genetic structure with as few as two individuals per population (Nazareno *et al.*, 2017). Here we apply double-digest restriction site associated DNA sequencing (ddRADseq; Peterson *et al.*, 2012) to investigate in more detail evolutionary process within the *L. tessellatus* species complex.

The onset of the relative volcanic quiescence within the island of Gran Canaria approximately 3 million years ago (Ma), known as the post-Roque Nublo period, predates estimates for the initiation of diversification within the *L. tessellatus* complex. Applying a general coleopteran COII mutation rate to mtDNA sequence variation within the complex, Faria *et al.* (2016) estimated the onset of diversification to have been approximately 2.7 Ma. More recently, Machado *et al.* (2017) used geological age constraints to calibrate their tree with a more complete sampling of the genus *Laparocerus*, and estimated the age of onset to be approximately 1.24 Ma. Thus, diversification falls within a period where volcanic activity has been characterised by localised low intensity activity in Gran Canaria, providing an opportunity to investigate diversification within a landscape subjected to the more subtle changes of millennial-scale erosional activity and climate variation.

In the present study, we first describe patterns of genomic relatedness among individuals, and then test the fit of competing hypotheses for species boundaries derived from taxonomy and RAD-seq data. We then use the best fit species model to test the

following three predictions from our ITQD model. Prediction 1 is that transitory interglacial conditions favour high elevation secondary contact and potential gene flow between species or populations previously isolated at lower altitudes during glacial conditions. Evidence for this prediction would be provided by signatures of admixture among species or populations at higher elevations. The more obvious potential mechanism for speciation within a topoclimate model would be through increased bioclimate fragmentation during glacial conditions, together with the colonisation of new favourable bioclimatic areas mediated by higher bioclimate connectivity during interglacial conditions (Fig. 3). Following from this, prediction 2 is that there would be lower genetic distance (higher genetic connectivity) among populations along altitudinal transects (i.e. down ridges and valleys), and higher genetic distance across radial transects (i.e. across ridges and valleys). A third prediction, derived from the expected higher genetic connectivity under interglacial conditions, is that populations should present signatures for demographic expansion consistent with the transition from glacial to interglacial conditions.

Materials and Methods

Geological context of Gran Canaria

Gran Canaria is located at the centre of the Canarian archipelago with a maximum elevation of 1950 metres above current sea level (macsl), and geologically it is likely one of the most comprehensively studied oceanic islands in the world (Carracedo & Troll, 2016). The geology of Gran Canaria can be broadly summarised as first involving a juvenile or shield forming stage (from 14.5-8.0 Ma), which includes basaltic shield growth on the submarine seamount, followed by a period of volcanic inactivity, and finally a stage involving renewed activity from 5.5 Ma to the present. This last stage is divided into two eruptive periods: Roque Nublo stratovolcanism and Post-Roque Nublo volcanism (Pérez-Torrado *et al.*, 1995; Carracedo & Day, 2002; Guillou *et al.*, 2004; Aulinas *et al.*, 2010). Since the end of the Roque Nublo eruptive period, approximately 3 Ma, Gran Canaria has been relatively inactive in terms of volcanic activity, characterised by local explosions related to hydromagmatic deposits (Anguita *et al.*, 2002), fissures and small-size monogenetic centers (Karátson *et*

al., 2016), with more recent activity limited to the north-northeast of the island (Rodriguez-Gonzalez *et al.*, 2012).

Sample collection and sample selection

Representative geographical sampling for the Gran Canarian species of the *L. tessellatus* complex was achieved by complementing the 10 sampling sites of Faria *et al.* (2016) with samples from 11 new sites. For each taxonomic species an average of three individuals from each sampling site were sequenced for a region of the mitochondrial COII gene. This was done to identify potential sites of sympatry for the two divergent mtDNA clades described by Faria *et al.* (2016) and García-Olivares *et al.* (2017), facilitating direct testing of their association with species boundaries. DNA was extracted using a Chelex extraction protocol (Casquet *et al.*, 2012) using two hind legs. PCR amplifications were performed using conditions described in Faria *et al.* (2016) and sequenced with the Sanger DNA sequencing service of Macrogen (www.macrogen.com). Sequences were edited with GENEIOUS R10.2.2 (http://geneious.com, Kearse *et al.*, 2012) and aligned with sequences from Faria *et al.* (2016) using MAFFT 6.814 (Katoh *et al.*, 2002). A Bayesian tree was then constructed using MRBAYES 3.2.6 (Ronquist *et al.*, 2012), applying the same parameters described in Faria *et al.* (2016). Four analyses were performed, each with 100 million generations using four Markov chain Monte Carlo (MCMC) chains, and sampling trees every 1000 generations, using *L. vicinus* as an outgroup. TRACER 1.6 (Rambaut *et al.*, 2018) was used to confirm that the average standard deviation of split frequencies was below 0.01 at the completion of the analysis; and to verify that effective sample size (ESS) values were above 200. Trees were visualized in FIGTREE 1.4.2 (Rambaut & Drummond, 2014).

RAD-seq library preparation

For each taxonomic species two individuals from each sampling site were selected for ddRAD-sequencing. Based on the results of the mtDNA sequencing, several additional samples were included to represent divergent mtDNA lineages sampled in sympatry. DNA extractions were performed using the Qiagen DNeasy Blood & Tissue kit following the manufacturer's instructions. A total of 51 individuals from the *L. tessellatus* complex were

analysed following modifications of the protocol of Mastretta-Yanes *et al.* (2015). Full details of the protocol are included in Appendix S1 (Supporting Information, Chapter II). After DNA extraction, digestion was performed using the enzymes EcoRI and MseI. Individuals from Gran Canaria were analysed together with a total of 224 individuals representing the remaining species of the complex from the western islands of the archipelago. In the light of complex patterns of mtDNA relatedness among individuals from Gran Canaria and other islands (Faria *et al.*, 2016; García-Olivares *et al.*, 2017), non-Gran Canaria samples were used to first assess relatedness among individuals of the complex from Gran Canaria and other islands. A total of 48 samples (including 11 individuals from Gran Canaria, four replicates and two negative controls) were first sequenced, randomly assigning samples to one of two sequencing indexes (ddRAD libraries hereafter). Both ddRAD libraries were pooled at equimolar ratios and size selected for fragments between 200-250 bp, and then sequenced using single-end reads (100bp long) in a single lane of an Illumina HiSeq2500 (Lausanne Genomic Technologies Facility, University of Lausanne, Switzerland). Based upon the mean depth from these first two libraries, a further 234 individuals were sequenced across 3 lanes (78 individuals, plus 1 replicate and 1 negative control). Samples within each lane were randomly assigned to one of four libraries for each (3 libraries with 24 samples, 1 library with 8 samples).

Bioinformatic and population genomic analysis

ddRAD-seq data were demultiplexed, quality filtered and de novo clustered using IPYRAD 0.7.19 (Eaton & Overcast, 2016). Only reads with unambiguous barcodes and fewer than 5 low quality bases (Phred quality score < 20), were retained, and a strict filter was applied to remove Illumina adapter contaminants. A first analysis was undertaken with all 273 individuals to assess patterns of relatedness among individuals of the complex from Gran Canaria and other islands. For this analysis, parameters were arbitrarily set to the following values: clust_threshold (the sequence similarity threshold) = 0.87, max_SNPs_locus (the maximum number of SNPs allowed in a locus) = 20, and min_samples_locus (the minimum number of samples that must have data at a given locus for that locus to be retained in the final data set) = 60%, with all remaining parameter values set to their default values.

We evaluated the congruence of the signal between two parameter combinations

identified for the analysis of individuals from Gran Canaria dataset (see Chapter II), one which yielded the highest number of loci, referred as the "relaxed" combination (clust_threshold = 0.85, max_SNPs_locus = 40, min_samples_locus = 80%), and the most "conservative" parameter combination (clust_threshold = 0.93, max_SNPs_locus = 5, min_sample_locus = 90%). To evaluate congruence between both parameter combinations we used principal component analysis (PCA) to describe the existence of groups of individuals and sNMF cross-entropy to compare the number of inferred ancestral populations, and individual ancestry coefficients. PCA analyses were performed using ADEGENET 2.1.0 package (Jombart & Ahmed, 2011) and sNMF using the LEA package (Frichot *et al.*, 2015) in R v. 3.4.2 (R Core Team 2013). The sNMF algorithm provides least-squares estimates of ancestry proportions to infer individual ancestry and population clustering (Frichot *et al.*, 2014). To obtain the best-fit number of ancestral populations (K) within Gran Canaria, K values from 1-10 were evaluated with 1000 replicates per K, using a cross-entropy criterion to identify the best fit value of K. Congruence between relaxed and conservative parameter combinations was accepted if the same groups are represented by PCA, and the same number and composition of ancestral populations were inferred by sNMF. In the absence of congruence stricter parameter combinations were evaluated until congruence with the relaxed parameter combinations was obtained. Upon identifying an appropriate parameter combination, replicate samples were used to estimate genotyping error (Mastretta-Yanes *et al.*, 2015).

Species delimitation

The Bayes factor delimitation (BFD) approach (Leache *et al.*, 2014) was implemented to evaluate competing species delimitation hypotheses, derived from taxonomy and ddRAD-seq data, using SNAPP (Bryant *et al.*, 2012). This approach uses an explicit multispecies coalescent (MSC) framework to calculate and compare marginal likelihood estimates (MLE) for alternative species delimitation hypotheses. While SNAPP is able to accommodate lineage sorting, it assumes that there is no gene flow between taxa (Bryant *et al.*, 2012). Thus, prior to the BFD analyses individuals with more than 10% assignment to an alternative ancestral population were considered admixed (Jombart & Collins, 2015) and removed from the dataset. These individuals were subsequently assessed for potential

hybrid origin (see following section). A path sampling analysis with 14 steps and an a-value of 0.3 with 100,000 MCMC generations and a pre burn-in of 10% was used.

Evaluating admixed individuals

Individuals identified as being of presumed admixed origin from sNMF and PCA analyses were further assessed using HYBRIDLAB (Nielsen *et al.*, 2006). The dataset was filtered using VCFTOOLS, to generate data sets comprising individuals of presumed admixed origin and their inferred parental populations. The set of recovered loci was then filtered for those loci presenting an F_{ST} estimate falling between 0.8 and 1.0 between parental populations. Selected loci were then used to simulate the following crosses: F1, F1 backcross with parent 1, F1 backcross to parent 2, F2. Simulated genotypes were then plotted to represent ancestry assignment and heterozygosity, together with estimates for parental and individuals of presumed admixed origin, using the graphics package in R v. 3.4.2.

Landscape patterns of genomic similarity and demography

To explore patterns of genetic distance among sampling sites within species inferred with BFD, the Neighbor-Net algorithm in SPLITSTREE v. 4.14.5 (Huson & Bryant, 2006) was used to summarise individual genomic relatedness, sampling a single SNP from each locus. Edge weights from splits graphs provide a measure of relatedness among nodes, facilitating their use as a proxy of genetic connectivity when nodes represent sampling sites and graphs are constructed from multiple genetic loci. By analysing a smaller number of more related individuals within species, more loci are expected to be recovered in the assembly process. Thus, to optimise the recovery of informative loci, individual species were processed with IPYRAD using the previously identified optimal parameter combination. To quantify differences in genetic distance among sampling sites, 100 bootstrap replicates were sampled from empirical SNP matrices and used to generate bootstrapped distributions for edge weights, which were corrected by geographic distance. Transformed edge weights were then used to generate mean bootstrapped edge weights and to test for significant differences between pairs of sampling sites using a non-parametric Kruskal-Wallis test

followed by a Nemenyi-test for multiple comparisons of (mean) rank sums of independent samples; both tests were performed in R v. 3.4.2 (R Core Team 2013).

To test for signatures of recent demographic expansion under the assumption of selective neutrality, we used Tajima's D (Tajima, 1989) and Fu and Li's D (Fu & Li, 1993) neutrality tests conducted in DnaSP v.6 (Rozas *et al.*, 2017), using all SNPs. Significantly negative values for Tajima's D and Fu and Li's D point to an excess of rare polymorphisms in a given population, which can be an indication of a recent increase in population size. In contrast, significantly positive values indicate a recent population contraction.

Landscape resistance analyses and isolation by distance

In order to make mechanistic inferences about what factor(s) could best explain geographic patterns of genetic structure within the *L. tessellatus* complex, we tested among alternative hypotheses, including isolation by distance, topographic-mediated isolation, and historical (glacial) and recent (interglacial) climate-driven isolation. To do this we used the R package ResistanceGA v 4.0 (Peterman, 2018) which both optimises and selects resistance surfaces to optimally fit genetic data. This approach circumvents typical issues such as spatial autocorrelation and high dimensionality that resistance surfaces can have, and subjectivity in assigning resistance values (Peterman *et al.*, 2014; Peterman, 2018). Pairwise genomic distances between individuals, estimated following the approach proposed by Petkova *et al.* (2015), were used as the dependent variable, while scaled and centred circuit resistance distance matrices between individuals were used as independent variables. Analyses were applied to inferred species and admixed individuals assigned to them (see population genomic analyses). For each species analysed, two data treatments were used: the first treatment included all individuals, while the second treatment excluded admixed individuals.

To calculate pairwise resistance distances between individuals, we used the random-walk commute time algorithm (function "commuteDistance" in "gdistance"), a genetic algorithm to maximise fit of resistance surfaces similar to CIRCUITSCAPE (McRae, 2006; McRae *et al.*, 2008). We used the wrapper function "all_comb" in ResistanceGA to implement single-surface and multiple-surface optimization, followed by a bootstrapping step. For the multiple-surface optimisation, we simultaneously combined two or three

resistance surfaces to optimise and create a novel composite resistance surface. Mixed models were fitted using the maximum-likelihood population effects (MLPE) parameterisation implemented in the R package LME4 (Bates *et al.*, 2014), as proposed in Peterman (2018) and Peterman *et al.* (2014).

We assessed the influence of eight climatic and topographic variables on genomic relatedness among individuals: (i) contemporary annual mean precipitation; (ii) annual mean precipitation at the Last Glacial Maximum (LGM); (iii) contemporary annual mean temperature; (iv) annual mean temperature at the LGM (Karger *et al.*, 2017); (v) a digital elevation model (DEM; Danielson & Gesch, 2011); and three topographic indexes estimated from the DEM layer in SAGA QGIS, including (vi) position index (TPI), (vii) ruggedness index (TRI) and (viii) wetness index (TWI). TPI is a measure which compares the elevation of each cell with the mean elevation of a specified neighbourhood around that cell, TRI describes the amount of elevation difference between adjacent cells of a digital elevation grid, and TWI quantifies topographic control on hydrological processes. All layers had a spatial resolution of 1 km x 1 km. In addition to the climatic and topographic resistance surfaces, we assessed Euclidean distance alone (isolation by distance) as well as an intercept only null model.

Results

Bioinformatic analyses

In contrast to the mtDNA results of Faria *et al.* (2016) and García-Olivares *et al.* (2017), nuclear genomic data revealed a simpler pattern of relatedness between individuals from Gran Canaria and other islands. A preliminary PCA using all 275 individuals from across all islands (Figure S1, Supporting Information) revealed individuals from Gran Canaria to form a cluster, being clearly distinct from other islands. Thus, for subsequent analyses only individuals from Gran Canaria were analysed. From this dataset two individuals were removed, one with a low number of reads and the other due to a high level of missing data (more than 30%).

A total of 178.37 million reads were sequenced for the dataset from Gran Canaria, of which 169.85 million reads passed the quality filtering steps of IPYRAD. Per sample an average of 3.46 (± 1.58 SD) million reads were recovered. Results from the optimization step are summarised in Figure S2 (Supporting Information, Chapter II). The relaxed parameter combination yielded a total of 4576 (± 228.14 SD) loci per sample, with 11.12% of missing data. In contrast to the relaxed parameter combination, the conservative parameter combination yielded an average of 512 (± 19.98 SD) loci per sample with 4.84% of missing data. Locus and allele error rates were calculated using the sample replicate approach of Mastretta *et al.* (2015) for the relaxed parameter combination revealing error rates of 0.029 and 0.002 respectively.

Population genomic analyses

A comparison of inferences derived from both the sNMF and PCA analyses for both the relaxed and conservative parameter combinations for genotype assembly in IPYRAD revealed congruence. The cross-entropy criterion identified four ancestral populations for both the relaxed (Fig. 4a) and conservative (Figure S2.1, Supporting Information) data sets, with consistent individual assignments inferred across both analyses. The relaxed parameter combination described six PCA groups with all but two groups (G4 and G5) showing clear separation (Fig. 4b). Genotype data assembled from the conservative parameter combination described four PCA groups (Figure S2.1, Supporting Information), three of which are described in Figure 4b (G1, G2, G3), with the fourth comprising the remaining groups in Figure 4b (G4, G5, G6). Comparing inferences from the sNMF ancestry coefficients and PCA analysis (Fig. 4), there is clear correspondence between both. PCA groups G1, G3, and G4 are exclusively comprised of all individuals assigned with high probability (> 90%; see Table S2.1, Supporting Information) to ancestral populations A, B and C respectively. PCA group G6 includes all individuals assigned with high ancestry to ancestral population D, but also includes 4 individuals with from 13% to 23% assignment to ancestral population C (Table S2.1, Supporting Information). The single individual comprising PCA group G2 is estimated to have shared ancestry between populations A and B, consistent with its intermediate position between G1 and G3 in the PCA. Finally, PCA group G5 comprises eight individuals with shared ancestry between populations C and D,

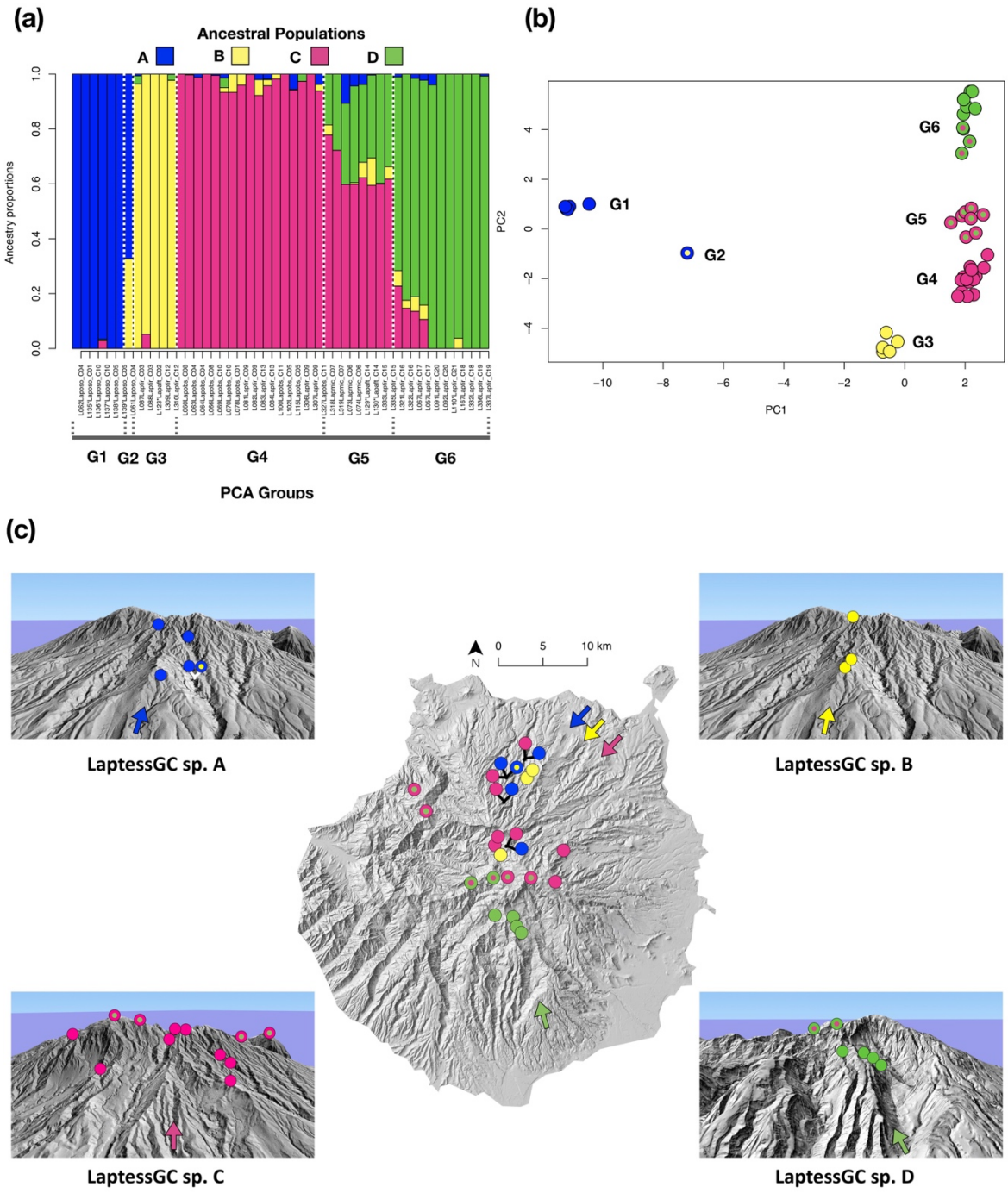

Figure 4. Ancestry assignment and individual clustering in the *Laparocerus tessellatus* complex. (a) sNMF assignment of individual ancestry to ancestral populations A, B, C and D. Individuals are grouped with respect to PCA clustering (see 4b). (b) Principal components analysis (PCA) of multilocus genotypes for individuals. Each point represents one individual, with colours corresponding to inferences of ancestry assignment with sNMF in (a). Individuals inferred to be of mixed ancestry with sNMF (more than 10% of the genome inferred to be from a second ancestral population) are represented with a coloured dot representing the minor representation genome. (c) Sampling sites are represented by circles and are colour coded with respect to probable genomic clusters identified by PCA (b). Black lines indicate sampling sites when more than one genomic cluster was sampled at a site. All sampling sites are represented in the central map. Sampled distributions of each the four species inferred by Bayes factor delimitation are shown using 3D digital terrain models, with orientation relative to the central map indicated with coloured arrows. Sites with admixed individuals are represented on the terrain model of the parental species with the higher contribution to the admixed genome.

consistent with the intermediate location of G5 between G4 and G6 in the PCA. *Laparocerus osorio* was the only taxonomically described species where all individuals were assigned to a single nuclear genomic population (A), to which no individuals from other taxonomic species were assigned. All but one individual of *L. osorio* was assigned with high probability to population A (PCA group G1), with the single exception also being assigned with 33% probability to population B (PCA group G2). The remaining taxonomic species did not segregate with nuclear data, with species either assigned to multiple populations, or to populations to which other species were also assigned, or both (Table S2.1, Supporting Information). No correspondence was found between patterns of nuclear genotype relatedness and the two mtDNA lineages described by Faria *et al.* (2016) and García-Olivares *et al.* (2017), with sympatric divergent mtDNA lineages associating with highly related nuclear genotypes.

Species delimitation

We identified seven initial competing species hypotheses derived from taxonomy and the population genomic analyses of RAD-seq data (Table 1). All samples from PCA groups G2 and G5, as well as four individuals from G6 were removed from the data set for SNAPP analyses because they presented signatures of admixture (i.e. more than 10% assignment to a second ancestral population). Removing these individuals reduced the final number of competing species hypotheses to four (Table 1). Bayes factor delimitation revealed highest support for hypothesis 3 (Table 1), in which four species are hypothesised (Fig. 4c) based on sNMF and PCA separation of the four inferred ancestral gene pools. The correspondences of inferred species with respect to the sNMF ancestral populations (Fig. 4a) and PCA groups (Fig. 4b) are as follows: LaptessGC sp. A (G1), LaptessGC sp. B (G3), LaptessGC sp. C (G4), and LaptessGC sp. D (G6 without admixed individuals).

Admixture

Two cases of presumed admixture were identified. In the first case a single individual comprising G2 (Fig. 4a) was inferred to be of admixed origin between LaptessGC sp. A and

Table 1. Bayes factor delimitation. Results of the Bayes factor delimitation analyses to test for the best support among competing species delimitation hypotheses (H) within the *Laparocerus tessellatus* complex in Gran Canaria. Initial hypotheses are refined to final hypotheses after the exclusion of admixed individuals. For each model, the marginal likelihood estimate (MLE), Bayes factors (BF) and rank are shown. The best fit model is highlighted in bold.

Initial hypotheses	Motivation	Groups	Final hypotheses	MLE	BF	Rank
H_a	2 major morphological groups	(G1, G2) (G3, G4, G5, G6)	H_1 2 species (G1) (G3, G4, G6)	-39,818.0	2,206.3	4
H_b	3 groups described by PC1 (PCA with conservative parameters)	(G1) (G2) (G3, G4, G5, G6)				
H_c	4 taxonomic species (*L. osorio, L.microphthalmus, L. obsitus, L. tirajana*)	(G1, G2) (G4) (G5) (G3, G4, G5, G6)	H_2 3 species (G1) (G4) (G3, G4, G6)	-40,357.0	2,745.3	º3
H_d	**5 groups described by PC1 and PC2 (PCA with conservative parameters)**	**(G1) (G2) (G3) (G4, G5) (G6)**	**H_3 4 species (G1) (G3) (G4) (G6)**	**-37,611.7**	**-**	**1**
H_e	**6 groups described by PC1 and PC2 (PCA with relaxed parameters)**	**(G1) (G2) (G3) (G4) (G5) (G6)**				
H_f	**4 groups described by sNMF (both conservative and relaxed parameter combinations)**	**(G1, G2) (G3) (G4, G5) (G6)**				
H_g	4 groups described by PC1 (PCA with relaxed parameters)	(G1) (G2) (G3) (G4, G5, G6)	H_4 3 species (G1) (G3) (G4, G6)	-38,221.1	609.3	2

LaptessGC sp. B. A total of 777 loci were identified as yielding an F_{ST} between 0.8 and 1 between LaptessGC sp. A and LaptessGC sp. B, providing strong diagnosability for first generation, second generation, or an older hybrid origin using HYBRIDLAB (Fig. 5a). These results clearly identify the G2 individual as being derived from an older admixture event between LaptessGC sp. A and LaptessGC sp. B. While the data does not allow us to say how far back in the past, the fact that only one of the parental species (LaptessGC sp. A) was sampled together with G2 suggests ancient rather than recent admixture. The sympatric sampling of G2 together with both LaptessGC sp. A and LaptessGC sp. C (Fig. 4c), with no signature of introgression, is consistent with reproductive isolation, and thus potential species status for G2. However, further sampling will be required to more rigorously assess the extent to which historical admixture between two morphologically distinct species, taxonomically assigned to the larger *L. osorio* and the smaller *L. tirajana*, has given rise to a new species that is morphologically cryptic with regard to *L. osorio*.

In the second case of inferred admixture, 12 individuals were inferred to be of admixed origin between LaptessGC sp. C and LaptessGC sp. D. The limited genetic differentiation between LaptessGC sp. C and LaptessGC sp. D resulted in only 26 loci with an F_{ST} between 0.8 and 1, providing only limited diagnosability of expected first and second-generation hybrid crosses (Fig. 5b). All 12 individuals were identified as derived from admixture older than F1, with several individuals providing strong signatures of an admixed origin going back multiple generations. It is interesting to note that individuals from the same sampling site tend to share similar values of heterozygosity and ancestry. This, together with PCA inferences that relatedness among admixed individuals is geographically structured (Figure S2.2, Supporting Information), and the absence of parental genotypes within any of the six sites with admixed individuals, suggests one or more admixture events of some antiquity.

Genomic distance and demographic signal

Of the four species inferred by BFD in SNAPP, LaptessGC sp. A and LaptessGC sp. B present geographically proximate distributions down the northern slopes of the island, with each showing greater separation among populations along an altitudinal axis relative to a radial axis (Fig. 4c). LaptessGC sp. D has a narrow distribution at higher altitudes of the southern

slopes of the island (Fig. 4c). The species with the broadest distribution is LaptessGC sp. C (Fig 4c). With a northern slope range that overlaps with LaptessGC sp. A, and further populations across the eastern slopes of the island, LaptessGC sp. C allows for the testing of higher genetic connectivity along altitudinal transects compared to radial transects. A SPLITSTREE representation of relatedness within LaptessGC sp. C reveals high separation among individuals, but lower genetic distance among individuals from the same sampling site, with the exception of sites C08 and C09, separated by a distance of less than 700 m (Fig. 6a). However, at a spatial separation from C08 and C09 of approximately 1.3 km, the two individuals from C10 are clearly differentiated (Fig. 6a). Distributions of bootstrapped edge lengths were generated from a data matrix representing each site with a single individual, collapsing C08 and C09 into a single site. Distributions were then used to calculate mean edge weight between sites capturing range limits, showing that values of genetic distance were significantly lower along altitudinal than across radial transects (Fig. 6b). Tajima's D and Fu and Li's D were non-significantly negative ($p > 0.10$) in all cases, with the exception of LaptessGC sp. D, which was non-significantly positive (Table 2).

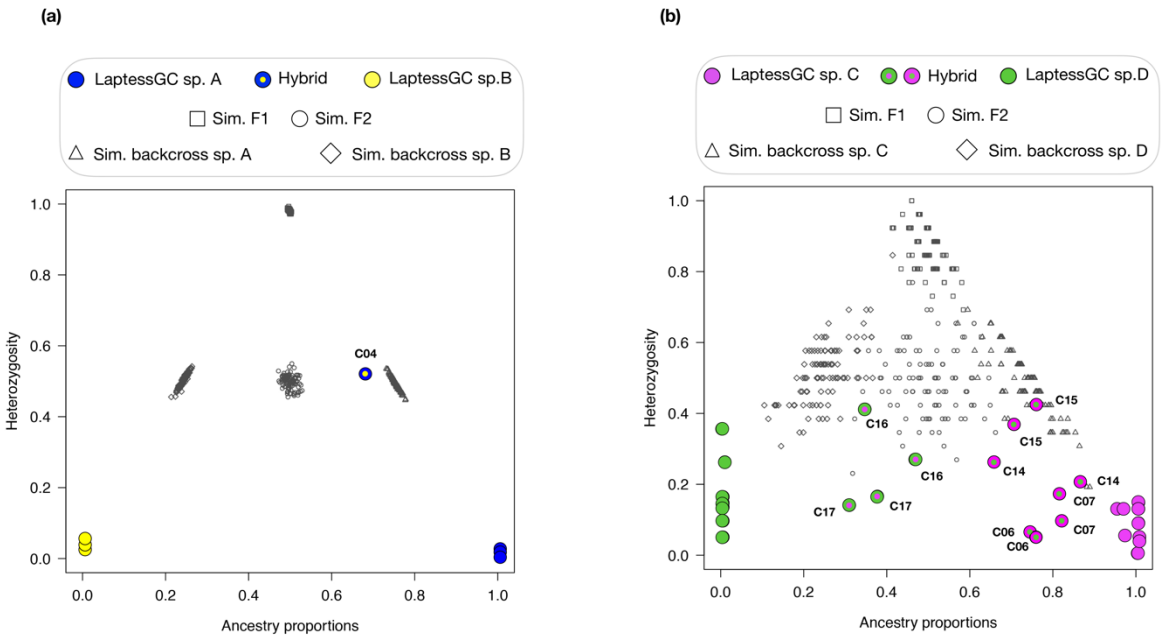

Figure 5. **Hybrid genome simulations.** Diagnostic loci from parental species are used to simulate expected genotypes for F1 and F2 hybrids, as well as F1 backcrosses with parental species. Sampling sites are indicated for admixed individuals (see Fig. 2). (a) High diagnosability of different hybrid classes clearly identifies an individual derived from admixture between LaptessGC sp. A and LaptessGC sp. B as not being of recent hybrid origin. (b) Despite limited diagnosability, all individuals derived from admixture between LaptessGC sp. C and LaptessGC sp. D are inferred to be older than F1 hybrids, and a smaller number can be diagnosed as being older than second generation hybrids.

Landscape resistance analyses

Landscape resistance analyses for LaptessGC sp. A identified genomic relatedness among individuals to be best explained by either geographic distance or a null model, while for LaptessGC sp. B geographic distance was identified as the model of best fit (Table 3). In contrast, for LaptessGC sp. C and LaptessGC sp. D, both of which presented individuals of admixed origin with the other species at higher elevations, genomic relatedness among individuals within each species was best explained by a single optimal model derived from landscape variation for annual precipitation during the LGM (Table 3). Landscape variation for annual precipitation during the LGM continued to be the single optimal model for LaptessGC sp. C even when admixed individuals were excluded, while for LaptessGC sp. D individual relatedness was best explained by a null model (Table 3), although with a very low R^2 value. Importantly, for all three analyses of LaptessGC sp. C and LaptessGC sp. D where landscape variation in precipitation during the LGM best explained genomic relatedness among individuals, a model derived from geographic distance was a substantially poorer fit, as measured by ΔAICc (Table 3).

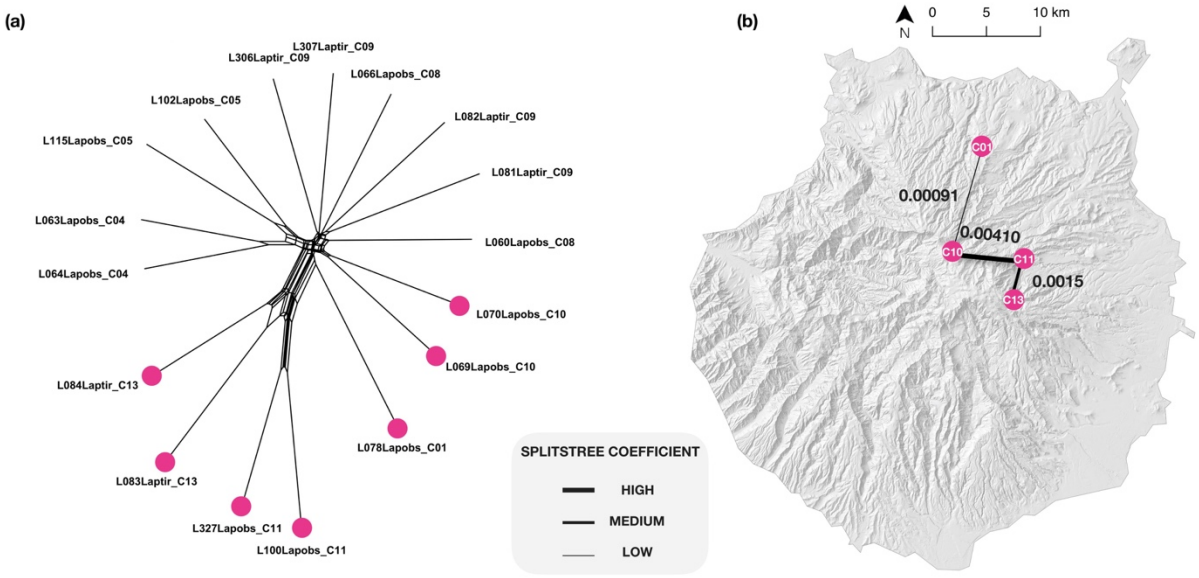

Figure 6. Altitudinal versus radial genomic relatedness. (a) Neighbor-Net phylogenetic network summarising genomic relatedness among individuals from LaptessGC sp. C. Individuals highlighted in pink represent sampling sites that capture altitudinal and radial limits of the distribution and were used to estimate genomic distance. (b) Mean edge weights calculated from 100 bootstrapped data sets were used to estimate genomic distance per kilometre among sampling sites. Genomic distance between C01 and C10 (9.1E-4 ± 3.9.1E-4) is significantly lower ($p < 0.05$ based on a Nemenyi test for multiple comparisons) than between C10 and C11 (4.1E-3 ± 1.0E-3) and C11 and C13 (1.5E-3 ± 5.9E-4).

Discussion

While the interaction between topography and climate across glacial cycles has been recognised as a driver of diversification in continental settings and among islands, its potential role as a driver of speciation within islands has been overlooked. Here we have presented a conceptual model for species distribution responses to the changing geography of local climate, an insular topoclimate model for Quaternary diversification (ITQD), as glacial-scale climate change plays out over topographically complex island landscapes. Our results provide support for the ITQD model, revealing a complex demographic history involving isolation, secondary contact and admixture. Signatures of admixture were associated with higher elevations, contrasting with an association of purer parental genomes at lower elevations, supporting prediction one. Higher genetic connectivity among individuals separated along an altitudinal axis compared to radially separation provides support for prediction two, while prediction three is unsupported, with no significant signatures for recent demographic expansion.

Table 2. Neutrality tests. Neutrality tests for the hypothesized species (see Table 1) in the *Laparocerus tessellatus* complex in Gran Canaria (genomic clusters identified in the PCA analyses are provided in brackets). All values for Tajima's D and Fu and Li's D are statistically non-significant ($p > 0.10$).

Genomic clusters	Tajima's D	Fu and Li's D
LaptessGC sp. A (G1)	-0.515	-0.291
LaptessGC sp. B (G3)	0.112	0.108
LaptessGC sp. C (G4)	-1.594	-1.846
LaptessGC sp. D (G6)	-0.728	-0.450

Admixture

Our results reveal two clear cases of admixture, one of which is largely characterised by higher altitudes in the centre of the island, from 1406 to 1813 macsl, involving the parental species LaptessGC sp. C and LaptessGC sp. D that were sampled at lower altitudes, from 708 to 1507 macsl (Fig. 4a). Specifically, LaptessGC sp. C is restricted to the northern and eastern slopes of Gran Canaria, while LaptessGC sp. D is restricted to southern slopes. To

explain population purity at lower elevations with admixture at higher elevations requires that the distribution of either one or both species has moved upslope facilitating contact and admixture. This is consistent with expectations following the Last Glacial Maximum (LGM), where warming temperatures and rising sea levels would have acted to enforce upslope shifts in species ranges (Fernández-Palacios *et al.*, 2016). Thus, the geography of admixture between LaptessGC sp. C and LaptessGC sp. D is consistent with a topoclimatic model.

Individuals derived from admixture between LaptessGC sp. C and LaptessGC sp. D were also sampled from two further sites, C06 and C07 (Fig. 2). These two sites fall outside the combined sampled ranges of LaptessGC sp. C and LaptessGC sp. D, being associated with the north-western Tamadaba massif, where altitude rises again from approximately 1000 macsl to exceed 1400 macsl. This regional topographic anomaly raises three possible explanations. The first is that there may be geographically close but unsampled pure parental populations in the Tamadaba region, consistent with recent (i.e. post LGM) admixture. The second possible explanation is that parental populations isolated locally during the LGM fully introgressed, which is again consistent with post LGM admixture. A third possible explanation is that admixture occurred prior to the LGM. Consistent with an older origin for the admixture of these populations is (i) their more distant relatedness to the parental populations in the PCA (Figure S2.2, Supporting Information), and (ii) their morphological differentiation from other individuals derived from admixture between LaptessGC sp. C and LaptessGC sp. D. Individuals from C06 and C07 are taxonomically described as *L. microphthalmus,* with the remaining admixed individuals from C14-C17 being taxonomically assigned to *L. tirajana*. To consider a dynamic under which genomic admixture might both arise during interglacial climatic conditions and persist through interglacial conditions, it is informative to draw comparison with population genetic expectations over glacial timescales within continental settings.

Table 3. Resistance analysis. Model rankings for landscape resistance variables tested against individual genomic relatedness for LaptessGC sp. A, LaptessGC sp. B, LaptessGC sp. C and LaptessGC sp. D, both with and without admixed individuals included. Only the five highest ranking models are presented in each case, with models identified as being optimal (ΔAIC_c ranges between 0-2) highlighted in bold. R^2m = marginal R^2 value; R^2c = conditional R^2 value; DIST = Euclidean distance, NULL = null model, P-LGM = annual precipitation at Last Glacial Maximum, (LGM) P-CT = contemporary annual mean precipitation, T-LGM = annual mean temperature at LGM, T-CT = annual mean temperature at current time, DEM = digital elevation model, TWI = topographic wetness index, TPI = topographic position index, TRI = topographic ruggedness index.

Species	Variable	AIC_c	ΔAIC_c	R^2_m	R^2_c
LaptessGC sp. A	**DIST**	**-88.86**	**0.00**	**0.31**	**0.33**
	NULL	-88.61	0.24	0.00	0.00
	TRI	-51.02	37.83	0.41	0.41
	TWI	-50.04	38.82	0.36	0.36
	TPI	-49.60	39.25	0.34	0.34
LaptessGC sp. A without admixed individuals	**NULL**	**-97.85**	**0.00**	**0.00**	**0.92**
	DIST	-97.52	0.33	0.01	0.94
	TRI	-76.90	20.95	0.02	0.94
	TPI	-76.80	21.05	0.02	0.94
	P-CT	-76.78	21.06	0.02	0.94
LaptessGC sp. B	**DIST**	**-56.19**	**0.00**	**0.56**	**0.88**
	NULL	-42.60	13.60	0.00	0.15
	TPI	-30.71	25.48	0.84	0.96
	TWI	-25.14	31.05	0.80	0.95
	T-LGM	-19.90	36.29	0.58	0.93
LaptessGC sp. C	**P-LGM**	**-1802.08**	**0.00**	**0.67**	**0.89**
	DEM	-1699.34	102.74	0.56	0.90
	T-LGM	-1690.64	111.44	0.54	0.91
	T-CT	-1689.18	112.90	0.54	0.91
	TWI	-1667.65	134.43	0.43	0.82
LaptessGC sp. C without admixed individuals	**P-LGM**	**-834.78**	**0.00**	**0.53**	**0.88**
	P-CT	-823.65	11.13	0.50	0.82
	DEM	-822.12	12.66	0.47	0.87
	TWI	-820.30	14.48	0.41	0.85
	P-LGM	-834.78	0.00	0.53	0.88

LaptessGC sp. D	**P-LGM**	**-339.60**	**0.00**	**0.68**	**0.89**
	TPI	-318.52	21.07	0.52	0.82
	DIST	-301.47	38.12	0.17	0.74
	TRI	-299.70	39.90	0.29	0.77
	TWI	-297.60	41.99	0.29	0.78
LaptessGC sp. D without admixed individuals	**NULL**	**-136.93**	**0.00**	**0.00**	**0.66**
	DIST	-133.74	3.18	0.02	0.67
	TWI	-118.00	18.93	0.55	0.65
	P-LGM	-114.32	22.60	0.05	0.69
	DEM	-114.13	22.79	0.07	0.63

Admixture and persistence

There is a rich literature on species demographic responses to Quaternary climate change, particularly within palearctic settings (e.g. Hewitt, 2000, 2004), with much empirical data demonstrating a dynamic where populations restricted to southern refugial areas during glacial periods expand and extend their distributions north as interglacial conditions unfold. Similar to our insular topoclimatic model, such range expansions create the potential for secondary contact and hybridisation, with many empirical examples of hybrid zones that have formed as a direct consequence of change in climate since the LGM (e.g. Hewitt, 2000, 2004). In a palearctic setting, such hybrid zones, and their genomic consequences, are transient. This transiency is a function of the typically vast distances between hybrid zones and refugial areas, separated by typically shallow elevational gradients. In the same way that post glacial northward range expansions from glacial refugia were typically rapid (Hewitt, 2000, 2004), so were southward contractions driven by the onset of glacial conditions, eliminating novel genomic variation from admixture as population extinction tracked south.

In an insular setting, the scale of range size change from glacial to interglacial conditions will be moderated by topography, whereby latitudinal and longitudinal changes are dampened by compensatory altitudinal shifts. It is this expectation for more limited change in the spatial dimensions of range size across glacial climate cycles, together with the potentially high topographic complexity within which these limited range changes may

occur, that may facilitate the persistence of novel admixed genomic variation across glacial cycles. Under a conceptual model where favourable habitat downslope from admixed populations is occupied by parental populations, extinction of admixed genomic variation would seem probable, due to priority effects (Alford & Wilbur, 1985). However, under a model where favourable downslope habitat is unoccupied, and generation-scale climate change across latitudinal and longitudinal axes are less than dispersal distance, descendants of admixed origin may potentially track climate change and habitat suitability downslope (Fig. 3). Under such a dynamic, the fate of admixed genomic variation from the four high altitude sampling sites of C14 to C17 (Fig. 2), under a future climate cooling scenario with the next glacial event, need not necessarily be one of extinction.

Admixed genomes sampled between the ranges of LaptessGC sp. C and LaptessGC sp. D span a geographic distance of approximately 7 km. Although we cannot definitively exclude that all favourable habitat downslope of the admixed range is populated by parental genotypes, it is improbable given the results of historical sampling efforts (AMC, unpublished data). Thus, there is potential for downslope movement of admixed genomes, and their survival through glacial maxima, providing a plausible mechanistic explanation for geographically disjunct populations of admixed genomes, such as those from the westernmost sampling sites (C06 and C07).

Admixture, persistence and speciation

It has recently been noted that admixture between divergent genomes could be a consequential process for insular speciation, potentially catalysing adaptive change and speciation (Emerson & Faria, 2014), and the more prevalent dynamic underpinning genomic admixture has been secondary contact arising from sequential colonisation of the same island by the same source species (e.g. Shaw, 2002; Jordal *et al.*, 2006; Nietlisbach *et al.*, 2013; Garrick *et al.*, 2014; Faria *et al.*, 2016). To our knowledge, our results are the first compelling evidence of genomic admixture within an island, without colonisation. Aside from the adaptive implications of admixture (Emerson & Faria, 2014), neutral processes of drift and recombination within admixed gene pools may also facilitate speciation through the generation of haplotypes and gene combinations that are incompatible with those of

parental populations (Abbott *et al.*, 2013). Thus, the persistence of admixed gene pools through time may contribute to both neutral and adaptive speciation.

The long-term fate of the admixed gene pools between LaptessGC sp. C and LaptessGC sp. D can only be speculated upon. Although there is tentative support for the admixed gene pools of the geographically disjunct populations of C06 and C07 having persisted through the LGM, the longer-term consequences of this, in terms of island community assembly, are unclear. Fortuitously the second admixture event that our analyses uncovered, involving the parental species LaptessGC sp. A and LaptessGC sp. B, provides some additional insight into community assembly consequences of admixture. The two parental species present similar distribution ranges in the northern slopes of the island, with our sampling suggesting them to be allopatric at the local scale (Fig. 4c). A strong signature of admixture between both parental genomes was revealed within an individual sampled at site C04. The sympatry of the admixed individual together with one of the parental species, LaptessGC sp. A, and a non-parental species, LaptessGC sp. C, suggests this admixed individual belongs to a fifth putative biological species, highlighting the potential for long-term persistence of admixed genomes, and their role in the origin of new species. However, further sampling of admixed individuals derived from LaptessGC sp. A and LaptessGC sp. B is required for a more robust inference.

Changing Quaternary bioclimate landscapes as drivers of population isolation and contact

The ITQD model makes the general prediction that connectivity between valleys is enhanced during interglacial conditions, as favourable climate is pushed upslope, where topographic heterogeneity, and thus environmental distance, is reduced among populations. In contrast, connectivity within valleys would remain relatively unchanged between both glacial and interglacial conditions, with the model making the general prediction that range limits should shift upslope. The species LaptessGC sp. C, which shows the broadest geographic distribution, revealed higher genetic connectivity among sites distributed along an altitudinal transect compared to populations separated radially around the island. These results are consistent with the prediction from the ITQD model that changes in climate throughout the Quaternary would result in higher potential bioclimate connectivity within valleys than among valleys. Indeed, topographic positions,

such as valley bottoms and basins, have been highlighted as ideal environments for microrefugia during Pleistocene glacial cycles (Dobrowski, 2011).

Landscape resistance analyses to test among mechanistic models for spatial structuring of genomic variation revealed evidence for geographic variation of annual precipitation during the LGM explaining contemporary geographic patterns of individual genomic relatedness. Admixed individuals assigned to either LaptessGC sp. C or LaptessGC sp. D were sampled from higher elevation areas characterised by high precipitation during the LGM. This is consistent with the origin of admixed individuals by upslope movement, and eventual secondary contact of parental species in response to increasingly favourable upslope climate as glacial conditions transitioned to interglacial. Phenological data for *Laparocerus* suggests that reduced levels of precipitation at higher altitudes are likely to have contributed to this dynamic together with increased temperature. Adult activity of *Laparocerus* species is typically concentrated in the more humid winter months. The few species whose maximum numbers shift to spring or early summer are notably found at higher elevations, where low winter temperatures are suggested to be a limiting factor (Machado & Aguiar, 2005).

None of the four species analysed presented significant support for recent demographic expansion from a bottleneck, although seven out of eight analyses presented values suggestive of expansion. These results perhaps highlight the complexity of demographic prediction within an insular geographic context. In the absence of a detailed understanding of probable species ranges during glacial climate conditions, it may be that simple predictions of demographic expansion are unrealistic. Upslope shifts in distribution limits may entail only limited increases in overall population size, compared to latitudinal range expansions in continental settings. An additional complication is that higher altitudes are precisely those areas where signatures for demographic expansion are expected to be strongest. However, estimation of any such signal would be further complicated by the existence of admixture at higher altitudes, and the necessary removal of such admixed individuals from demographic analyses, as was the case for two of our four species.

Conclusions

Our topoclimatic model for insular diversification places emphasis on the role of topography and changes in climate throughout the Quaternary for the process of diversification within islands. Using ddRAD-seq data for a beetle taxon with low-dispersal ability and affinity for areas of higher humidity within the pluviseasonal bioclimate of Gran Canaria, we found general support for the ITQD model, with evidence for isolation and admixture consistent with expectations as climate transitions between glacial and interglacial conditions. With regard to the generality of our model, it is likely to be less consequential within islands that present little topographic complexity, or for species that are highly dispersive, or with broad environmental tolerances. However, as topographic complexity increases, and as species traits tend toward low dispersal ability and limited environmental tolerances, we suggest the ITQD model will be a useful framework for interpreting patterns of genomic relatedness across insular landscapes.

References

Abbott, R., Albach, D., Ansell, S., Arntzen, J.W., Baird, S.J., Bierne, N., Boughman, J., Brelsford, A., Buerkle, C.A., Buggs, R., Butlin, R.K., Dieckmann, U., Eroukhmanoff, F., Grill, A., Cahan, S.H., Hermansen, J.S., Hewitt, G., Hudson, A.G., Jiggins, C., Jones, J., Keller, B., Marczewski, T., Mallet, J., Martinez-Rodriguez, P., Most, M., Mullen, S., Nichols, R., Nolte, A.W., Parisod, C., Pfennig, K., Rice, A.M., Ritchie, M.G., Seifert, B., Smadja, C.M., Stelkens, R., Szymura, J.M., Vainola, R., Wolf, J.B. & Zinner, D. (2013) Hybridization and speciation. *Journal of Evolutionary Biology*, **26**, 229-46.

Alford, R.A. & Wilbur, H.M. (1985) Priority effects in experimental pond communities: competition between Bufo and Rana. *Ecology*, **66**, 1097-1105.

Ali, J.R., Aitchison, J.C. & Fernández-Palacios, J.M. (2014) Exploring the combined role of eustasy and oceanic island thermal subsidence in shaping biodiversity on the Galápagos. *Journal of Biogeography*, **41**, 1227-1241.

Anguita, F., Márquez, A., Castiñeiras, P. & Hernán, F. (2002) *Los Volcanes de Canarias. Guía geológica e itinerarios*. Editorial Rueda, Madrid.

Aulinas, M., Gimeno, D., Fernandez-Turiel, J.L., Perez-Torrado, F.J., Rodriguez-Gonzalez, A. & Gasperini, D. (2010) The Plio-Quaternary magmatic feeding system beneath Gran Canaria (Canary Islands, Spain): constraints from thermobarometric studies. *Journal of the Geological Society*, **167**, 785-801.

Bates, D.M., Maechler, M., Bolker, B.M. & Walker, S. (2014) *lme4: Linear mixed-effects models using Eigen and S4.*

Brown, R.M. & Diesmos, A.C. (2002) Application of lineage-based species concepts to oceanic island frog populations: the effects of differing taxonomic philosophies on the estimation of Philippine biodiversity. *Silliman Journal*, **42**, 133-162.

Brown, R.M., Siler, C.D., Diesmos, A.C. & Alcala, A.C. (2009) Philippine Frogs of the Genus Leptobrachium (Anura; Megophryidae): Phylogeny-based Species Delimitation, Taxonomic Review, and Descriptions of Three New Species. *Herpetological Monographs*, **23**, 1-44.

Bryant, D., Bouckaert, R., Felsenstein, J., Rosenberg, N.A. & RoyChoudhury, A. (2012) Inferring species trees directly from biallelic genetic markers: bypassing gene trees in a full coalescent analysis. *Molecular Biology and Evolution*, **29**, 1917-32.

Carracedo, J. & Troll, V. (2016) *The geology of the Canary Islands*. Elsevier, Amsterdam.

Carracedo, J.C. & Day, S. (2002) *Canary Islands. Classic Geology in Europe Series Volume 4.* Terra Publishing, Harpenden.

Casquet, J., Thebaud, C. & Gillespie, R.G. (2012) Chelex without boiling, a rapid and easy technique to obtain stable amplifiable DNA from small amounts of ethanol-stored spiders. *Molecular Ecology Resources*, **12**, 136-41.

Contreras-Diaz, H.G., Moya, O., Oromi, P. & Juan, C. (2007) Evolution and diversification of the forest and hypogean ground-beetle genus Trechus in the Canary Islands. *Molecular Phylogenetics and Evolution*, **42**, 687-99.

Danielson, J.J. & Gesch, D.B. (2011) Global multi-resolution terrain elevation data 2010 (GMTED2010). In: *U.S. Geological Survey Open-File Report*, p. 26.

del-Arco, M., Salas, M., Acebes, J.R., del C. Marrero, M., Reyes-Betancort, J.A. & Pérez-de-Paz, J.A. (2002) Bioclimatology and climatophilous vegetation of Gran Canaria (Canary Islands). *Annales Botanici Fennici*, **39**, 15-41.

Dimitrov, D., Arnedo, M.A. & Ribera, C. (2008) Colonization and diversification of the spider genus Pholcus Walckenaer, 1805 (Araneae, Pholcidae) in the Macaronesian archipelagos: evidence for long-term occupancy yet rapid recent speciation. *Molecular Phylogenetics and Evolution*, **48**, 596-614.

Dobrowski, S.Z. (2011) A climatic basis for microrefugia: the influence of terrain on climate. *Global Change Biology*, **17**, 1022-1035.

Eaton, D.A.R. & Overcast, I. (2016) ipyrad: interactive assembly and analysis of RADseq data sets. *Available from:* http://ipyrad.readthedocs.io/.

Emerson, B.C. (2003) Genes, geology and biodiversity: faunal and floral diversity on the island of Gran Canaria. *Animal Biodiversity and Conservation*, **26**, 9-20.

Emerson, B.C. & Oromi, P. (2005) Diversification of the forest beetle genus Tarphius on the Canary Island, and the evolutionary origins of island endemics. *Evolution*, **59**, 586-598.

Emerson, B.C. & Gillespie, R.G. (2008) Phylogenetic analysis of community assembly and structure over space and time. *Trends in Ecology & Evolution*, **23**, 619-630.

Emerson, B.C. & Faria, C.M. (2014) Fission and fusion in island taxa–serendipity, or something to be expected? *Molecular ecology*, **23**, 5132-5134.

Esselstyn, J.A. & Brown, R.M. (2009) The role of repeated sea-level fluctuations in the generation of shrew (Soricidae: Crocidura) diversity in the Philippine Archipelago. *Molecular Phylogenetics and Evolution*, **53**, 171-81.

Faria, C.M.A., Machado, A., Amorim, I.R., Gage, M.J.G., Borges, P.A.V. & Emerson, B.C. (2016) Evidence for multiple founding lineages and genetic admixture in the evolution of species within an oceanic island weevil (Coleoptera, Curculionidae) super-radiation. *Journal of Biogeography*, **43**, 178-191.

Fernández-Palacios, J.M., Rijsdijk, K.F., Norder, S.J., Otto, R., de Nascimento, L., Fernández-Lugo, S., Tjørve, E. & Whittaker, R.J. (2016) Towards a glacial-sensitive model of island biogeography. *Global Ecology and Biogeography*, **25**, 817-830.

Frichot, E., François, O. & O'Meara, B. (2015) LEA: An R package for landscape and ecological association studies. *Methods in Ecology and Evolution*, **6**, 925-929.

Frichot, E., Mathieu, F., Trouillon, T., Bouchard, G. & Francois, O. (2014) Fast and efficient estimation of individual ancestry coefficients. *Genetics*, **196**, 973-83.

Fu, Y.X. & Li, W.H. (1993) Statistical tests of neutrality of mutations. *Genetics*, **133**, 693-709.

García-Olivares, V., López, H., Patiño, J., Alvarez, N., Machado, A., Carracedo, J.C., Soler, V. & Emerson, B.C. (2017) Evidence for mega-landslides as drivers of island colonization. *Journal of Biogeography*, **44**, 1053-1064.

Garrick, R.C., Benavides, E., Russello, M.A., Hyseni, C., Edwards, D.L., Gibbs, J.P., Tapia, W., Ciofi, C. & Caccone, A. (2014) Lineage fusion in Galápagos giant tortoises. *Molecular Ecology*, **23**, 5276-5290.

Gillespie, R.G. & Roderick, G.K. (2014) Geology and climate drive diversification. *Nature*, **509**, 297.

Guillou, H., Torrado, F.J.P., Hansen Machin, A.R., Carracedo, J.C. & Gimeno, D. (2004) The Plio–Quaternary volcanic evolution of Gran Canaria based on new K–Ar ages and magnetostratigraphy. *Journal of Volcanology and Geothermal Research*, **135**, 221-246.

Heaney, L.R. (1985) Zoogeographic evidence for middle and late Pleistocene land bridges to the Philippine Islands. *Modern Quaternary Research in Southeast Asia*, **9**, 127-144.

Hendrickx, F., Backeljau, T., Dekoninck, W., Van Belleghem, S.M., Vandomme, V. & Vangestel, C. (2015) Persistent inter- and intraspecific gene exchange within a parallel radiation of caterpillar hunter beetles (Calosoma sp.) from the Galapagos. *Molecular Ecology*, **24**, 3107-21.

Hewitt, G.M. (2000) The genetic legacy of the Quaternary ice ages. *Nature*, **405**, 907-913.

Hewitt, G.M. (2004) Genetic consequences of climatic oscillations in the Quaternary. *Philosophical Transactions of the Royal Society B: Biological Sciences*, **359**, 183-195.

Huson, D.H. & Bryant, D. (2006) Application of phylogenetic networks in evolutionary studies. *Molecular Biology and Evolution*, **23**, 254-67.

Jombart, T. & Ahmed, I. (2011) adegenet 1.3-1: new tools for the analysis of genome-wide SNP data. *Bioinformatics*, **27**, 3070-1.

Jombart, T. & Collins, C. (2015) A tutorial for discriminant analysis of principal components (DAPC) using adegenet 2.0.0. *Available from:* http://adegenet.r-forge.r-project.org/files/tutorial-dapc.pdf.

Jordal, B.H., Emerson, B.C. & Hewitt, G.M. (2006) Apparent 'sympatric' speciation in ecologically similar herbivorous beetles facilitated by multiple colonizations of an island. *Molecular Ecology*, **15**, 2935-47.

Jordan, S., Simon, C., Foote, D. & Englund, R.A. (2005) Phylogeographic patterns of Hawaiian Megalagrion damselflies (Odonata: Coenagrionidae) correlate with Pleistocene island boundaries. *Molecular Ecology*, **14**, 3457-3470.

Karátson, D., Yepes, J., Favalli, M., Rodríguez-Peces, M.J. & Fornaciai, A. (2016) Reconstructing eroded paleovolcanoes on Gran Canaria, Canary Islands, using advanced geomorphometry. *Geomorphology*, **253**, 123-134.

Karger, D.N., Conrad, O., Böhner, J., Kawohl, T., Kerft, H., Soria-Auza, R.W., Zimmermann, N.E., Linder, H.P. & Kessler, M. (2017) Climatologies at high resolution for the earth's land surface areas. *Scientific Data*, **4**, 170122.

Katoh, K., Misawa, K., Kuma, K.I. & Miyata, T. (2002) MAFFT: a novel method for rapid multiple sequence alignment based on fast Fourier transform. *Nucleic acids research*, **30**, 3059-3066.

Kearse, M., Moir, R., Wilson, A., Stones-Havas, S., Cheung, M., Sturrock, S., Buxton, S., Cooper, A., Markowitz, S., Duran, C., Thierer, T., Ashton, B., Meintjes, P. & Drummond, A. (2012) Geneious Basic: An integrated and extendable desktop software platform for the organization and analysis of sequence data. *Bioinformatics*, **28**, 1647-1649.

Leache, A.D., Fujita, M.K., Minin, V.N. & Bouckaert, R.R. (2014) Species delimitation using genome-wide SNP data. *Systematic Biology*, **63**, 534-42.

Machado, A. & Aguiar, A. (2005) Phenology of *Laparocerus* species in Tenerife, Canary Islands (Coleoptera, Curculionidae). *Boletim do Museu Municipal do Funchal*, **56**, 5-21.

Machado, A., Rodriguez-Exposito, E., Lopez, M. & Hernandez, M. (2017) Phylogenetic analysis of the genus *Laparocerus*, with comments on colonisation and diversification in Macaronesia (Coleoptera, Curculionidae, Entiminae). *Zookeys*, 1-77.

Mastretta-Yanes, A., Arrigo, N., Álvarez, N., Jorgensen, T.H., Pinero, D. & Emerson, B.C. (2015) Restriction site-associated DNA sequencing, genotyping error estimation and de novo assembly optimization for population genetic inference. *Molecular Ecology Resources*, **15**, 28-41.

McRae, B.H. (2006) Isolation by resistance. *Evolution*, **60**, 1551-1561.

McRae, B.H., Dickson, B.G., Keitt, T.H. & Shah, V.B. (2008) Using circuit theory to model connectivity in ecology, evolution, and conservation. *Ecology*, **89**, 2712-2724.

Nazareno, A.G., Bemmels, J.B., Dick, C.W. & Lohmann, L.G. (2017) Minimum sample sizes for population genomics: an empirical study from an Amazonian plant species. *Molecular Ecology Resources*, **17**, 1136-1147.

Nielsen, E.E., Bach, L.A. & Kotlicki, P. (2006) Hybridlab (version 1.0): a program for generating simulated hybrids from population samples. *Molecular Ecology Notes*, **6**, 971-973.

Nietlisbach, P., Wandeler, P., Parker, P.G., Grant, P.R., Grant, B.R., Keller, L.F. & Hoeck, P.E. (2013) Hybrid ancestry of an island subspecies of Galapagos mockingbird explains discordant gene trees. *Molecular Phylogenetics and Evolution*, **69**, 581-92.

Papadopoulou, A. & Knowles, L.L. (2015a) Genomic tests of the species-pump hypothesis: Recent island connectivity cycles drive population divergence but not speciation in Caribbean crickets across the Virgin Islands. *Evolution*, **69**, 1501-1517.

Papadopoulou, A. & Knowles, L.L. (2015b) Species-specific responses to island connectivity cycles: refined models for testing phylogeographic concordance across a Mediterranean Pleistocene Aggregate Island Complex. *Molecular Ecology*, **24**, 4252-68.

Patiño, J., Whittaker, R.J., Borges, P.A.V., Fernández-Palacios, J.M., Ah-Peng, C., Araújo, M.B., Ávila, S.P., Cardoso, P., Cornuault, J., de Boer, E.J., de Nascimento, L., Gil, A., González-Castro, A., Gruner, D.S., Heleno, R., Hortal, J., Illera, J.C., Kaiser-Bunbury, C.N., Matthews, T.J., Papadopoulou, A., Pettorelli, N., Price, J.P., Santos, A.M.C., Steinbauer, M.J., Triantis, K.A., Valente, L., Vargas, P., Weigelt, P. & Emerson, B.C. (2017) A roadmap for island biology: 50 fundamental questions after 50 years of The Theory of Island Biogeography. *Journal of Biogeography*, **44**, 963-983.

Pérez-Torrado, F.J., Carracedo, J.C. & Mangas, J. (1995) Geochronology and stratigraphy of the Roque Nublo Cycle, Gran Canaria, Canary Islands. *Journal of the Geological Society*, **152**, 807-818.

Peterman, W.E. (2018) ResistanceGA: An R package for the optimisation of resistance surfaces using genetic algorithms. *Methods in Ecology and Evolution*, **9**, 1638-1647.

Peterman, W.E., Connette, G.M., Keitt, T.H. & Shah, V.B. (2014) Ecological resistance surfaces predict fine-scale genetic differentiation in a terrestrial woodland salamander. *Molecular Ecology*, **23**, 2402-2413.

Peterson, B.K., Weber, J.N., Kay, E.H., Fisher, H.S. & Hoekstra, H.E. (2012) Double digest RADseq: an inexpensive method for de novo SNP discovery and genotyping in model and non-model species. *PLoS One*, **7**, e37135.

Petkova, D., Novembre, J. & Stephens, M. (2015) Visualising spatial population structure with estimated effective migration surfaces. *Nature Genetics*, **48**, 94-100.

Rambaut, A. & Drummond, A. (2014) FigTree v.1.4.2: Tree Figure Drawing Tool. *Available from :* http://tree.bio.ed.ac.uk/software/figtree.

Rambaut, A., Drummond, A.J., Xie, D., Baele & G., S., M. A (2018) Posterior summarisation in Bayesian phylogenetics using Tracer 1.7. *Systematic Biology*, **10**

Rijsdijk, K.F., Hengl, T., Norder, S.J., Otto, R., Emerson, B.C., Ávila, S.P., López, H., van Loon, E.E., Tjørve, E., Fernández-Palacios, J.M. & Heaney, L. (2014) Quantifying surface-area changes of volcanic islands driven by Pleistocene sea-level cycles:

biogeographical implications for the Macaronesian archipelagos. *Journal of Biogeography*, **41**, 1242-1254.

Rodríguez-González, A., Fernández-Turiel, J.L., Pérez-Torrado, F.J., París, R., Gimeno, D., Carracedo, J.C. & Aulinas, M. (2012) Factors controlling the morphology of monogenetic basaltic volcanoes: The Holocene volcanism of Gran Canaria (Canary Islands, Spain). *Geomorphology*, **136**, 31-44.

Roesch, K.G., Welter, S.C. & Roderick, G.K. (2012) Genetic divergence is decoupled from ecological diversification in the Hawaiian *Nesosydne* planthoppers. *Evolution*, **66**, 2798-2814.

Ronquist, F., Teslenko, M., van der Mark, P., Ayres, D.L., Darling, A., Hohna, S., Larget, B., Liu, L., Suchard, M.A. & Huelsenbeck, J.P. (2012) MrBayes 3.2: efficient Bayesian phylogenetic inference and model choice across a large model space. *Systematic Biology*, **61**, 539-42.

Rozas, J., Ferrer-Mata, A., Sánchez-DelBarrio, J.C., Guirao-Rico, S., Librado, P., Ramos-Onsins, S.E. & Sánchez-Gracia, A. (2017) DnaSP 6: DNA Sequence Polymorphism Analysis of Large Data Sets. *Molecular Biology and Evolution*, **34**, 3299-3302.

Sequeira, A.S., Lanteri, A.A., Albelo, L.R., Bhattacharya, S. & Sijapati, M. (2008) Colonization history, ecological shifts and diversification in the evolution of endemic Galápagos weevils. *Molecular Ecology*, **17**, 1089-1107.

Shapiro, L.H., Strazanac, J.S. & Roderick, G.K. (2006) Molecular phylogeny of Banza (Orthoptera: Tettigoniidae), the endemic katydids of the Hawaiian Archipelago. *Molecular Phylogenetics and Evolution*, **41**, 53-63.

Shaw, K.L. (2002) Conflict between nuclear and mitochondrial DNA phylogenies of a recent species radiation: What mtDNA reveals and conceals about modes of speciation in Hawaiian crickets. *Proceedings of the National Academy of Sciences*, **99**, 16122-16127.

Shaw, K.L. & Gillespie, R.G. (2016) Comparative phylogeography of oceanic archipelagos: Hotspots for inferences of evolutionary process. *Proceedings of the National Academy of Sciences*, **113**, 7986-7993.

Tajima, F. (1989) Statistical method for testing the neutral mutation hypothesis by DNA polymorphism. *Genetics*, **123**, 585-595.

Vandergast, A.G., Gillespie, R.G. & Roderick, G.K. (2004) Influence of volcanic activity on the population genetic structure of Hawaiian Tetragnatha spiders: fragmentation, rapid population growth and the potential for accelerated evolution. *Molecular Ecology*, **13**, 1729-43.

Weigelt, P., Steinbauer, M.J., Cabral, J.S. & Kreft, H. (2016) Late Quaternary climate change shapes island biodiversity. *Nature*, **532**, 99-102.

Supporting information

Appendix S1. Exploratory analysis using all 275 individuals sampled within the *L. tessellatus* complex.

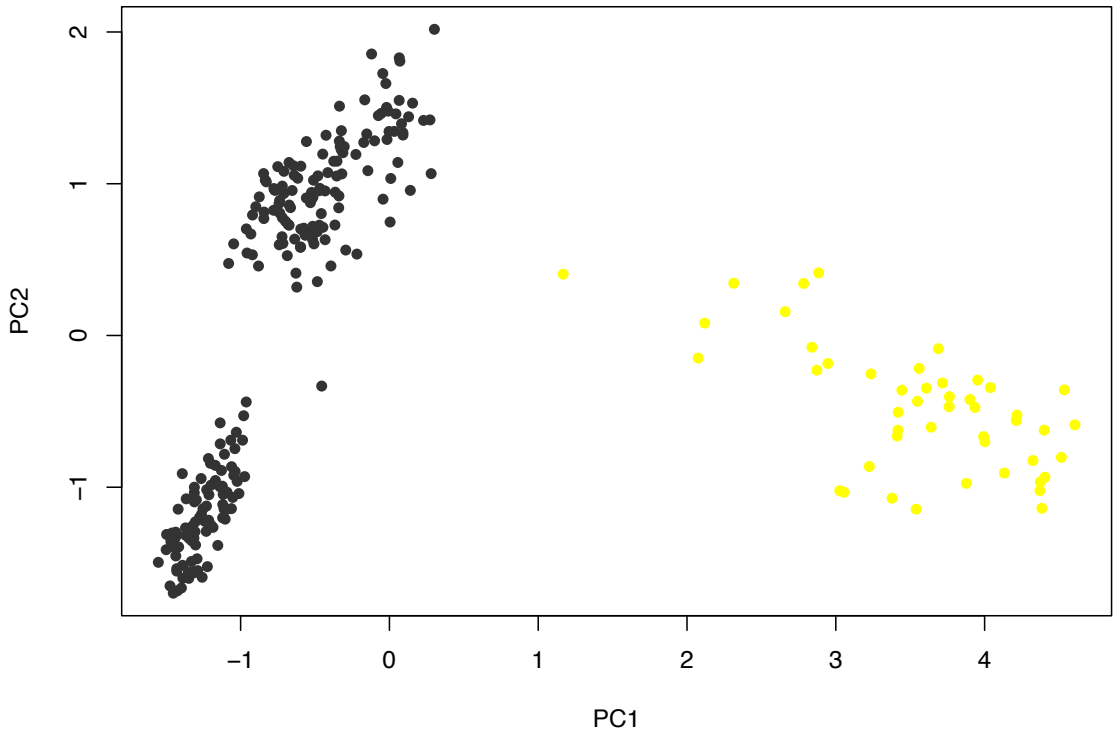

Figure S1. Exploratory analysis of the *Laparocerus tessellatus* species complex across the Canary Islands. Principal components analysis (PCA) of multilocus genotypes for the individuals sampled. Each point represents one individual. Whereas the individuals from Gran Canaria are represented with yellow colour, the individuals from Gran Tenerife, La Palma and El Hierro are represented in black colour.

Appendix S2. Table S2.1 and Figures S2.1 – S2.2

Table S2.1. sNMF ancestry coefficients (i.e probabilities of assignment to inferred ancestral populations) for each of the four inferred ancestral populations using genotypes derived from assembly with the relaxed parameter combination.

Individuals	Taxonomy	A	B	C	D
L318Lapmic_C07	*L. microphthalmus*	9.9991E-05	0.0371861	0.777792	0.184922
L319Lapmic_C07	*L. microphthalmus*	9.9982E-05	9.9982E-05	0.722439	0.277361
L074Lapmic_C06	*L. microphthalmus*	0.043507	0.0057993	0.598642	0.352052
L073Lapmic_C06	*L. microphthalmus*	0.106653	0.000397027	0.597985	0.294965
L060Lapobs_C08	*L. obsitus*	9.998E-05	9.998E-05	0.9997	9.998E-05
L066Lapobs_C08	*L. obsitus*	9.998E-05	9.998E-05	0.9997	9.998E-05
L102Lapobs_C05	*L. obsitus*	9.998E-05	9.998E-05	0.9997	9.998E-05
L063Lapobs_C04	*L. obsitus*	9.9982E-05	9.9982E-05	0.997109	0.00269139
L069Lapobs_C10	*L. obsitus*	0.0044504	9.9982E-05	0.99535	9.9982E-05
L064Lapobs_C04	*L. obsitus*	0.0117716	9.9982E-05	0.988028	9.9982E-05
L100Lapobs_C11	*L. obsitus*	9.9982E-05	0.0173816	0.982418	9.9982E-05
L115Lapobs_C05	*L. obsitus*	0.0553148	0.00300875	0.941576	9.9991E-05
L327Lapobs_C11	*L. obsitus*	0.0377896	0.0236061	0.938504	9.9991E-05
L070Lapobs_C10	*L. obsitus*	0.0142199	0.0170389	0.933511	0.0352303
L078Lapobs_C01	*L.obsitus*	9.9982E-05	0.0663112	0.933489	9.9982E-05
L062Laposo_C04	*L. osorio*	0.9997	9.998E-05	9.998E-05	9.998E-05
L135Laposo_C01	*L. osorio*	0.9997	9.998E-05	9.998E-05	9.998E-05
L136Laposo_C10	*L. osorio*	0.9997	9.998E-05	9.998E-05	9.998E-05
L138Laposo_C05	*L. osorio*	0.9997	9.998E-05	9.998E-05	9.998E-05
L139Laposo_C05	*L. osorio*	0.9997	9.998E-05	9.998E-05	9.998E-05
L137Laposo_C10	*L. osorio*	0.966173	9.9991E-05	0.0286126	0.00511416
L061Laposo_C04	*L. osorio*	0.672839	0.326961	9.9982E-05	9.9982E-05
L123Lapaft_C02	*L. tirajana*	9.998E-05	0.9997	9.998E-05	9.998E-05
L309Laptir_C12	*L. tirajana*	9.998E-05	0.9997	9.998E-05	9.998E-05
L088Laptir_C03	*L. tirajana*	9.9982E-05	0.947662	0.0521384	9.9982E-05
L087Laptir_C03	*L. tirajana*	0.00610788	0.96426	9.9991E-05	0.0295324
L310Laptir_C12	*L. tirajana*	0.00145776	0.977111	9.9991E-05	0.0213317
L307Laptir_C09	*L. tirajana*	9.998E-05	9.998E-05	0.9997	9.998E-05
L082Laptir_C09	*L. tirajana*	9.9982E-05	0.00129132	0.998509	9.9982E-05
L306Laptir_C09	*L. tirajana*	9.9982E-05	9.9982E-05	0.973705	0.0260952
L081Laptir_C09	*L. tirajana*	9.9982E-05	0.0397396	0.96006	9.9982E-05
L084Laptir_C13	*L. tirajana*	0.0180139	0.0218433	0.957439	0.00270433
L083Laptir_C13	*L. tirajana*	0.020511	0.0567137	0.922675	9.9991E-05
L129Lapaft_C14	*L. tirajana*	0.038317	0.0557084	0.622777	0.283198
L335Laptir_C15	*L. tirajana*	9.9991E-05	0.0449201	0.61764	0.33734
L333Laptir_C15	*L. tirajana*	9.9991E-05	0.0032789	0.599277	0.397344
L130Lapaft_C14	*L. tirajana*	0.00363042	0.0994095	0.594738	0.302222
L092Laptir_C20	*L. tirajana*	9.998E-05	9.998E-05	9.998E-05	0.9997
L110Laptir_C21	*L. tirajana*	9.998E-05	9.998E-05	9.998E-05	0.9997
L332Laptir_C18	*L. tirajana*	9.998E-05	9.998E-05	9.998E-05	0.9997
L336Laptir_C19	*L. tirajana*	9.998E-05	9.998E-05	9.998E-05	0.9997
L337Laptir_C19	*L. tirajana*	0.00707153	9.9982E-05	9.9982E-05	0.992729
L167Laptir_C18	*L. tirajana*	9.9982E-05	0.0370518	9.9982E-05	0.962748
L091Laptir_C20	*L. tirajana*	0.0395451	9.9982E-05	9.9982E-05	0.960255
L322Laptir_C16	*L. tirajana*	9.9991E-05	0.029206	0.146733	0.823961
L057Laptir_C17	*L. tirajana*	0.0225678	0.0527392	0.105654	0.819039
L067Laptir_C17	*L. tirajana*	0.0155539	0.0526422	0.135628	0.796176
L321Laptir_C16	*L. tirajana*	0.0101628	0.0566325	0.227272	0.705932

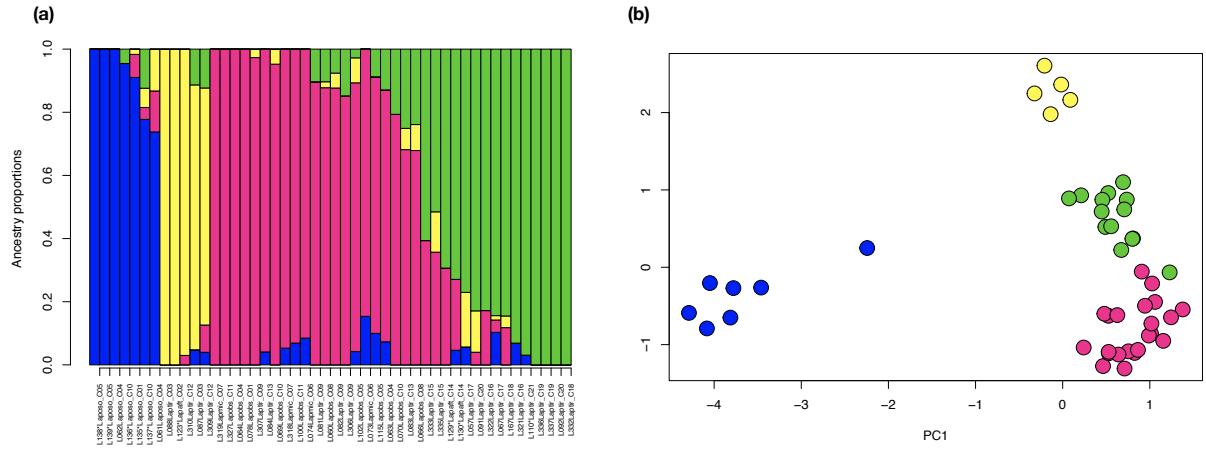

Figure S2.1. Ancestry assignment and individual clustering within the *L. tessellatus* complex using genotypes derived from assembly with the conservative parameter combination**.** (a) sNMF assignment of individual ancestry to ancestral populations: A (blue), B (yellow), C (pink) and D (green). (b) Principal components analysis of multilocus genotypes for individuals. Each point represents one individual, with colors corresponding to inferences of ancestry assignment with sNMF in (a).

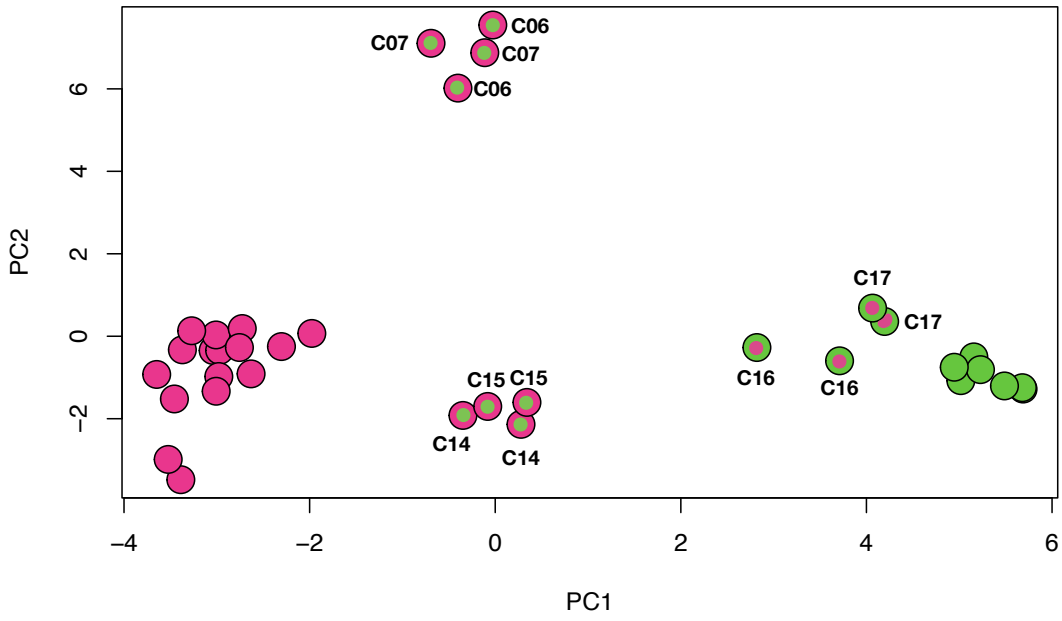

Figure S2.2. Principal components analysis of multilocus genotypes for individuals from groups G4 (pink), G5 (pink with green dot) and G6 (green and green with pink dot). Each point represents one individual, with colours corresponding to inferences of ancestry assignment with sNMF (see Figure 4a). Individuals inferred to be of mixed ancestry with sNMF (more than 10% of the genome inferred to be from a second ancestral population) are represented with a coloured dot representing the minor representation genome. Sampling sites are indicated for individuals of mixed ancestry.

▶ CHAPTER IV

Unravelling a complex genomic history within a geologically dynamic island

Unravelling a complex genomic history within a geologically dynamic island

Abstract

Oceanic islands, due to their geological history characterized by three key processes of eruptive volcanic activity, millennial-scale erosional activity, and catastrophic flank collapse, can be considered as natural laboratories to understand the evolutionary consequences of geomorphological dynamics. Islands that are well-documented from a geological point of view may thus provide a suitable environment to develop our understanding regarding the evolutionary consequences of such dynamics. Within the Canary Islands, Tenerife, has a well-understood geological history, thus providing an excellent model to investigate the role of mega-landslides on species history. We use RAD-seq data sampled within a complex of weevil species on Tenerife to quantify relatedness within and among areas of different geological stability through time. Our findings suggest that geological events such as flank collapses, frequent in geological active islands, promote a dynamic of range fragmentations and isolation, together with subsequent range expansions and secondary contact, which may have a positive effect on regional genetic variation over the long term.

Introduction

Oceanic archipelagos are considered to serve as natural laboratories for evolutionary biologists and ecologists, providing an important framework to improve our understanding about the drivers of speciation. Frequently diversification is associated with ecological gradients, but non-ecological mechanisms are also expected to promote speciation within insular settings by local geographic isolation (Patiño *et al.*, 2017). Otto *et al.* (2016) have argued for the need to focus attention on geomorphological dynamics within islands, highlighting the role of volcanic eruptions and other major landform-changing events, such as mega-landslides, in the evolutionary process. During the typical developmental life cycle of oceanic islands, geological activity acts to remodel existing landscapes. This geological dynamic is represented by three major events, eruptive volcanic activity, millennial scale erosional activity and catastrophic flank collapse. Of these three phenomena, the immediate consequences of eruptive events and flank collapses may directly impact island biotas by provoking local extinction in geologically affected zones (Borges & Hortal, 2009). Such extinctions driven by landslides (e.g. Juan, 2000; Brown *et al.*, 2006; Macías-Hernández *et al.*, 2013; Mairal *et al.*, 2015) or by volcanism (Carson, 1990; Pestano & Brown, 1999; Malhotra & Thorpe, 2000; Beheregaray *et al.*, 2003; Vandergast *et al.*, 2004; Gubitz *et al.*, 2005; Bloor *et al.*, 2008) may be followed by long-term habitat discontinuities generating genetic differentiation among populations. As conditions in the empty ecological space generated by a catastrophic geological event become suitable, recolonization from adjacents zones could promote episodes of secondary contact. Evidence for such a dynamic is limited, but several phylogeographic studies within Tenerife do provide some support. Brown *et al.* (2006) revealed the potential role of the Güímar flank collapse on cladogenesis through population fragmentation and isolation within the reptile *Gallotia galloti*, based on genetic and morphological data. Population differentiation within the spider species *Dysdera verneaui*, coincides with the western and eastern division of the Anaga peninsula by the flanks of a mega-landslide. An estimated landslide age of 0.5 - 1.0 Ma (Watts, 2001) was interpreted as support for a potential causal relationship, as it

coincides with the estimated divergence time between the eastern and western *D. verneaui* lineages (Macías-Hernández *et al.*, 2013). However, more recent evidence for a much older origin for the landslide between 4.2 - 4.7 Ma (Walter *et al.*, 2005) questions such a causal relationship. In any case, the limited evidence to date is likely, at least in part, due to the need for detailed population-level sampling together with genetic markers that provide enough resolution to elucidate such a dynamic, while at the same time allowing fundamental predictions from such a dynamic to be tested.

Generalised volcanic island ontogeny has been characterized by four phases. The first phase is one of a geologically eruptive period of island building, followed by a second phase of immaturity in which there is a deceleration of eruptive processes in parallel with an increase in erosional activity and topographical complexity. A third phase is characterised by a cessation of constructive volcanism, loss of elevation and flank collapses, although flank collapses may also feature within the second phase. The final phase comprises a reduction of area, elevation and topographic complexity, and eventual loss of subaerial mass. While this stylised ontogenetic roadmap necessarily ignores the individual idiosyncrasies of islands, it does argue for catastrophic eruptive and erosional activity to be a consistent feature throughout much of the life cycle of an oceanic island. This in turn suggests a consequential evolutionary impact, and the potential for hypothesis testing when such events are clearly documented in the geological record. One of the best characterised archipelagos, from a geological point of view, is that of the Canary Islands (Carracedo & Troll, 2016). The Canary Island of Tenerife presents a complex geological history, in which three older volcanic massifs were merged into a single island within the last 3.5 Ma (Carracedo, 2006), due to successive volcanic activity (Ancochea *et al.*, 1990; Cantagrel *et al.*, 1999). During the last 2 Ma, Tenerife has suffered several major eruptions (Ancochea *et al.*, 1990; Ancochea *et al.*, 1999; Huertas, 2002), and has been the subject of many flank collapses (García-Olivares *et al.*, 2017), including some of the largest recorded mega-landslides within the archipelago.

The well documented geological history of Tenerife provides a suitable framework to investigate the role of the geological events in shaping oceanic island diversification.

Recent or ongoing diversification in turn constitutes a fertile ground for the investigation of the mechanisms which promote divergence among populations. Such investigations require a molecular focus that provides high information content at intraspecific level (e.g. Jordal *et al.*, 2006; Spurgin *et al.*, 2011) together with a representative geographic sampling. Until recently phylogeographic and population genetic studies have typically been reliant upon a limited number of mitochondrial and nuclear markers, or microsatellites (Brito & Edwards, 2008). Recent advances in DNA sequencing technology have improved our capability to obtain large amounts of comparative genomic data from non-model organisms (e.g. Emerson, 2010; Lemmon & Lemmon, 2013; Pyron *et al.*, 2014; Leache & Oaks, 2017), greatly increasing information content and thus statistical power. Reduced representation genome sequencing approaches, such as restriction site-associated DNA sequencing (RAD-seq), represent low-cost and efficient techniques for the analysis of potentially thousands of homologous DNA sequence regions sampled from the genomes of species with no prior genomic information. Such markers, when applied to species that have evolved within geologically dynamic landscapes, offer the best opportunity to reveal demographic signatures to reconstruct such events.

The *Laparocerus tessellatus* complex of weevil species has been demonstrated to be a suitable model to assess the influence of landscape history on geographic patterns of individual relatedness (Chapter III). The combination of dispersal limitation within a changing landscape provides a suitable framework to investigate how geological dynamics impact intraspecific diversification within an island. A population genomic study within the *L. tessellatus* complex on the island of Gran Canaria has revealed the combined impact of topographic complexity and climate change during the Quaternary on diversification within the complex, in a background of relative geological quiescence (Chapter III). In addition to topoclimatic variation, geologically active islands are also likely to structure genetic variation within species. The close relationship between both geological and phylogeographic history have been clearly demonstrated (e.g. Brown *et al.*, 2000; Juan, 2000; Contreras-Díaz *et al.*, 2003; Moya *et al.*, 2004; Brown *et al.*, 2006; Emerson *et al.*, 2006), with insular examples including the importance of the lava flows for spider

population dynamics (Vandergast *et al.*, 2004; Bidegaray-Batista *et al.*, 2007; Macías-Hernández *et al.*, 2013) and gravitational flank collapses generating phylogeographic breaks in lizards (Thorpe *et al.*, 1996; Gübitz, 2000; Brown *et al.*, 2006). In contrast to the relative geological dormancy of Gran Canaria over the last 3 million years, Tenerife represents an island characterised by explosive volcanic activity and numerous gravitational flank collapses over the same period of time. It thus provides an excellent geological framework to investigate the role of catastrophic geological activity, in particular mega-landslides, on evolutionary dynamics within islands.

In the present study, we evaluate the evolutionary within-island consequences of mega-landslides using the *L. tessellatus* species complex on Tenerife, which is comprised of four taxonomically described species *L. tessellatus* Brullé, 1839, *L. freyi*, Uyttenboogaart, 1940, *L. canescens*, Machado, 2016 and *L. punctiger*, Machado 2016. Two testable predictions can be made to evaluate the role of mega-landslides on the evolutionary history within the *L. tessellatus* species complex. The first prediction is that geologically more stable areas within an island may act as reservoirs for population persistence, unlike areas that have suffered catastrophic flank collapses. The second prediction is that areas derived from catastrophic flank collapses are likely to promote admixture among genomically divergent populations colonising from areas peripheral to the landslide. To test these predictions, the *L. tessellatus* complex on Tenerife was sampled representatively across its range, and double-digest restriction site associated DNA sequence data (ddRADseq; Peterson *et al.*, 2012) generated to quantify genomic relatedness within and among areas of different geological stability through time.

Materials and Methods

Geological context of Tenerife

Within the Canary Islands, Tenerife is the largest and highest island, reaching 2058 km^2 of emerged area and 3,718 macsl. It has a complex geological history in comparison with other

islands within the archipelago. The more accepted model for the island of Tenerife is that during the Miocene three separate proto-islands formed: Roque del Conde (11.9–8.9 Ma), Teno (6.2–5.6 Ma) and Anaga (4.9–3.9 Ma) (Guillou *et al.*, 2004; Walter *et al.*, 2005). These then became fused into the single present-day island within the last 3.5 Ma (Carracedo, 2006), followed by 3 cycles of volcanic activity, ending approximately 0.2 Ma (Ancochea *et al.*, 1999; Cantagrel *et al.*, 1999). The recent volcanic activity on the island is evidenced by a high number of maif monogenetic cones distributed across the island, more than 297, formed within the last 1 Ma (Dóniz *et al.*, 2008). The most recent volcanic activity was concentrated in the north, where the Pico Viejo and Teide stratovolcanoes formed (Ablay & Martí, 2000). As the island reached a higher elevation, the edifice became gravitationally unstable and thus more prone to suffer flank collapses due to volcanic or tectonic seismicity, and dyke injections (McGuire, 2003). Tenerife has suffered numerous large landslides, approximately every 150 to 250 ky, with volumes often over 300 km^3 (Hunt *et al.*, 2018). Across the island, 11 documented landslides have left lasting signatures across the landscape (summarised in García-Olivares *et al.*, 2017). Vast areas were affected by these mega-landslides, with prominent scarps along the northern flank of the island representing the mega-landslides of Icod (0.15-0.17 Ma, Masson *et al.*, 2002), Orotava (0.54-0.69 Ma, Acosta *et al.*, 2003) and Roques de García (0.6-1.3 Ma, Watts & Masson, 1998; Acosta *et al.*, 2003), Micheque (0.83 Ma, Carracedo *et al.*, 2010) and Güímar (0.83-0.85 Ma, Giachetti *et al.*, 2011; Hunt *et al.*, 2013); the last one in the southern flank.

Sample collection and sample selection

To obtain a representative geographic sampling of the *L. tessellatus* complex on Tenerife we improved the number of localities sampled based on known sampling records for the species complex (A. Machado, pers. comm). We increased by sampling an additional 85 sites, yielding a total of 103 sites within the island (Fig. 1).

MtDNA sequencing and Bayesian tree construction

For each site, an average of three individuals were sequenced for a region of the mtDNA COII gene, and an alignment constructed together with sequences from García-Olivares *et al.* (2017; Chapter I). DNA sequencing was undertaken using the same protocol as that described in García-Olivares *et al.* (2017; see Chapter I). A Bayesian tree was constructed from the alignment, using the same parameters described in García-Olivares *et al.* (2017; Chapter I).

ddRAD-seq library preparation

For the preparation of genomic libraries, one individual per sampling site was selected, increasing the number of individuals sequenced in localities those with divergent mtDNA lineages in sympatry, adding one individual per each divergent lineage. DNA extractions were performed using the Qiagen DNeasy Blood & Tissue kit following the manufacturer's instructions. Genomic library construction was performed following the protocol described in Chapter III for a total of 132 individuals from the *L. tessellatus* complex within Tenerife. To assess the relatedness among individuals from Tenerife with respect to individuals from other islands, the approach described in Chapter III was followed, in which individuals from Tenerife were processed together with a total of 144 individuals sampled from the remaining species of the complex from the other islands within the archipelago. ddRADseq libraries were pooled at equimolar ratios and size selected for fragments between 200-250 bp, and then sequenced using single-end reads (100bp long) under four independently runs (see chapter III) on the Illumina HiSeq2500 platform.

Bioinformatic analysis

ddRAD-seq data were demultiplexed, quality filtered and de novo clustered using IPYRAD 0.7.19 (Eaton & Overcast, 2016). Only reads with unambiguous barcodes and fewer than five low quality bases (Phred quality score < 20), were retained, and a strict filter was applied to remove Illumina adapters. Following the same protocol used in Chapter III, a first analysis was undertaken using all the individuals within the *L. tessellatus* complex in order

to assess patterns of relatedness among individuals of the complex from Tenerife and other islands. For subsequent analyses of individuals from Tenerife, the optimal parameter values identified for the analysis of individuals from Gran Canaria dataset (see Chapter II) were used (clust_treshold = 0.85, max_SNPs_locus = 40, min_individuals_Locus = 80).

Population genomic analyses

In order to explore population structure within the *L. tessellatus* complex, we applied an individual-based multivariate method, principal component analysis (PCA), and two independent clustering methods, a discriminant analysis of principal components (DAPC) by using Bayesian Information Criteria (BIC), and an estimation of ancestry coefficients with sNMF cross-entropy algorithm. The PCA analysis summarises highly multivariate genetic information into several synthetic variables, providing an unsupervised clustering method which allow one to discern underlying population structure from a visual point of view. DAPC and sNMF methods apply a quantitative clustering approach, allowing for the inference of the number of potential clusters and ancestral populations, respectively, and their individual probabilities of assignment to each. To evaluate congruence of the groupings inferred by different methods, the number and composition of clusters and ancestral populations inferred by BIC and sNMF algorithms respectively, were compared. Congruence between the results of DAPC and sNMF and the spatial relationships of individuals within the PCA was assessed visually by incorporating cluster and population assignment information from DAPC and sNMF, respectively, into the graphical PCA output. The results provided by sNMF were also used to discriminate between pure and admixed individuals, fixing a threshold value of more than 10% assignment to an alternative ancestral population to be considered admixed (Jombart & Collins, 2015). For all population genomic analyses, a single SNP was randomly sampled from each locus. PCA and DAPC analyses were performed using ADEGENET 2.1.0 package (Jombart & Ahmed, 2011) and sNMF using the LEA package (Frichot *et al.*, 2015) in R v. 3.4.2 (R Core Team 2013). To explore overall genomic patterns within Tenerife a Neighbor-Net tree was used to generate an unrooted phylogenetic network in SPLITSTREE v. 4.14.5 (Huson & Bryant, 2006). The Neighbor-Net algorithm constructs highly resolved networks represented as a splits graph, providing a general visualisation of relatedness among individuals.

Genetic diversity was estimated as the mean allele richness (A_r) and private allele richness (Pa_r) calculated and corrected for sample size by rarefaction using HP-RARE 1.0 (Kalinowski, 2005), whereas the observed heterozygosity (H_o) and expected heterozygosity (H_s) were calculated by Genodive (Meirmans & Van Tienderen, 2004).

Results

Summary of RADseq Data

The exploratory PCA using all 275 individuals sampled within the *L. tessellatus* complex across all islands revealed individuals from Tenerife to form a cluster of individuals, clearly differentiated from the other islands (Figure S1, Supporting Information). This clustering of individuals from Tenerife revealed by the PCA fits with the phylogenomic reconstruction performed in Chapter II, where individuals from this island form part of the same clade. Thus, subsequent analyses only included the 132 individuals sampled from Tenerife.

A first filter was performed in order to remove individuals with a low number of reads or high level of missing data (more than 30%), resulting in the removal of 4 individuals, and a final dataset of 128 individuals (Table S1, Supporting Information) from 103 localities (Fig. 1). A total of 447.96 million reads were sequenced, of which 426.10 millions reads passed the quality filtering steps of IPYRAD. On average 3.32 (± 2.03 SD) millions reads were recovered per individual. After running all the steps of IPYRAD pipeline, a single SNP per locus was randomly sampled for the final dataset, yielding 5,718 parsimonious informative SNPs with 9.99% of missing data.

Populations inference and geographical delimitation

Variation across the two first components of the PCA analysis (Fig. 2a) revealed three axes of variation. Variation across the principal axis PC1 conformed to a more-or-less continuous gradient, while the remaining two axes, largely described by variation along the second principal component, presented signatures for distinct clusters (TF1-TF5). Substructuring

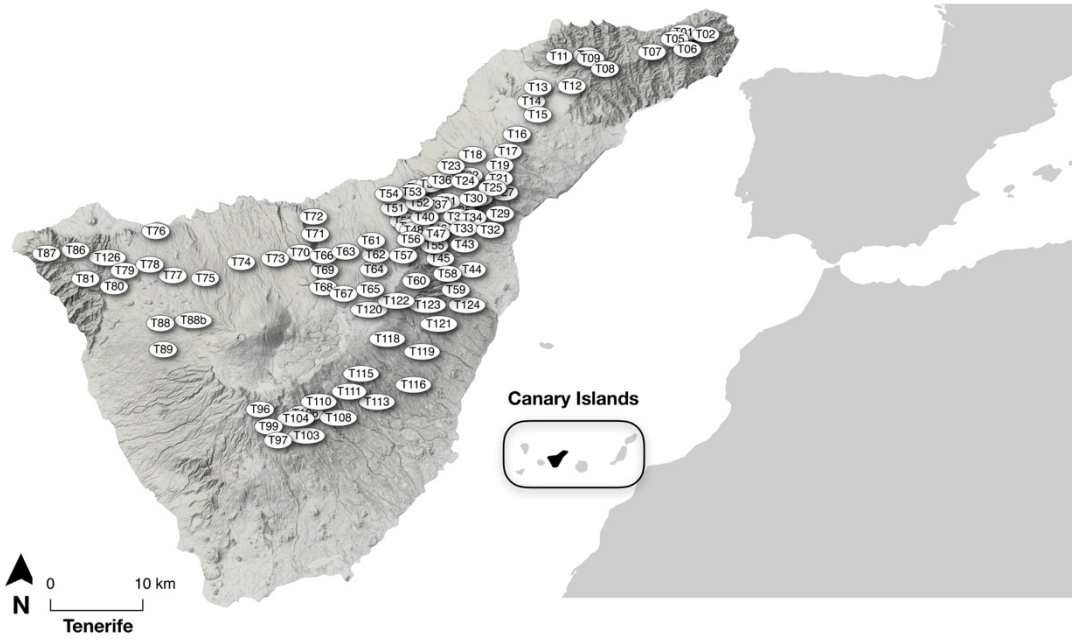

Figure 1. Sampling of the *Laparocerus tessellatus* species complex on Tenerife. Map showing the location of the Canary Islands relative to Northwest Africa, and the geography of the archipelago with Tenerife highlighted in black. Sampling sites are shown within the island of Tenerife (for the details of each sampling site, see Table S1).

was statistically supported within the DAPC analysis (Fig. 2b), with BIC scores pointing to the presence of five clusters, with spatial relationships among individuals consistent with those observed in the PCA. Individuals at the extremes of the three PCA axes were identified as distinct groups within the DAPC (TF1, TF2, TF3) while remaining individuals distributed along the first component of the PCA were partitioned into two clusters (TF4 and TF5). Groups were non-overlapping across both axes of PCA and DAPC variation, with the exception of TF4 and TF5, which presented some overlap along both axes of the DAPC.

The cross-entropy criterion identified five ancestral populations in the sNMF analysis, with assignments of individuals to each of the five ancestral populations being in strong agreement with DAPC group assignments. Groups TF1, TF2 and TF3 from the DAPC analysis were also recovered with the same composition with sNMF (Fig. 2b and 2c). Groups approximating TF4 and TF5 were also recovered, but with minor compositional differences involving individuals presenting strong signatures of admixture in the sNMF analysis. Congruent results were also revealed between individual sNMF ancestry coefficients and their spatial distribution within the PCA (Fig. 2a and 2c). Individuals inferred to be of admixed origin with sNMF were consistently found to be intermediate in the PCA ordination space between inferred parental populations (Fig. 2a and 2c). In a spatial context

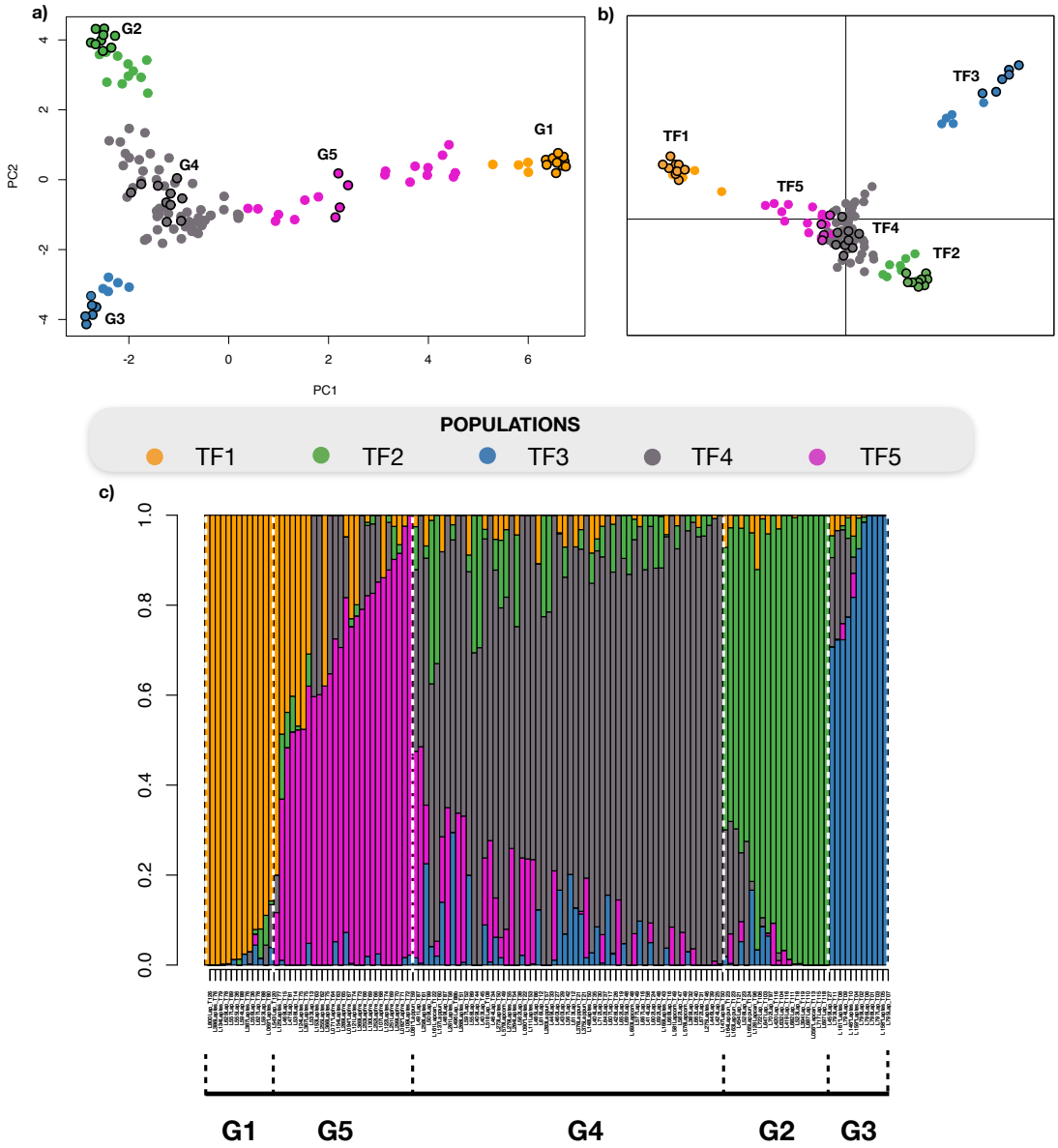

Figure 2. Discriminant analysis and individual ancestry assignment inference. (a) PCA of individuals within Tenerife, in which each point represents one individual, with colours corresponding to inferences of the five clusters inferred by discriminant analysis of principal components (DAPC). (b) DAPC of individuals within Tenerife, in which, each point represents one individual, with colours corresponding to the five clusters inferred by the analysis. Points with a black edge in (a) and (b) represent individuals with 90% or higher assignment to an individual ancestral population. (c) sNMF plot representing each individual as a column and the probability of assignment to the five different populations inferred.

individuals inferred to be of single ancestry, almost exclusively clustered together geographically, and in the majority of the cases these areas border the scarps of mega-landslides (Fig. 3a). Individuals assigned with high probability (>90%) to population TF1 are distributed in the northwest of the island, with the exception of a single individual sampled within the northeast rift. Individuals assigned with high probability to population TF2, in

contrast, are distributed across higher elevations of the southern flank, close to the back scar of the Roques de García landslide, with the exception of two individuals sampled within the northeast rift. Individuals with high assignment to population TF3 were sampled exclusively within the northeastern peninsula of Anaga. Individuals with high assignment to population TF4 are distributed along the northeast rift, coincident with the limits of the Micheque mega-landslide, with the exception of a single individual sampled along the northern lateral scarp of the Güímar Valley. Population TF5 was represented by only 4 individuals of high ancestry assignment, with three sampled above the western lateral scarp of the Orotava valley (Fig. 3a), and the fourth individual sampled along the northern lateral scarp of the Güímar Valley. Therefore, the distribution of individuals observed in both the DAPC and PCA are highly congruent with their geographical distribution within the Tenerife island (Fig. 3b).

The phylogenetic network revealed a similar pattern of relationships, with individuals assigned by sNMF analysis to populations TF1, TF2 and TF3 forming more clearly defined groups, among which TF4 and TF5 were differentiated, but intermediate within the network topology (Figure S2a, Supporting Information). When individuals of inferred admixed ancestry are removed from the analysis, a much clearer pattern of close relatedness within and high divergence among groups is revealed (Figure S2b, Supporting Information).

Incongruences between mitochondrial and nuclear data were also revealed, with the mitochondrial Bayesian tree revealing two main clades that were not reflected by ddRADseq data. From the fifteen sites identified with divergent mtDNA lineages in sympatry, in only one case were the two individuals also inferred to belong to different groups inferred from ddRAD-seq data (Figure S3, Supporting Information).

Contact zones between populations

The broad correspondence between the distribution of individuals with high assignment probability to single ancestral populations in both PCA space and geographic space (Fig. 3a) was also reflected in individuals of inferred admixed origin (Fig. 3b). Individuals inferred to be of admixed origin were similarly intermediately placed between inferred parental populations in both PCA space and geographic space, albeit with some exceptions in

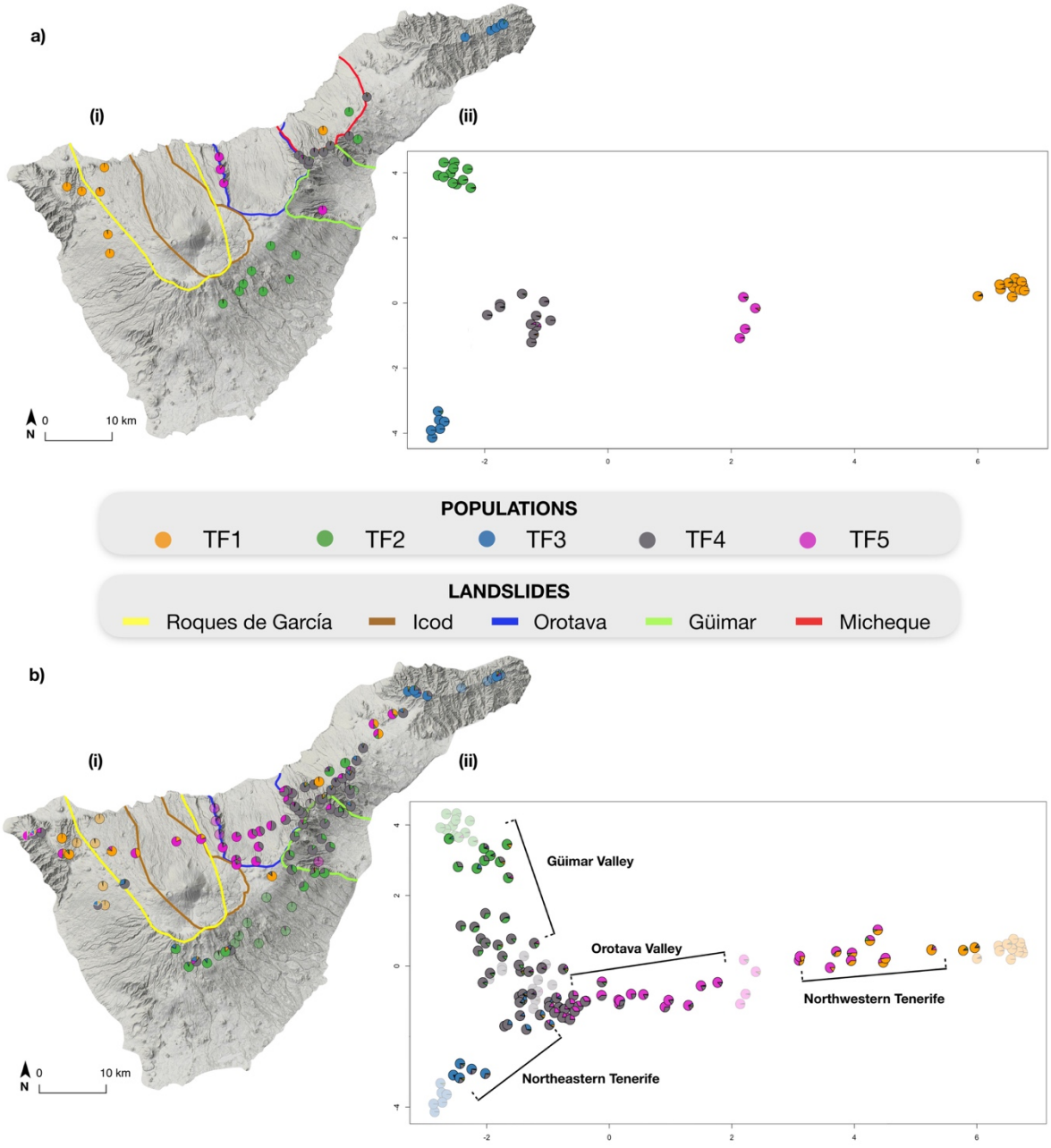

Figure 3. Genomic spatial and geographic distribution within Tenerife. A general representation of the genomic patterns revealed within Tenerife is shown (i) over a geographic framework in where each locality is defined by a pie-chart, and (ii) in a PCA in which each individual is defined by a pie-chart containing the ancestry population proportions inferred by sNMF. Localities compound by a unique individual are represented by its respective ancestry proportion and, in the case of localities grouping more than one individual, an average of the ancestry proportion inferred was performed. Localities, in which different ancestry proportions were inferred, were represented by two independent pie-charts surrounded with a white edge. Limits of each landslide within the last 2 Ma is drawn as a line with colour coded according to the inset. a) Representation exclusively of individuals with high assignment (>90%) to an unique ancestral population from the five populations inferred by sNMF. b) Representation of all individuals analyzed within Tenerife, highlighting the admixed individuals with more than 10% or more assignment more than 10% assignment to an alternative ancestral population inferred by sNMF.

geographic space (Fig. 3b). A total of four gradients of admixture were identified within the PCA plot (Fig. 3b), three of which were delimited within zones where mega-landslides have occurred during the last 2 Ma. Each case was subsequently analysed independently, with parental populations represented by individuals with 90% or higher assignment, and admixed individuals with 10% or more assignment to the second population. Thus, for each case the data set was reduced to include only those individuals assigned to one or both of the parental populations, and new sNMF and PCA analyses were undertaken to explore in more detail where the two parental populations may have contacted and admixed.

Northwestern Tenerife

When limiting analysis to individuals that assigned to TF1 and TF5 in the northwest of Tenerife, two ancestral populations were optimally inferred with sNMF, with four individuals presenting strong signatures of admixture (Fig. 4a). The PCA analysis for this subset of four individuals clearly identifies their intermediate position along the first principal component that separates TF1 and TF5. In addition to the Teno flank collapse approximately 6 Ma (Walter & Schmincke, 2002; Longpré *et al.*, 2009), the northwest of Tenerife has been subject to two more recent and more extensive flank collapses. The Roques de Garcia mega-landslide is estimated to have occurred between 0.6 and 1.3 Ma (Watts & Masson, 1998; Acosta *et al.*, 2003), followed by the geographically overlapping Icod mega-landslide approximately 165 Ka (thousand years ago, Masson *et al.*, 2002). It is between the western limits of both landslides, where an area of potential secondary contact between TF1 and TF4 is inferred (Fig. 4a).

Orotava Valley

Reducing the dataset to include only individuals assigned to TF4 and TF5 distributed across the central region of the northern flank of Tenerife, two ancestral populations were again inferred by the cross-entropy sNMF algorithm, among which 15 individuals presented clear signatures of admixture. The PCA revealed a clear gradient of admixture between both ancestral populations along the first component of the PCA (Fig. 4b). To the east and adjacent to both the Roques García and Icod flank collapse limits, there is a valley formed by the Orotava flank collapse that is estimated to have occurred between 0.54 and 0.69 Ma (Acosta *et al.*, 2003). All individuals assigned to TF5 were sampled along the western flank

or at geographically proximate locations within the valley. All individuals assigned to TF4 were sampled outside the valley, along the eastern flank. Individuals with clear signature of admixture were sampled in the valley of at lower elevation sites along the eastern flank (Fig. 4b).

Güímar Valley

When limiting analysis to individuals that assigned to TF2 and TF4, two ancestral populations were optimally inferred with sNMF. Nine individuals were designated as admixed, and these were broadly, but not perfectly distributed within PCA space between clusters of individuals assigned to a single population, albeit clustered toward the ancestral population to which they were predominantly assigned (Fig. 4c). Individuals inferred to be of single ancestry from TF2 were sampled south of the southern lateral flank of the Güímar valley (Fig. 4c), formed by a flank collapse (0.83-0.85 Ma, Giachetti *et al.*, 2011; Hunt *et al.*, 2013). In contrast, individuals inferred to be of single ancestry from TF5 were sampled both within the Güímar valley and along its northern and western margins. Admixed individuals were largely confined to sites either within or along the margins of the southwestern limits of the valley.

Northeastern Tenerife

Reducing the dataset to include only individuals assigned to TF3 and TF4 resulted in an optimal inference of two ancestral populations. Six individuals were inferred to be of admixed origin, and as in the case for the Güímar Valley scenario, they were broadly, but not perfectly, distributed within PCA space between clusters of individuals assigned to a single population, but clustering toward the population to which they were predominantly assigned (Fig. 4d). All individuals inferred to be of single ancestry from TF4 were sampled exclusively within the Anaga peninsula, while those assigned to be on single ancestry from TF3 were exclusively sampled outside the peninsula. All but one admixed individual were sampled at the western limits of the Anaga peninsula, with the exception being an individual of inferred admixed origin in the east of Anaga (Fig. 4d).

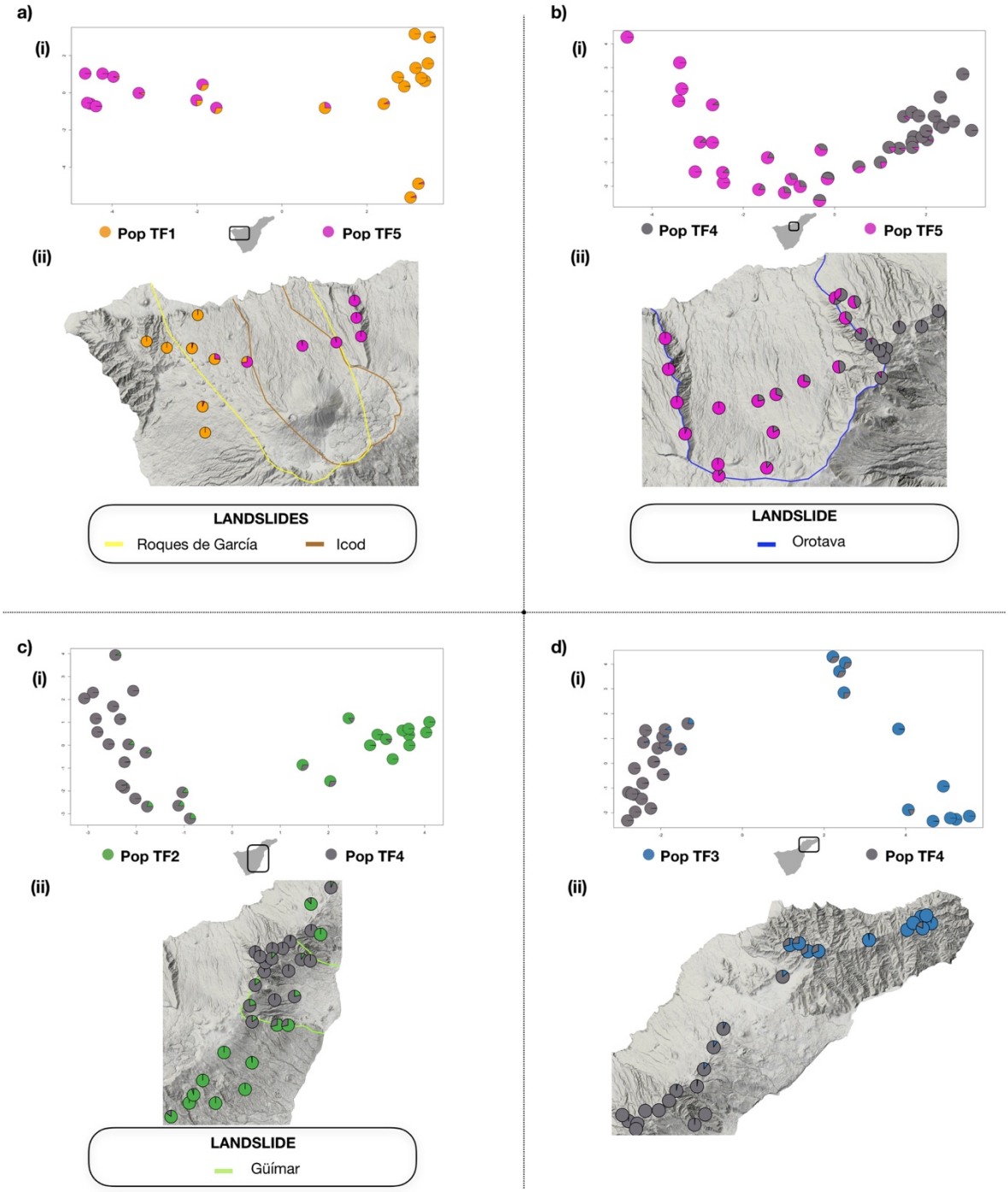

Figure 4. Contact zones between populations. Each contact zone between pairs of populations was represented with more detail, i) in a PCA in which each individual is defined by a pie-chart containing the ancestry population proportions inferred by sNMF, and ii) over a geographic framework in where each locality is defined by a pie-chart. Localities compound by a unique individual are represented by its respective ancestry proportion inferred, in the case of localities forming by more than one individual, an average of the ancestry proportion of all individuals. Limits of each landslide within the last 2 Ma is drawn as a line with colour coded according to the inset. a) Contact zone between TF1 and TF5, Northwestern Tenerife. b) Contact zone between TF4 and TF5, Orotava Valley. c) Contact zone between TF3 and TF4, Güímar Valley. d) Contact zone between TF2 and TF4, Northeastern Tenerife.

Analysis of genetic diversity

Mean observed heterozygosity (H_o), mean expected heterozygosity (H_s), mean allele richness (A_r) and private allele richness (Pa_r) were evaluated for each subset of genetic clusters involved in contact zones, establishing three groups: the parental populations, in which were including individuals with 90% or higher assignment; and a group compound by individuals with 10% or more assignment to the second population, the admixed population. The summary statistics showed, in all the cases analysed, that admixed population values were positioned between the estimated parental ranges, with the exception of A_r and Pa_r parameters within northwestern Tenerife, in which lower values that those within parental populations were found (Table 1).

Table 1. Genetic diversity within each contact zone. Results of the population genetics statistics estimated in the four secondary contact zones revealed within the *Laparocerus tessellatus* species complex in Tenerife, for which, three groups were established: the two groups defined by the parental populations and the resulting admixed populations. Mean observed heterozygosity (H_o), mean expected heterozygosity (H_s), mean allele richness (A_r) and private allele richness (Pa_r).

Contacts zone	Pop	H_o	H_s	A_r	Pa_r
Northwestern Tenerife	TF1	0.023	0.036	1.19	0.12
	TF5	0.028	0.041	1.15	0.09
	Adm	0.027	0.038	1.1	0.03
Orotava Valley	TF4	0.029	0.039	1.29	0.18
	TF5	0.028	0.041	1.17	0.08
	Adm	0.028	0.039	1.25	0.12
Güímar Valley	TF2	0.022	0.03	1.12	0.06
	TF4	0.03	0.039	1.27	0.18
	Adm	0.022	0.036	1.16	0.07
Northeastern Tenerife	TF3	0.019	0.026	1.1	0.03
	TF4	0.029	0.039	1.31	0.25
	Adm	0.02	0.033	1.11	0.04

Discussion

Our results support a role for gravitational flank collapses promoting a dynamic of population isolation and secondary contact. In support of our predictions, we found: (i) populations characterised by individuals with ancestry assignments to single populations were associated with areas of relative geological stability, having suffered neither recent volcanic activity nor flank collapse, and (ii) individuals with signatures of mixed ancestry were typically sampled within areas having suffered flank collapses.

Geological stability and population stability

Our findings reveal how variation in geological activity across an island can directly impact geographical patterns of individual relatedness, leaving genomic signatures of geological events dating back several hundreds of thousands of years. The geographic distribution of individuals assigned to a single ancestral population within the *L. tessellatus* species complex of Tenerife largely corresponds to areas characterised by long-term geological stability. Five populations were consistently inferred with a variety of population genomic analyses. Populations TF1 and TF3 are distributed in northwest Tenerife and Anaga respectively. These two areas have been long considered as paleo-islands, and have remained relatively stable geologically since the end of the Miocene and beginning of the Pliocene (Ancochea *et al.*, 1990; Cantagrel *et al.*, 1999; Guillou *et al.*, 2004), the time interval that encompasses the evolutionary history of the *L. tessellatus* complex (Faria *et al.*, 2016; Machado *et al.*, 2017). The distribution of the remaining populations inferred, populations TF2, TF4 and TF5, are almost exclusively associated with areas above scarps defining the Orotava, Güímar and Roques García flank collapse limits, respectively. These are terrains that predate the flank collapses with which they are associated (Fig. 3a), thus providing the opportunity for the persistence of genomic variation related to that extirpated within the areas of each flank collapse.

Landslides and their demographic consequences

While individuals inferred to be of single ancestry were found to be associated with areas of geological stability, a contrasting pattern was observed for individuals of mixed ancestry. Excluding the ancestral population TF3, admixed individuals showed greater association with areas of flank collapse within the combined ranges of their parental populations, implicating a cause and effect relationship between flank collapses and an isolation followed by secondary contact dynamic. Thus, while hybrid zones of recent origin often exhibit predictable placement and width with respect to parental populations (McEntee *et al.*, 2018), it is less clear what would happen to such zones over a longer temporal window. Continental hybrid zone arising from postglacial secondary contact are short-lived, as they are erased with every subsequent glacial period. However, insular hybrid zones derived from geological events might not be erased if they occur within areas that remain climatically favourable during both glacial and interglacial conditions.

Species within the *L. tessellatus* complex have limited dispersal ability, contributing to geographic structuring of their genetic variation over small spatial scales (Chapter III). Thus, one could expect that a simple dynamic of range fragmentation and isolation caused by flank collapse, followed by range expansion and secondary contact within the area of the flank collapse, might lead to geographically restricted areas of secondary contact. However, limited divergence among taxa can act to broaden the geography of hybrid zones, even when dispersal is limited, with a useful example being provided by the European grass snake *Natrix natrix*. Two secondary contact zones have been identified within the range of *N. natrix*, involving contrasting levels of divergence between parental populations, providing for a comparison of the influence of divergence on hybrid zone with no variation in dispersal ability (Kindler *et al.*, 2013). A detailed geographic sampling, together with mtDNA and microsatellite markers, revealed that gene flow and thus hybrid zone width was substantially greater when parental populations were of limited genetic divergence (Kindler *et al.*, 2017). Thus, given the typically limited genomic divergences describing the different populations within *L. tessellatus* on Tenerife, together with the probable ancient origin for their secondary contact, based on the ages of flank collapses (> 0.5 Ma), it would seem reasonable to assume that admixture should not be geographically limited.

For the case of admixture between TF1 and TF5 within northwestern Tenerife, admixed individuals are geographically localised, sampled from two neighbouring populations within the area of the older Roques de García flank collapse, which was not affected by the more recent Icod flank collapse. This is consistent with recolonisation into the flank collapse area by TF1 from the west, and TF5 from the east, with a relatively limited area of admixture. However, because of the more recent Icod flank collapse, individuals to the east of the area of admixture are of more recent origin, with the genomic record of the Roques de García flank collapse in this area having been overwritten. Thus, the true geographic extent of admixture following the Roques de García flank collapse is uncertain. In contrast to the pattern in northwestern Tenerife, much broader distributions of admixed individuals are associated with both the Orotava and Güímar flank collapses, distributed across areas of at least 136 km^2 and 130 km^2 respectively.

Isolation and secondary contact in the north east

The fourth area of admixture, between TF3 and TF4 in the north east of Tenerife, is conspicuously remote from any recent geological activity that could explain the contemporary pattern of genomic relatedness among individuals from these two populations. Both on the neighbouring island of Gran Canaria, and within the Anaga peninsula itself, the interaction of climatic change throughout the Quaternary together with topographic variation have been shown to be a strong driver of both range fragmentation and secondary contact (Chapter III; Salces-Castellano *et al.*, In preparation A; Salces-Castellano *et al.*, In preparation B), and may potentially be implicated in the pattern observed between TF3 and TF4. However, in the absence of a specific explanatory topoclimate model as in Salces-Castellano *et al.* (In preparation A), such an explanation would require a more rigorous assessment, potentially sampling co-distributed species for similar signatures, an expectation of such a model (Salces-Castellano *et al.*, In preparation A).

Geological process as a driver of genetic variation in oceanic islands

Emerson and Faria (2014) have previously pointed out how genomic admixture may act to overcome the negative population genetic consequences associated with the founding of new island populations. Under their model, genetic admixture can provide a potential escape from reduced genetic variation via the production of novel genotypic combinations of alleles, coupled with new opportunities for recombination among divergent genomes that may also facilitate adaptation within novel adaptive landscapes (Mallet, 2007). The emergent patterns from ddRAD-seq data for the *L. tessellatus* complex within the island of Tenerife also suggest an important role for admixture in generating novel genetic variation within islands.

The notion that islands are typically characterised by low levels of genetic diversity within species, compared to continental settings, has been of interest since Frankham (1997) presented evidential support for this hypothesis. However, the supporting data presented by Frankham (1997) was largely biased toward vertebrates and plants, where species might reasonably be assumed to approximate panmixia within islands, due to minimal dispersal limitations within the geographic confines of an island. Under such conditions fundamental population genetic theory predicts lower genetic variation in populations of smaller size (e.g. Crow & Kimura, 1970), and as noted by Frankham (Frankham, 1997), lower genetic variation within island species should increase their extinction probability. However, the generality of this pattern in plants has been questioned by recent studies (e.g. Fernandez-Mazuecos & Vargas, 2011; Hutsemekers *et al.*, 2011; García-Verdugo *et al.*, 2015), and Patiño *et al.* (2017) have identified the "island impoverishment" syndrome as requiring more critical analysis.

While our data does not provide a direct comparison between island and continental invertebrate species, it does provide insight into conditions that can promote the generation of novel genetic variation within insular invertebrate species. The geographic structuring of genetic variation into five regional ancestral populations clearly demonstrates the influence of dispersal limitation in enhancing genetic variation at the insular scale. At such a local spatial scale, where dispersal limitation structures genetic variation regionally within islands, genetic variation at the individual level is unlikely to differ from that within a continental setting, assuming all other factors (e.g. environmental

effects) are similar. However, under conditions that promote admixture, genetic variation will increase dramatically (Emerson & Faria, 2014), with Garrick *et al.* (2019) noting that genetic diversity will spike above equilibrium values before returning to equilibrium expectations through the action of genetic drift. Thus, at the scale of the individual, an immediate consequence of admixture is increased heterozygosity, but this gain is of limited temporal duration. However, at the local and regional scales, increases in genetic variation through admixture will leave a more permanent record. At the local scale, after returning to equilibrium, genetic variation will be enhanced through increased allelic diversity (alleles derived from two population sources). At the regional scale, genotypic diversity will be increased through the existence of both parental and admixed genotypes. Our data thus suggest that for dispersal limited species in geologically active islands, wherein geological events such as flank collapses are relatively frequent, a dynamic of range fragmentations and isolation, together with subsequent range expansions and secondary contact, may have a positive effect on regional genetic variation over the long term.

References

Ablay, G.J. & Martí, J. (2000) Stratigraphy, structure, and volcanic evolution of the Pico Teide-Pico Viejo formation, Tenerife, Canary Islands. *Journal of Volcanology and Geothermal Research*, **103**, 175-208.

Acosta, J., Uchupi, E., Muñoz, A., Palomo, C., Ballesteros, M. & ZEE Working Group (2003) Geologic evolution of the Canarian Islands of Lanzarote, Fuerteventura, Gran Canaria and La Gomera and comparison of landslides at these islands with those at Tenerife, La Palma and El Hierro. *Marine Geophysical Researches*, **24**, 1-40.

Ancochea, E., Huertas, M.J., Cantagrel, J.M., Coello, J., Fúster, J.M., Arnaud, N. & Ibarrola, E. (1999) Evolution of the Cañadas edifice and its implications for the origin of the Cañadas Caldera (Tenerife, Canary Islands). *Journal of Volcanology and Geothermal Research*, **88**, 177-179.

Ancochea, E., Fuster, J.M., Ibarrola, E., Cendrero, A., Coello, J., Hemán, F., Cantagrel, J.M. & Jamond, C. (1990) Volcanic evolution of the island of Tenerife (Canary Islands) in the light of new K-Ar data. *Journal of Volcanology and Geothermal Research* **44**, 231-249.

Beheregaray, L.B., Ciofi, C., Geist, D., Gibbs, J.P., Caccone, A. & Powell, J.R. (2003) Genes Record a Prehistoric Volcano Eruption in the Galápagos. *Science*, **302**, 75.

Bidegaray-Batista, L., Macías-Hernández, N., Oromí, P. & Arnedo, M.A. (2007) Living on the edge: demographic and phylogeographical patterns in the woodlouse-hunter spider Dysdera lancerotensis Simon, 1907 on the eastern volcanic ridge of the Canary Islands. *Mol Ecol*, **16**, 3198-214.

Bloor, P., Kemp, S.J. & Brown, R.P. (2008) Recent volcanism and mitochondrial DNA structuring in the lizard Gallotia atlantica from the island of Lanzarote. *Molecular Ecology*, **17**, 854-66.

Borges, P.A.V. & Hortal, J. (2009) Time, area and isolation: factors driving the diversification of Azorean arthropods. *Journal of Biogeography*, **36**, 178-191.

Brito, P.H. & Edwards, S.V. (2008) Multilocus phylogeography and phylogenetics using sequence-based markers. *Genetica*, **135**, 439-455.

Brown, R.P., Campos-Delgado, R. & Pestano, J. (2000) Mitochondrial DNA evolution and population history of the Tenerife skink Chalcides viridanus. *Molecular Ecology*, **9**, 1061-1067.

Brown, R.P., Hoskisson, P.A., Welton, J.H. & Báez, M. (2006) Geological history and within-island diversity: a debris avalanche and the Tenerife lizard Gallotia galloti. *Molecular Ecology*, **15**, 3631-40.

Cantagrel, J.M., Arnaud, N.O., Ancochea, E., Fuster, J.M. & Huertas, M.J. (1999) Repeated debris avalanches on Tenerife and genesis of Las Canadas caldera wall (Canary islands). *Geology*, **27**, 739-742.

Carracedo, J.C. (2006) *El volcán Teide. Volcanología, interpretación de paisajes e itinerarios comentados*. Obra Social y Cultural de CajaCanarias, Santa Cruz de Tenerife.

Carracedo, J.C. & Troll, V. (2016) *The geology of the Canary Islands*. Elsevier, Amsterdam.

Carracedo, J.C., Guillou, H., Nomade, S., Rodríguez-Badiola, E., Pérez-Torrado, F.J., Rodríguez-Gonzalez, A., Paris, R., Troll, V.R., Wiesmaier, S., Delcamp, A. & Fernandez-Turiel, J.L. (2010) Evolution of ocean-island rifts: The northeast rift zone of Tenerife, Canary Islands. *Geological Society of America Bulletin*, **123**, 562-584.

Carson, H.L.L., J.P.; Elysse, M.C. (1990) Extinction and Recolonization of Local Populations on a Growing Shield Volcano. *Proceedings of the National Academy of Sciences of the United States of America*, **87**, 7055-7057.

Contreras-Díaz, H.G., Moya, O., Oromí, P. & Juan, C. (2003) Phylogeography of the endangered darkling beetle species of Pimelia endemic to Gran Canaria (Canary Islands). *Molecular Ecology*, **12**, 2131-2143.

Crow, J.F. & Kimura, M. (1970) *An introduction to population genetics theory*. Harper & Row, New York.

Dóniz, J., Romero, C., Coello, E., Guillén, C., Sánchez, N., García-Cacho, L. & García, A. (2008) Morphological and statistical characterisation of recent mafic volcanism on Tenerife (Canary Islands, Spain). *Journal of Volcanology and Geothermal Research*, **173**, 185-195.

Eaton, D.A. & Overcast, I. (2016) ipyrad: interactive assembly and analysis of RADseq data sets. *Available from:* http://ipyrad.readthedocs.io/.

Emerson, B.C. & Faria, C.M.A. (2014) Fission and fusion in island taxa – serendipity, or something to be expected? *Molecular Ecology*, **23**, 5132-5134.

Emerson, B.C., Forgie, S., Goodacre, S. & Oromí, P. (2006) Testing phylogeographic predictions on an active volcanic island: Brachyderes rugatus (Coleoptera: Curculionidae) on La Palma (Canary Islands). *Mol Ecol*, **15**, 449-58.

Emerson, K.J.M., Clayton R.; Catchen, Julian M.; Hohenlohe, Paul A.; Cresko, William A.; Bradshaw, William E.; Holzapfel, Christina M. (2010) Resolving postglacial phylogeography using high-throughput sequencing. *Proceedings of the National Academy of Sciences*, **107**, 16196-16200.

Faria, C.M.A., Machado, A., Amorim, I.R., Gage, M.J.G., Borges, P.A.V. & Emerson, B.C. (2016) Evidence for multiple founding lineages and genetic admixture in the evolution of species within an oceanic island weevil (Coleoptera, Curculionidae) super-radiation. *Journal of Biogeography*, **43**, 178-191.

Fernandez-Mazuecos, M. & Vargas, P. (2011) Genetically depauperate in the continent but rich in oceanic islands: Cistus monspeliensis (Cistaceae) in the Canary Islands. *PLoS One*, **6**, e17172.

Frankham, R. (1997) Do island populations have less genetic variation than mainland populations? *Heredity*, **78**, 311-327.

Frichot, E., François, O. & O'Meara, B. (2015) LEA: AnRpackage for landscape and ecological association studies. *Methods in Ecology and Evolution*, **6**, 925-929.

García-Olivares, V., López, H., Patiño, J., Alvarez, N., Machado, A., Carracedo, J.C., Soler, V. & Emerson, B.C. (2017) Evidence for mega-landslides as drivers of island colonization. *Journal of Biogeography*, **44**, 1053-1064.

García-Verdugo, C., Sajeva, M., La Mantia, T., Harrouni, C., Msanda, F. & Caujape-Castells, J. (2015) Do island plant populations really have lower genetic variation than mainland populations? Effects of selection and distribution range on genetic diversity estimates. *Mol Ecol*, **24**, 726-41.

Garrick, R.C., Banusiewicz, J.D., Burgess, S., Hyseni, C. & Symula, R.E. (2019) Extending phylogeography to account for lineage fusion. *Journal of Biogeography*, **46**, 268-278.

Giachetti, T., Paris, R., Kelfoun, K. & Pérez-Torrado, F.J. (2011) Numerical modelling of the tsunami triggered by the Güìmar debris avalanche, Tenerife (Canary Islands): Comparison with field-based data. *Marine Geology*, **284**, 189-202.

Gübitz, R.T.R.S.M., A. (2000) Phylogeography and natural selection in the Tenerife gecko Tarentola delalandii: testing historical and adaptive hypotheses. *Molecular Ecology*, **9**, 1213-1221.

Gubitz, T., Thorpe, R.S. & Malhotra, A. (2005) The dynamics of genetic and morphological variation on volcanic islands. *Proceedings of the National Academy of Sciences*, **272**, 751-7.

Guillou, H., Torrado, F.J.P., Hansen Machin, A.R., Carracedo, J.C. & Gimeno, D. (2004) The Plio–Quaternary volcanic evolution of Gran Canaria based on new K–Ar ages and magnetostratigraphy. *Journal of Volcanology and Geothermal Research*, **135**, 221-246.

Huertas, M.J.A., N.O.; Ancochea, E.; Cantagrel, J.M.; Fúster, J.M. (2002) 40Ar/39Ar stratigraphy of pyroclastic units from the Can‹adas VolcanicEdi¢ce(Tenerife,CanaryIslands)andtheirbearing on the structural evolution. *Journal of Volcanology and Geo- thermal Research*, **115**, 351–365.

Hunt, J.E., Cassidy, M. & Talling, P.J. (2018) Multi-stage volcanic island flank collapses with coeval explosive caldera-forming eruptions. *Scientific Reports*, **8**, 1146.

Hunt, J.E., Wynn, R.B., Talling, P.J. & Masson, D.G. (2013) Turbidite record of frequency and source of large volume (>100 km3) Canary Island landslides in the last 1.5 Ma: Implications for landslide triggers and geohazards. *Geochemistry, Geophysics, Geosystems*, **14**, 2100-2123.

Huson, D.H. & Bryant, D. (2006) Application of phylogenetic networks in evolutionary studies. *Mol Biol Evol*, **23**, 254-67.

Hutsemekers, V., Szövényi, P., Shaw, A.J., González-Mancebo, J.M., Muñoz, J.V. & Vanderpoorten, A. (2011) Oceanic islands are not sinks of biodiversity in spore-producing plants. *Proceedings of the National Academy of Sciences of the USA*, **108**, 18989 –18994.

Jombart, T. & Ahmed, I. (2011) *adegenet 1.3-1: new tools for the analysis of genome-wide SNP data*.

Jombart, T. & Collins, C. (2015) A tutorial for discriminant analysis of principal components (DAPC) using adegenet 2.0.0. *Available from :* http://adegenet.r-forge.r-project.org/files/tutorial-dapc.pdf.

Jordal, B.H., Emerson, B.C. & Hewitt, G.M. (2006) Apparent 'sympatric' speciation in ecologically similar herbivorous beetles facilitated by multiple colonizations of an island. *Molecular Ecology*, **15**, 2935-2947.

Juan, C.E., B. C; Oromí, P; Hewitt, G. M. (2000) Colonization and diversification: towards a phylogeographic synthesis for the Canary Islands. *Trends in Ecology & Evolution*, **15**, 104-109.

Kindler, C., Chevre, M., Ursenbacher, S., Bohme, W., Hille, A., Jablonski, D., Vamberger, M. & Fritz, U. (2017) Hybridization patterns in two contact zones of grass snakes reveal a new Central European snake species. *Sci Rep*, **7**, 7378.

Kindler, C., Böhme, W., Corti, C., Gvoždík, V., Jablonski, D., Jandzik, D., Metallinou, M., Široký, P. & Fritz, U. (2013) Mitochondrial phylogeography, contact zones and taxonomy of grass snakes (Natrix natrix,N. megalocephala). *Zoologica Scripta*, **42**, 458-472.

Leache, A.D. & Oaks, J.R. (2017) The Utility of Single Nucleotide Polymorphism (SNP) Data in Phylogenetics. *The Annual Review of Ecology, Evolution, and Systematics*, **48**, 69-84.

Lemmon, E.M. & Lemmon, A.R. (2013) High-Throughput Genomic Data in Systematics and Phylogenetics. *Annual Review of Ecology, Evolution, and Systematics*, **44**, 99-121.

Longpré, M.-A., Troll, V.R., Walter, T.R. & Hansteen, T.H. (2009) Volcanic and geochemical evolution of the Teno massif, Tenerife, Canary Islands: Some repercussions of giant landslides on ocean island magmatism. *Geochemistry, Geophysics, Geosystems*, **10**, Q12017.

Machado, A., Rodríguez-Expósito, E., López, M. & Hernandez, M. (2017) Phylogenetic analysis of the genus *Laparocerus*, with comments on colonisation and diversification in Macaronesia (Coleoptera, Curculionidae, Entiminae). *Zookeys*, **651**, 1-77.

Macías-Hernández, N., Bidegaray-Batista, L., Emerson, B.C., Oromí, P. & Arnedo, M. (2013) The imprint of geologic history on within-island diversification of woodlouse-hunter spiders (Araneae, Dysderidae) in the Canary Islands. *Journal of Heredity*, **104**, 341-56.

Mairal, M., Sanmartin, I., Aldasoro, J.J., Culshaw, V., Manolopoulou, I. & Alarcon, M. (2015) Palaeo-islands as refugia and sources of genetic diversity within volcanic archipelagos: the case of the widespread endemic Canarina canariensis (Campanulaceae). *Molecular Ecology*, **24**, 3944-63.

Malhotra, A. & Thorpe, R.S. (2000) A phylogeny of the trimeresurus group of pit vipers: new evidence from a mitochondrial gene tree. *Mol Phylogenet Evol*, **16**, 199-211.

Mallet, J. (2007) Hybrid speciation. *Nature*, **446**, 279-83.

Masson, D., Watts, A., Gee, M., Urgeles, R., Mitchell, N., La Bas, T. & Canals, M. (2002) Slope failures on the flanks of the western Canary Islands. *Earth-Science Reviews*, **57**, 33-45.

McEntee, J.P., Burleigh, J.G. & Singhal, S. (2018) Dispersal predicts hybrid zone widths across animal diversity: Implications for species borders under incomplete reproductive isolation. *BioRxiv*.

McGuire, W.J. (2003) Volcanic instability and lateral collapse. *Revista*, **1**, 33-45.

Meirmans, P.G. & Van Tienderen, P.H. (2004) genotype and genodive: two programs for the analysis of genetic diversity of asexual organisms. *Molecular Ecology Notes*, **4**, 792-794.

Moya, O., Contreras-Díaz, H.G., Oromí, P. & Juan, C. (2004) Genetic structure, phylogeography and demography of two ground-beetle species endemic to the Tenerife laurel forest (Canary Islands). *Molecular Ecology*, **13**, 3153-67.

Otto, R., Whittaker, R.J., von Gaisberg, M., Stierstorfer, C., Naranjo-Cigala, A., Steinbauer, M.J., Borregaard, M.K., Arévalo, J.R., Garzón-Machado, V., del Arco, M. & Fernández-Palacios, J.M. (2016) Transferring and implementing the general dynamic model of oceanic island biogeography at the scale of island fragments: the roles of geological age and topography in plant diversification in the Canaries. *Journal of Biogeography*, **43**, 911-922.

Patiño, J., Whittaker, R.J., Borges, P.A.V., Fernández-Palacios, J.M., Ah-Peng, C., Araújo, M.B., Ávila, S.P., Cardoso, P., Cornuault, J., de Boer, E.J., de Nascimento, L., Gil, A., González-Castro, A., Gruner, D.S., Heleno, R., Hortal, J., Illera, J.C., Kaiser-Bunbury, C.N., Matthews, T.J., Papadopoulou, A., Pettorelli, N., Price, J.P., Santos, A.M.C., Steinbauer, M.J., Triantis, K.A., Valente, L., Vargas, P., Weigelt, P. & Emerson, B.C. (2017) A roadmap for island biology: 50 fundamental questions after 50 years of The Theory of Island Biogeography. *Journal of Biogeography*, **44**, 963-983.

Pestano, J. & Brown, R.P. (1999) Geographical structuring of mitochondrial DNA in Chalcides sexlineatus within the island of Gran Canaria. *Proceedings of the Royal Society*, **266**, 805-812.

Peterson, B.K., Weber, J.N., Kay, E.H., Fisher, H.S. & Hoekstra, H.E. (2012) Double digest RADseq: an inexpensive method for de novo SNP discovery and genotyping in model and non-model species. *PLoS One*, **7**, e37135.

Pyron, R.A., Hendry, C.R., Chou, V.M., Lemmon, E.M., Lemmon, A.R. & Burbrink, F.T. (2014) Effectiveness of phylogenomic data and coalescent species-tree methods for resolving difficult nodes in the phylogeny of advanced snakes (Serpentes: Caenophidia). *Mol Phylogenet Evol*, **81**, 221-31.

Salces-Castellano, A., Stankowski, S., Arribas, P., Patiño, J., Butlin, R.K. & Emerson, B.C. (In preparation B) An idiosyncratic response to Quaternary climate change drives speciation in an insular cloud forest.

Salces-Castellano, A., Patiño, J., Arribas, P., Andújar, C., Karger, D., Manolopoulou, I., Peterman, W.E., López, H., Pérez-Delgado, A., García-Olivares, V., Braojos-Ruiz, J.J., Alvarez, N., Oromí, P. & Brent, C.E. (In preparation A) Microclimate drives community-wide speciation on an oceanic island.

Spurgin, L.G., van Oosterhout, C., Illera, J.C., Bridgett, S., Gharbi, K., Emerson, B.C. & Richardson, D.S. (2011) Gene conversion rapidly generates major histocompatibility complex diversity in recently founded bird populations. *Molecular Ecology*, **20**, 5213-25.

Thorpe, R.S., Black, H. & Malhotra, A. (1996) Matrix correspondence tests on the DNA phylogeny of the Tenerife Lacertid elucidate both historical causes and morphological adapation. *Systematic Biology*, **45**, 335-343.

Vandergast, A.G., Gillespie, R.G. & Roderick, G.K. (2004) Influence of volcanic activity on the population genetic structure of Hawaiian Tetragnatha spiders: fragmentation, rapid population growth and the potential for accelerated evolution. *Molecular Ecology*, **13**, 1729-43.

Walter, T. & Schmincke, H.U. (2002) Rifting, recurrent landsliding and Miocene structural reorganization on NW-Tenerife (Canary Islands). *International Journal of Earth Sciences*, **91**, 615-628.

Walter, T.R., Troll, V.R., Cailleau, B., Belousov, A., Schmincke, H.U., Amelung, F. & v.d. Bogaard, P. (2005) Rift zone reorganization through flank instability in ocean island volcanoes: an example from Tenerife, Canary Islands. *Bulletin of Volcanology*, **67**, 281-291.

Watts, A.B. & Masson, D.G. (1998) Reply [to “Comment on “A giant landslide on the north flank of Tenerife, Canary Islands” by A. B. Watts and D. G. Masson”]. *Journal of Geophysical Research: Solid Earth*, **103**, 9949-9952.

Watts, A.B.M., D. G. (2001) New sonar evidence for recent catastrophic collapses of the north flank of Tenerife, Canary Islands. *Bulletin of Volcanology*, **63**, 8-19.

Supporting information

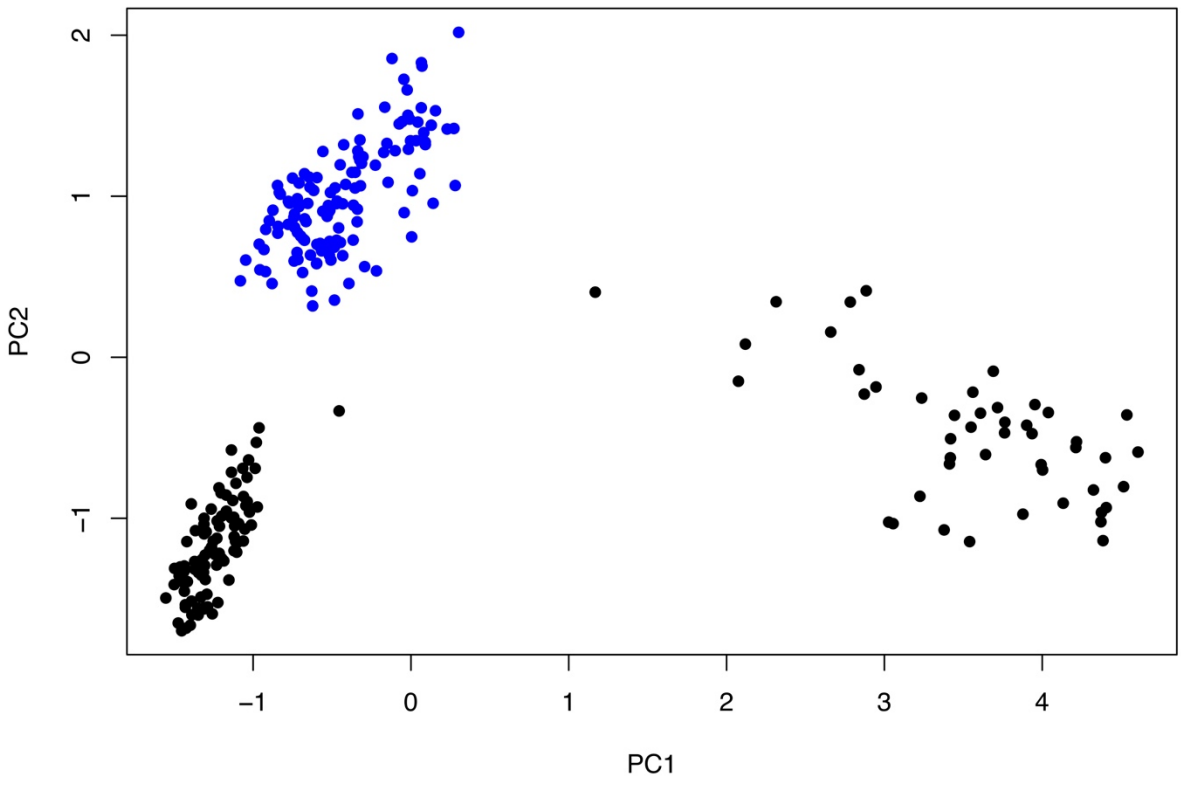

Figure S1. Exploratory analysis of the *Laparocerus tessellatus* species complex across the Canary Islands. Principal components analysis (PCA) of multilocus genotypes for the individuals sampled. Each point represents one individual. Whereas the individuals from Tenerife are represented with blue colour, the individuals from Gran Canaria, La Palma and El Hierro are represented in black colour.

Table S1. Details of sampling locations and the number of individuals sampled at each location for the *Laparocerus tessellatus* complex from Tenerife.

Island	Locality Code	Latitude	Longitude	No. Individuals
Tenerife	T01	28.56202	-16.17140	1
Tenerife	T02	28.56020	-16.16920	1
Tenerife	T03	28.55930	-16.17323	1
Tenerife	T04	28.55856	-16.17519	1
Tenerife	T05	28.55558	-16.18118	1
Tenerife	T06	28.55196	-16.18923	1
Tenerife	T07	28.54243	-16.22830	1
Tenerife	T08	28.53192	-16.28007	1
Tenerife	T09	28.53550	-16.29620	1
Tenerife	T10	28.53869	-16.30013	1
Tenerife	T11	28.53731	-16.30938	1
Tenerife	T12	28.50834	-16.31650	2
Tenerife	T13	28.50689	-16.33226	1
Tenerife	T14	28.49309	-16.36113	1
Tenerife	T15	28.48003	-16.35396	1
Tenerife	T16	28.46071	-16.37668	2
Tenerife	T17	28.44379	-16.38644	1
Tenerife	T18	28.44044	-16.40373	1
Tenerife	T19	28.42999	-16.39546	1
Tenerife	T21	28.42381	-16.39610	2
Tenerife	T22	28.42011	-16.40750	1
Tenerife	T23	28.42914	-16.42743	1
Tenerife	T24	28.41455	-16.41713	1
Tenerife	T25	28.40815	-16.40306	1
Tenerife	T26	28.40458	-16.39634	1
Tenerife	T27	28.40373	-16.39002	2
Tenerife	T29	28.38285	-16.39437	1
Tenerife	T30	28.40399	-16.42423	1
Tenerife	T31	28.39480	-16.43165	1
Tenerife	T32	28.37345	-16.40509	1
Tenerife	T33	28.37479	-16.41268	1
Tenerife	T34	28.37879	-16.42473	1
Tenerife	T35	28.39203	-16.43736	1
Tenerife	T36	28.41501	-16.44292	2
Tenerife	T37	28.39117	-16.44142	1
Tenerife	T38	28.41115	-16.45066	1
Tenerife	T39	28.38607	-16.44199	1
Tenerife	T40	28.38550	-16.45585	1
Tenerife	T42	28.40752	-16.46434	1

Tenerife	T43	28.35901	-16.43337	1
Tenerife	T44	28.32805	-16.42484	1
Tenerife	T45	28.33887	-16.43794	1
Tenerife	T46	28.37383	-16.46376	1
Tenerife	T47	28.36885	-16.46501	1
Tenerife	T48	28.37258	-16.46783	3
Tenerife	T49	28.37591	-16.47280	4
Tenerife	T50	28.38143	-16.47936	3
Tenerife	T51	28.39032	-16.48924	1
Tenerife	T52	28.39917	-16.48384	1
Tenerife	T53	28.40304	-16.49229	1
Tenerife	T54	28.40121	-16.49567	1
Tenerife	T55	28.35769	-16.46667	1
Tenerife	T56	28.36350	-16.49301	1
Tenerife	T57	28.34126	-16.47891	1
Tenerife	T58	28.32366	-16.45176	1
Tenerife	T59	28.30806	-16.44236	1
Tenerife	T60	28.31639	-16.48614	1
Tenerife	T61	28.35539	-16.51461	1
Tenerife	T62	28.34795	-16.53172	1
Tenerife	T63	28.34423	-16.54283	2
Tenerife	T64	28.32716	-16.53320	1
Tenerife	T65	28.30758	-16.53692	1
Tenerife	T66	28.34006	-16.56710	2
Tenerife	T67	28.30291	-16.56654	1
Tenerife	T68	28.30911	-16.56722	1
Tenerife	T69	28.32569	-16.58786	2
Tenerife	T70	28.34282	-16.59322	1
Tenerife	T71	28.36096	-16.59862	1
Tenerife	T72	28.37783	-16.60095	1
Tenerife	T73	28.33658	-16.62066	1
Tenerife	T74	28.33271	-16.65817	2
Tenerife	T75	28.31620	-16.71957	3
Tenerife	T76	28.36146	-16.77505	2
Tenerife	T77	28.31853	-16.75554	1
Tenerife	T78	28.32877	-16.78104	2
Tenerife	T79	28.32896	-16.80887	1
Tenerife	T80	28.31338	-16.82018	1
Tenerife	T81	28.31413	-16.82984	1
Tenerife	T86	28.34167	-16.86331	1
Tenerife	T87	28.33848	-16.87357	2
Tenerife	T88	28.27160	-16.76831	2
Tenerife	T88b	28.27495	-16.73553	1
Tenerife	T89	28.24605	-16.76495	2
Tenerife	T96	28.18893	-16.65695	1

Tenerife	T97	28.16540	-16.63680	1
Tenerife	T99	28.17253	-16.62525	1
Tenerife	T103	28.17035	-16.60902	1
Tenerife	T104	28.18068	-16.59173	1
Tenerife	T106	28.18591	-16.58145	1
Tenerife	T108	28.18815	-16.57393	1
Tenerife	T110	28.19746	-16.56724	1
Tenerife	T111	28.20746	-16.56141	1
Tenerife	T113	28.19770	-16.53115	1
Tenerife	T115	28.22499	-16.54904	1
Tenerife	T116	28.21490	-16.49102	2
Tenerife	T118	28.25931	-16.52052	1
Tenerife	T119	28.24721	-16.48191	1
Tenerife	T120	28.28796	-16.51247	1
Tenerife	T121	28.27462	-16.46414	1
Tenerife	T122	28.29692	-16.48256	1
Tenerife	T123	28.29324	-16.44798	2
Tenerife	T124	28.29325	-16.43329	1
Tenerife	T126	28.33486	-16.83157	1

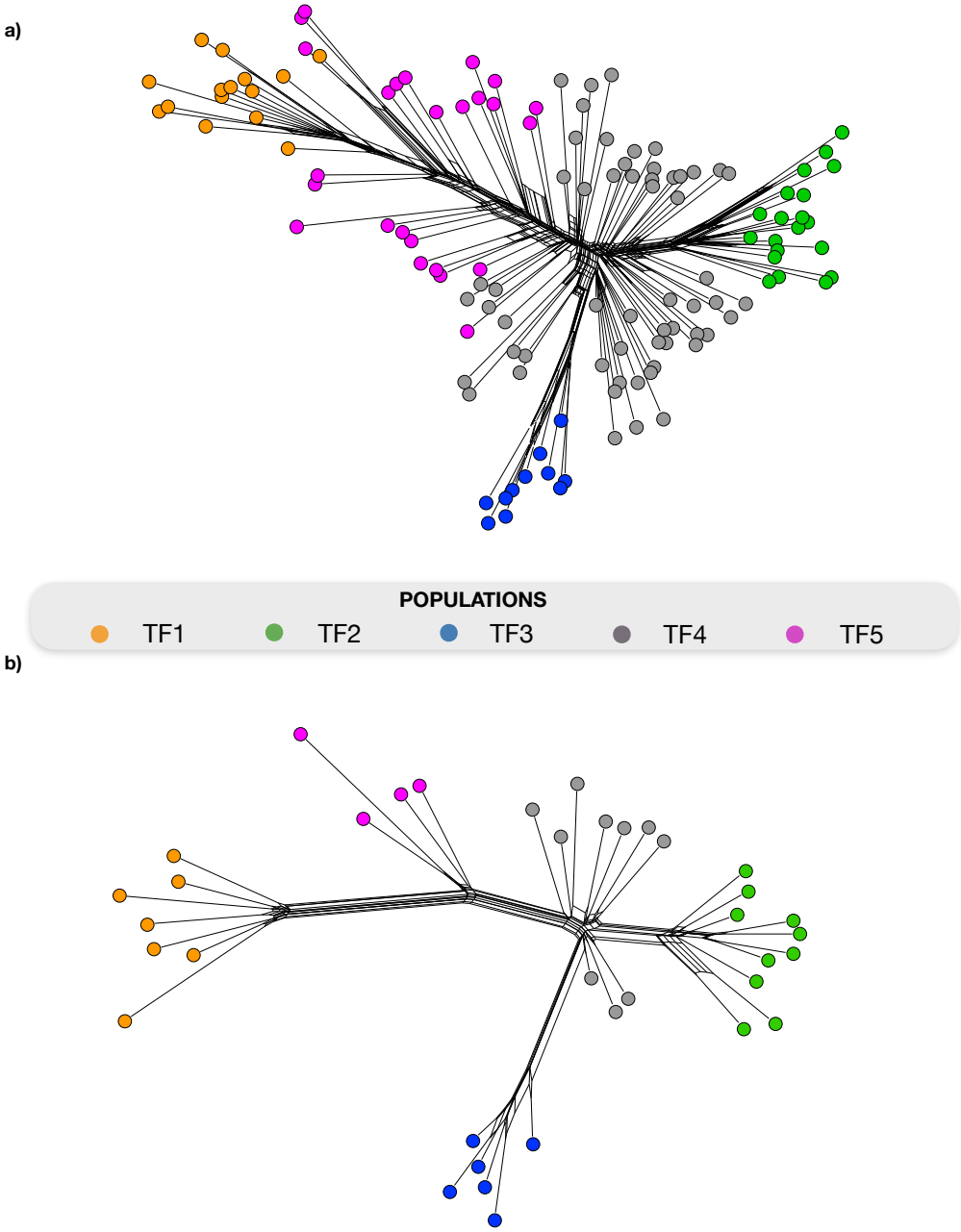

Figure S2. Phylogenomic network within Tenerife. Neighbor-Net phylogenomic network summarising genomic relatedness among individuals within Tenerife. Each point represents one individual, with colours corresponding to inferences of the five ancestral populations inferred by sNMF. (a) Network including all the individuals sequenced. The population colour assignment to each individual was established from probabilities higher than 50% to a particular ancestral population. (b) Network including only individuals with higher assignment (>90%) to an unique ancestral population.

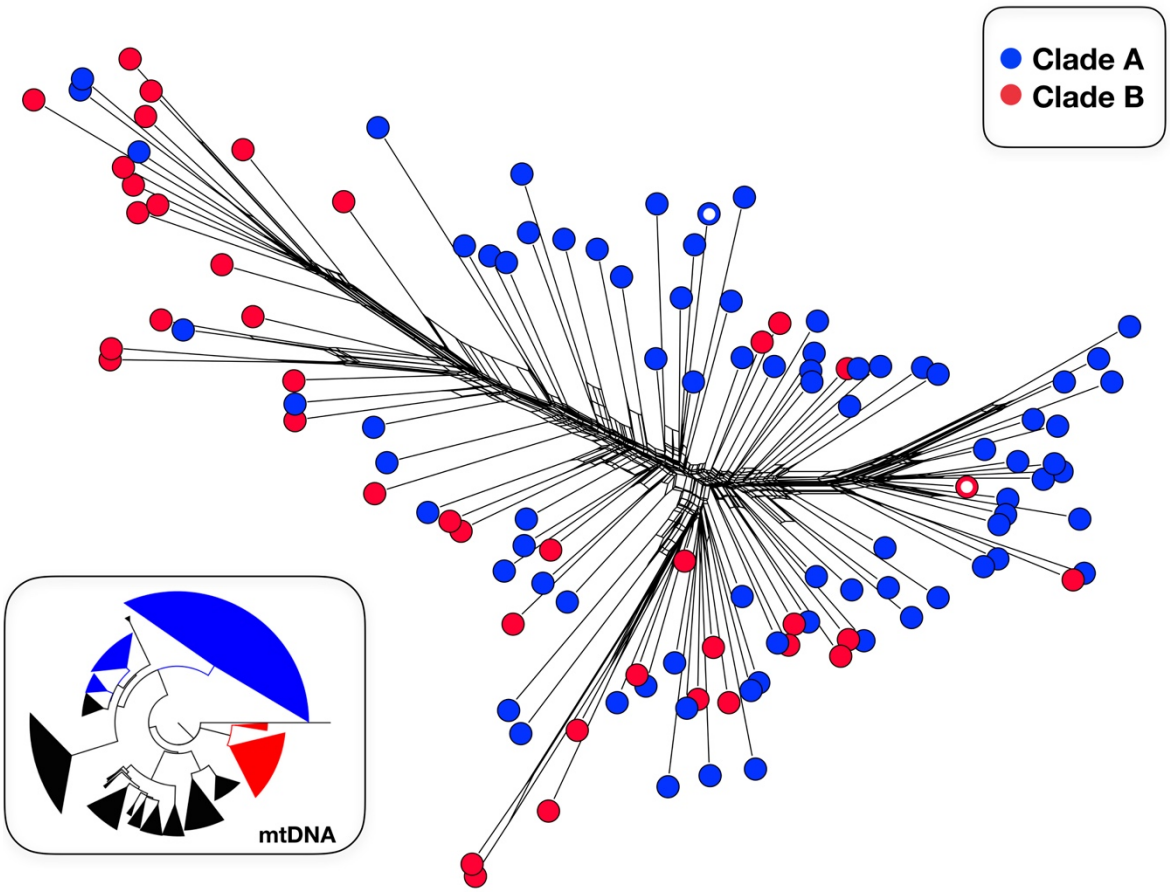

Figure S3. Representing mtDNA clades within the phylogenomic network. Neighbor-Net phylogenomic network summarising genomic relatedness among individuals within Tenerife. Each point represents one individual, with different colour corresponding to both mitochondrial clades inferred by the Bayesian tree. Those individuals which were revealed as divergent mtDNA in sympatry which were inferred at different clades from ddRAD-seq data, were identified with a white coloured dot. A Bayesian tree shown the three differentiated clades identified by mtDNA.

CONCLUSIONS

Conclusions

1. Mitochondrial data from the *Laparocerus tessellatus* complex provides strong evidence for multiple founding individuals to La Palma that share a common geographic origin from Tenerife, originating specifically within the limits of the La Orotava mega-landslide (Chapter I).

2. Geological and genetic data support a hypothesis of mega-landslides as an important driver of inter-island colonization by oceanic rafting. This mechanism may facilitate movement between islands involving multiple individuals from the same source. In the context of island biogeographic theory, mega-landslides may be an important driver of colonization and subsequent lineage diversification (Chapter I).

3. The nuclear genome phylogeny inferred for the *L. tessellatus* species complex is consistent with the origin of each island from a single founding event, although with some minor exceptions (Chapter II).

4. The nuclear genomic data provide strong support for a Gran Canaria origin for the *L. tessellatus* complex (Chapter II).

5. The Bayesian species delimitation method applied to sub-genomic data sampled from the *L. tessellatus* complex from Gran Canaria rejected species hypothesis based on taxonomy, finding highest support for the hypothesis based on results provides by sNMF and PCA analyses, which describe four species (Chapter III).

6. Individual-level genomic relationships within the *L. tessellatus* complex from Gran Canaria revealed strong genomic signatures of admixture at higher elevations and, at lower elevations, purer parental genomes. Furthermore, higher genetic connectivity among individuals along an altitudinal gradient in comparison with radial connectivity

was found, consistent with a higher potential bioclimate connectivity within valleys than among valleys throughout the Quaternary (Chapter III).

7. The ddRAD-seq data generated for *L. tessellatus* complex from Gran Canaria, reveals a complex speciation history involving population isolation and admixture, supporting an insular topoclimate model for Quaternary diversification (ITQD). This conceptual model explains the responses of species distribution to the changing geography of local climate under a topographically complex island landscape through glacial-scale climate dynamics. The ITQD model, therefore, will be a useful framework for interpreting patterns of genomic relatedness across insular landscapes (Chapter III).

8. Within the *L. tessellatu*s complex from Tenerife, five ancestral populations were inferred, with individuals inferred to have single ancestry distributed respectively in, the northwest of the island, Anaga, and associated with areas above scarps defining the Orotava, Güímar and Roques García flank collapse limits. Areas of secondary contact were detected among these pure populations, which were associated with areas within of close to flank collapses (Chapter IV).

9. Genomic patterns of individual relatedness within Tenerife give support a role for gravitational flank collapses promoting a dynamic of population isolation and secondary contact. This finding, in relation to the frequent occurrence of flank collapses in oceanic islands, could be considered an important mechanism at the regional scale for the generation of novel genetic variation within islands over the long term (Chapter IV).

ACKNOWLEDGMENTS

Para culminar esta tesis doctoral me gustaría dedicar unas palabras de agradecimiento a aquellas personas e instituciones que me han acompañado durante todo este trayecto, que tanto de forma directa e indirecta, han formado parte activa de este proceso.

En primer lugar, quiero agradecer a mi familia, por el apoyo y cariño que me han dado durante el desarrollo de la tesis, y por inculcarme desde siempre el valor del esfuerzo, la perseverancia y la humildad como modo de vida. A Lida, por su incondicional apoyo en esta travesía, su comprensión y su paciencia, mi línea de vida durante todos estos años. A mis amigos pepineros, a los "Alcarreños", a los latinos, y a muchos otros, por permanecer siempre a mi lado a pesar de la lejanía. A los miembros del Grupo de Ecología y Evolución en Islas, por su cariño y su amistad durante todos estos años, por apoyarme durante todas las vicisitudes doctorales, y por aguantar mis delirantes monólogos durante el almuerzo de cada día. Y a los nuevos compañeros de esta nueva etapa laboral, por su cálido recibimiento y su cariño desde el primer día.

Esta tesis no hubiera sido posible sin Brent Emerson, brindándome la oportunidad de realizar el doctorado bajo su dirección, a quien agradezco su entrega y su dedicación durante toda la tesis. A Jairo Patiño, por su apoyo, su cercanía y su continúa disposición durante toda la tesis doctoral. A Heriberto López, por su apoyo incondicional desde el inicio y por transmitirme todo su conocimiento. A Antonio Machado, por transmitirme su pasión por la investigación y por su ayuda prestada durante la tesis. A la gerencia y dirección del Instituto de Productos Naturales y Agrobiología, por facilitar cada trámite administrativo, además de su atención y preocupación durante todo este tiempo. A Unai López de Heredia y a Fernando Mora por su cercanía, su inestimable ayuda bioinformática, y su dedicación durante la estancia en la Universidad Politécnica de Madrid. A Mike Hickerson, Isaac Overcast y Laura Bertola por facilitarme en todo momento mi estadía por la City College of New York, por su cercanía, su y su conocimiento compartido.

También quería agradecer de manera especial a Carlos Ruiz, por rescatarme de la crisis laboral española, otorgándome su confianza, su conocimiento y su ayuda, reimpulsando mi carrera para llegar hasta el lugar donde me hallo ahora. A Ecuador, por proveerme de aquello que España no supo ofrecerme al finalizar mi carrera, un trabajo dónde poder seguir aprendiendo y formándome. Sin lugar a duda, la experiencia ecuatoriana me enriqueció no solo como persona, sino que me ayudó a catapultar mi valía profesional para poder logar obtener el contrato predoctoral que me permitió llevar a cabo esta tesis doctoral. Por último, agradecer a mi compañero de viaje ecuatoriano Carlos Zaragoza, con quien además de compartir un trayecto importante de mi vida, ha permanecido atento y cercano a esta travesía académica.

Por último, agradecer al Ministerio de Economía y Empresa, y por ende a todos los contribuyentes que aportan al estado, la financiación otorgada a través del programa de Formación de Personal Investigador para realizar esta tesis doctoral, además de la financiación obtenida para las dos estancias disfrutadas durante estos cuatro años.

VÍCTOR M. GARCÍA OLIVARES
2019

Universidad de La Laguna
IPNA CSIC
CSIC
Consejo Superior de Investigaciones Científicas